→ 10th COASTAL ALTIMETRY WORKSHOP

SAR Altimetry Training Course

SAR and SARin L1A to L2 processing: Strategies for different applications

Salvatore Dinardo (HeSpace)

21–24 February 2017 | Florence, Italy

Presentation Content

- SAR (Delay-Doppler) Background
- L1A to L1b Processing Walk-Through (using CryoSat-2 Data)
- From L1b to L2
- Conclusions

Expected advantages of SAR (Delay-Doppler) Altimetry

- More independent looks ➔ improved retrieval precision
  - ~0.9 cm in range (@1 Hz)

Expected advantages of SAR (Delay-Doppler) Altimetry

- More independent looks ➔ improved retrieval precision
  - ~0.9 cm in range (@1 Hz)
- Finer spatial resolution along track ➔ capacity to retrieve short scale signal
  - ~300 meters along-track

Expected advantages of SAR (Delay-Doppler) Altimetry

- More independent looks → improved retrieval precision
  - ~0.9 cm in range (@1 Hz)
- Finer spatial resolution along track → capacity to retrieve short scale signal
  - ~300 meters along-track
- Higher SNR
  - ~10 db more
  -

Expected advantages of SAR (Delay-Doppler) Altimetry

- More independent looks ➔ improved retrieval precision
  - ~0.9 cm in range (@1 Hz)
- Finer spatial resolution along track ➔ capacity to retrieve short scale signal
  - ~300 meters along-track
- Higher SNR
  - ~10 db more
- Better performance close to land
  - especially for track ~90° to coastline

Expected advantages of SAR (Delay-Doppler) Altimetry

- More independent looks ➔ improved retrieval precision
  - ~0.9 cm in range (@1 Hz)
- Finer spatial resolution along track ➔ capacity to retrieve short scale signal
  - ~300 meters along-track
- Higher SNR
  - ~10 db more
- Better performance close to land
  - especially for track ~90° to coastline
- Less sensitivity to sea state (constant footprint with SWH)

Expected advantages of SAR (Delay-Doppler) Altimetry

- More independent looks ➔ improved retrieval precision
  - ~0.9 cm in range (@1 Hz)
- Finer spatial resolution along track ➔ capacity to retrieve short scale signal
  - ~300 meters along-track
- Higher SNR
  - ~10 db more
- Better performance close to land
  - especially for track ~90° to coastline
- Less sensitivity to sea state (constant footprint with SWH)
- Less sensitive to antenna mispointing (especially pitch)

Pulse Transmission Schemes

Classic Altimetry (Pulse-Limited,LRM): PRF @ 1970hz, Posting Rate @ 21hz (350 m)

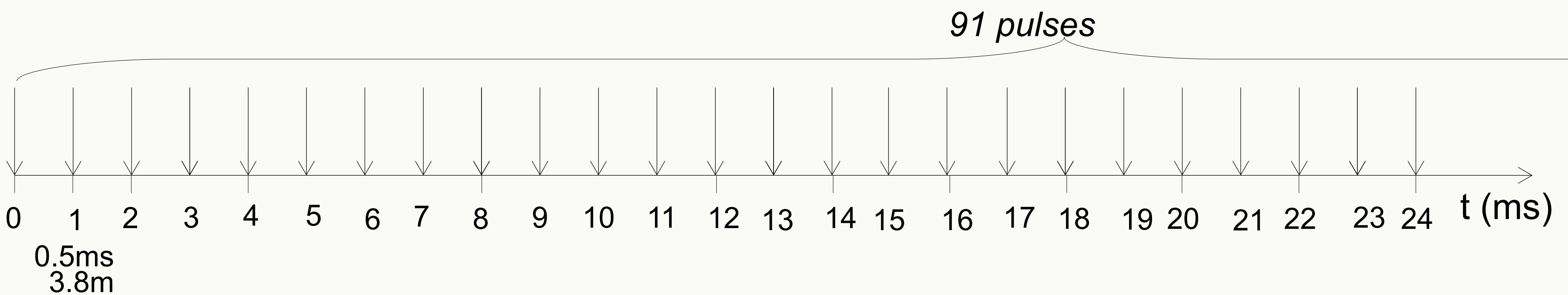

Pulse Transmission Schemes

Pulse-Limited Altimetry (LRM): PRF @ 1970hz, Posting Rate @ 21hz (350 m)

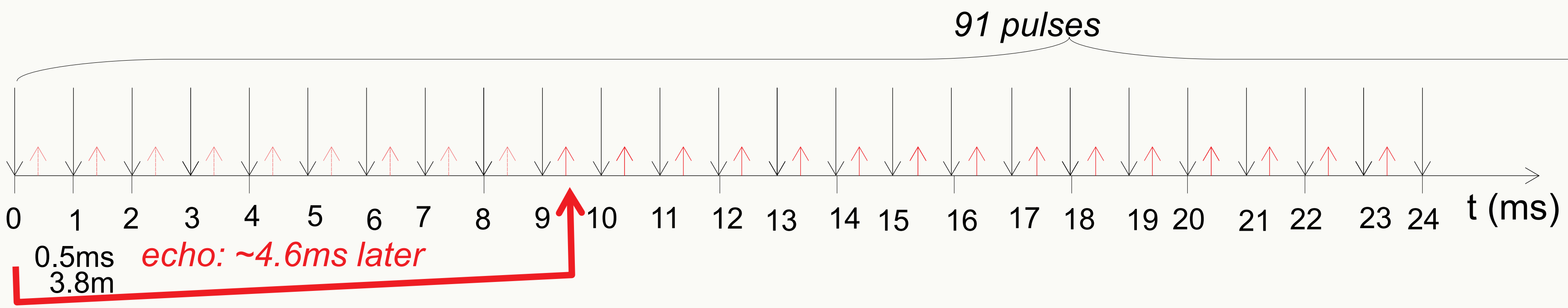

Pulse Transmission Schemes

Pulse-Limited Altimetry (LRM): PRF @ 1970hz, Posting Rate @ 21hz (350 m)

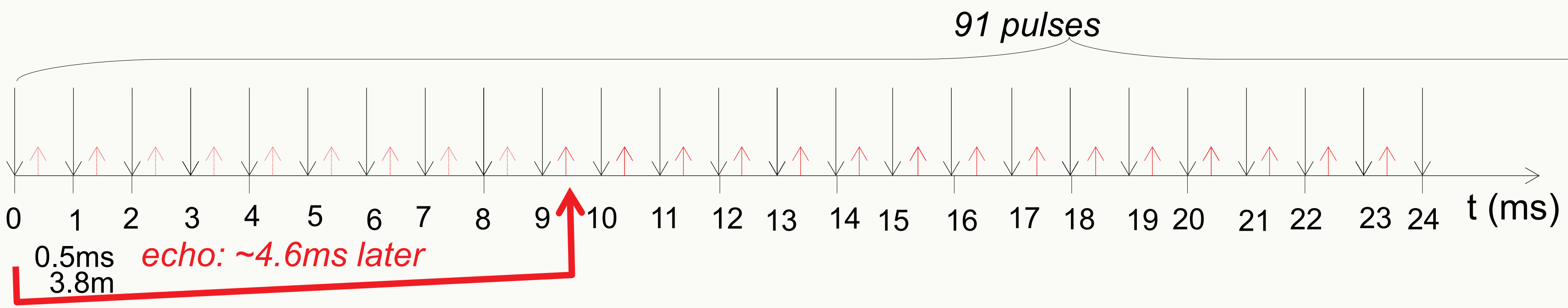

SAR: PRF @ 17800hz, bursts @ 84hz, Posting Rate @ 21hz (350 m)

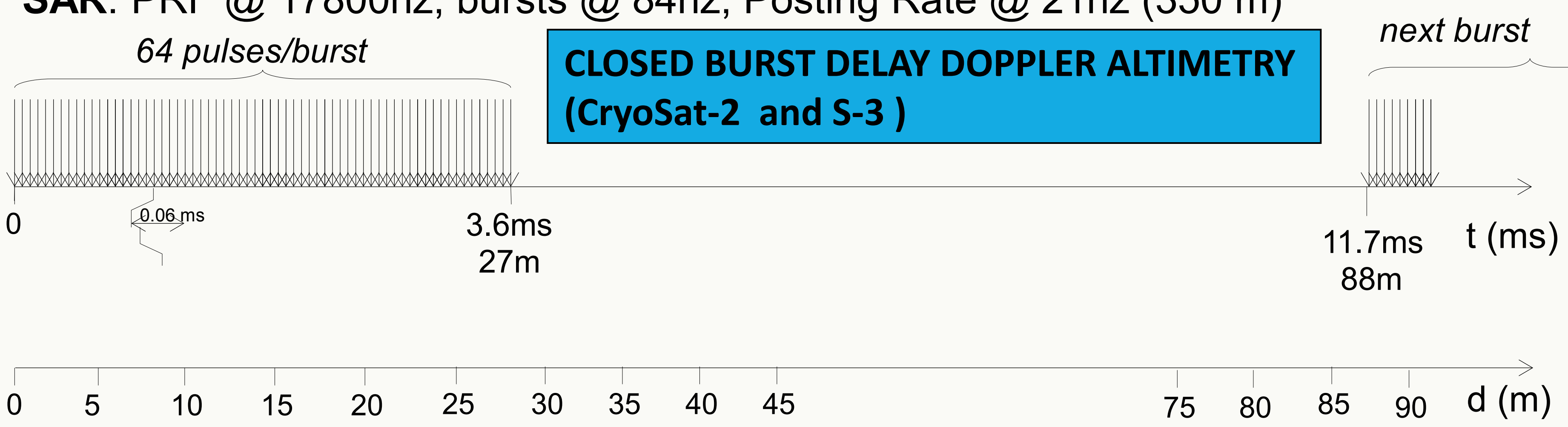

Pulse Transmission Schemes

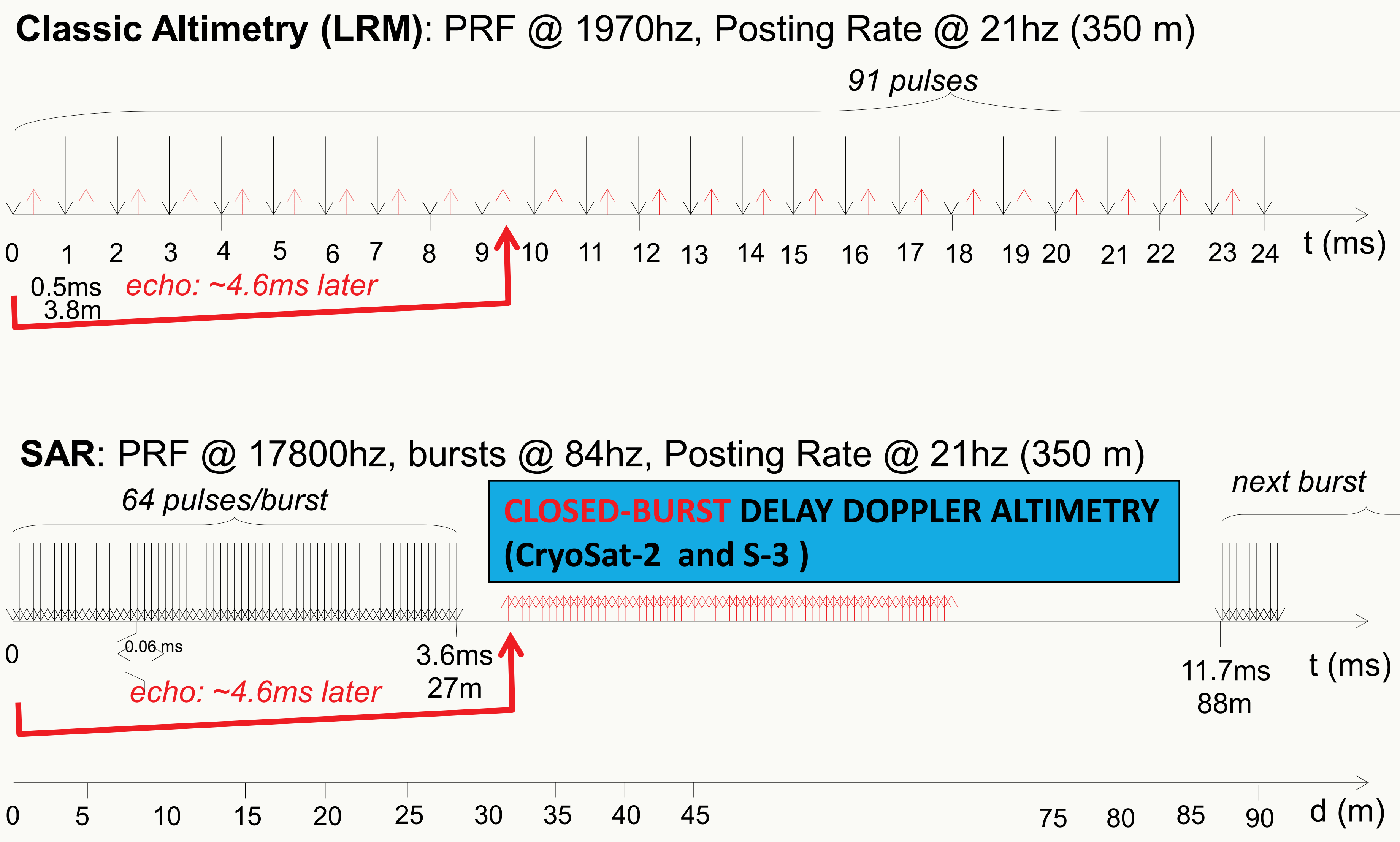

Picture by Nicolas Bercher

DATA PRODUCTS LEVEL TERMINOLOGY

- **L1A** (or Full Bit Rate, aka FBR) → *un-calibrated complex (I and Q) individual echoes, unpacked from telemetries, posted at full PRF Rate and deramped in time domain.*
- **L1b-S** (Level 1b-Stack or simply Stack)→ *Stack of Geo-located, calibrated, beam-formed power echoes, after slant range correction, all reflected by a given ground cell along the ground-track (i.e. looks).* No averaging of individual waveforms (i.e. multi-looking) is applied.
- **L1b** (Level 1 b)→ *Geo-located, calibrated multi-looked power echoes reflected by a ground cell along the ground-track*

Delay-Doppler (SAR) Processing → FROM L1A to L1b

DELAY-DOPPLER ALGORITHM PAPER
by K. Raney + CryoSat Team Heritage

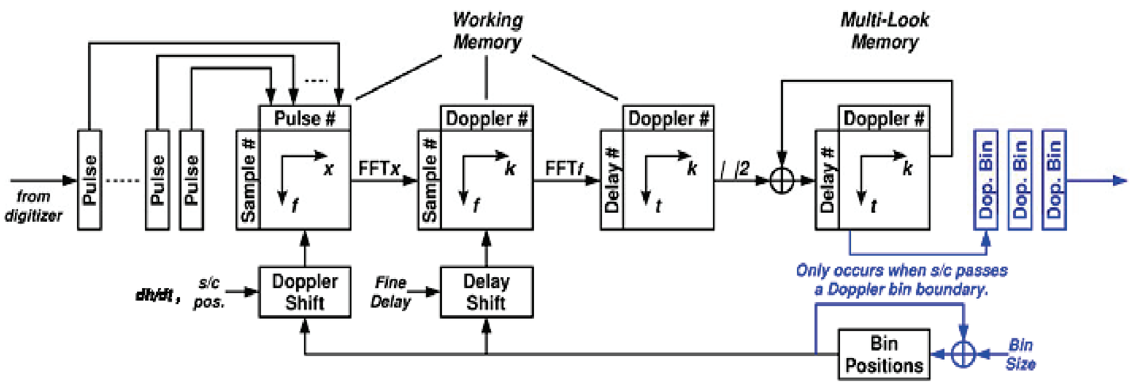

The Delay/Doppler Radar Altimeter

R. Keith Raney, *Fellow, IEEE*

***Abstract*—The key innovation in the delay/Doppler radar altimeter is delay compensation, analogous to range curvature correction in a burst-mode synthetic aperture radar (SAR). Following delay compensation, height estimates are sorted by Doppler frequency, and integrated in parallel. More equivalent looks are accumulated than in a conventional altimeter. The relatively small along-track footprint size is a constant of the system, typically on the order of 250 m for a Ku-band altimeter. The flat-surface response is an impulse rather than the more familiar step function produced by conventional satellite radar altimeters. The radar equation for the delay/Doppler radar altimeter has an $h^{-5/2}(c\tau)^{1/2}$ dependence on height h and compressed pulse length τ, which is more efficient than the corresponding $h^{-3}c\tau$ factor for a pulse-limited altimeter. The radiometric response obtained by the new approach would be 10 dB stronger than that of the TOPEX/Poseidon altimeter, for example, if the same hardware were used in the delay/Doppler altimeter mode. This new technique leads to a smaller instrument that requires less power, yet performs better than a conventional radar altimeter. The concept represents a new generation of altimeter for earth observation, with particular suitability for coastal ocean regions and polar ice sheets as well as open oceans.**

***Index Terms*—Doppler beam sharpening, radar altimeter, synthetic aperture radar.**

I. Introduction

THE PRINCIPAL objective of a satellite radar altimeter is to measure the height of reflecting facets scanned by passage of the instrument overhead. Geophysical elevation is derived from the record of radar height measurements, corrected with respect to precise orbit knowledge and path delays. Height precision is set by the radar pulse length and by the amount of averaging available for each estimate. Height is defined in the context of this paper as the minimum range between the radar and scatterers that lie along the ground track of the satellite.

By definition, a conventional satellite altimeter [Fig. 1(a) and (b)] uses the echo delays from within the pulse-limited footprint to estimate minimum radar range [8]. Outside of the pulse-limited footprint, each scatterer's echo appears at relatively greater delay. The (compressed) pulse length determines the diameter of the pulse-limited footprint associated with a quasiflat surface [2]. For a typical radar altimeter, such as GEOSAT, the pulse-limited footprint is on the order of 2 km in diameter [6], expanding to many kilometers as large-scale surface roughness increases.

Manuscript received April 1, 1997; revised October 27, 1997.
The author is with The Johns Hopkins University Applied Physics Laboratory, Laurel, MD 20723-6099 USA (e-mail: keith.raney@jhuapl.edu).
Publisher Item Identifier S 0196-2892(98)04976-6.

Pulse-limited operation necessarily implies that conventional altimeters are relatively wasteful of radiated power. For example, the footprint diameter of GEOSAT over a quasiflat surface is less than 1/10 of the antenna pattern within the half-power width. Hence, most of the radiated power falls outside of the pulse-limited area and cannot be used for height estimation. Other disadvantages of conventional radar altimeters include footprint dilation over rougher terrain, and the tendency of the footprint location to hop from one elevated region to another rather than to trace out the elevation profile without negative influence from the topography. Footprint dilation leads to less than optimal estimation of surface height and roughness.

Doppler beam-sharpened (DBS) altimeters have been proposed as a means of reducing the along-track footprint size of a radar altimeter. The performance of DBS altimeters has proven to be very disappointing. The main reason is that relatively few "looks" are available, virtually eliminating most of the incoherent averaging that is essential to precision altimetric measurements. The Johns Hopkins University Applied Physics Laboratory (JHU/APL) delay/Doppler approach is fundamentally different; there is far more averaging in the delay/Doppler approach than is possible from a DBS altimeter.

The principal objectives of the delay/Doppler altimeter [12], [13] are to operate more efficiently and more effectively. The first objective is met by compensating for systematic range delay errors; thus, the entire (beam-limited) along-track signal history contributes to height measurement rather than only the much smaller pulse-limited area. Stated another way, the delay/Doppler altimeter uses much more of the instrument's radiated energy than does a conventional beam-limited altimeter. The second objective is met by using Doppler selectivity to reduce the width of the postprocessing along-track footprint; this minimizes unwanted terrain dependency of the footprint size and position.

The delay/Doppler altimeter uses pulse compression in the range dimension, just as is customary for incoherent radar altimeters [5]. The range signal is a long linearly frequency modulated (FM) pulse, which is multiplied by a delayed replica FM pulse immediately upon reception, and low-pass filtered. The delay is chosen to match the expected range to the mean reflecting surface, the so-called track point. This "deramp" strategy transforms "range" into a continuous wave (CW) signal whose frequency is proportional to height, relative to the track point [7], [15], [16]. A conventional altimeter and the delay/Doppler altimeter both complete range compression by application of an inverse Fourier transform (IFFT) to convert the CW signals into height. These are summed to produce

DELAY-DOPPLER ALGORITHM PAPER
by K. Raney + CryoSat Team Heritage

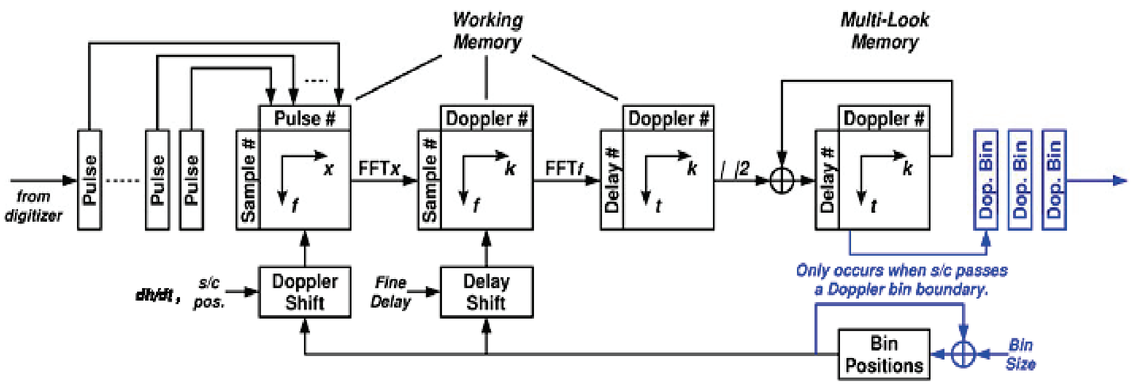

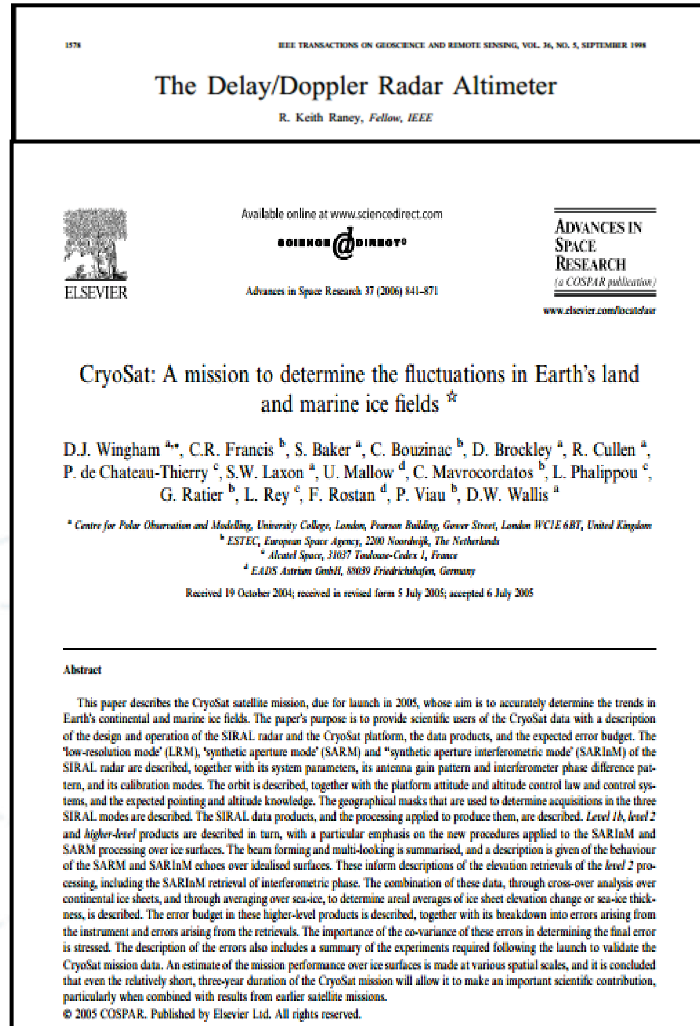

1578 IEEE TRANSACTIONS ON GEOSCIENCE AND REMOTE SENSING, VOL. 36, NO. 5, SEPTEMBER 1998

The Delay/Doppler Radar Altimeter

R. Keith Raney, *Fellow, IEEE*

ELSEVIER

Available online at www.sciencedirect.com

SCIENCE @ DIRECT®

Advances in Space Research 37 (2006) 841–871

ADVANCES IN SPACE RESEARCH (a COSPAR publication)

www.elsevier.com/locate/asr

CryoSat: A mission to determine the fluctuations in Earth's land and marine ice fields ☆

D.J. Wingham [a,*], C.R. Francis [b], S. Baker [a], C. Bouzinac [b], D. Brockley [a], R. Cullen [a], P. de Chateau-Thierry [c], S.W. Laxon [a], U. Mallow [d], C. Mavrocordatos [b], L. Phalippou [c], G. Ratier [b], L. Rey [c], F. Rostan [d], P. Viau [b], D.W. Wallis [a]

[a] *Centre for Polar Observation and Modelling, University College, London, Pearson Building, Gower Street, London WC1E 6BT, United Kingdom*
[b] *ESTEC, European Space Agency, 2200 Noordwijk, The Netherlands*
[c] *Alcatel Space, 31037 Toulouse-Cedex 1, France*
[d] *EADS Astrium GmbH, 88039 Friedrichshafen, Germany*

Received 19 October 2004; received in revised form 5 July 2005; accepted 6 July 2005

Abstract

This paper describes the CryoSat satellite mission, due for launch in 2005, whose aim is to accurately determine the trends in Earth's continental and marine ice fields. The paper's purpose is to provide scientific users of the CryoSat data with a description of the design and operation of the SIRAL radar and the CryoSat platform, the data products, and the expected error budget. The 'low-resolution mode' (LRM), 'synthetic aperture mode' (SARM) and "synthetic aperture interferometric mode' (SARInM) of the SIRAL radar are described, together with its system parameters, its antenna gain pattern and interferometer phase difference pattern, and its calibration modes. The orbit is described, together with the platform attitude and altitude control law and control systems, and the expected pointing and altitude knowledge. The geographical masks that are used to determine acquisitions in the three SIRAL modes are described. The SIRAL data products, and the processing applied to produce them, are described. *Level 1b*, *level 2* and *higher-level* products are described in turn, with a particular emphasis on the new procedures applied to the SARInM and SARM processing over ice surfaces. The beam forming and multi-looking is summarised, and a description is given of the behaviour of the SARM and SARInM echoes over idealised surfaces. These inform descriptions of the elevation retrievals of the *level 2* processing, including the SARInM retrieval of interferometric phase. The combination of these data, through cross-over analysis over continental ice sheets, and through averaging over sea-ice, to determine areal averages of ice sheet elevation change or sea-ice thickness, is described. The error budget in these higher-level products is described, together with its breakdown into errors arising from the instrument and errors arising from the retrievals. The importance of the co-variance of these errors in determining the final error is stressed. The description of the errors also includes a summary of the experiments required following the launch to validate the CryoSat mission data. An estimate of the mission performance over ice surfaces is made at various spatial scales, and it is concluded that even the relatively short, three-year duration of the CryoSat mission will allow it to make an important scientific contribution, particularly when combined with results from earlier satellite missions.

© 2005 COSPAR. Published by Elsevier Ltd. All rights reserved.

DELAY-DOPPLER ALGORITHM PAPER
by K. Raney + CryoSat Team Heritage

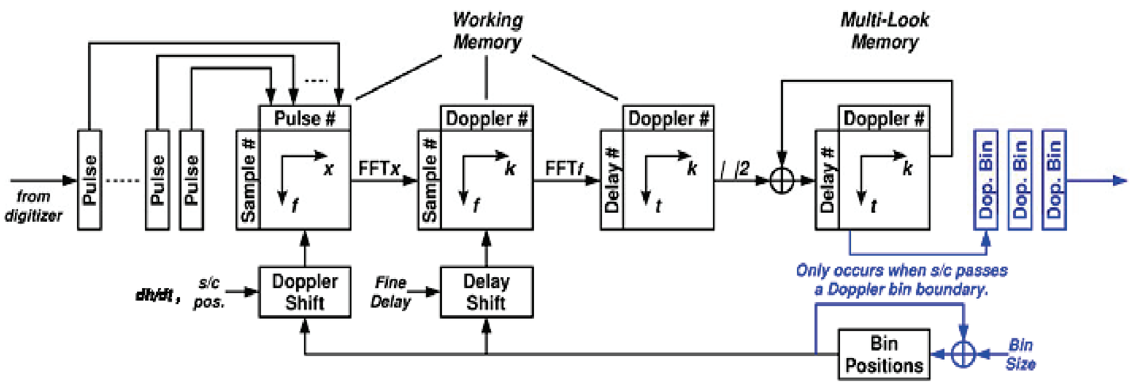

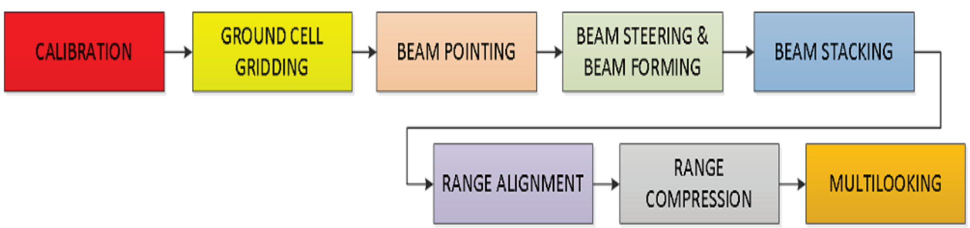

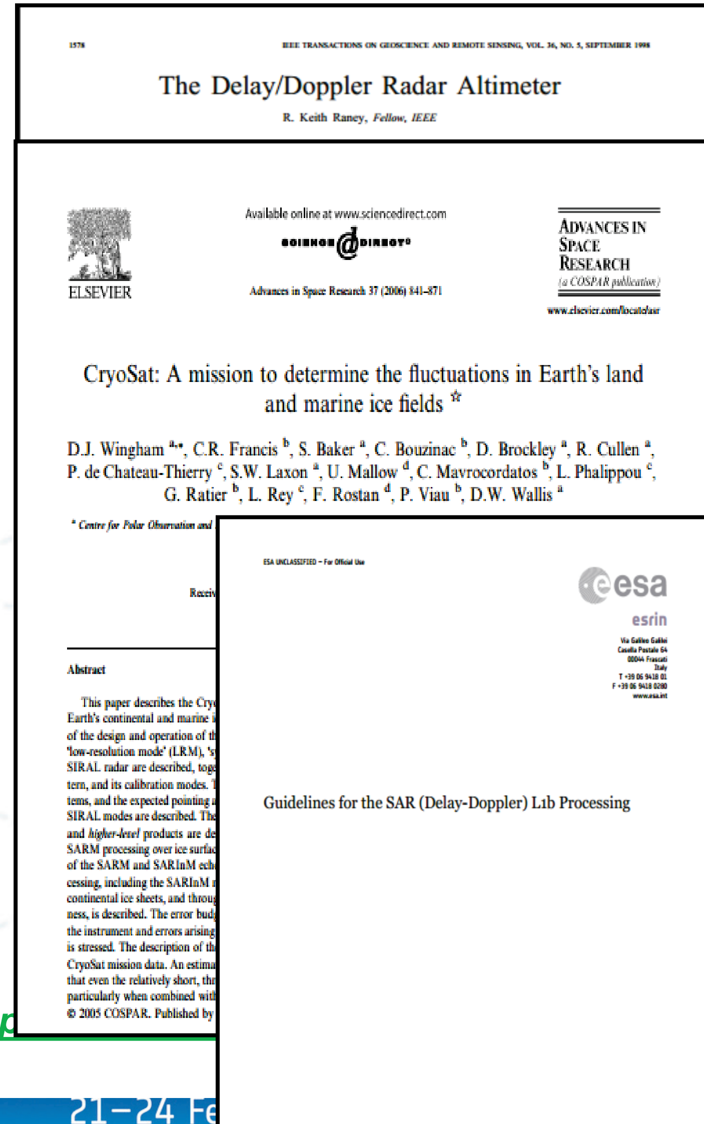

1578 IEEE TRANSACTIONS ON GEOSCIENCE AND REMOTE SENSING, VOL. 36, NO. 5, SEPTEMBER 1998

The Delay/Doppler Radar Altimeter

R. Keith Raney, *Fellow, IEEE*

ELSEVIER

Available online at www.sciencedirect.com

SCIENCE @ DIRECT®

Advances in Space Research 37 (2006) 841–871

ADVANCES IN SPACE RESEARCH (a COSPAR publication)

www.elsevier.com/locate/asr

CryoSat: A mission to determine the fluctuations in Earth's land and marine ice fields ☆

D.J. Wingham [a,*], C.R. Francis [b], S. Baker [a], C. Bouzinac [b], D. Brockley [a], R. Cullen [a], P. de Chateau-Thierry [c], S.W. Laxon [a], U. Mallow [d], C. Mavrocordatos [b], L. Phalippou [c], G. Ratier [b], L. Rey [c], F. Rostan [d], P. Viau [b], D.W. Wallis [a]

ESA UNCLASSIFIED – For Official Use

esa esrin

Guidelines for the SAR (Delay-Doppler) L1b Processing

ESA\Esrin GUIDELINES (<u>Didactic Material</u>) available here:

http://wiki.services.eoportal.org/tiki-download_wiki_attachment.php

CALIBRATION In Power and Time

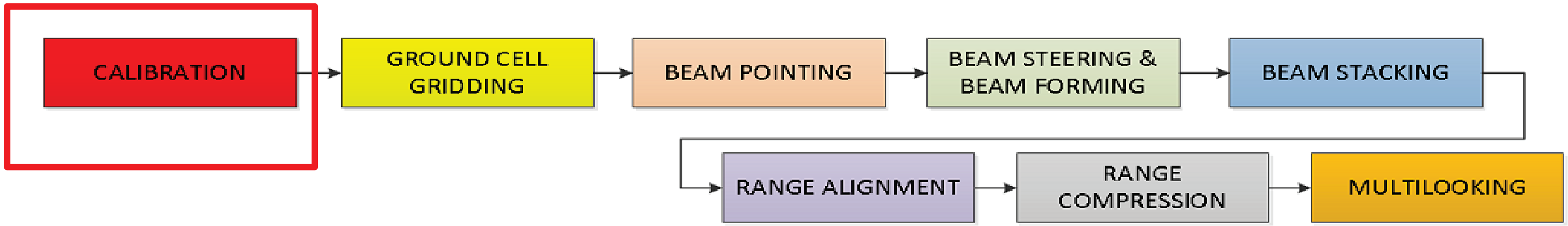

The SAR FBR waveforms need to be **calibrated**

The following internal calibration corrections are applied to SAR data:

CALIBRATION In Power and Time

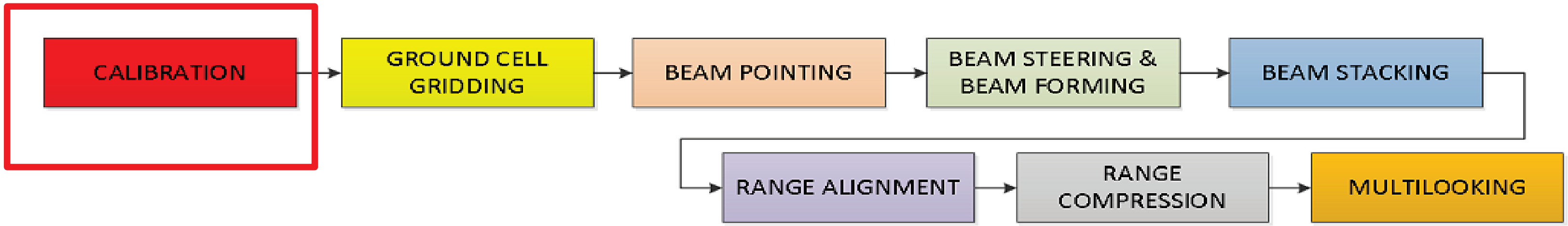

The SAR FBR waveforms need to be **calibrated**

The following internal calibration corrections are applied to SAR data:

1) **Internal Path Delay Calibration**: to calibrate the range drift of the RIR (or Range Point Target Response, PTR) due to instrument aging

CALIBRATION In Power and Time

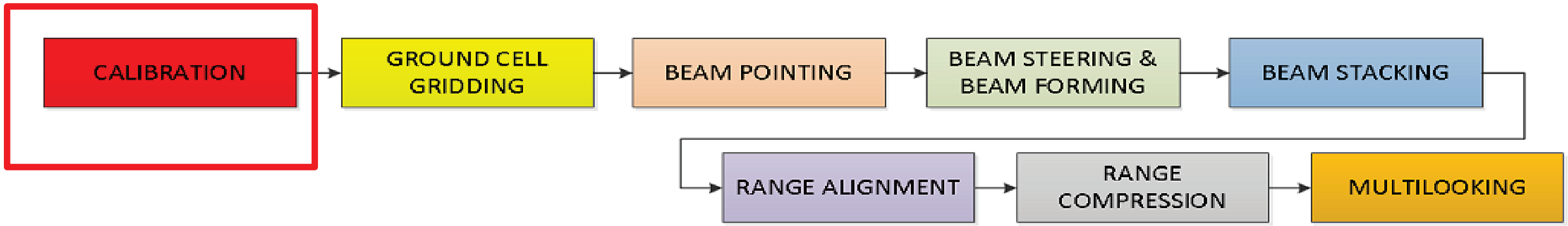

The SAR FBR waveforms need to be **calibrated**

The following internal calibration corrections are applied to SAR data:

1) **Internal Path Delay Calibration**: to calibrate the range drift of the RIR (or Range Point Target Response, PTR) due to instrument aging
2) **Internal Power Drift Calibration**: to calibrate the power level drift of the rage PTR due to instrument aging

CALIBRATION In Power and Time

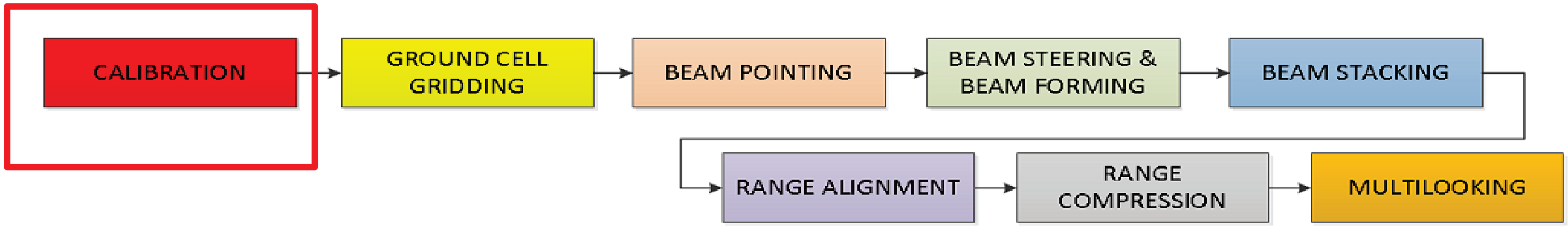

The SAR FBR waveforms need to be **calibrated**

The following internal calibration corrections are applied to SAR data:

1) **Internal Path Delay Calibration**: to calibrate the range drift of the RIR (or Range Point Target Response, PTR) due to instrument aging
2) **Internal Power Drift Calibration**: to calibrate the power level drift of the rage PTR due to instrument aging
3) **Receiver Transfer Function Mask Calibration**: to calibrate the received waveform's shape for the LPF Mask

CALIBRATION In Power and Time

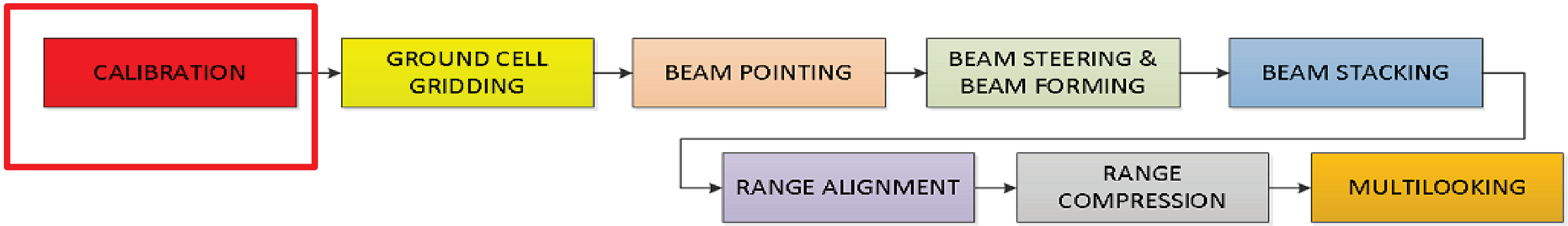

The SAR FBR waveforms need to be **calibrated**

The following internal calibration corrections are applied to SAR data:

1) **Internal Path Delay Calibration**: to calibrate the range drift of the RIR (or Range Point Target Response, PTR) due to instrument aging

2) **Internal Power Drift Calibration**: to calibrate the power level drift of the rage PTR due to instrument aging

3) **Receiver Transfer Function Mask Calibration**: to calibrate the received waveform's shape for the LPF Mask

4) **SAR Intra-Burst Phase and Amplitude Differences Calibration**: to calibrate variation in phase and amplitude between the pulses within each burst

CALIBRATION In Power and Time

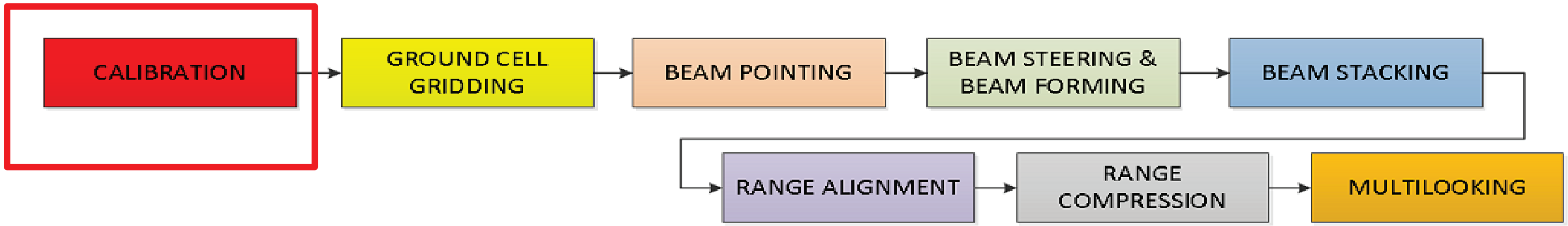

The SAR FBR waveforms need to be **calibrated**

The following internal calibration corrections are applied to SAR data:

1) **Internal Path Delay Calibration**: to calibrate the range drift of the RIR (or Range Point Target Response, PTR) due to instrument aging
2) **Internal Power Drift Calibration**: to calibrate the power level drift of the rage PTR due to instrument aging
3) **Receiver Transfer Function Mask Calibration**: to calibrate the received waveform’s shape for the LPF Mask
4) **SAR Intra-Burst Phase and Amplitude Differences Calibration**: to calibrate variation in phase and amplitude between the pulses within each burst

In addition to internal calibration, the power level is compensated for:

1) **AGC values** (dynamic correction, updated every 20 Hz).
2) Fixed Receiver Chain Gains, as characterized prior to launch

CALIBRATION In Power and Time

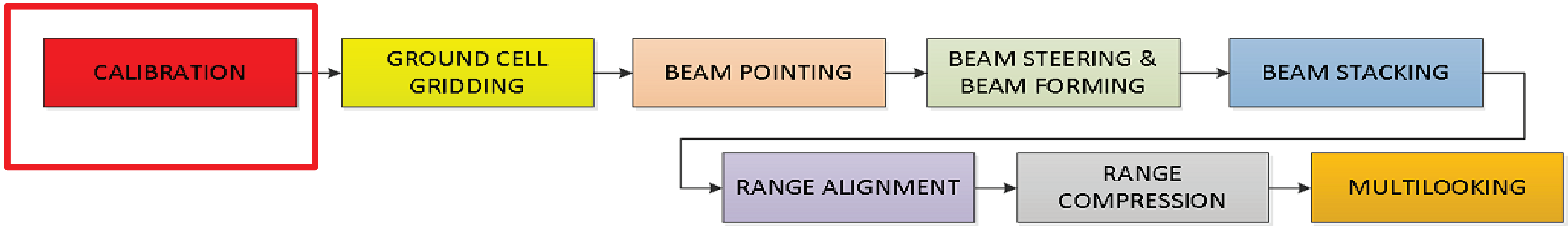

Echogram: Image of Pass’s Multilooked Echoes stacked in sequence

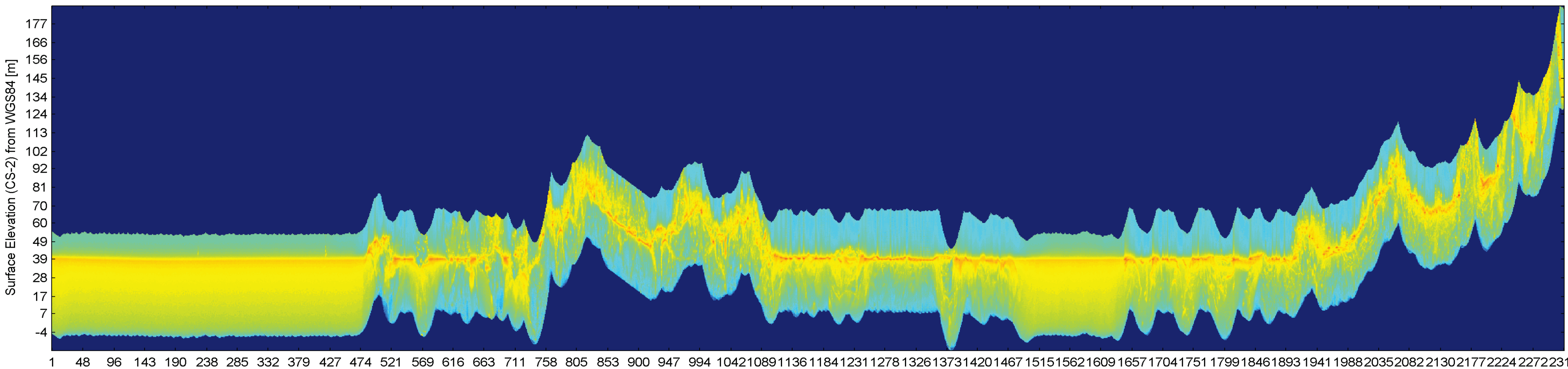

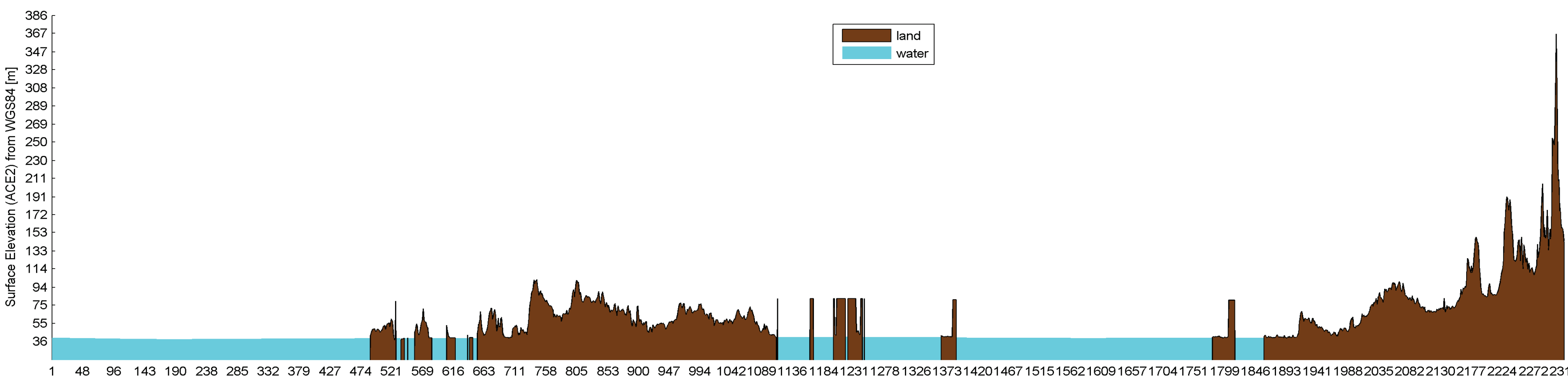

CALIBRATION In Power and Time

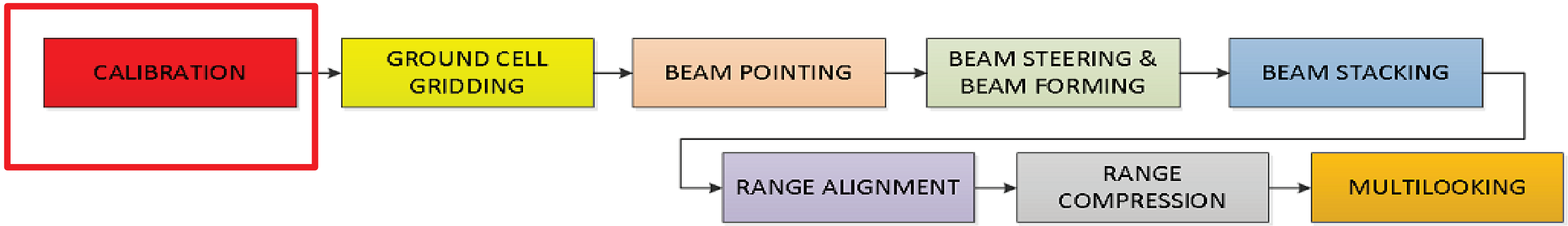

Echogram: Image of Pass's Multilooked Echoes stacked in sequence

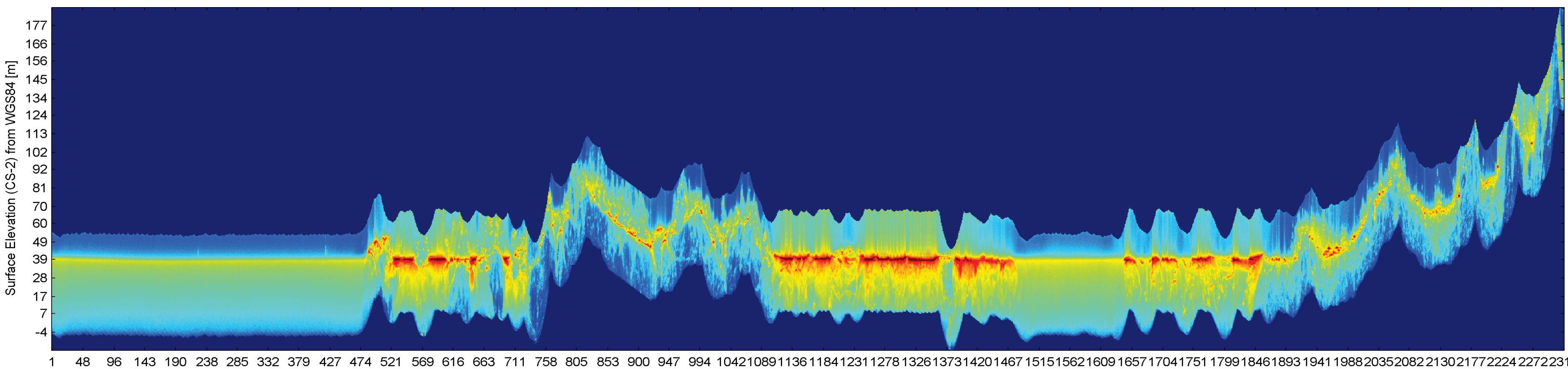

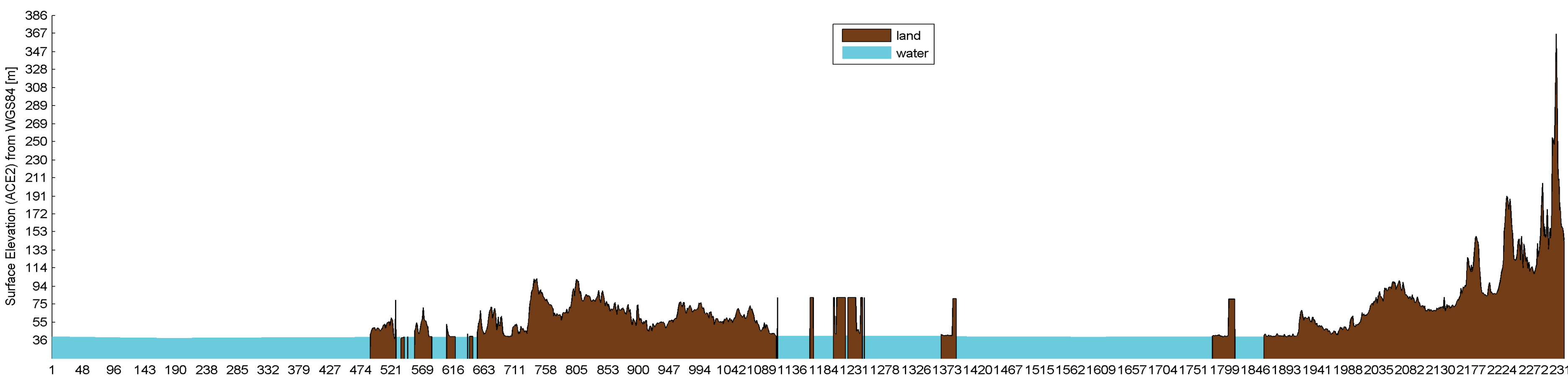

CALIBRATION In Power and Time

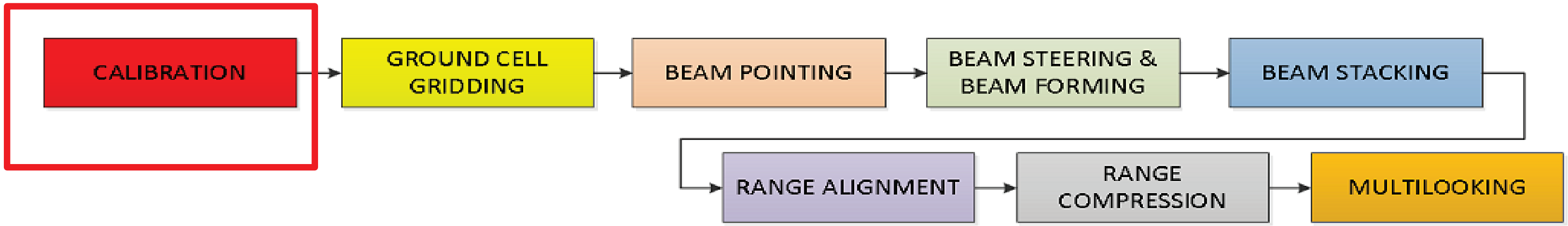

More details about how to compute and apply the gain calibration correction (CryoSat-2 mission)in the TN on the right

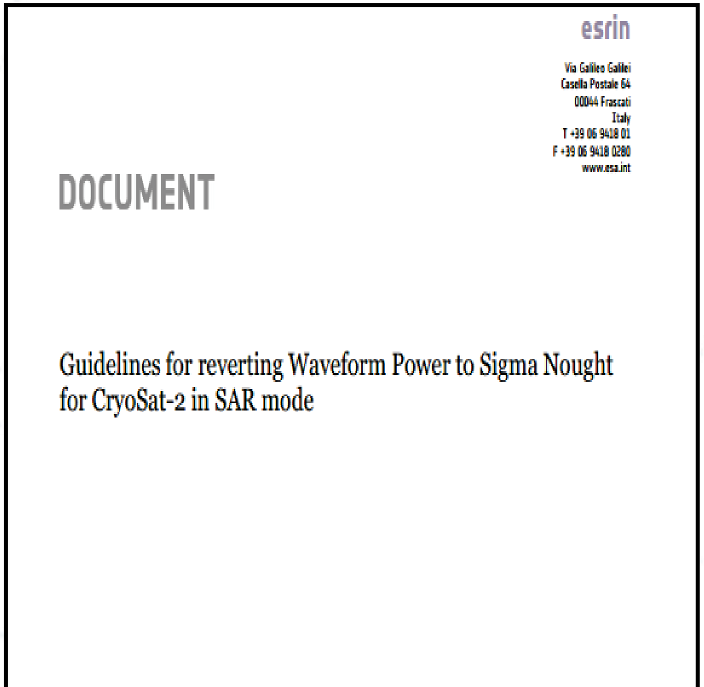
esrin

Via Galileo Galilei
Casella Postale 64
00044 Frascati
Italy
T +39 06 9418 01
F +39 06 9418 0280
www.esa.int

DOCUMENT

Guidelines for reverting Waveform Power to Sigma Nought for CryoSat-2 in SAR mode

ESA GUIDELINES For Power Calibration (Didactic Material) Available here:
https://wiki.services.eoportal.org/tiki-download_wiki_attachment.php?attId=2927

GROUND CELL GRIDDING

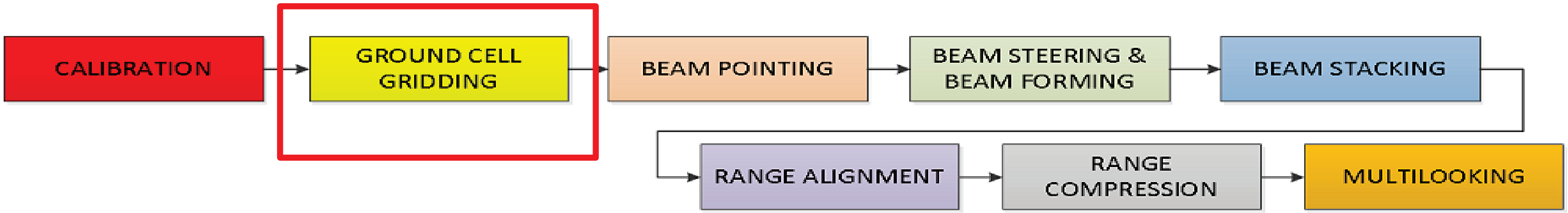

The purpose of this stage is to place along the over-flown surface elevation profile a set of surface locations wherein the synthetized Doppler Beams will be afterwards focused, steered and multilooked

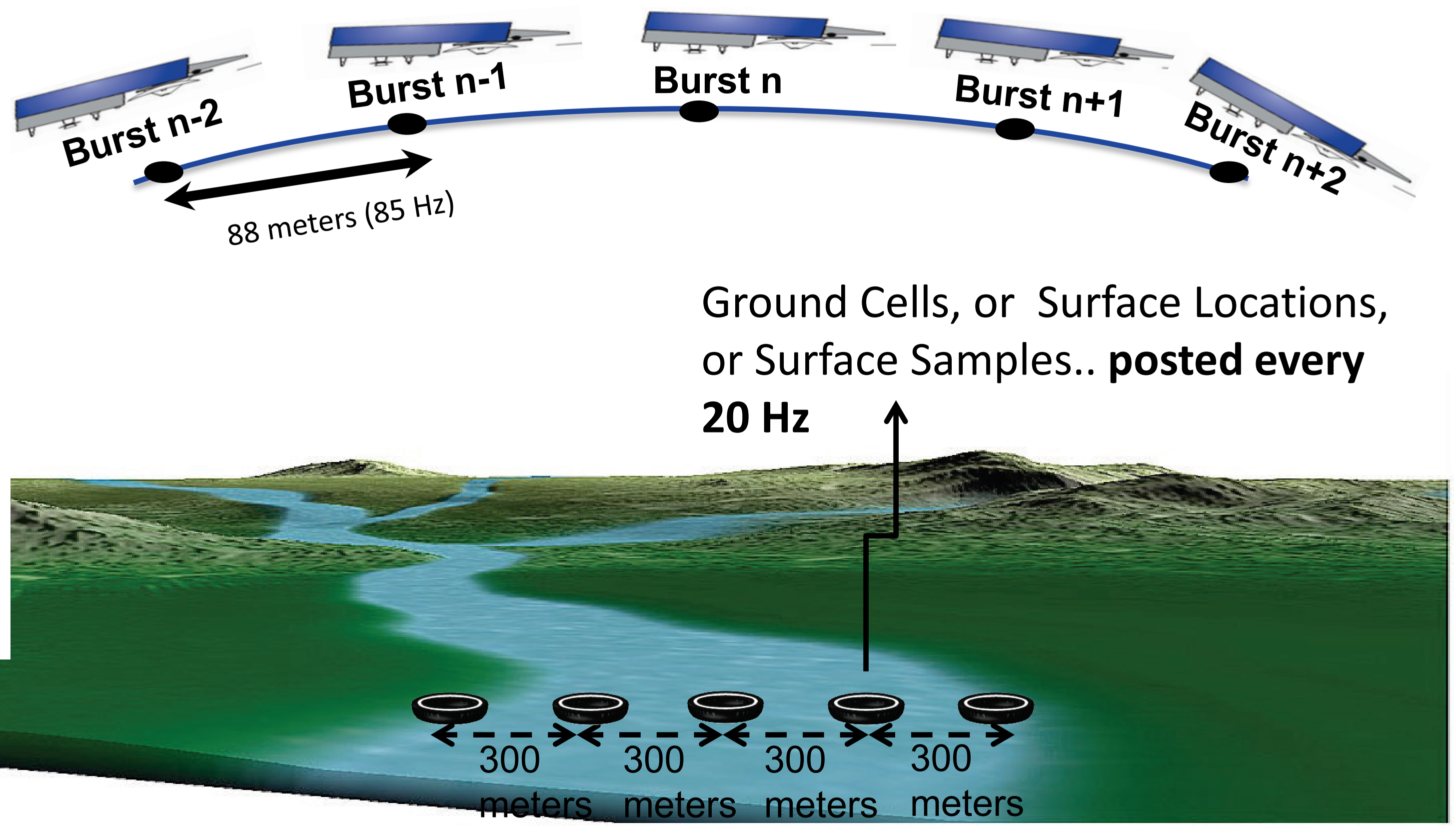

GROUND CELL GRIDDING

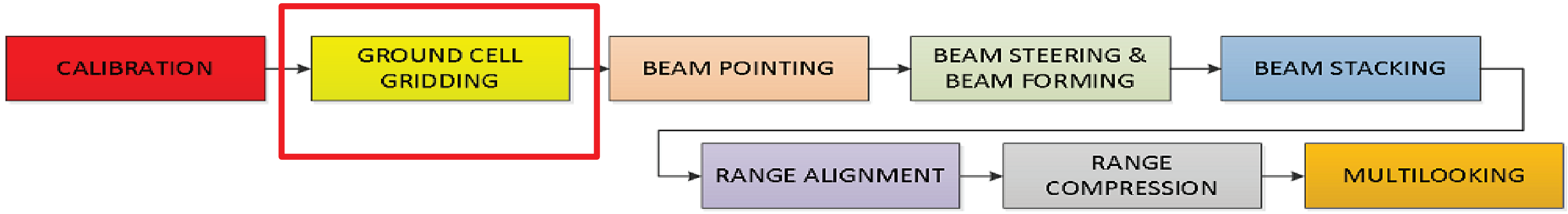

To place the ground cell on Earth's surface, is used a first-approximation elevation profile derived from the on-board calculated tracker range.

Important to remark that the posting rates of the FBR (85 Hz) and Level 1b data (20 Hz) are **independent** of each other

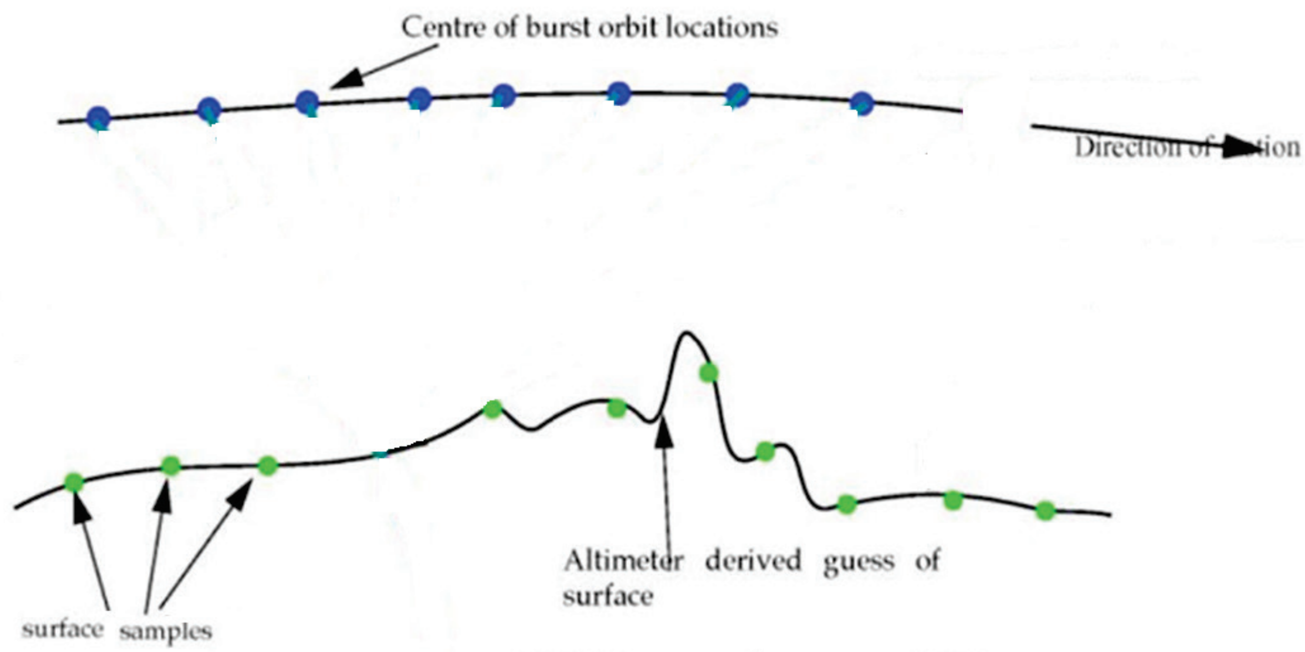

BEAM POINTING

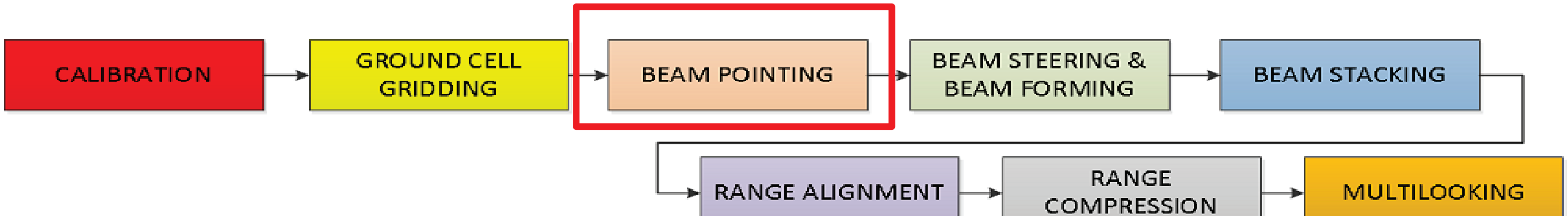

Given the set of surface sample locations, the purpose of this stage is to calculate for each burst center the scene geometry: range between the burst center and each ground cell, angles that vectors joining burst-ground cell form with velocity vectors, etc

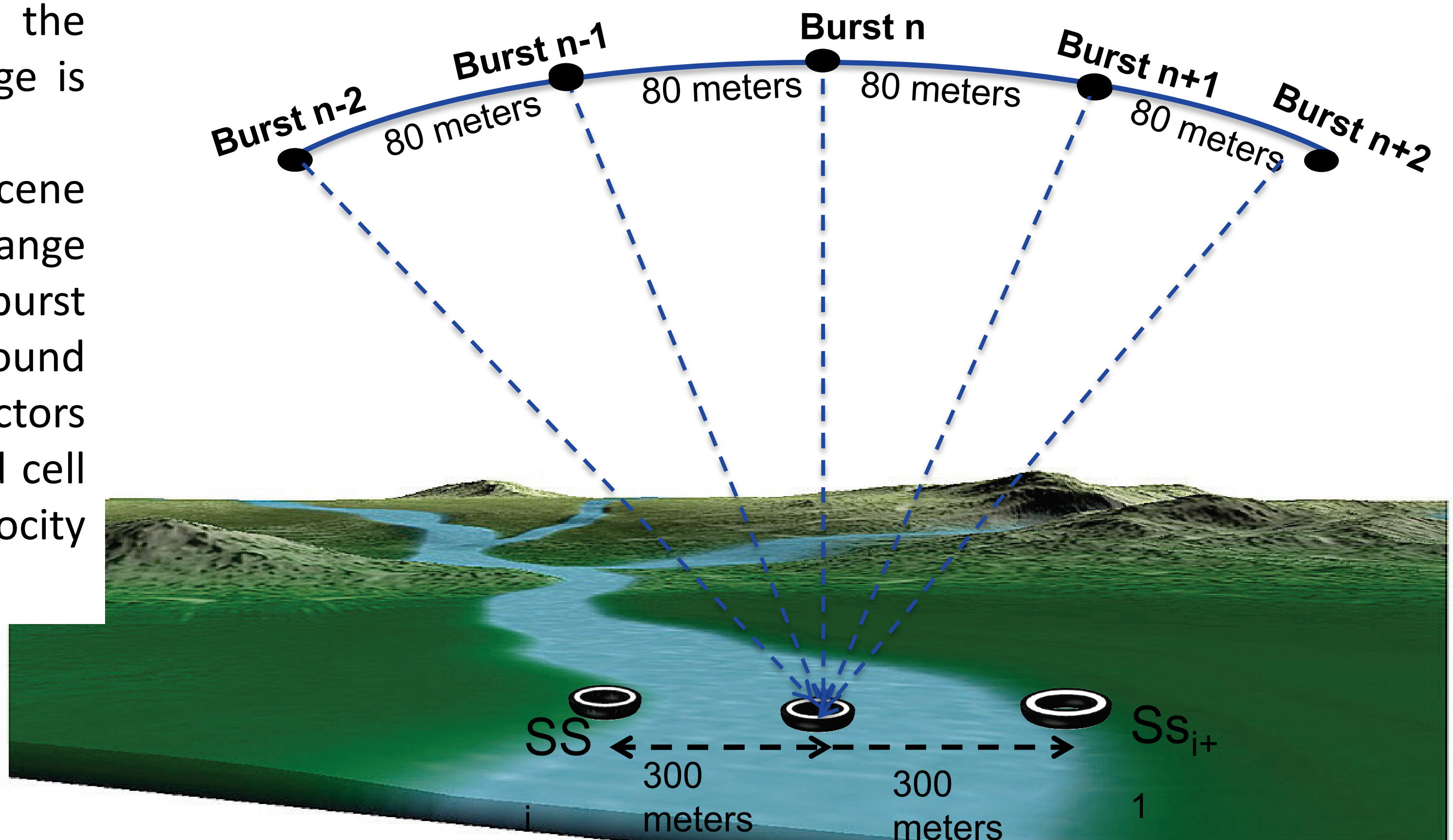

BEAM STEERING & BEAM FORMING

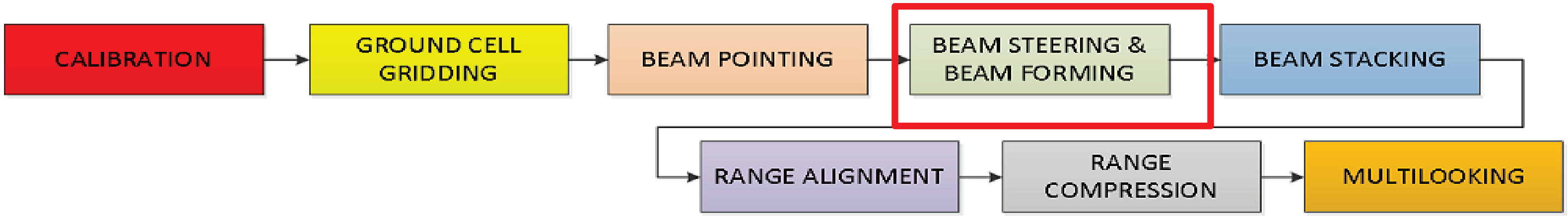

The purpose of this Beam Forming is to synthetize a set of 64 Doppler Beams per burst, exploiting the Doppler effect due to the satellite motion with respect the ground.

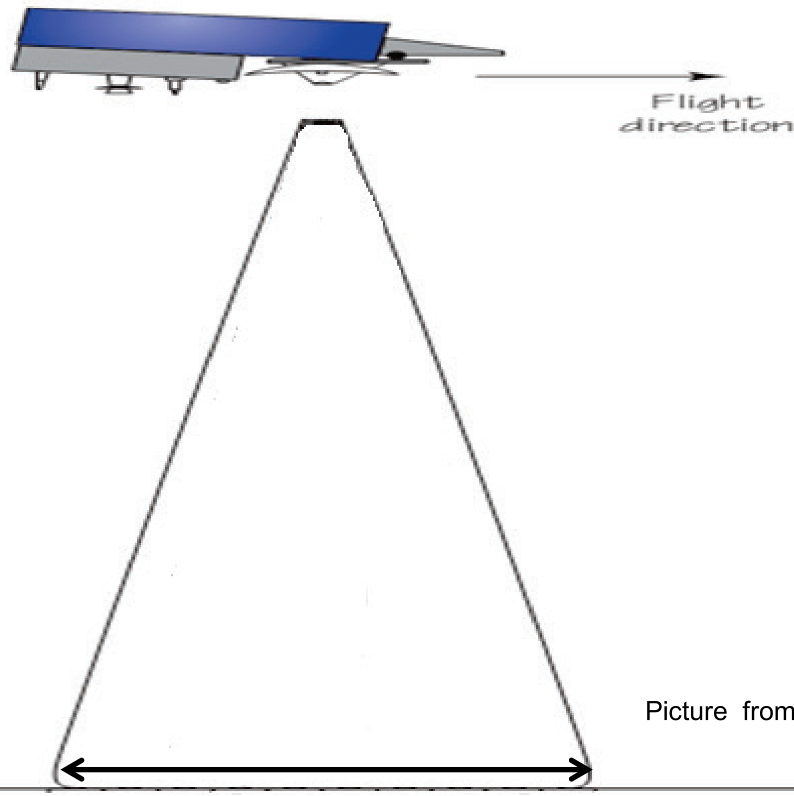

Picture from CryoSat Mission Document

CryoSat-2 Antenna Pattern Footprint: ~ 18 km

BEAM STEERING & BEAM FORMING

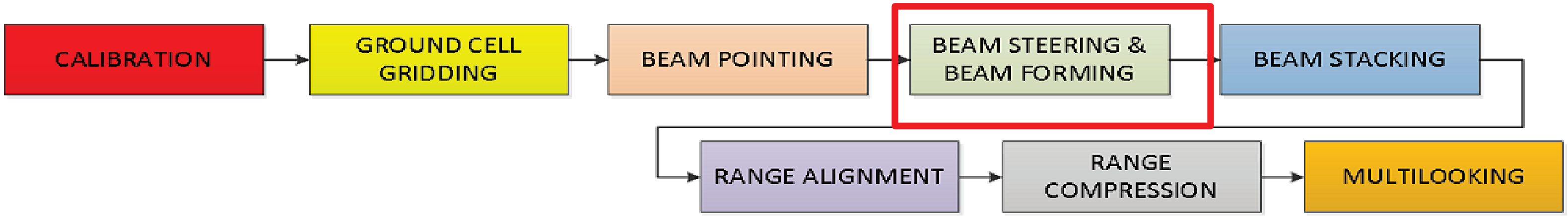

The purpose of this Beam Forming is to synthetize a set of 64 Doppler Beams per burst, exploiting the Doppler effect due to the satellite motion with respect the ground.

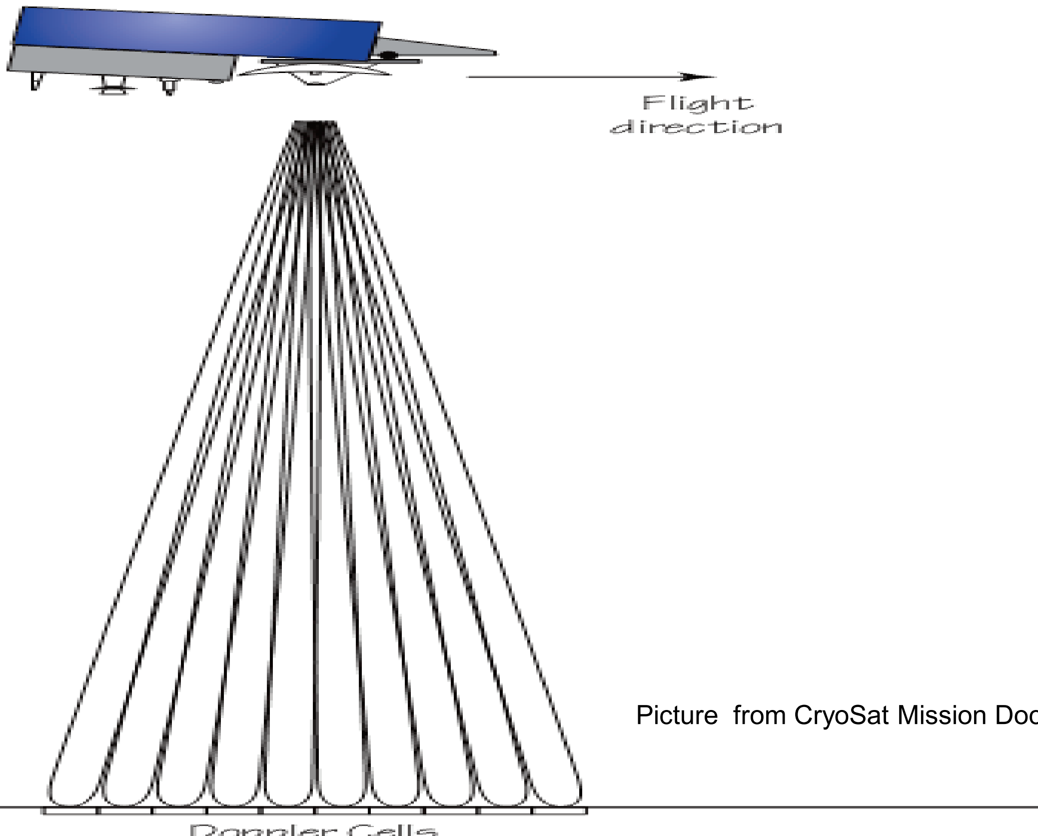

Picture from CryoSat Mission Document

BEAM STEERING & BEAM FORMING

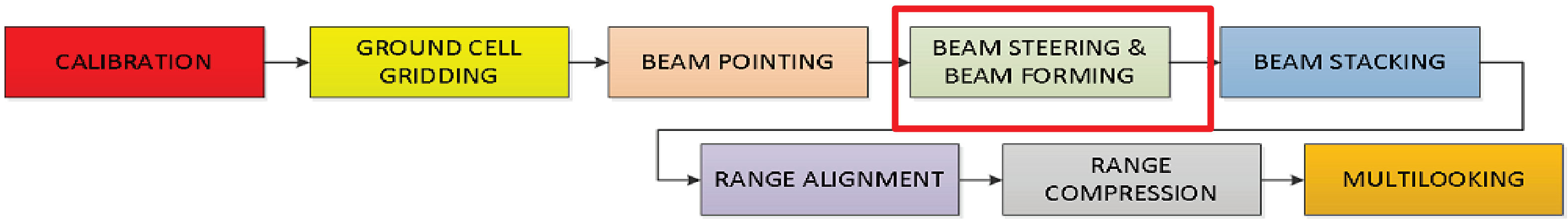

The purpose of this Beam Forming is to synthetize a set of 64 Doppler Beams per burst, exploiting the Doppler effect due to the satellite motion with respect the ground.

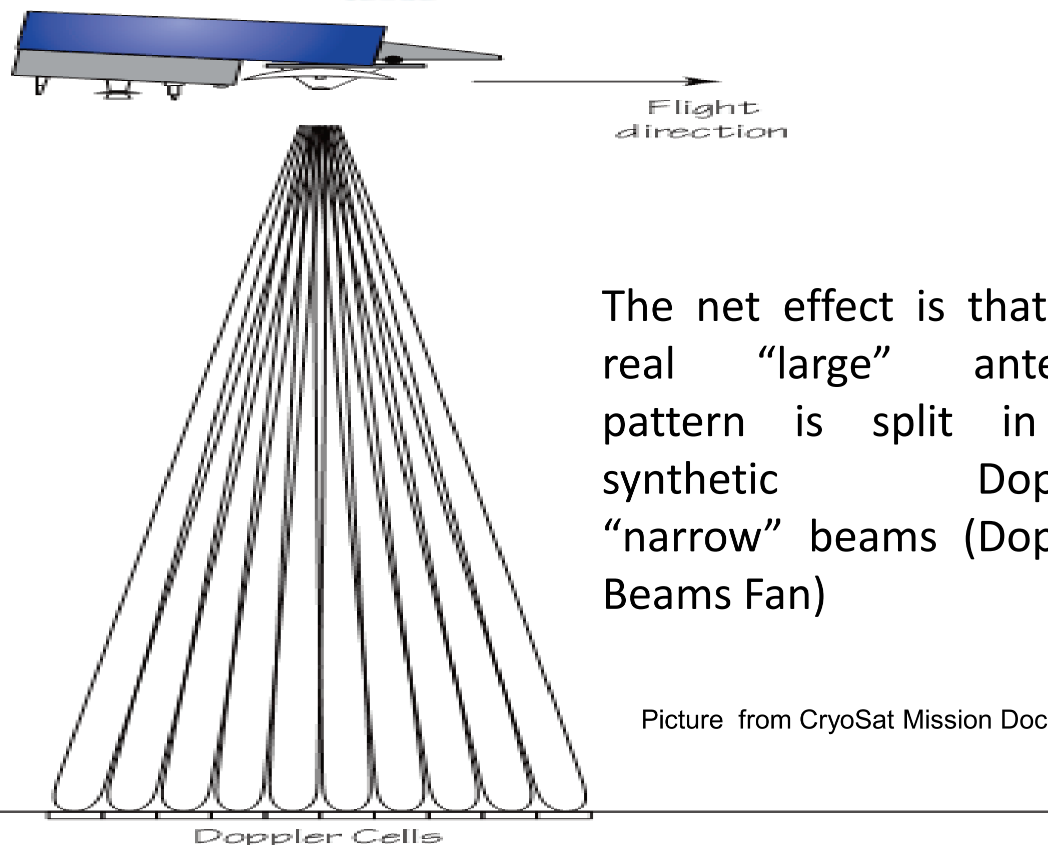

The net effect is that the real "large" antenna pattern is split in 64 synthetic Doppler "narrow" beams (Doppler Beams Fan)

Picture from CryoSat Mission Document

BEAM STEERING & BEAM FORMING

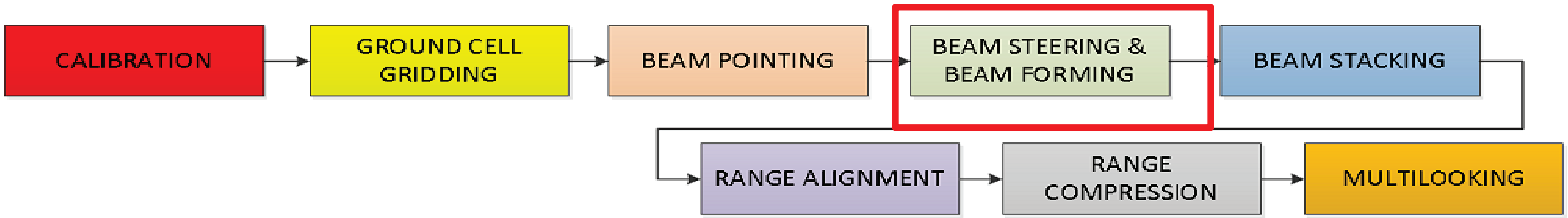

The purpose of this Beam Forming is to synthetize a set of 64 Doppler Beams per burst, exploiting the Doppler effect due to the satellite motion with respect the ground.

Each Doppler Cell has a size of around 300 metes

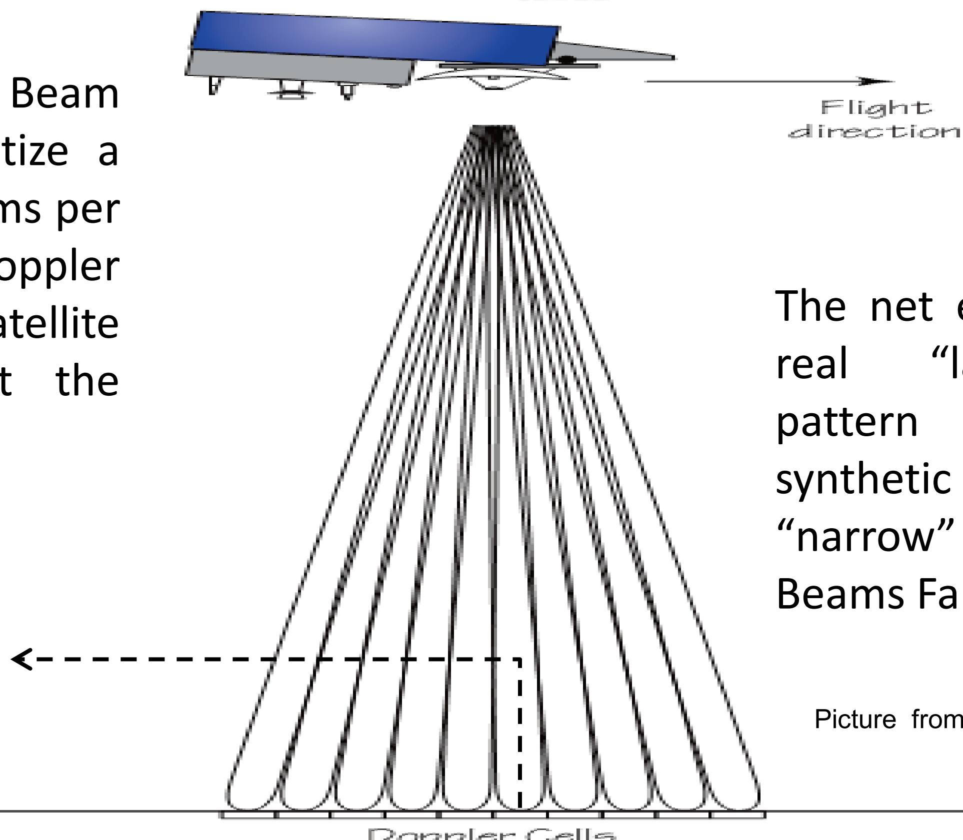

The net effect is that the real "large" antenna pattern is split in 64 synthetic Doppler "narrow" beams (Doppler Beams Fan)

Picture from CryoSat Mission Document

BEAM STEERING & BEAM FORMING

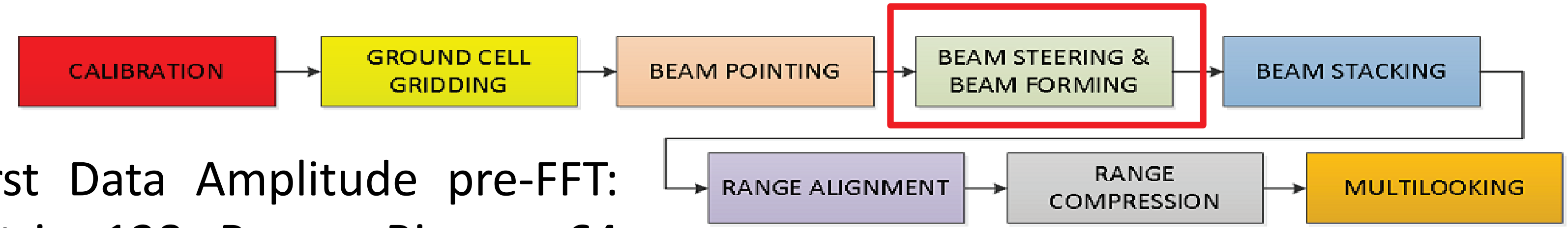

Burst Data Amplitude pre-FFT: Matrix 128 Range Bins x 64 Doppler Bins

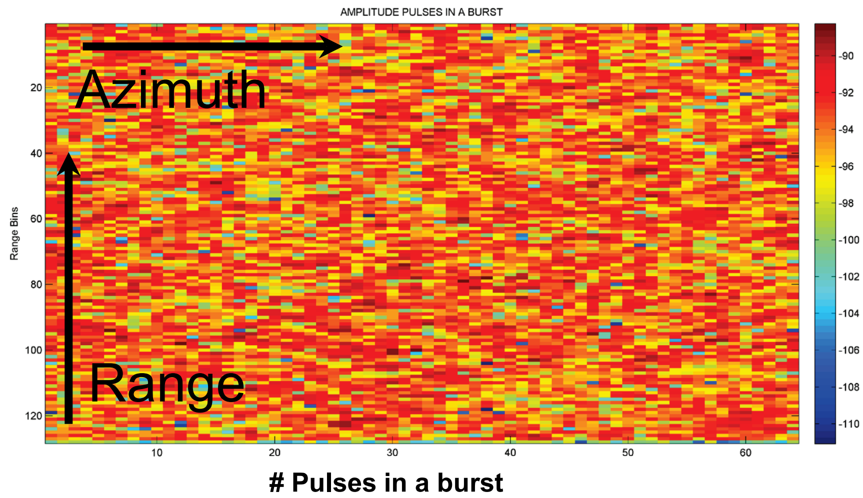

BEAM STEERING & BEAM FORMING

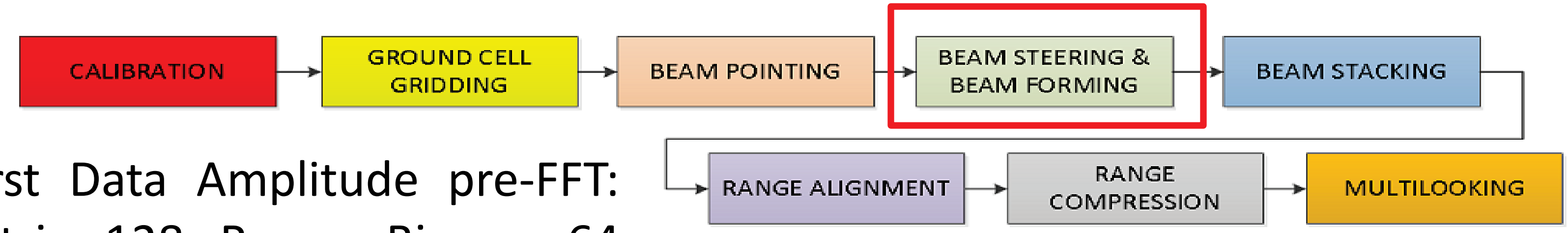

Burst Data Amplitude pre-FFT: Matrix 128 Range Bins x 64 Doppler Bins

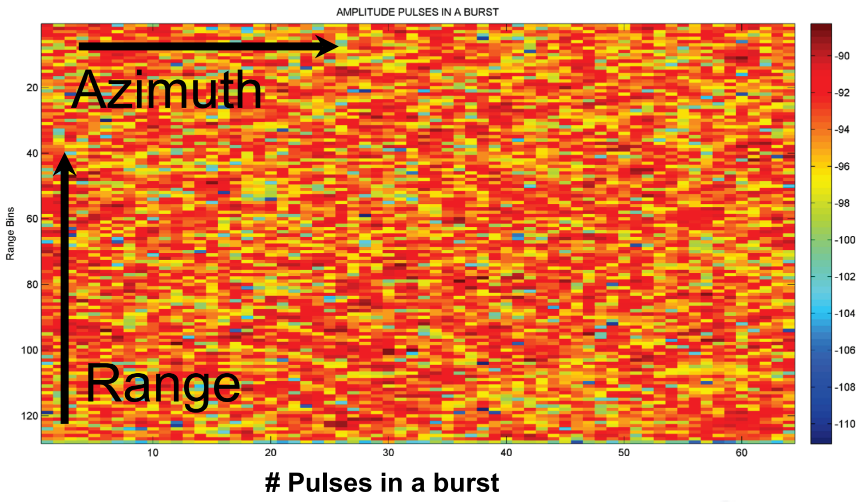

Beam Forming: simply a Fast Fourier Transform of the complex burst data in azimuth (along track) direction

BEAM STEERING & BEAM FORMING

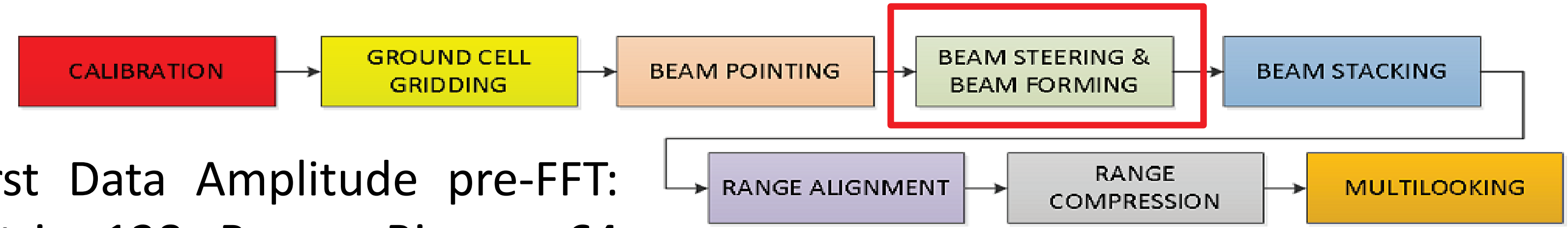

Burst Data Amplitude pre-FFT: Matrix 128 Range Bins x 64 Doppler Bins

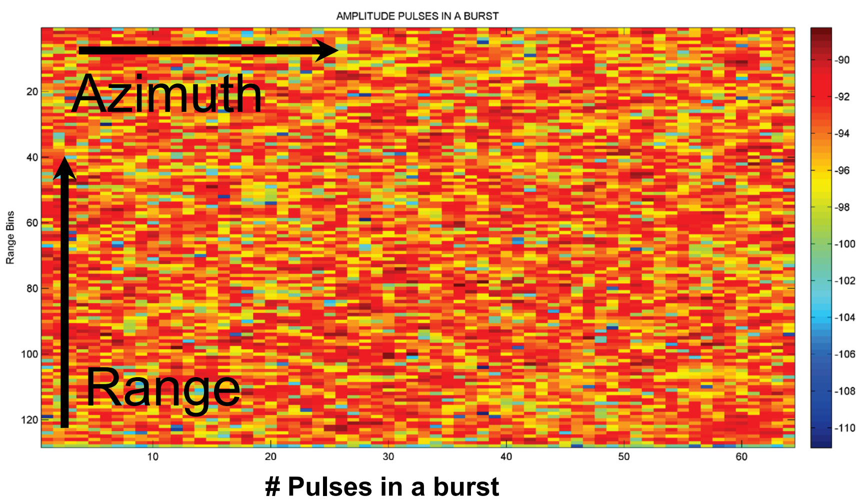

Beam Forming: simply a Fast Fourier Transform of the complex burst data in azimuth (along track) direction

Burst Data Amplitude post-FFTs (Range-azimuth): Matrix 128 Range Bins x 64 Doppler Bins: Delay-Doppler Spectrum

BEAM STEERING & BEAM FORMING

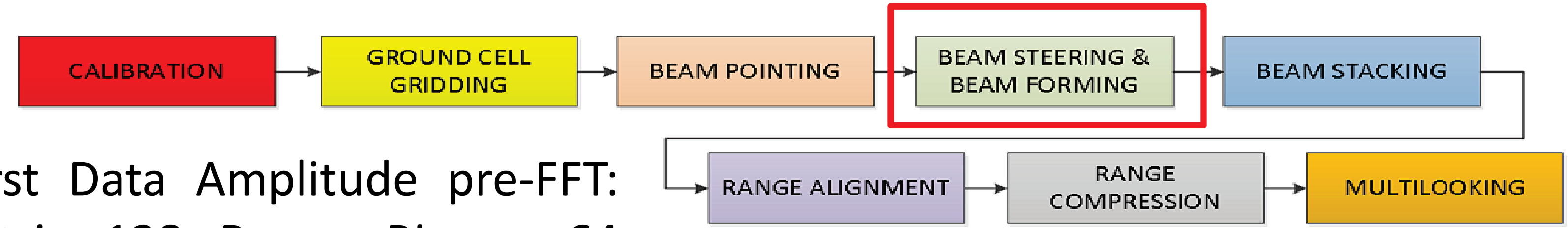

Burst Data Amplitude pre-FFT: Matrix 128 Range Bins x 64 Doppler Bins

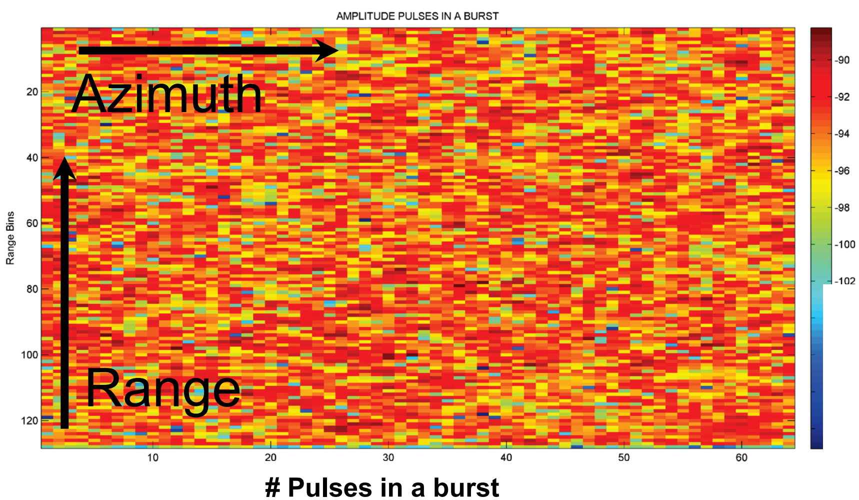

Beam Forming: simply a Fast Fourier Transform of the complex burst data in azimuth (along track) direction

Burst Data Amplitude post-FFTs (Range-azimuth): Matrix 128 Range Bins x 64 Doppler Bins: Delay-Doppler Spectrum

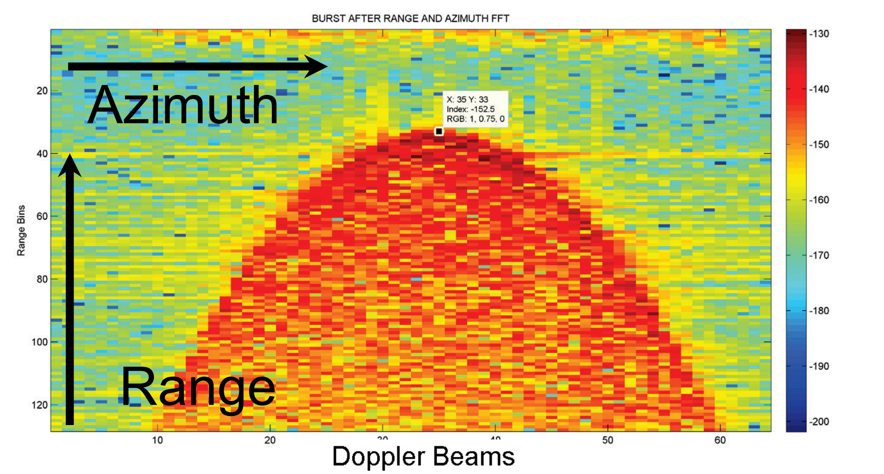

BEAM STEERING & BEAM FORMING: Doppler Centroid

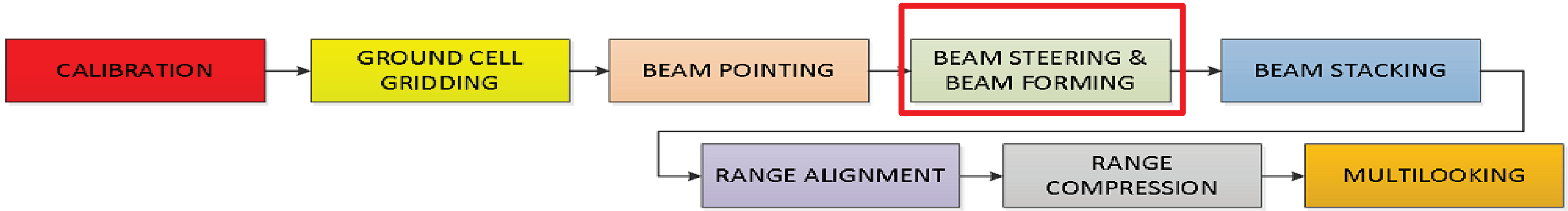

For an efficient SAR L1b Processing, It's mandatory a very precise compensation for Doppler Centroid: we rotate the Doppler Beam Fan by Doppler centroid angle (function of radial velocity) to steer it at nadir direction

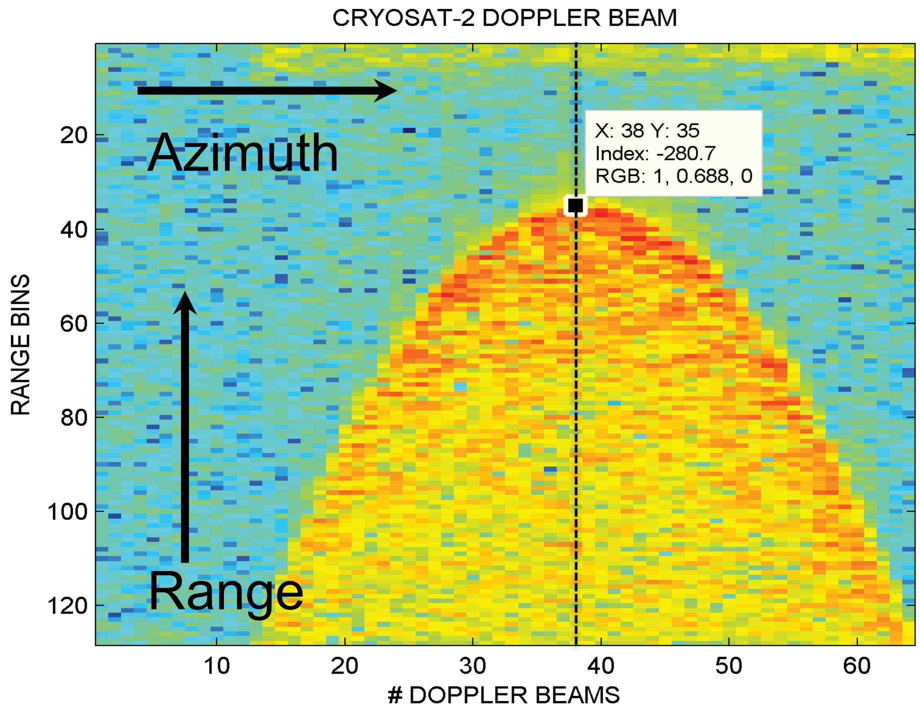

BEAM STEERING & BEAM FORMING: *Doppler Centroid*

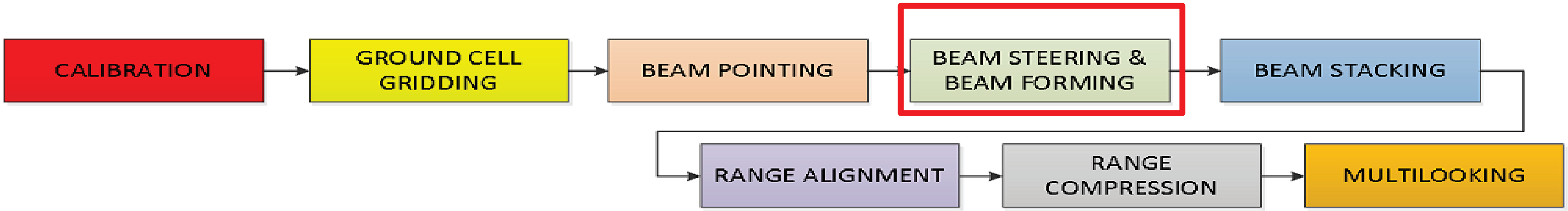

For an efficient SAR L1b Processing, It's mandatory a very precise compensation for Doppler Centroid: we rotate the Doppler Beam Fan by Doppler centroid angle (function of radial velocity) to steer it at nadir direction

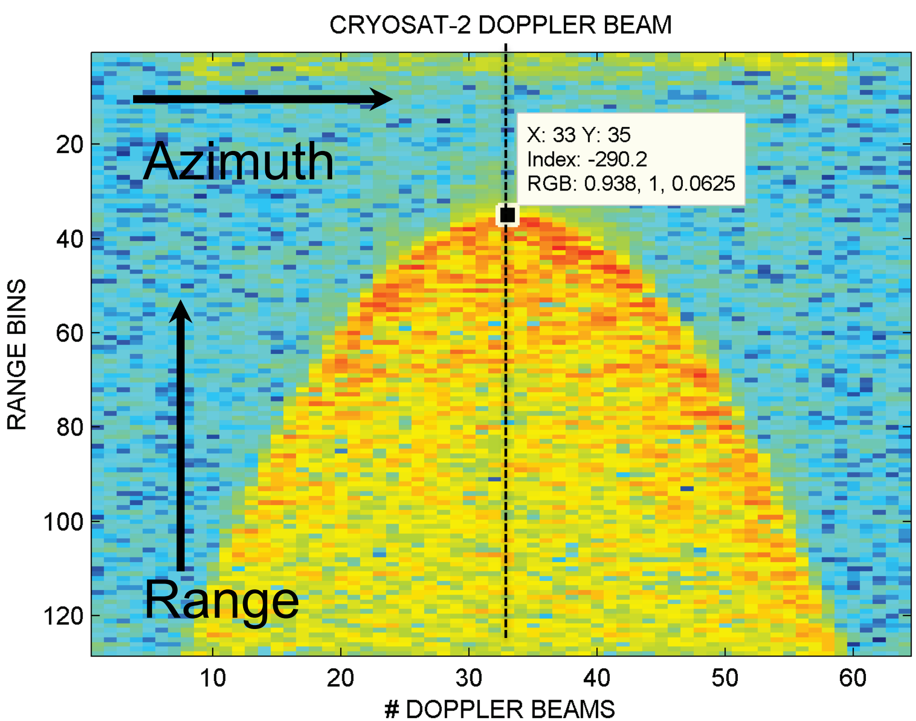

BEAM STEERING & BEAM FORMING: Doppler Centroid

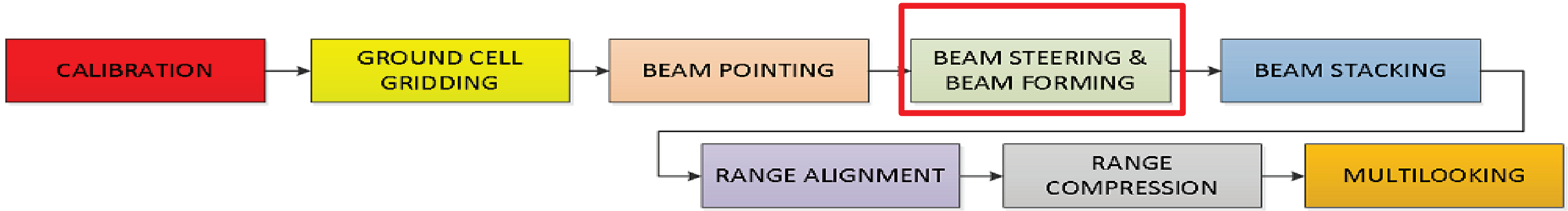

For an efficient SAR L1b Processing, It's mandatory a very precise compensation for Doppler Centroid: we rotate the Doppler Beam Fan by Doppler centroid angle (function of radial velocity) to steer it at nadir direction

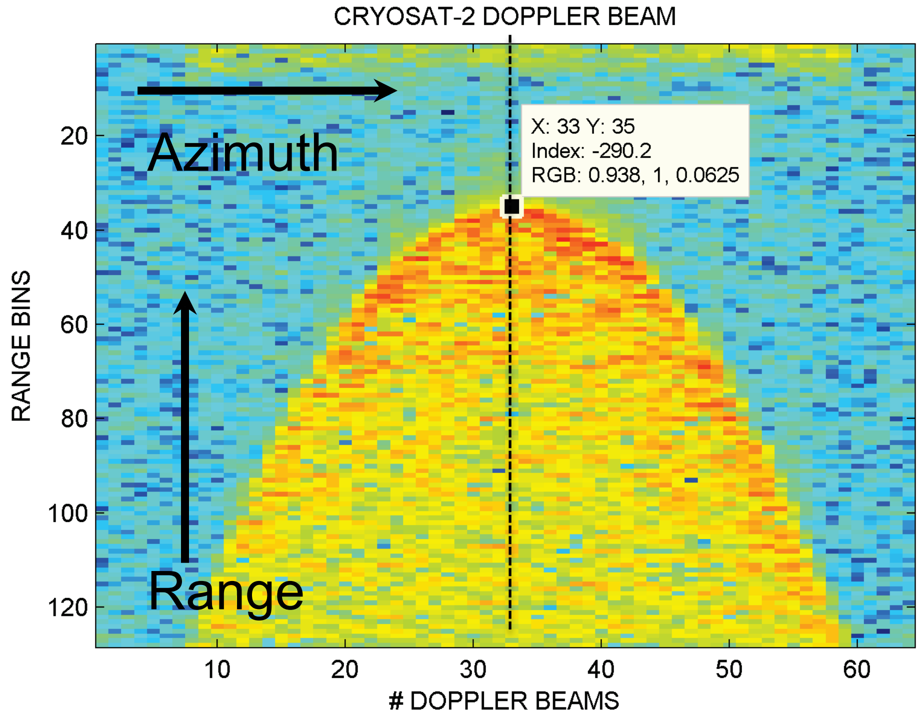

This is carried out by a pre azimuth-FFT multiplication of the burst matrix with a phasor (shift's theorem)

BEAM STEERING & BEAM FORMING: Doppler Beams co-located with ground cell

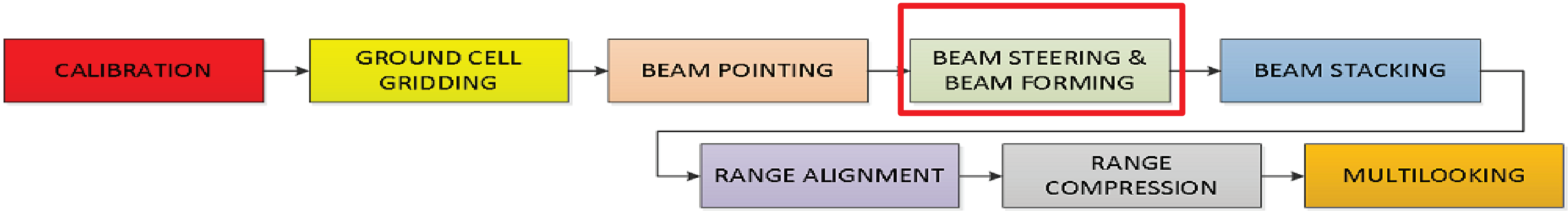

After the Doppler Centroid compensation, none of the Doppler beam will be perfectly centered to any of the 64 surface sample locations actually in view by the current burst. Hence, a further steering of the Doppler beams in order to make the 64 Doppler footprints perfectly co-located with the 64 surface sample locations is necessary.

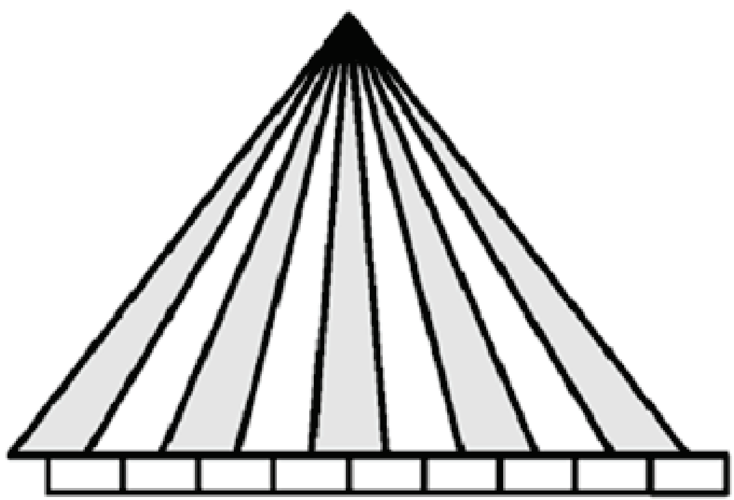

Pictures by Keith Raney

BEAM STEERING & BEAM FORMING: Doppler Beams co-located with ground cell

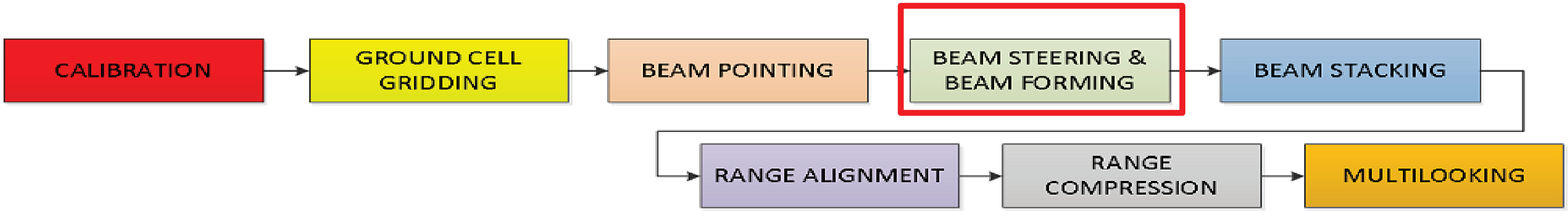

After the Doppler Centroid compensation, none of the Doppler beam will be perfectly centered to any of the 64 surface sample locations actually in view by the current burst. Hence, a further steering of the Doppler beams in order to make the 64 Doppler footprints perfectly co-located with the 64 surface sample locations is necessary.

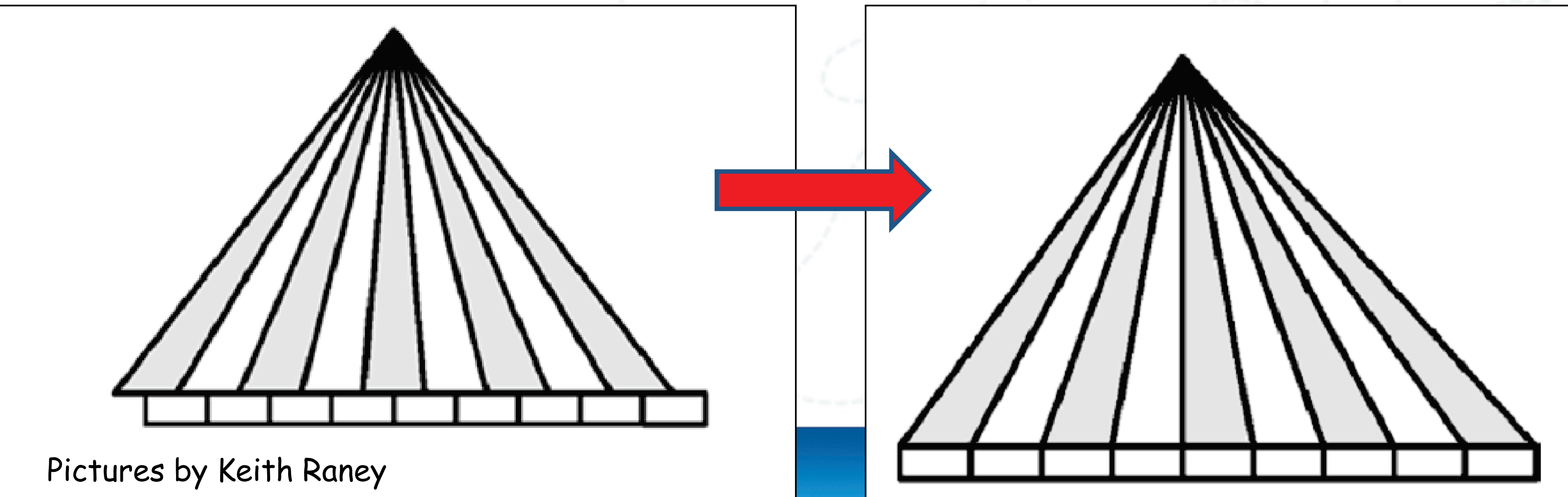

Pictures by Keith Raney

BEAM STEERING & BEAM FORMING:
Doppler Beams co-located with ground cell

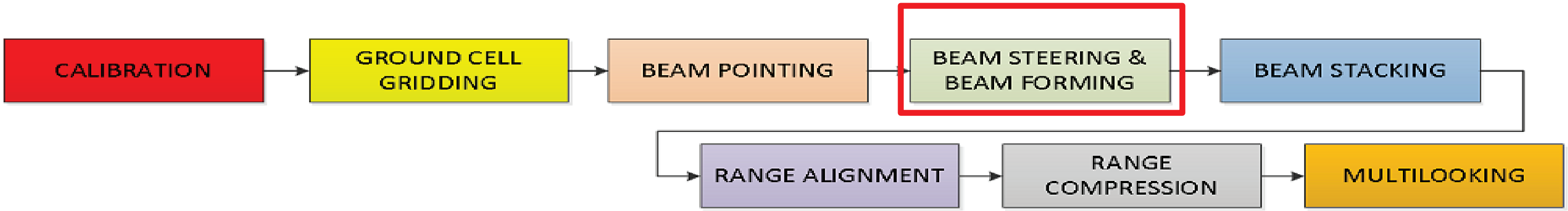

After the Doppler Centroid compensation, none of the Doppler beam will be perfectly centered to any of the 64 surface sample locations actually in view by the current burst. Hence, a further steering of the Doppler beams in order to make the 64 Doppler footprints perfectly co-located with the 64 surface sample locations is necessary.

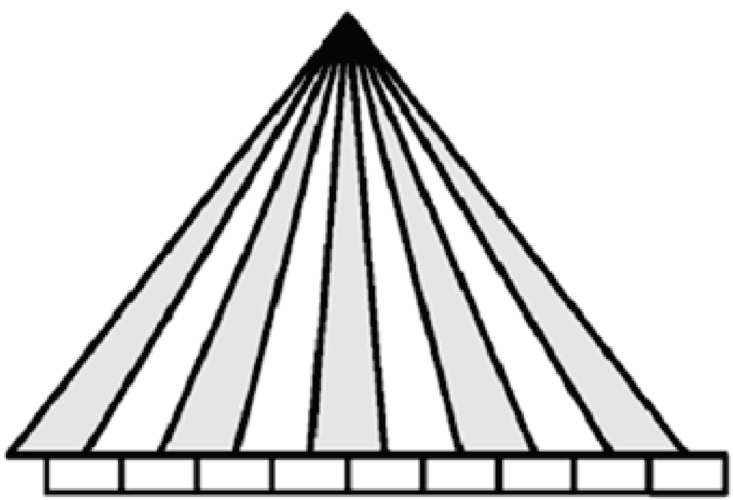

Pictures by Keith Raney

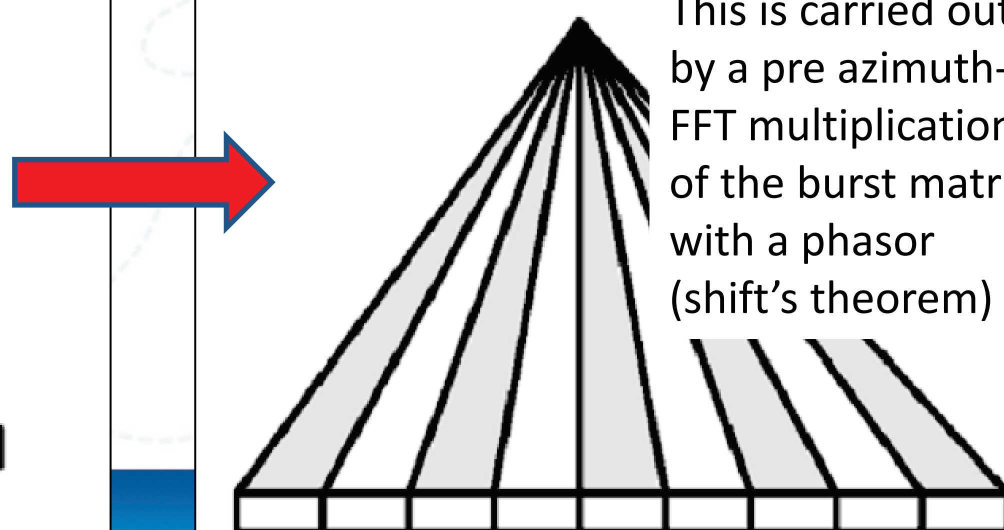

This is carried out by a pre azimuth-FFT multiplication of the burst matrix with a phasor (shift's theorem)

BEAM STEERING & BEAM FORMING

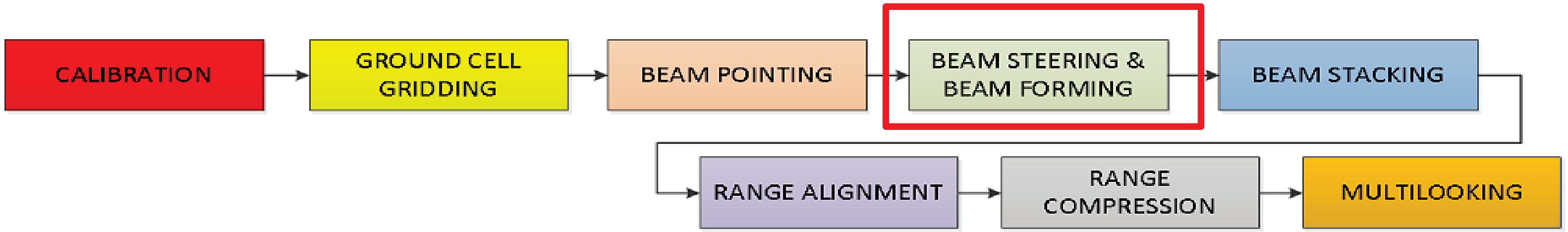

Picture Courtesy of Rober Cullen

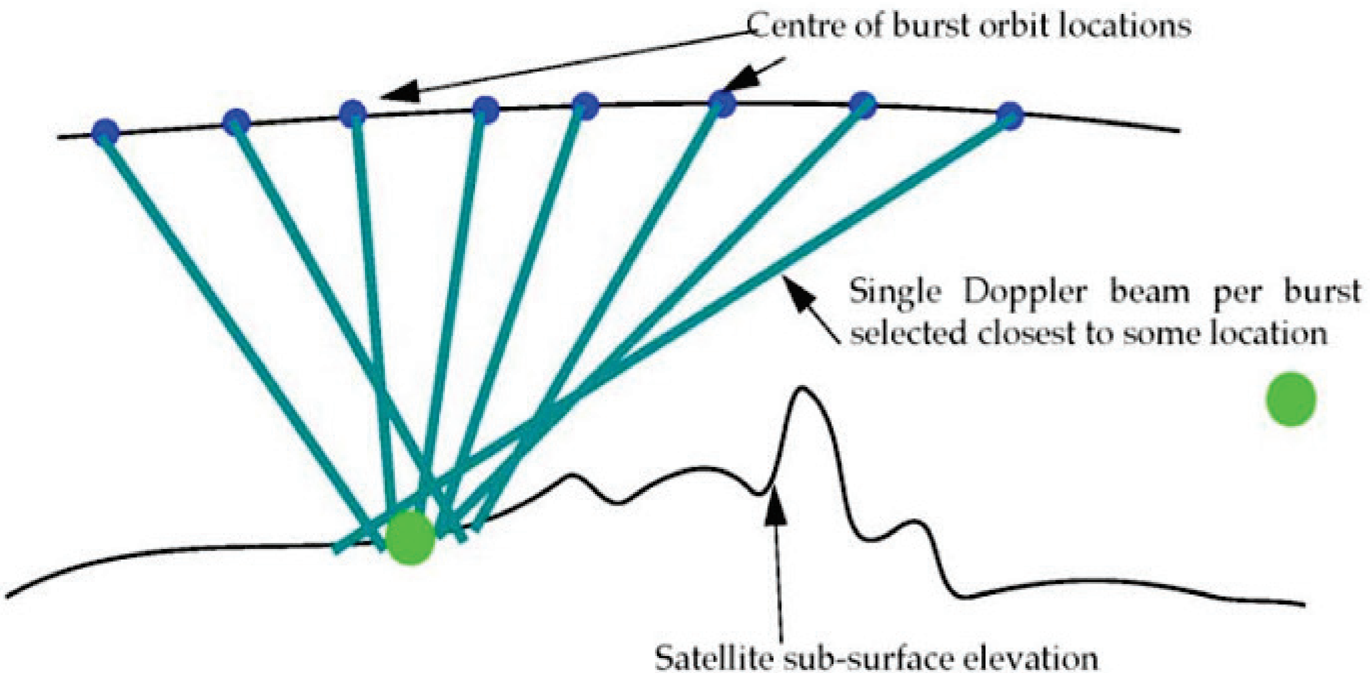

BEAM STEERING & BEAM FORMING

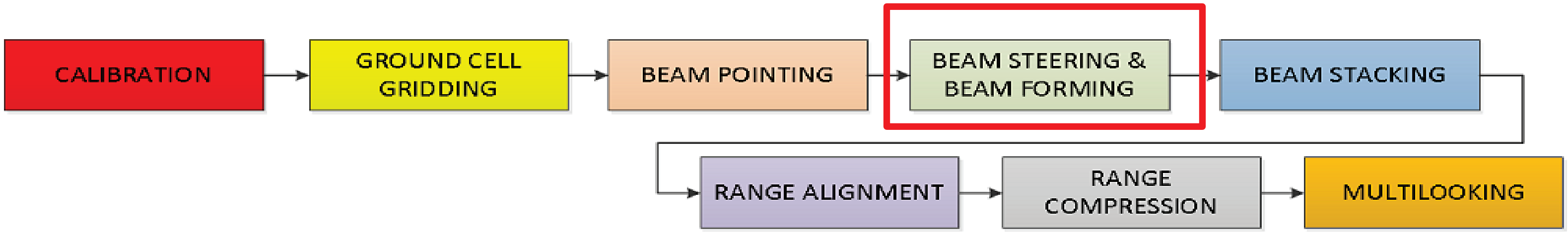

Picture Courtesy of Rober Cullen

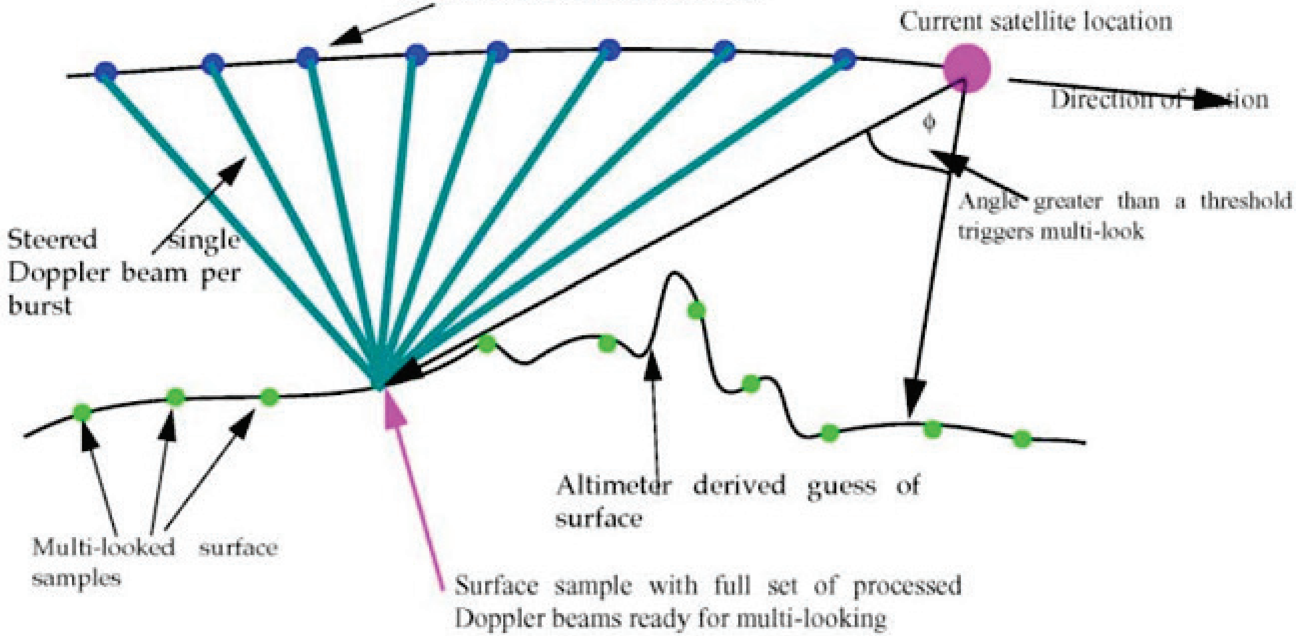

BEAM STEERING & BEAM FORMING

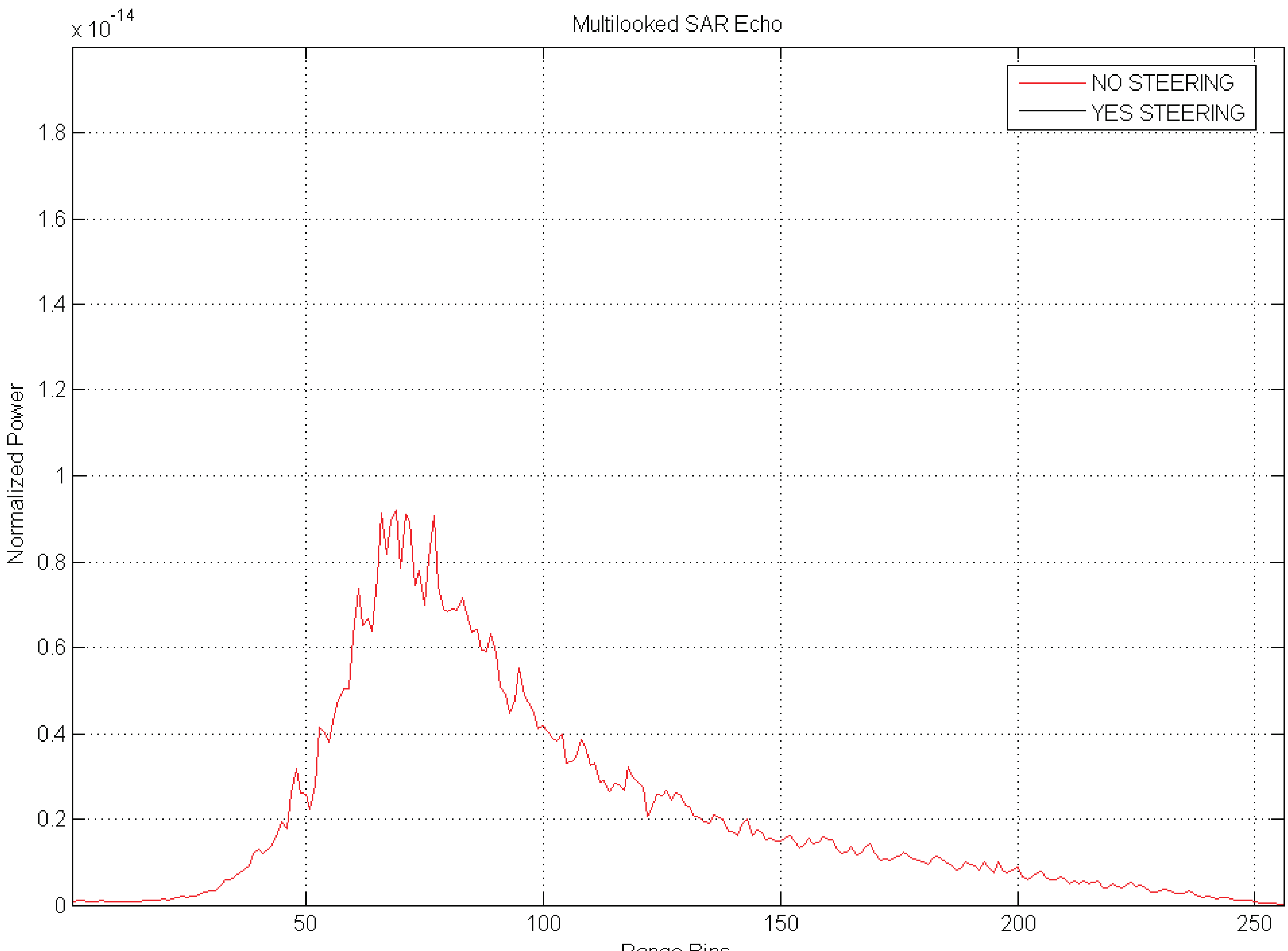

BEAM STEERING & BEAM FORMING

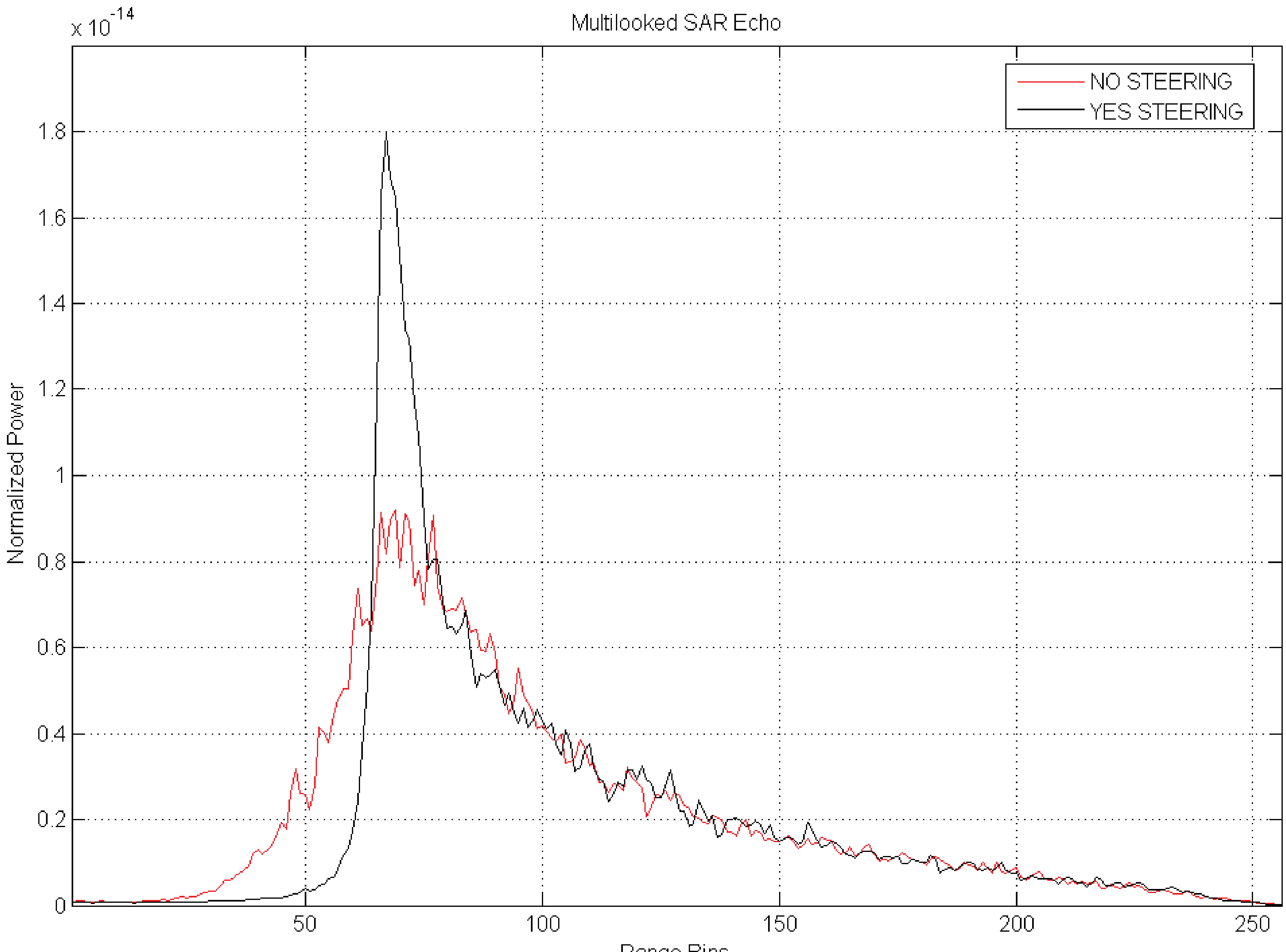

BEAM STEERING & BEAM FORMING: Exact / Approximated

— In the "**approximate"** beam steering, all the Doppler Beams in the fan will be steered by the **same** angle. This approximation can be considered acceptable on gentle undulating surfaces (open sea).

— In the **"exact"** beam steering, each of the Doppler Beams will be steered by a **different** angle; by effect of these phase rotations, all Doppler beam footprint will be now co-located "exactly" with the own surface sample location. The exact beam forming needs to be applied in case of highly variable topographic surfaces but is more time-consuming operation.

Burst Weighting Function

Ghostings: AZIMUTH AMBIGUITIES OVER SPECULAR WATER SURFACES

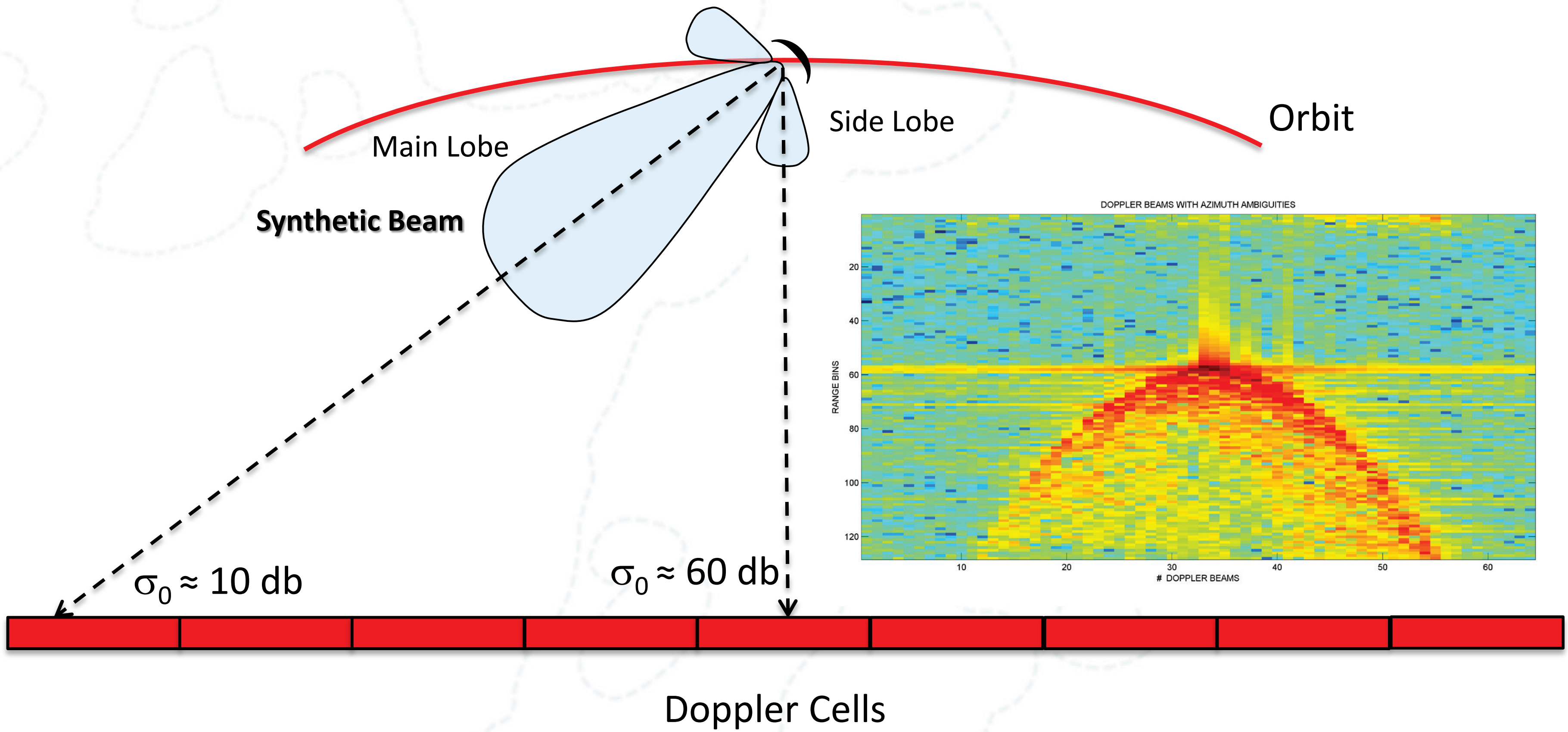

Burst Weighting Function

In order to mitigate the effect of ghostings, one way is to apply a Weighting Function (Hamming) in Doppler Domain to Delay-Doppler Spectrum before the Beam Forming

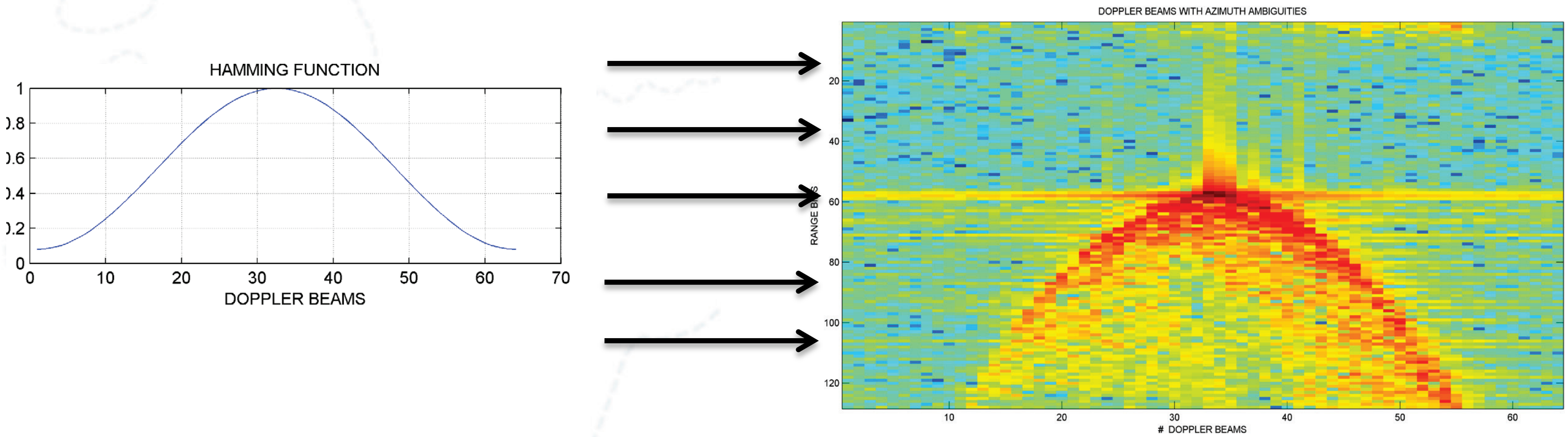

Effect of the application of Weighting Function to eliminate parabolic artifacts on echogram

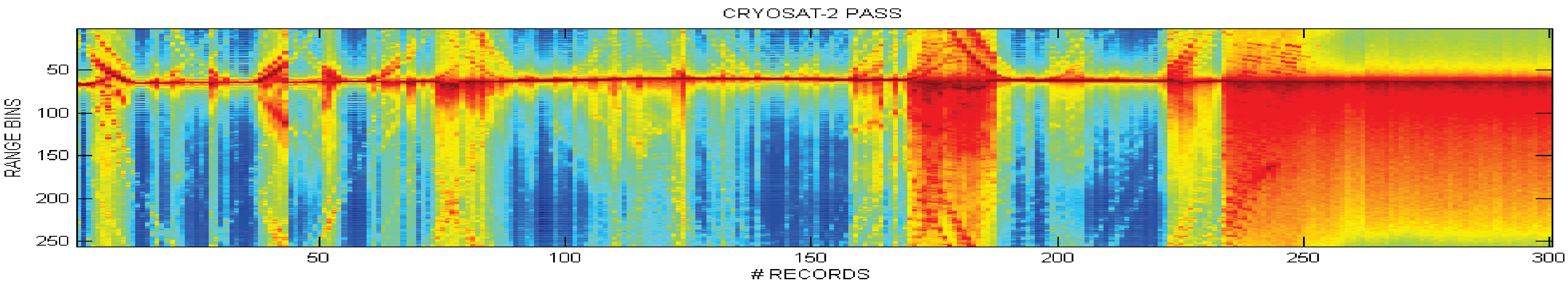

Burst Weighting Function

In order to mitigate the effect of ghostings, one way is to apply a Weighting Function (Hamming) in Doppler Domain to Delay-Doppler Spectrum before the Beam Forming

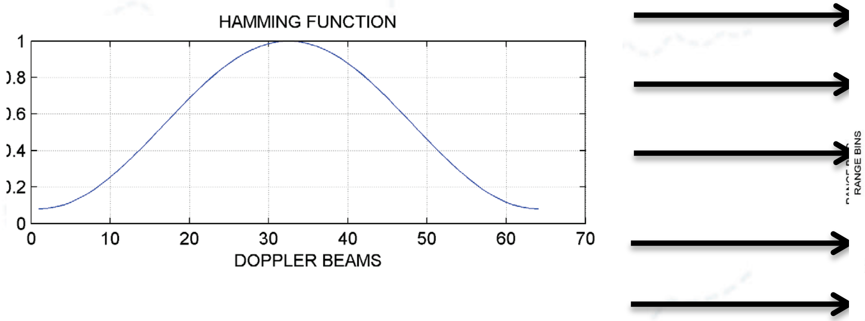

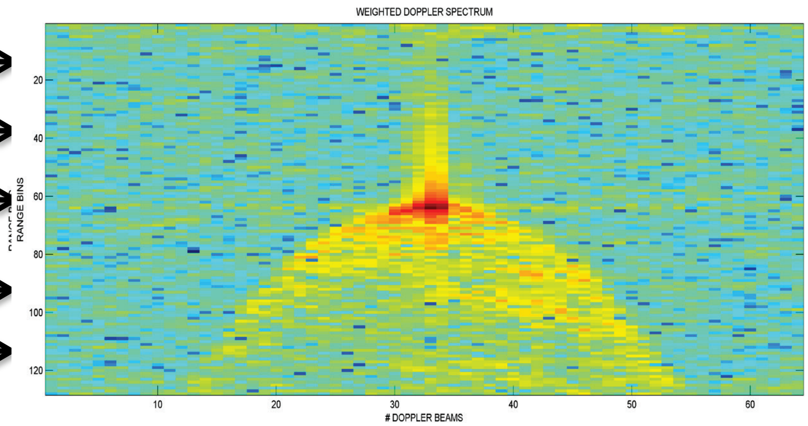

Effect of the application of Weighting Function to eliminate parabolic artifacts on echogram

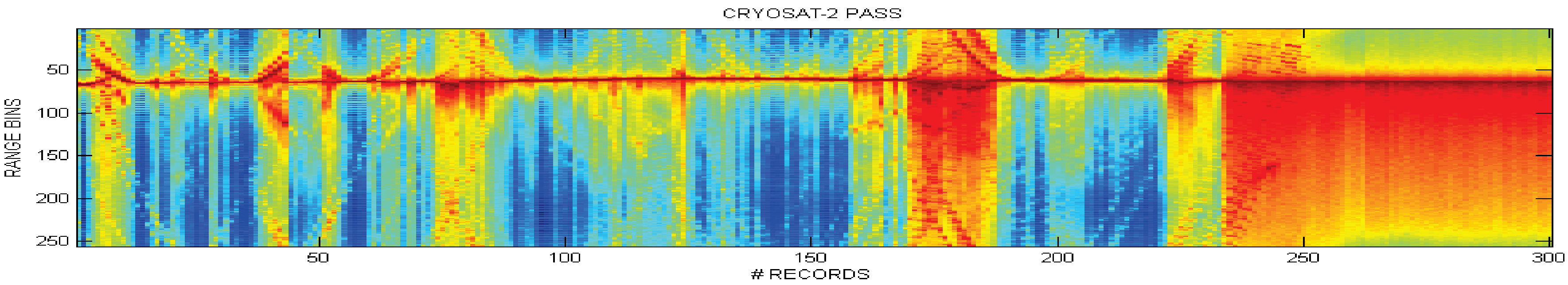

Burst Weighting Function

In order to mitigate the effect of ghostings, one way is to apply a Weighting Function (Hamming) in Doppler Domain to Delay-Doppler Spectrum before the Beam Forming

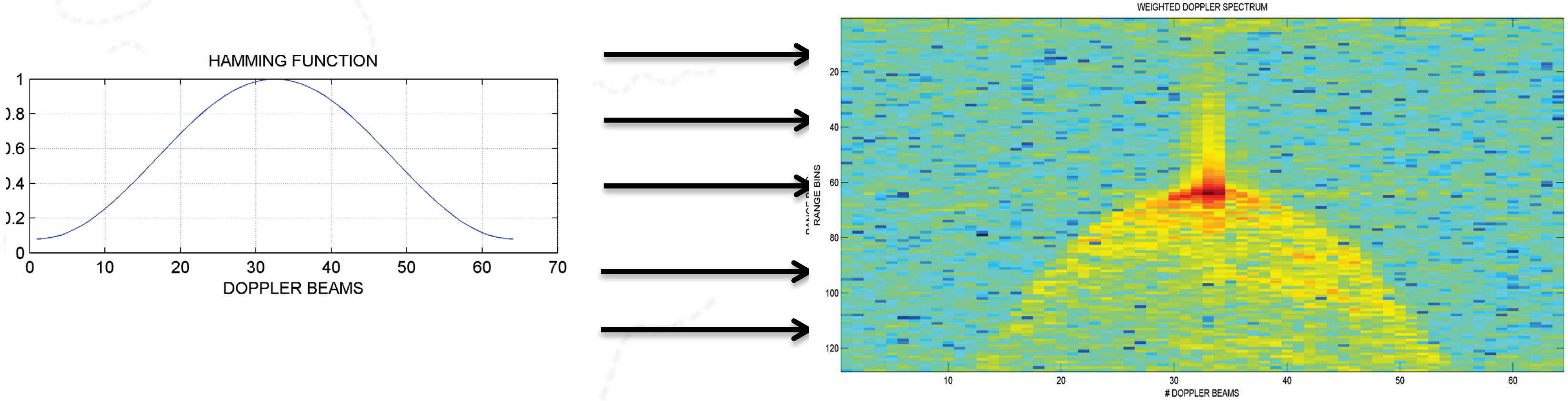

Effect of the application of Weighting Function to eliminate parabolic artifacts on echogram

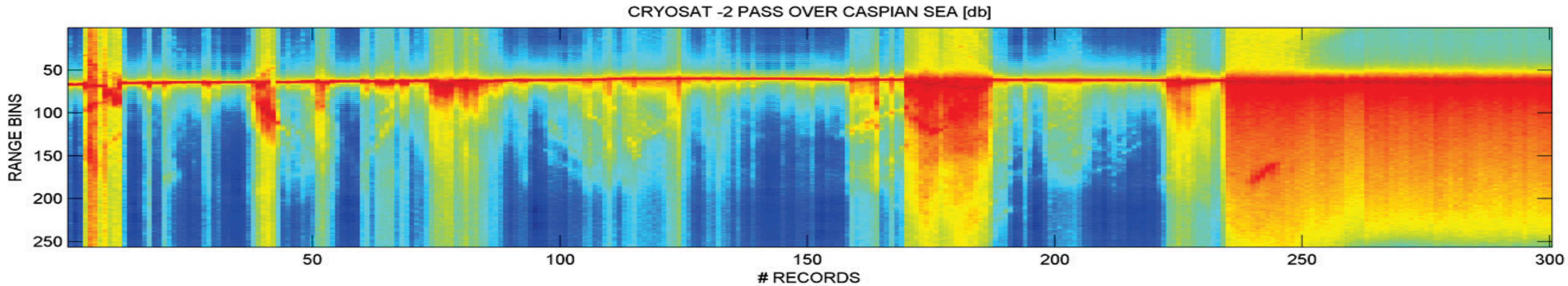

Case over sea ice

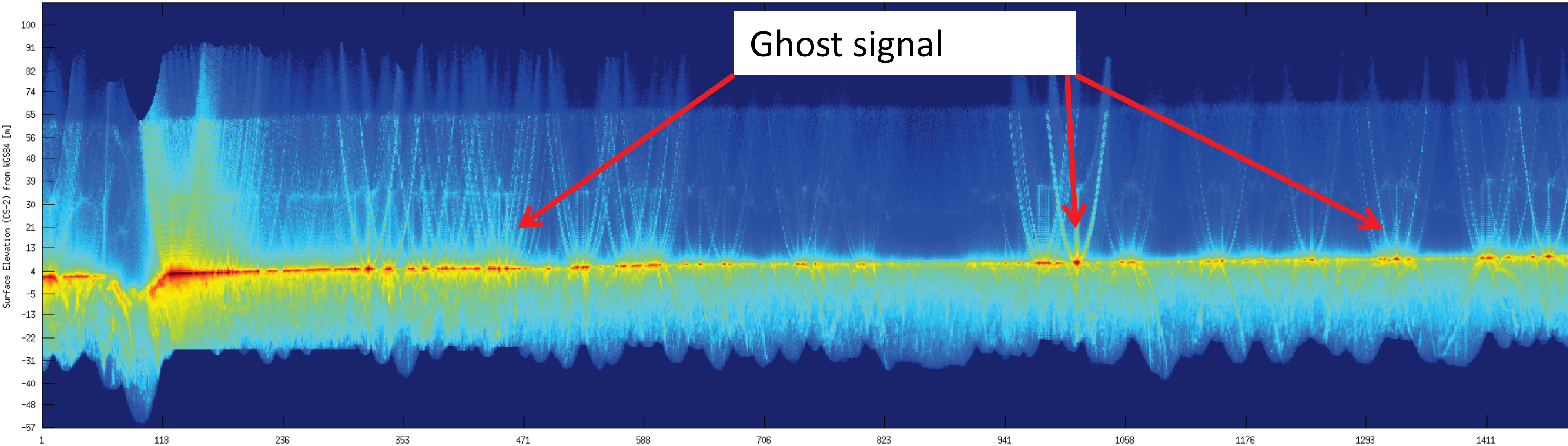

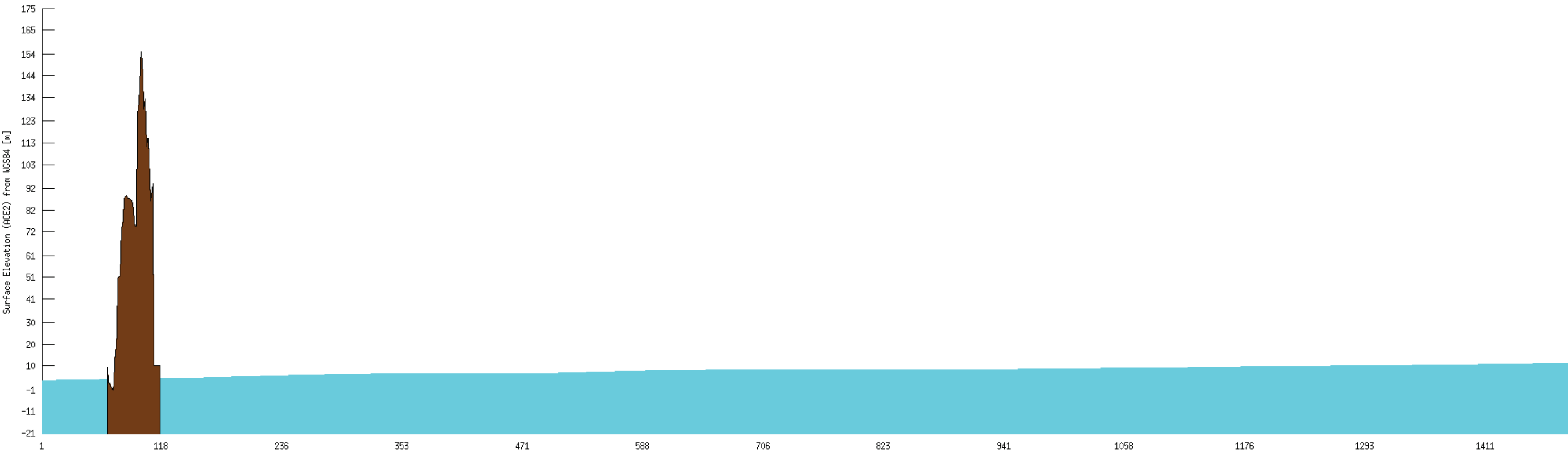

Case over sea ice

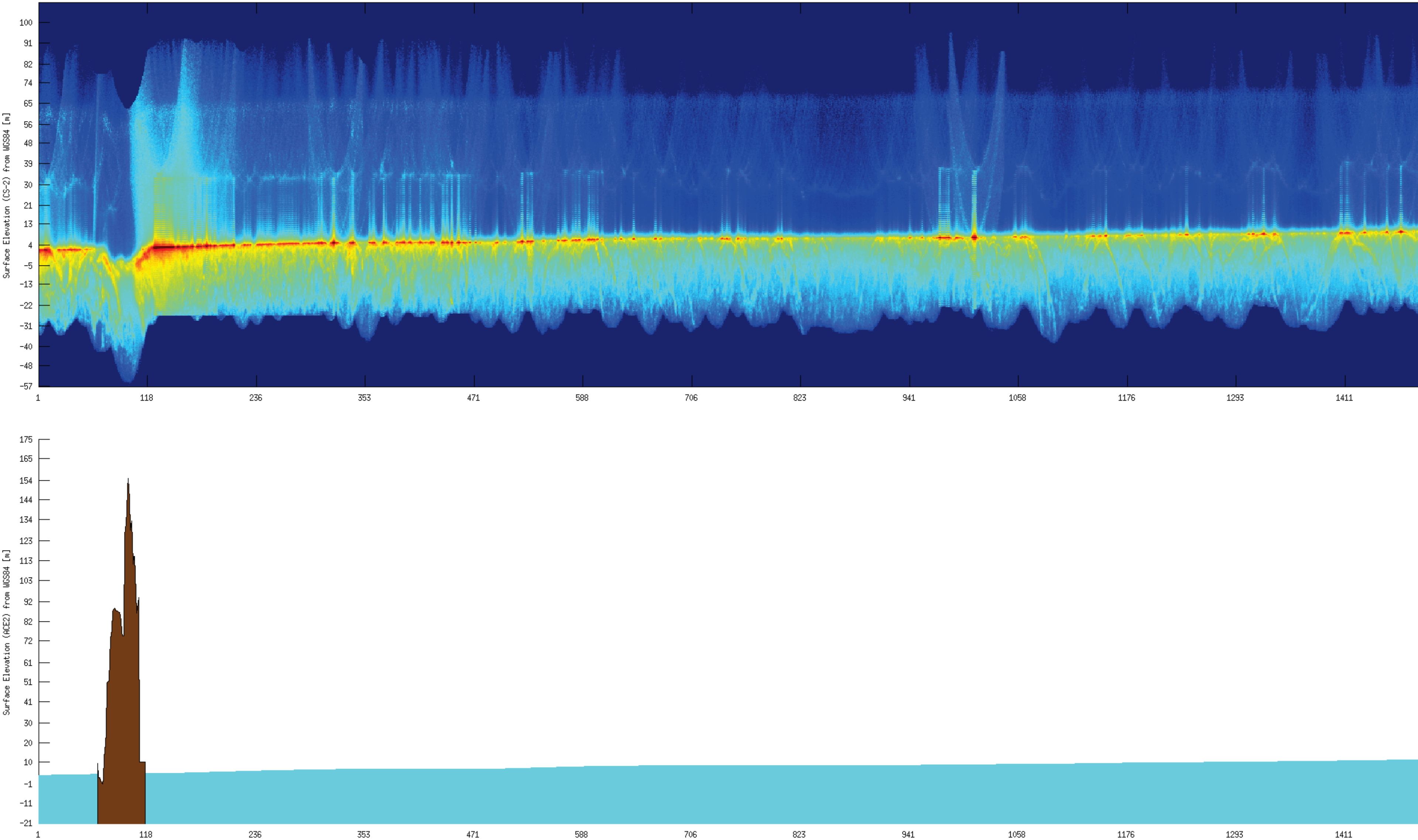

Burst Weighting Function: Be careful!

PRICE TO PAY:

Burst Weighting Function: Be careful!

PRICE TO PAY:

- Along track resolution get worst (from 300 meters to 500 meters)

Burst Weighting Function: Be careful!

PRICE TO PAY:

- Along track resolution get worst (from 300 meters to 500 meters)
- Max Power get lower (attenuation effect)

Burst Weighting Function: Be careful!

PRICE TO PAY:

- Along track resolution get worst (from 300 meters to 500 meters)
- Max Power get lower (attenuation effect)
- Raise a question .. Which is the best weighting function ? (Hamming, Hanning, Blackmann, etc..) or are they others methods to solve the ambiguities problem ?

Burst Weighting Function: Be careful!

PRICE TO PAY:

- Along track resolution get worst (from 300 meters to 500 meters)
- Max Power get lower (attenuation effect)
- Raise a question .. Which is the best weighting function ? (Hamming, Hanning, Blackmann, etc..) or are they others methods to solve the ambiguities problem ?
- In case of usage of a physical retracker, it needs to proper model the weighting function in the retracker's functional model to avoid side effects

Burst Weighting Function: Be careful!

PRICE TO PAY:

- Along track resolution get worst (from 300 meters to 500 meters)
- Max Power get lower (attenuation effect)
- Raise a question .. Which is the best weighting function ? (Hamming, Hanning, Blackmann, etc..) or are they others methods to solve the ambiguities problem ?
- In case of usage of a physical retracker, it needs to proper model the weighting function in the retracker's functional model to avoid side effects
- Dynamic application of Weighting Function: no over open ocean and yes in coastal zone

Burst Weighting Function: Be careful!

PRICE TO PAY:

- Along track resolution get worst (from 300 meters to 500 meters)
- Max Power get lower (attenuation effect)
- Raise a question .. Which is the best weighting function ? (Hamming, Hanning, Blackmann, etc..) or are they others methods to solve the ambiguities problem ?
- In case of usage of a physical retracker, it needs to proper model the weighting function in the retracker's functional model to avoid side effects
- Dynamic application of Weighting Function: no over open ocean and yes in coastal zone

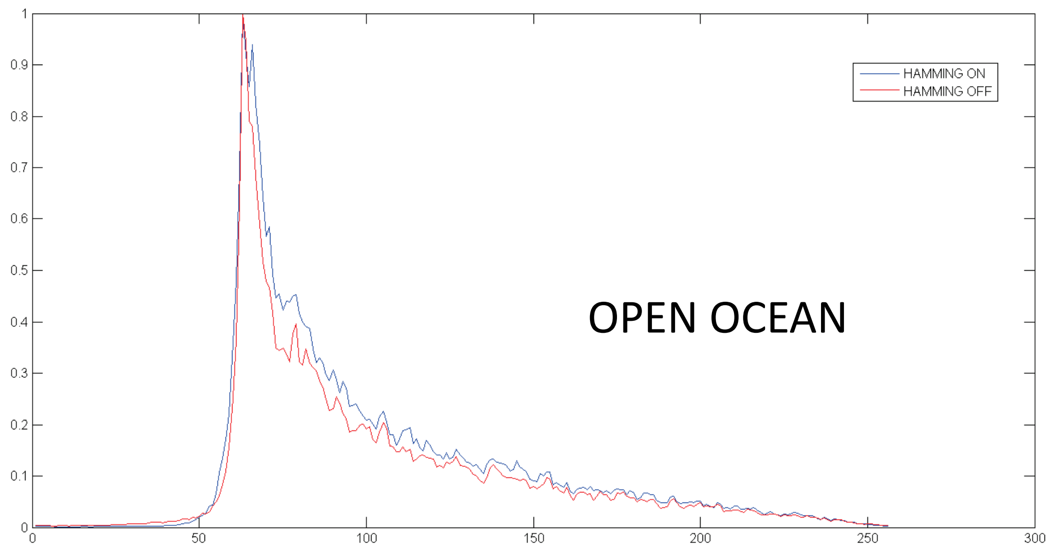

BEAM STACKING

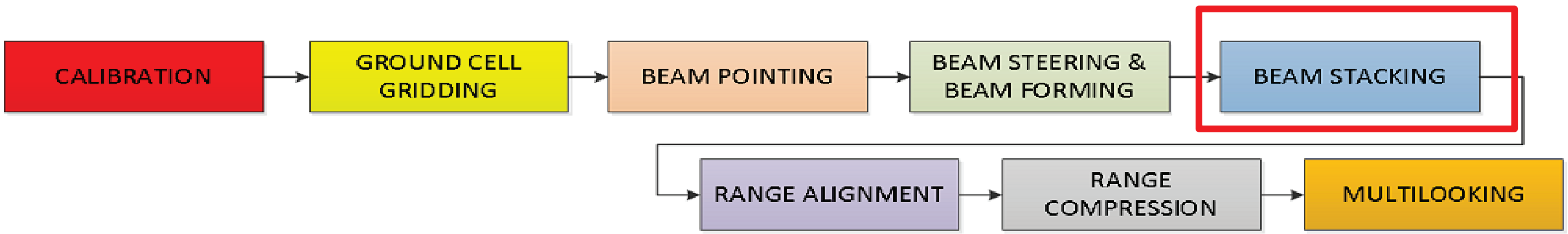

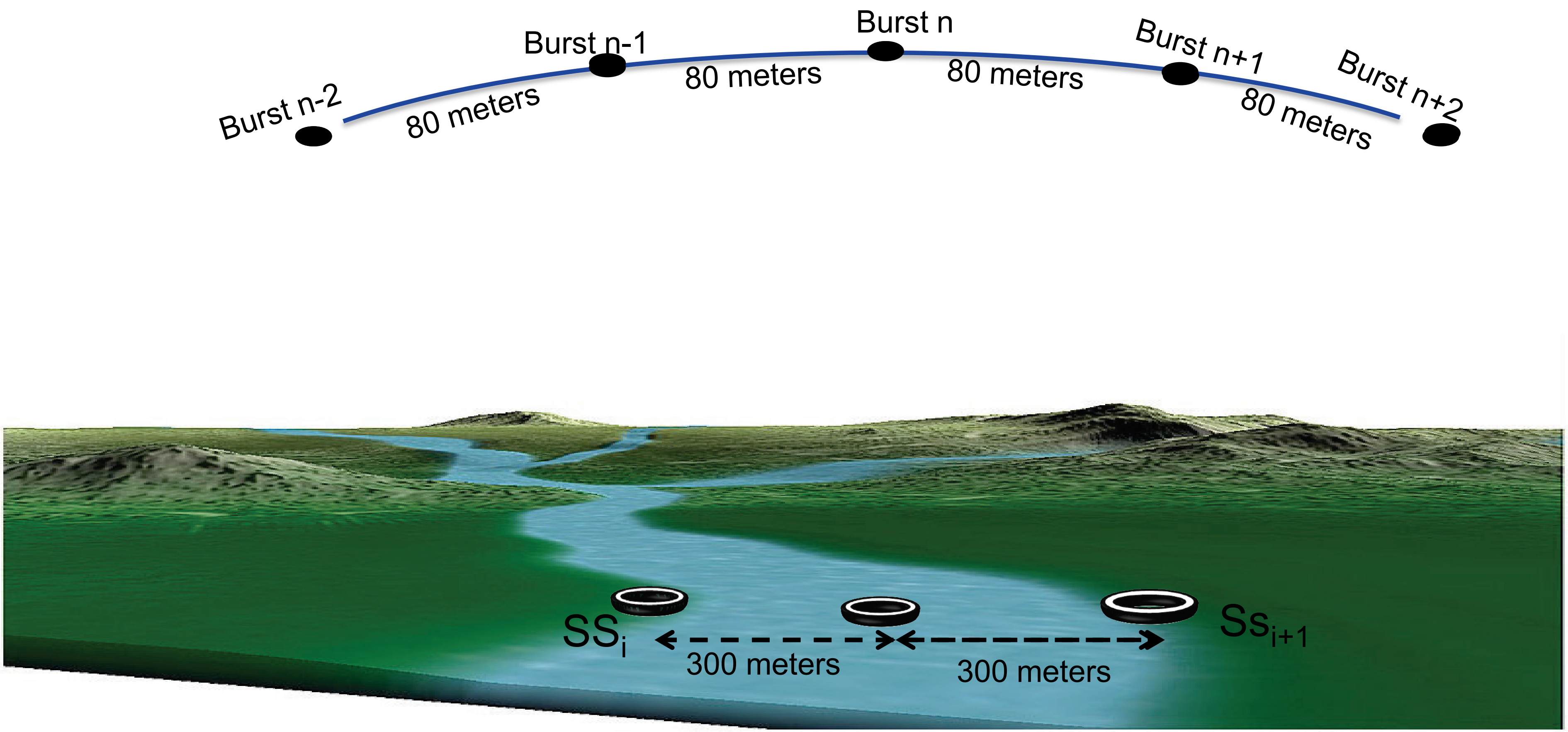

BEAM STACKING

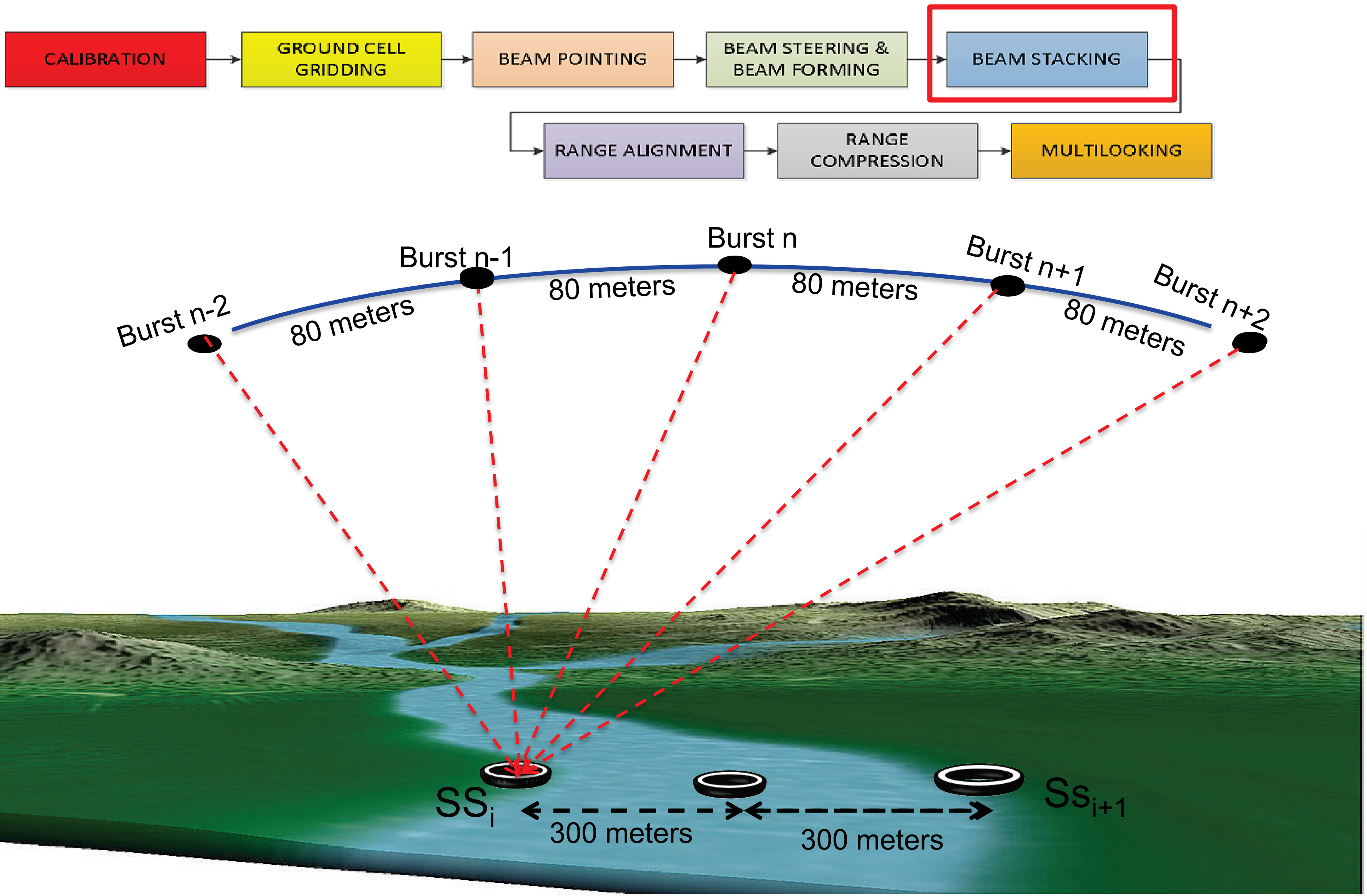

BEAM STACKING

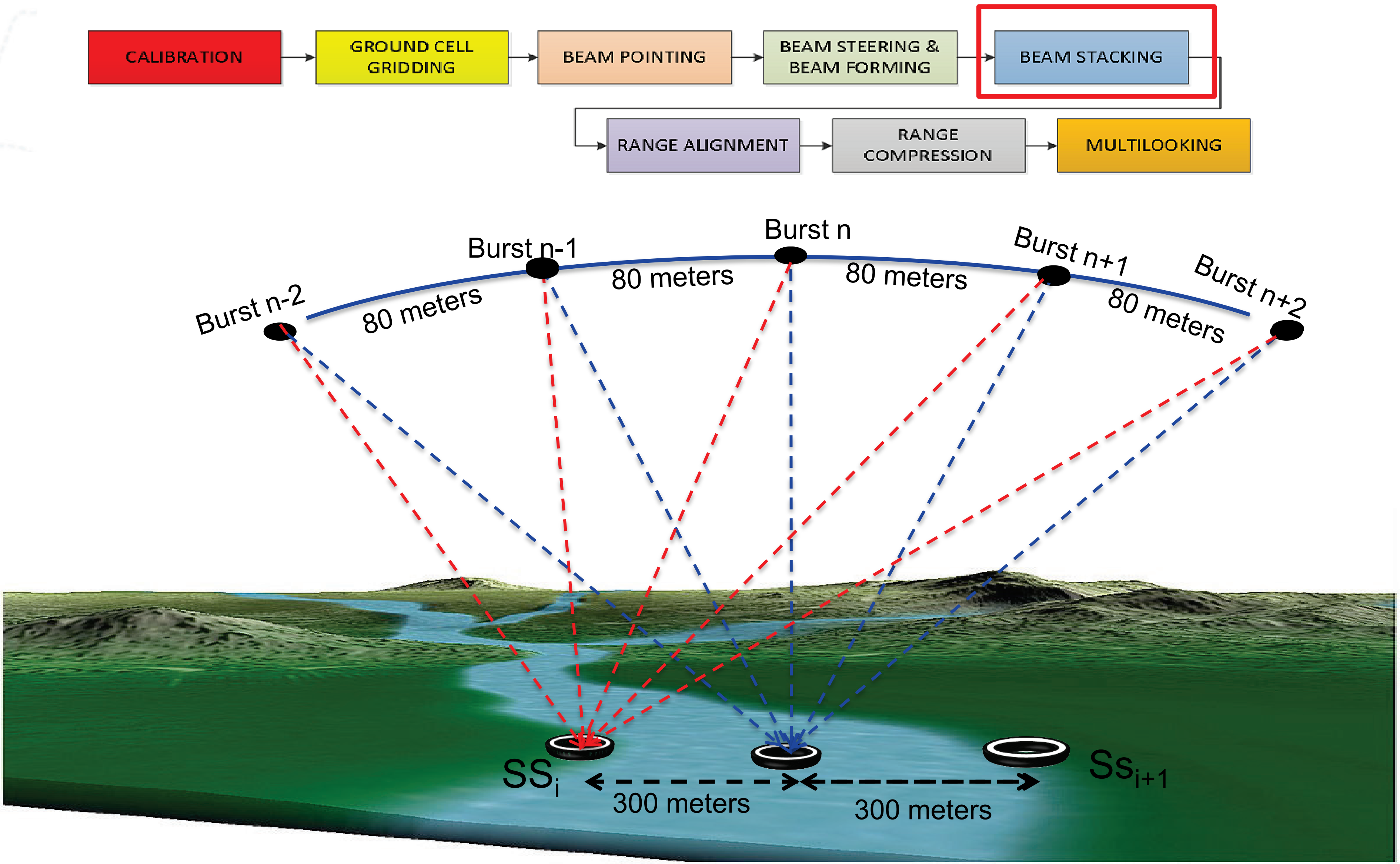

BEAM STACKING

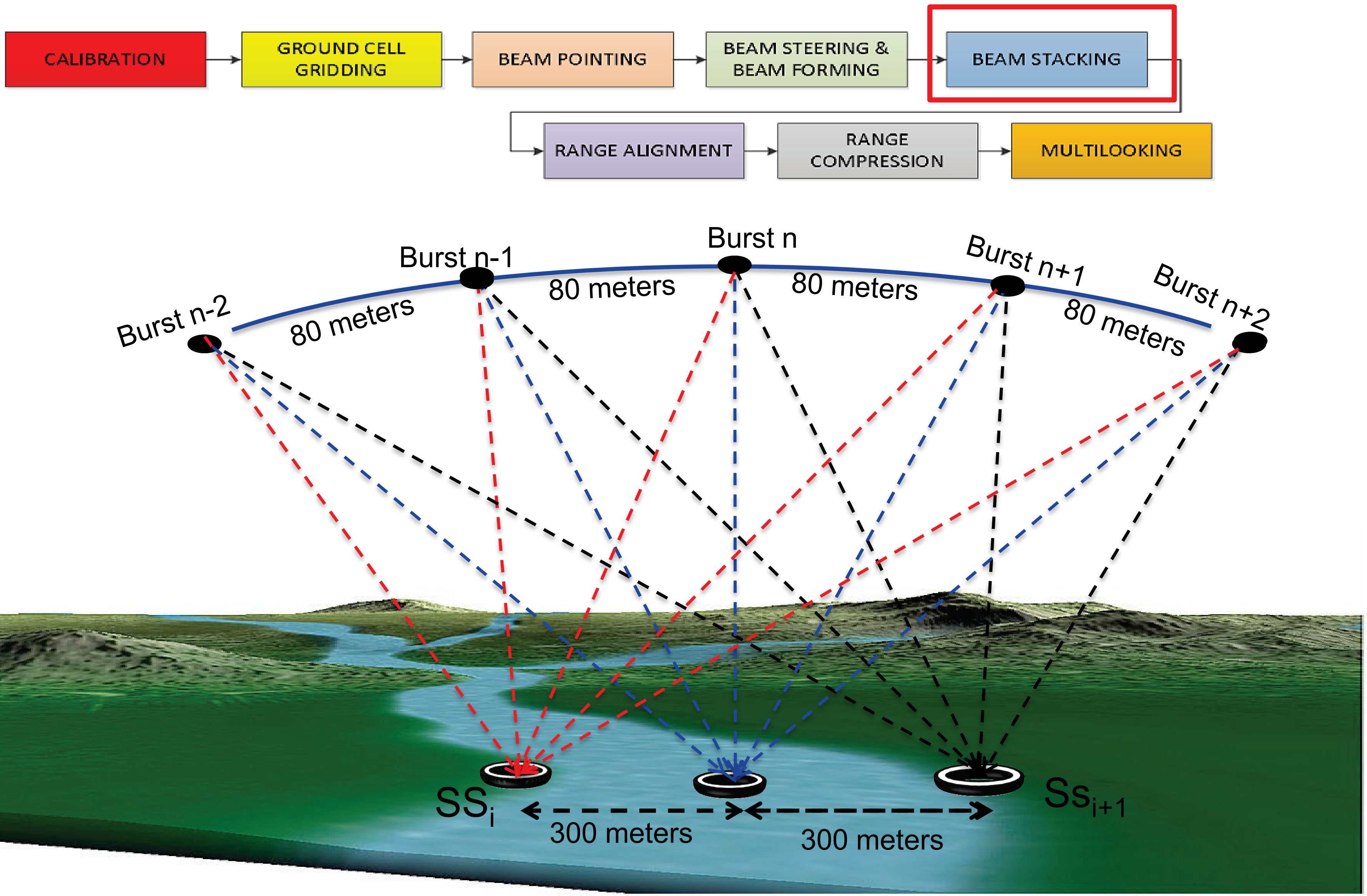

BEAM STACKING

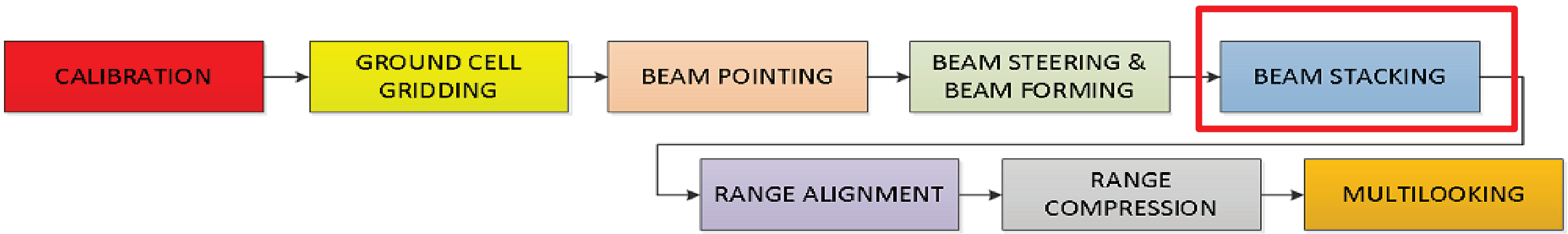

Around 220 burst in view for each ground cell

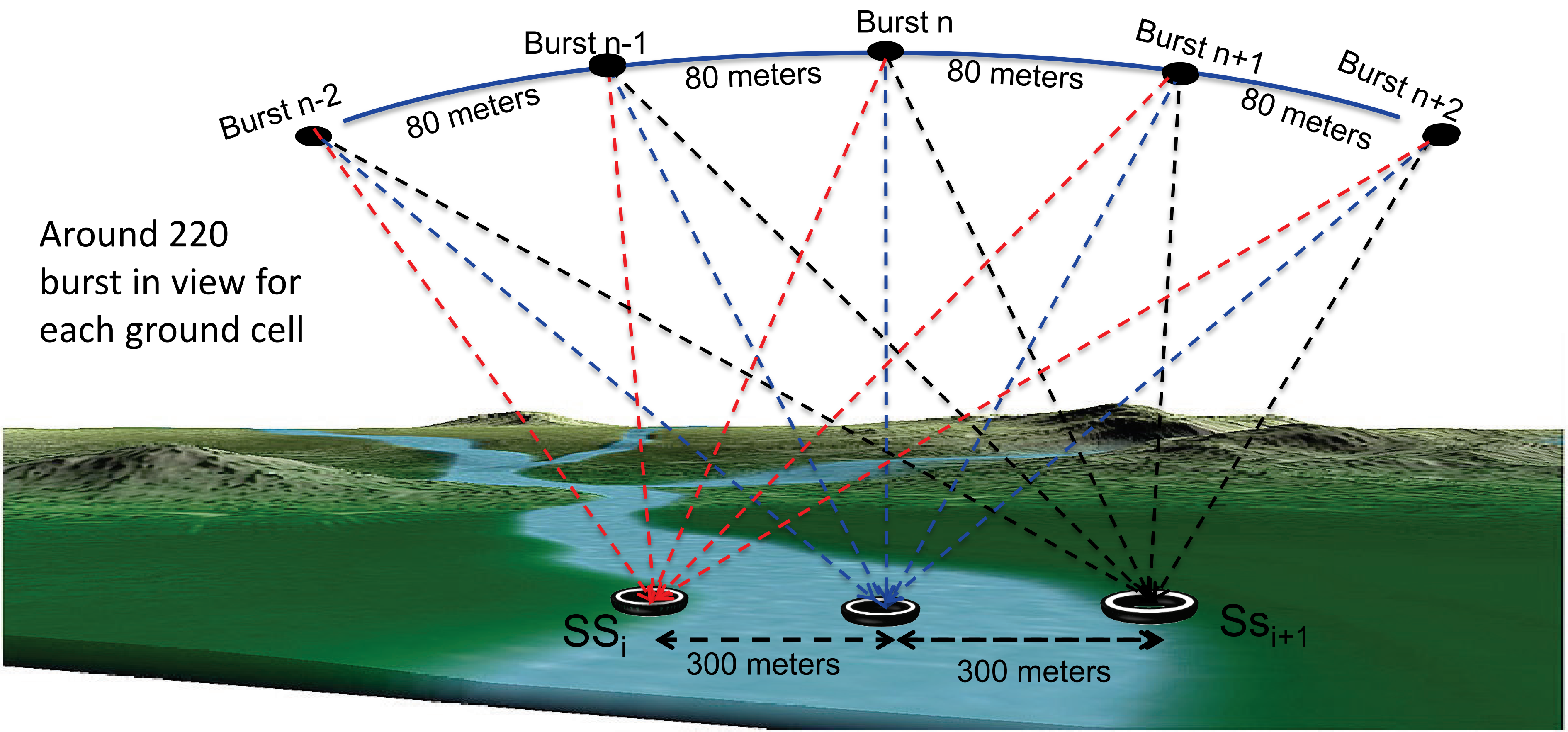

BEAM STACKING

STACK: Collection of the looks, staring at the same ground cell and gathered in sequence in a data matrix

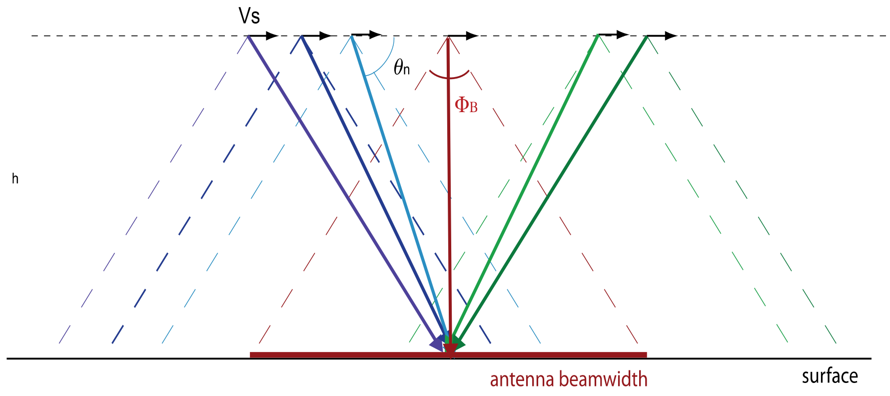

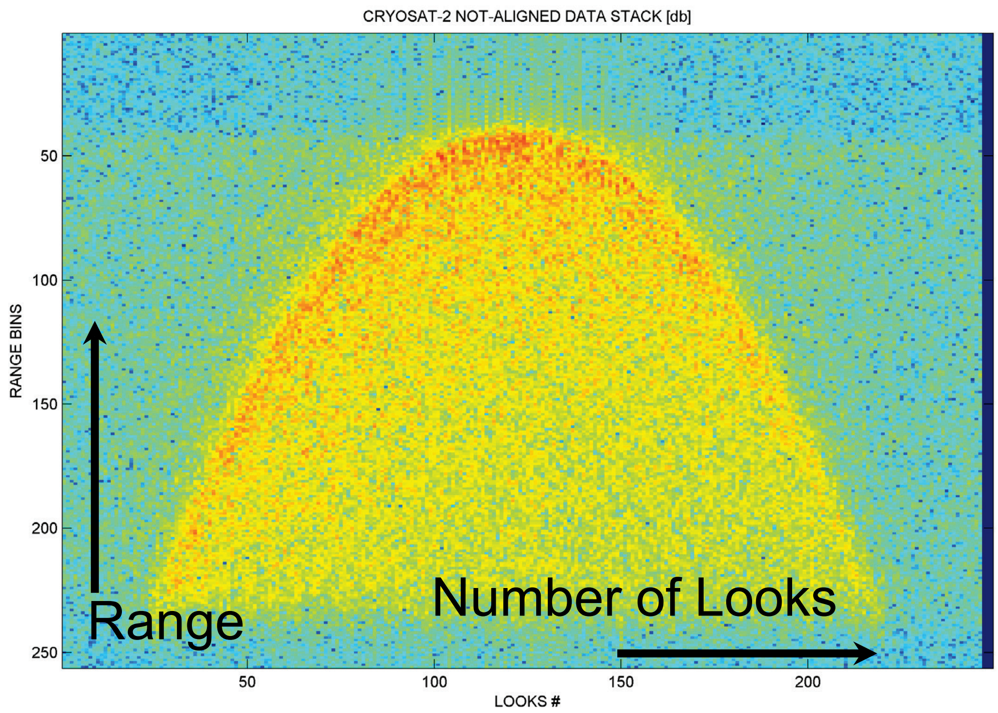

RANGE ALIGNMENT

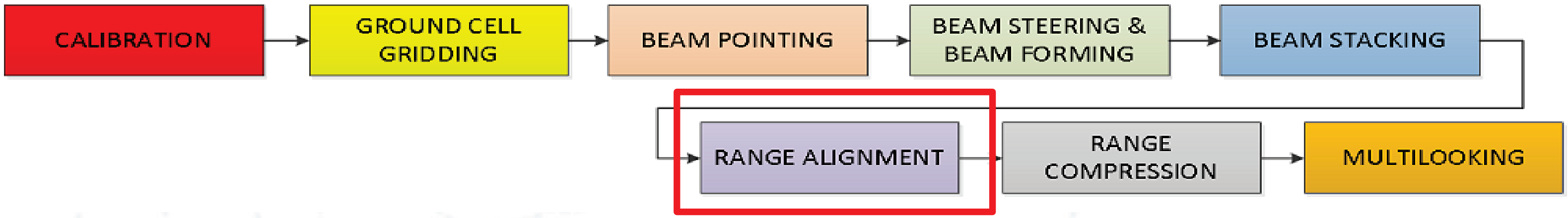

The purpose of this stage is to correct all the misalignment in range between the beams of the same stack.
Three range misalignment needs to be corrected:

- Misalignment for on board **Tracker Shift** Correction
- Misalignment for **Slant Range** Correction
- Misalignment for **Doppler Shift** Correction

TRACKER RANGE ALIGNMENT

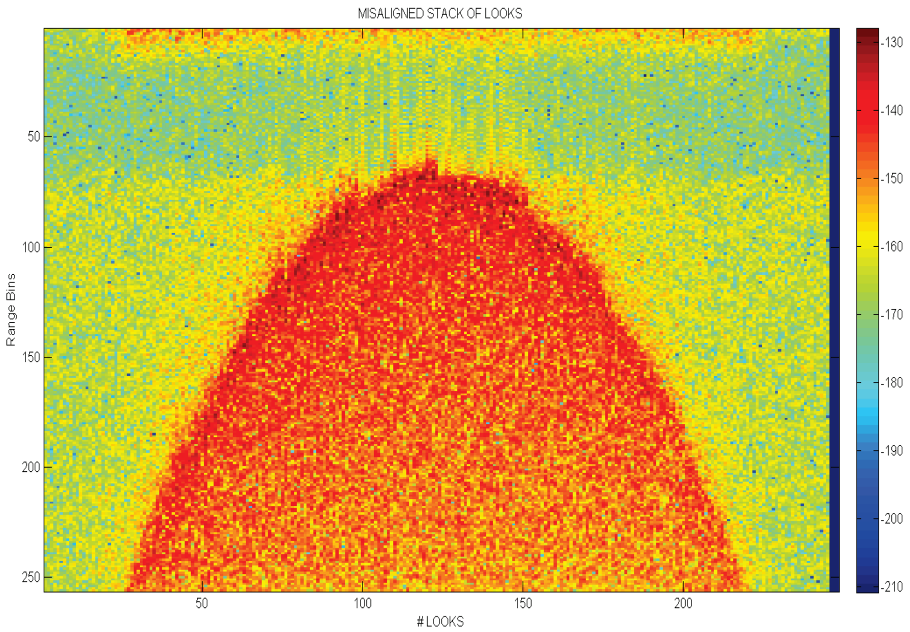

TRACKER RANGE ALIGNMENT

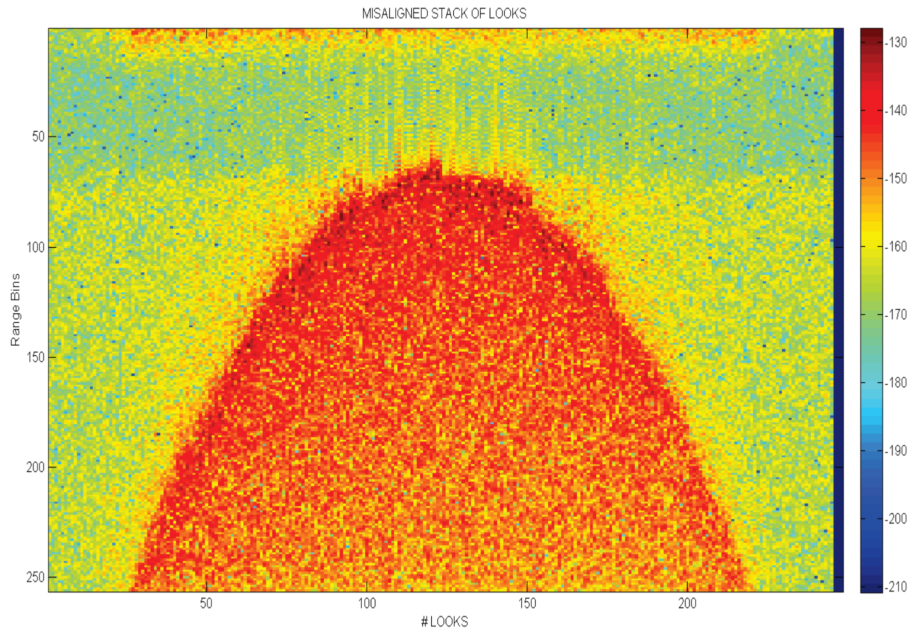

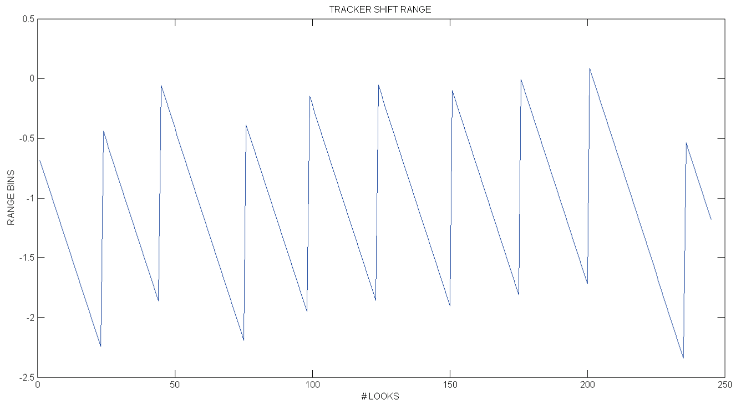

TRACKER RANGE ALIGNMENT

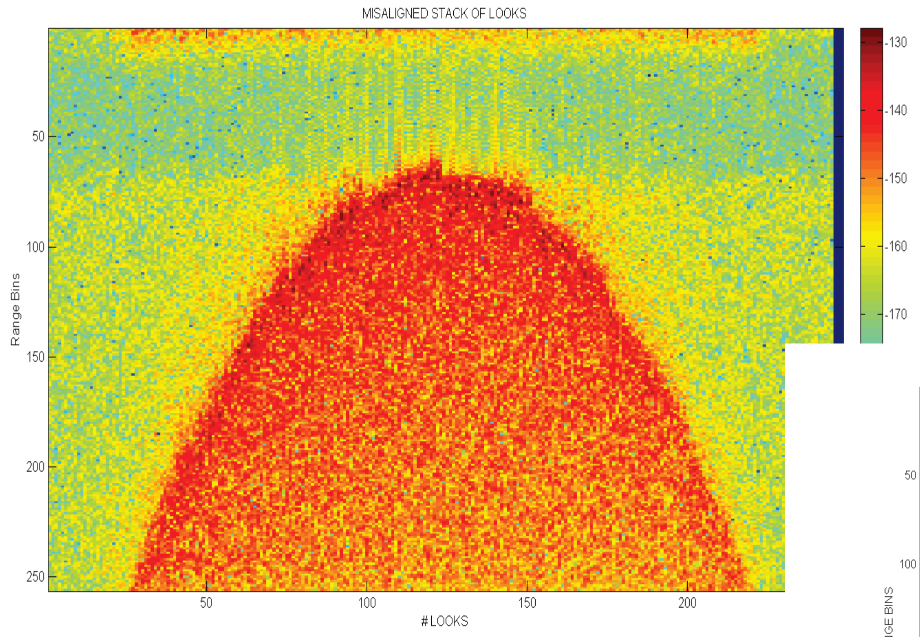

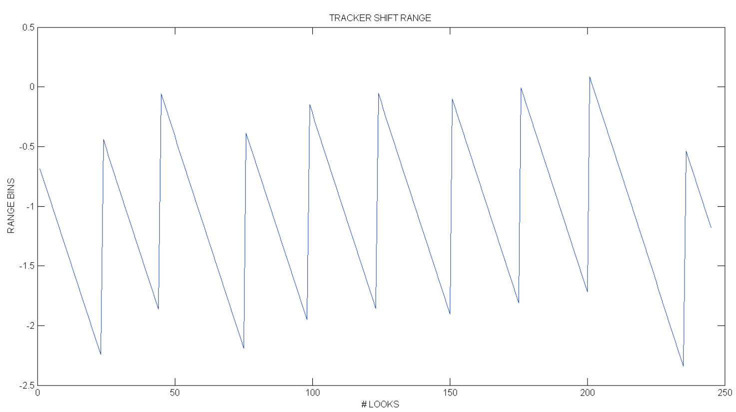

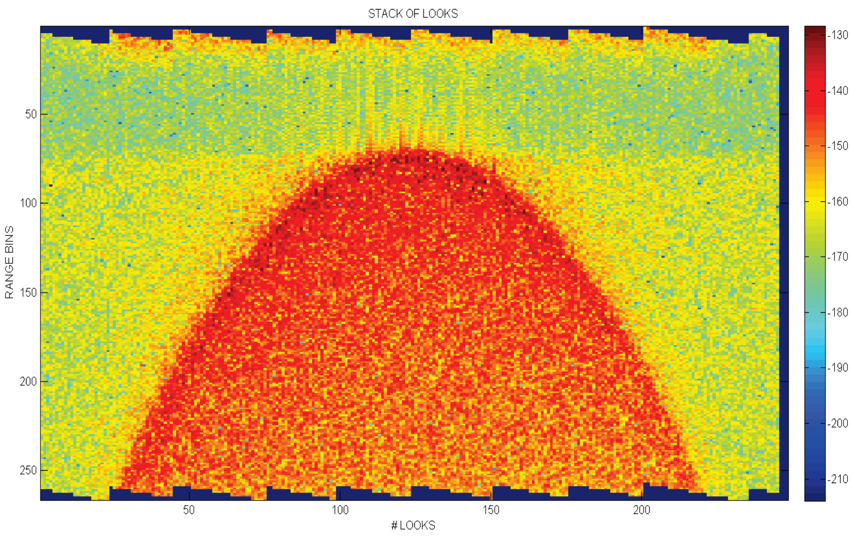

SLANT RANGE ALIGNMENT

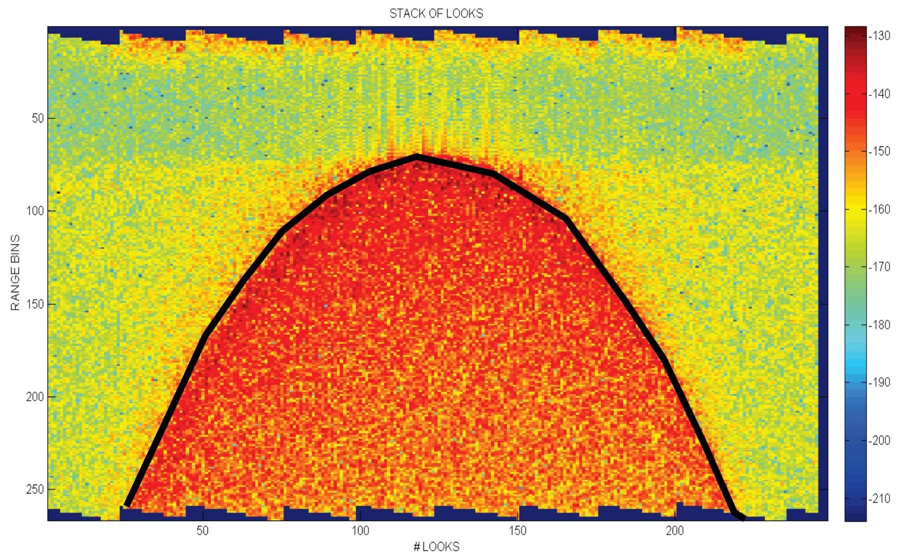

SLANT RANGE ALIGNMENT

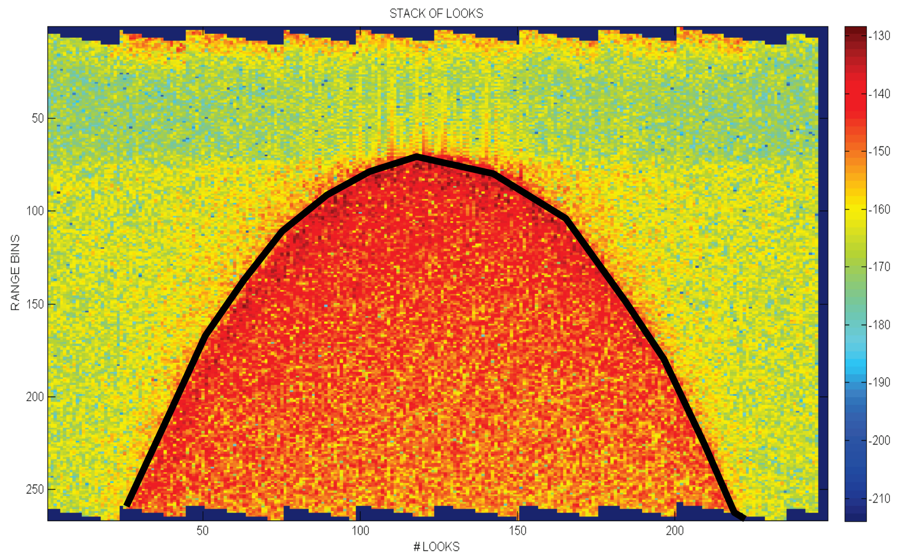

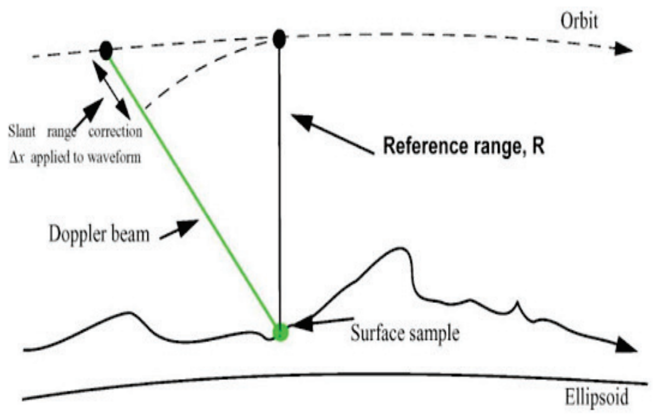

SLANT RANGE ALIGNMENT

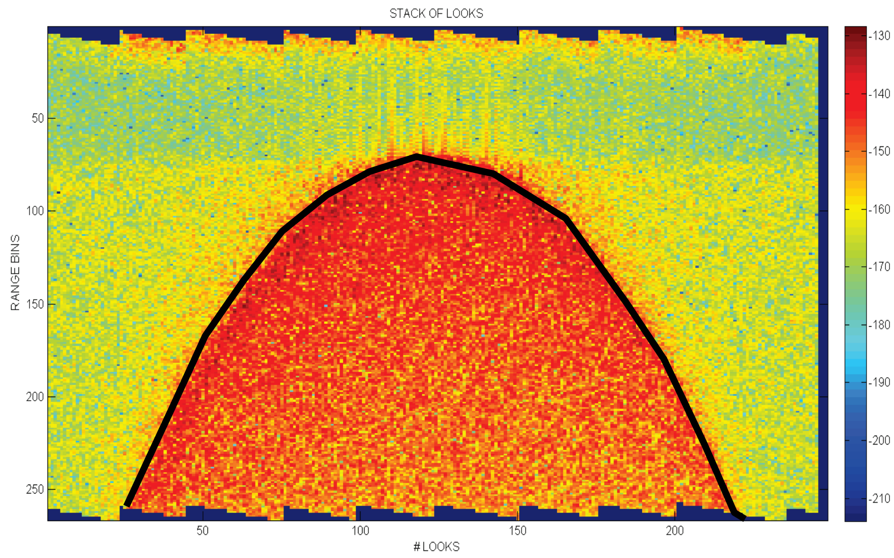

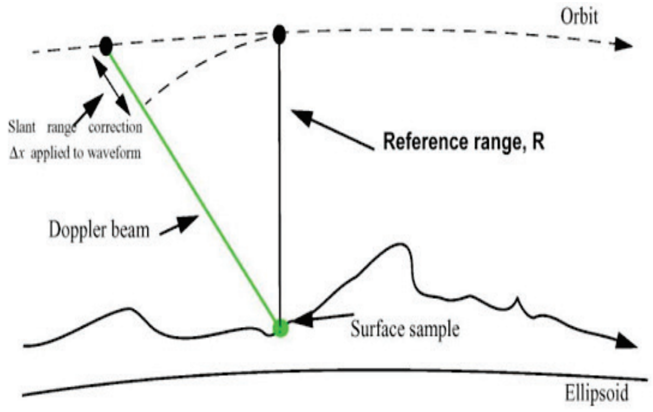

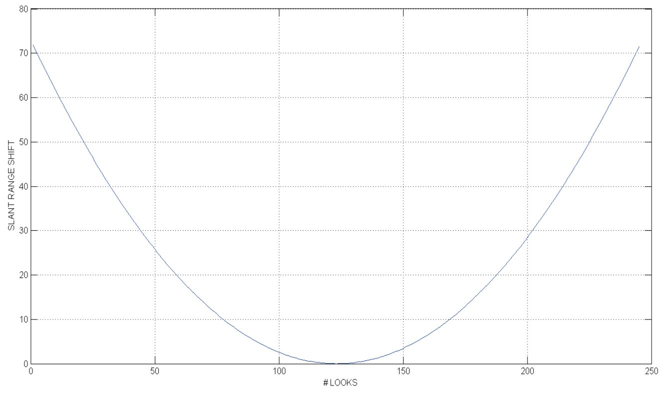

SLANT RANGE ALIGNMENT

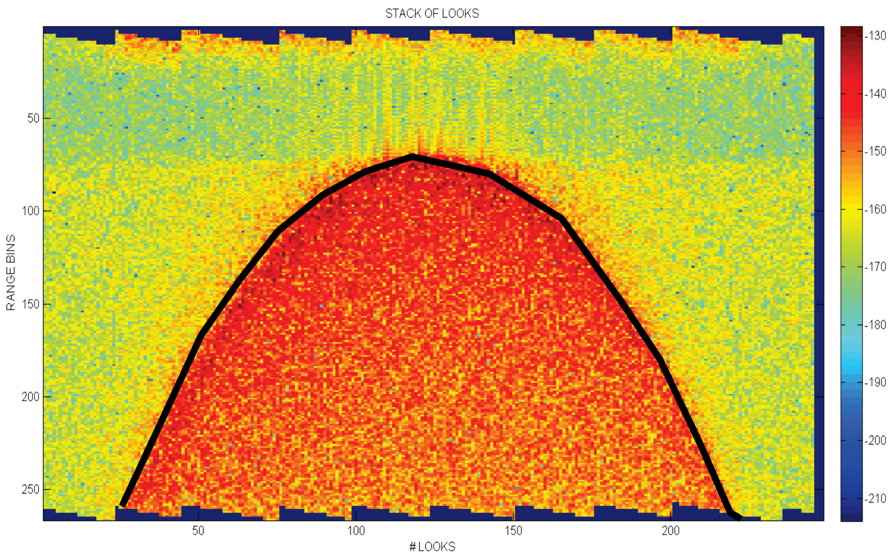

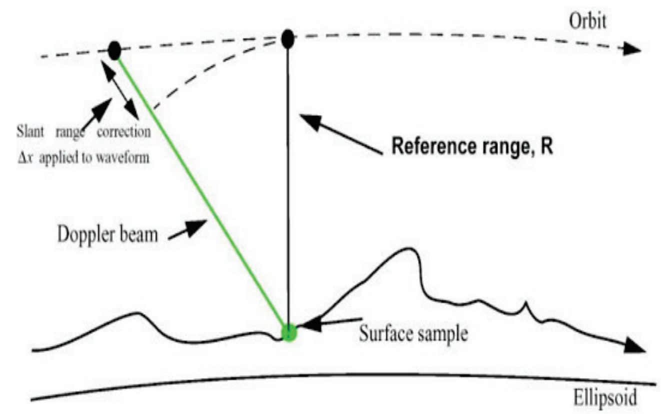

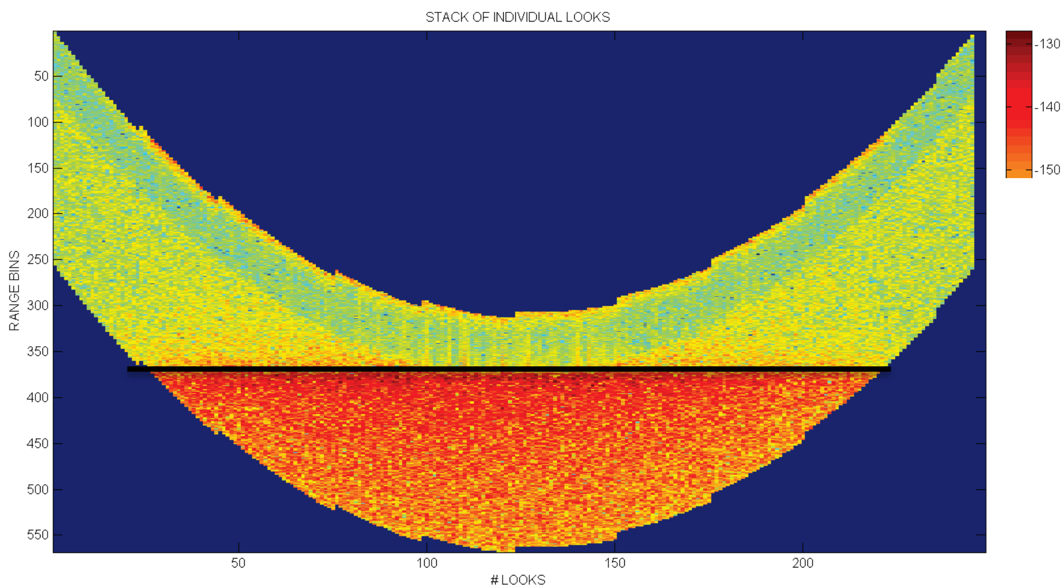

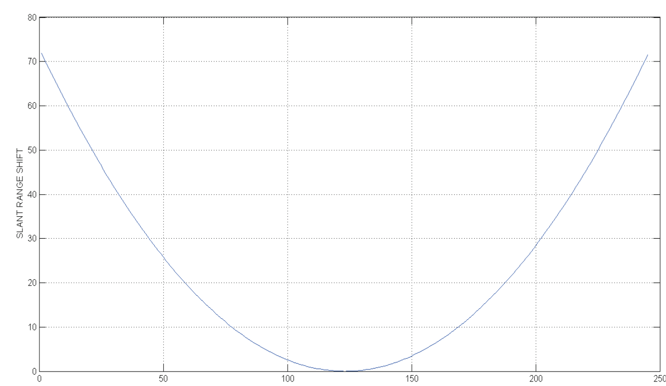

DOPPLER SHIFT ALIGNMENT

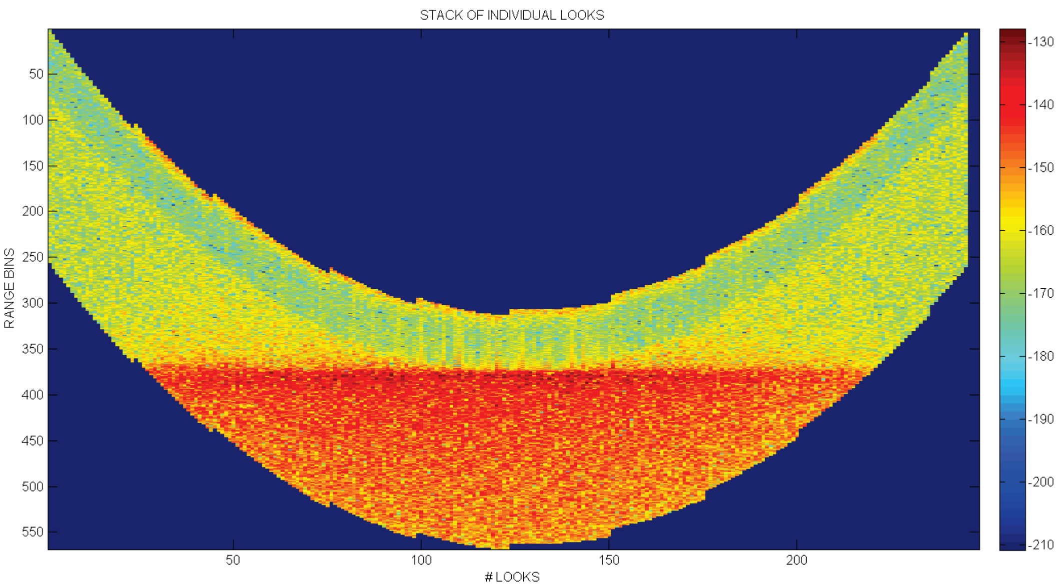

DOPPLER SHIFT ALIGNMENT

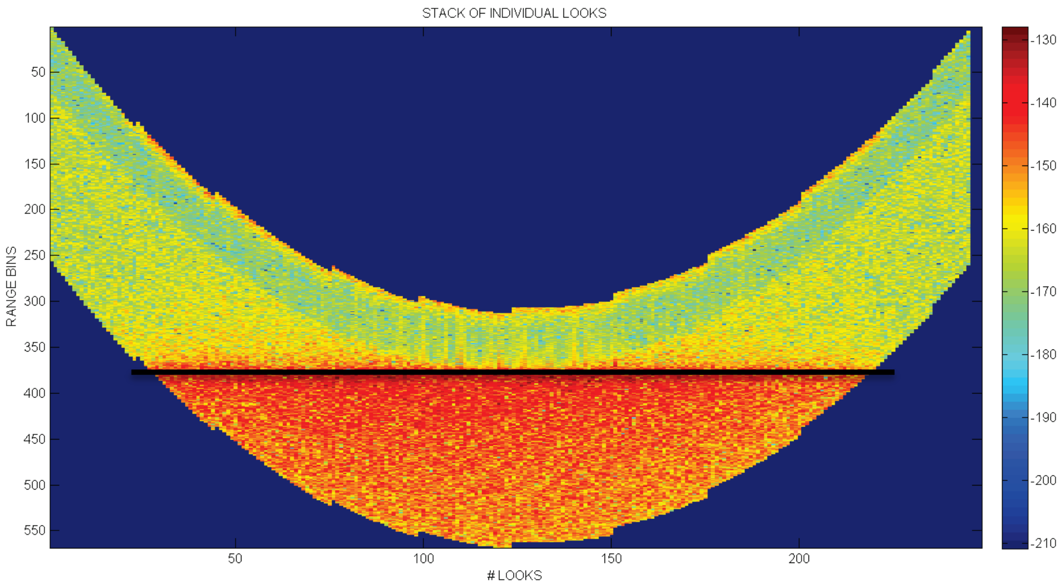

DOPPLER SHIFT ALIGNMENT

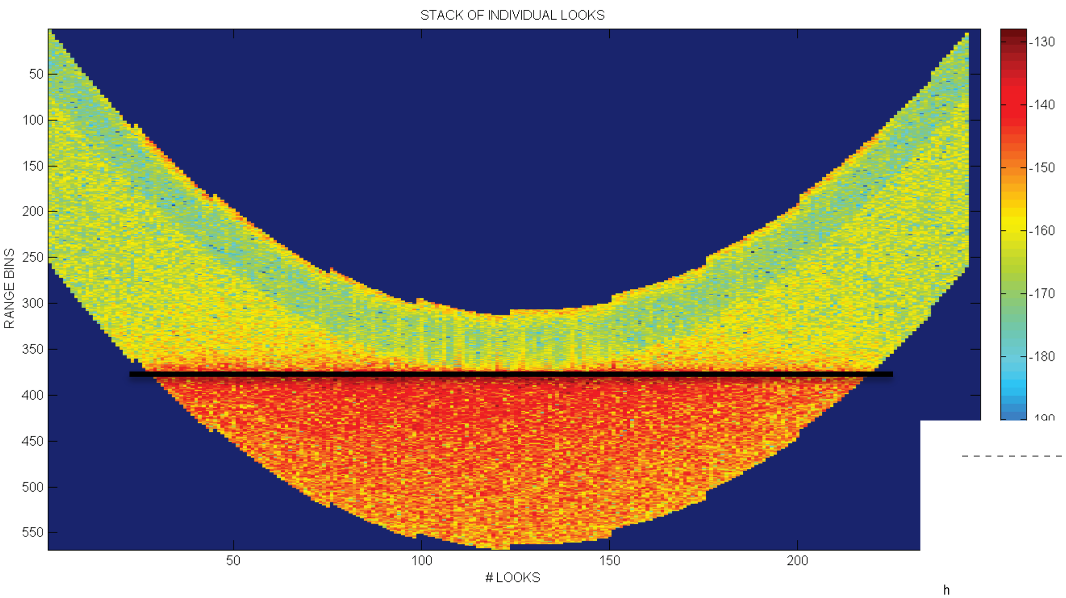

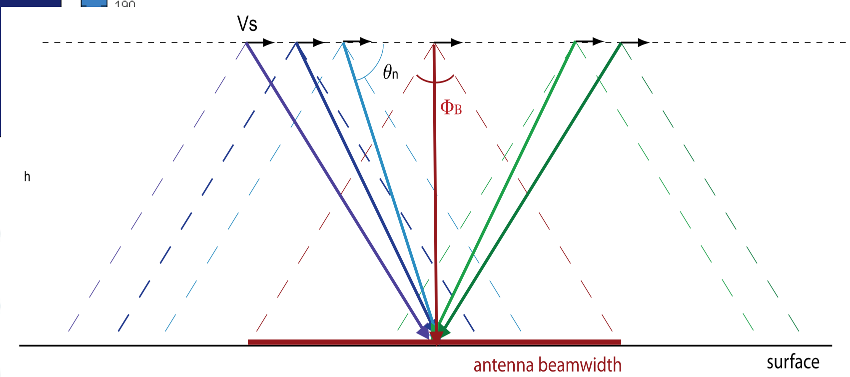

DOPPLER SHIFT ALIGNMENT

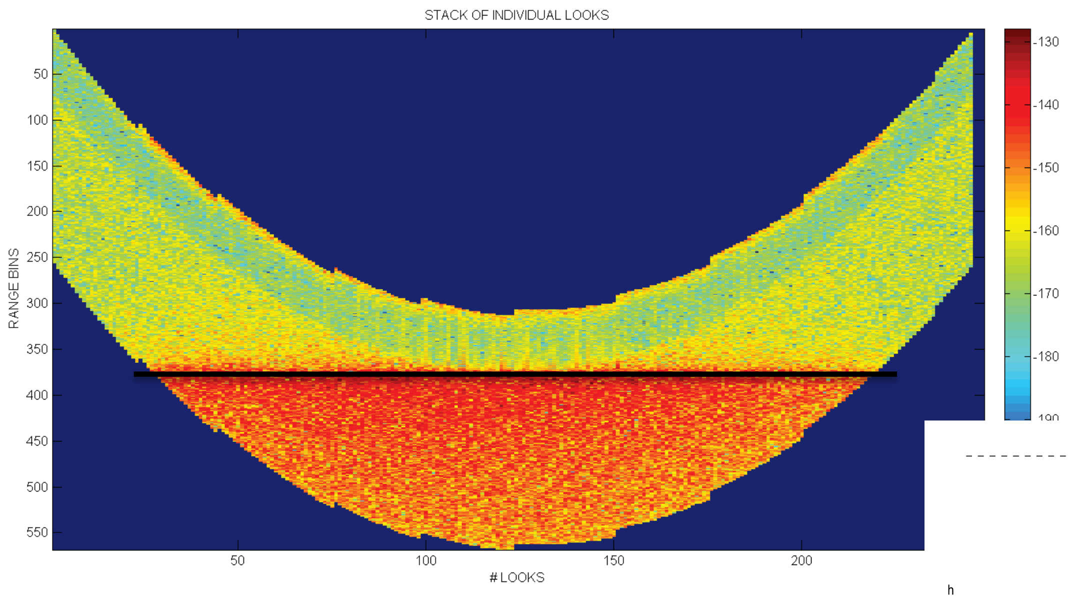

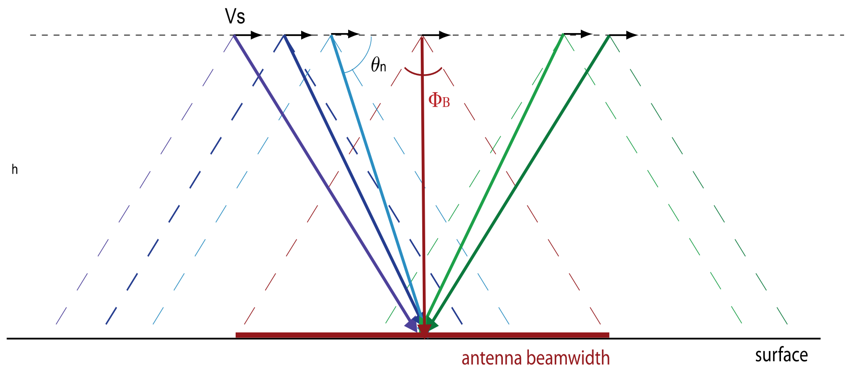

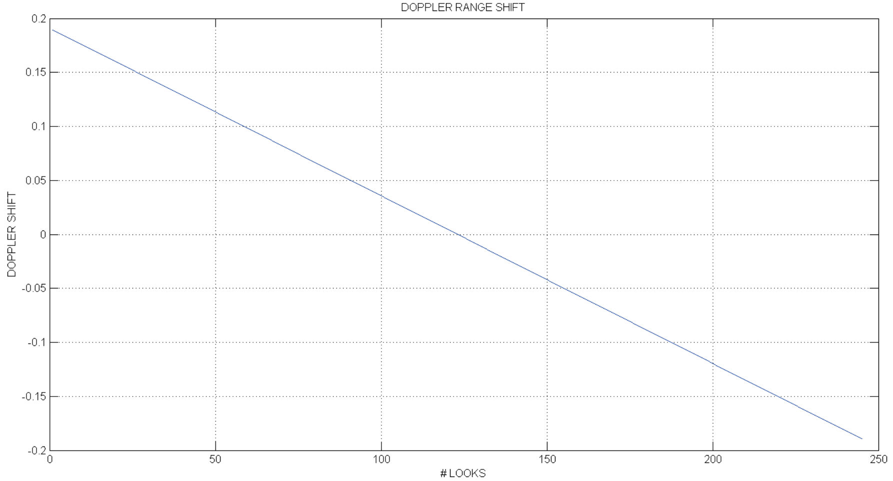

RANGE ALIGNMENT MUST BE PRECISE !

A way to verify the quality of the range alignment operation is to perform an over-sampled stacking on a transponder data pass.
The looks alignment in range is as much precise as half centimeter.

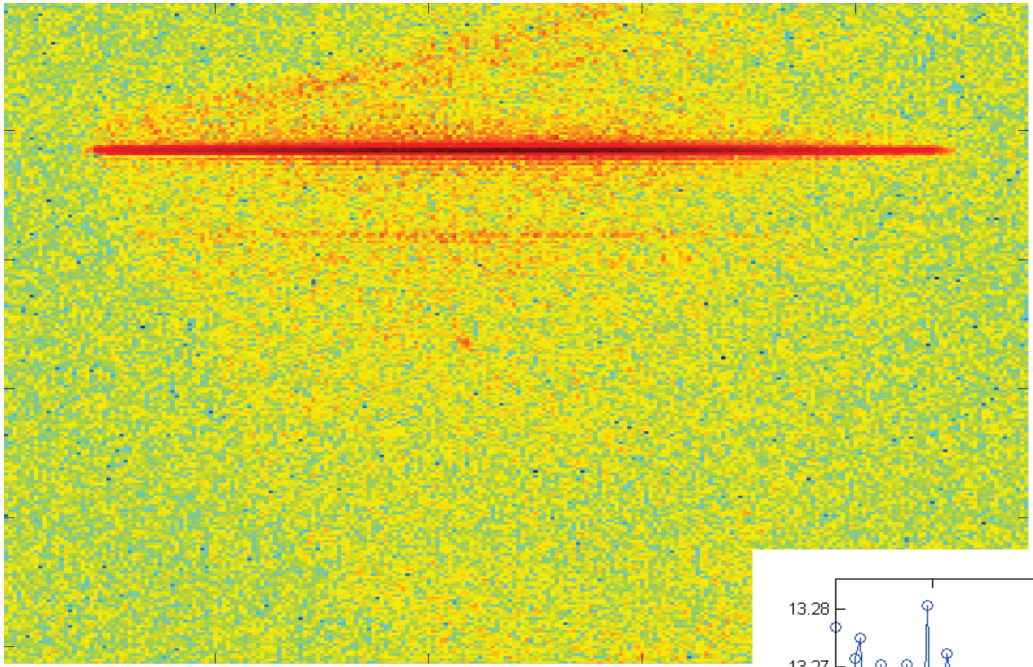

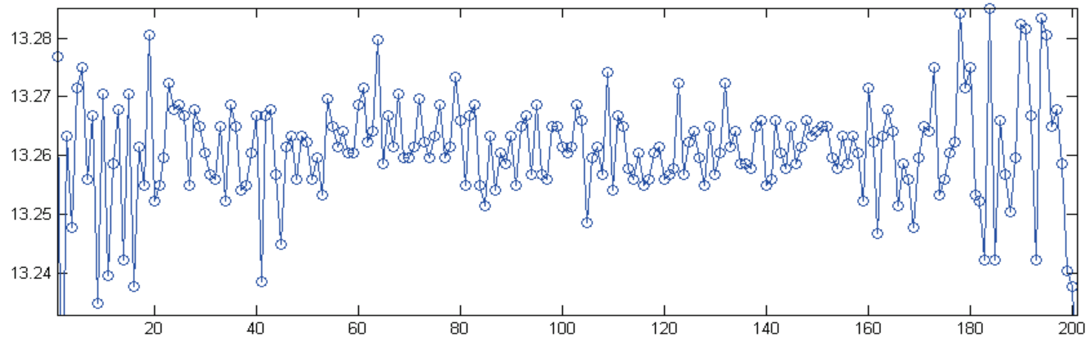

RANGE ALIGNMENT MUST BE PRECISE !

A way to verify the quality of the range alignment operation is to perform an over-sampled stacking on a transponder data pass.
The looks alignment in range is as much precise as half centimeter.

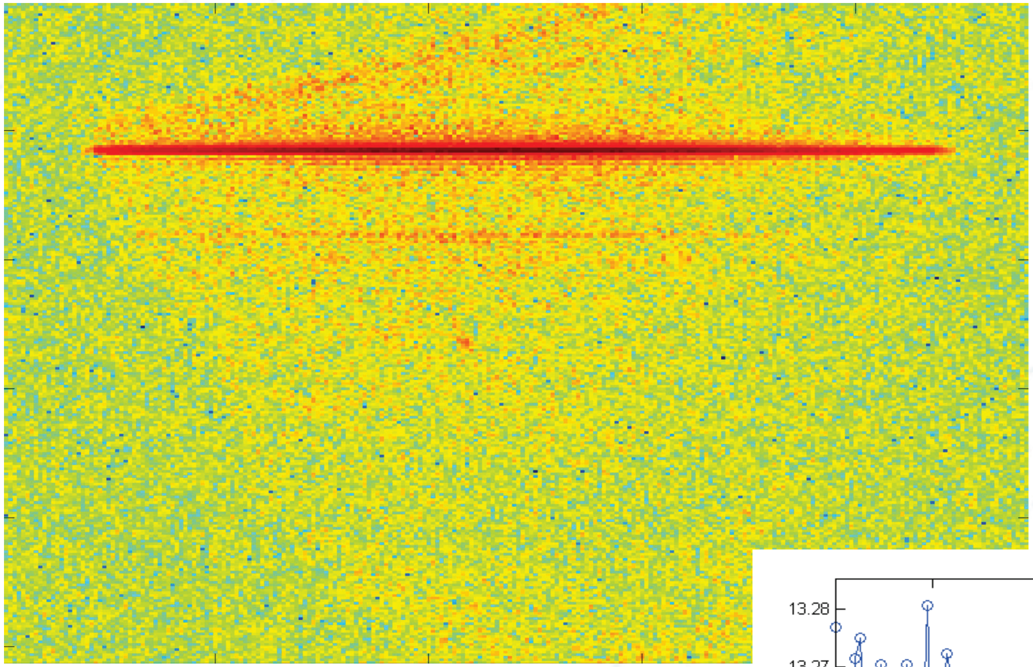

Range Alignment is carriot out by a pre range-FFT multiplication of the burst with a phasor (shift's theorem) for the fine delay's part

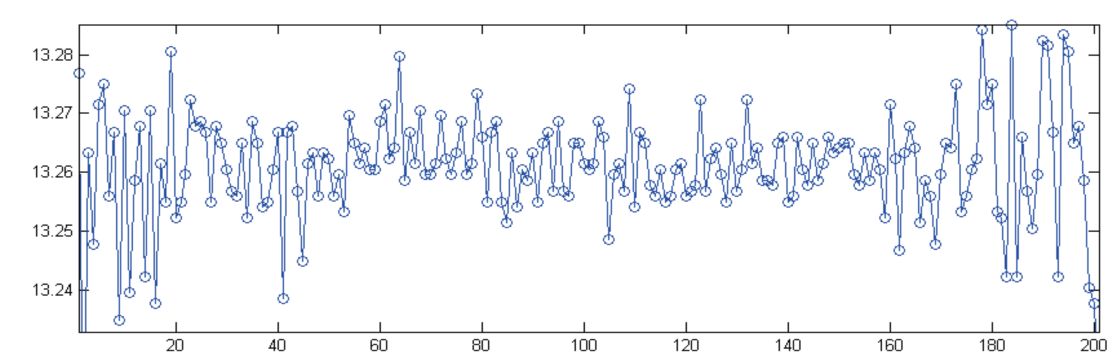

RANGE COMPRESSION

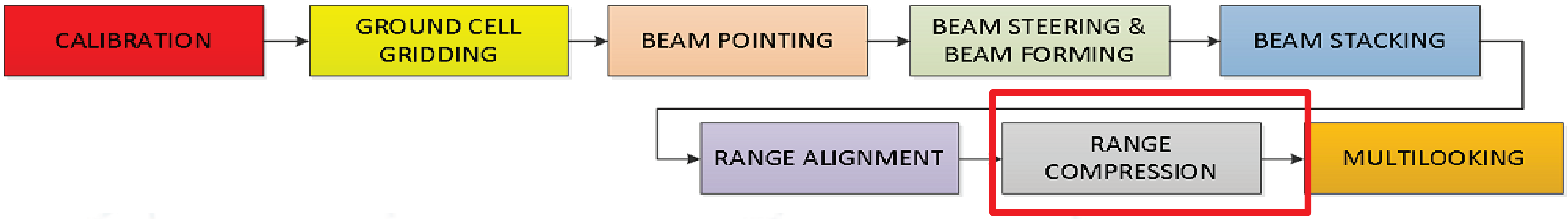

As consequence of deramping theory, Range Compression is carried out as simply Fast Fourier Transform in range direction of the stack data.

This processing step is common with Classic Altimetry.

After this step, we have around half meter of vertical resolution

ZERO-PADDING =>DOUBLE SAMPLING

In order to avoid aliasing of the signal that would normally occur due to the doubling of the signal bandwidth when square-law detecting the signal itself, prior of the range compression the Doppler Beams waveforms can be zero-padded (Jensen's sampling), doubling this way the number of samples. The net effect is to over-sample the range compressed signal by a factor of 2. This is particularly useful over specular surfaces

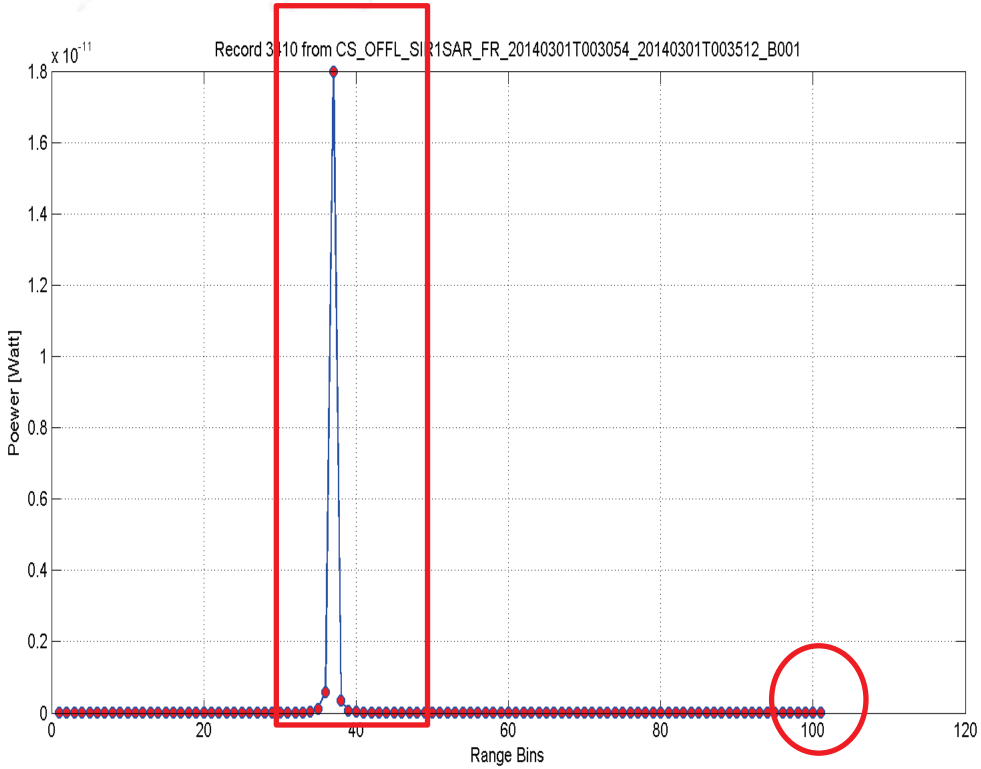

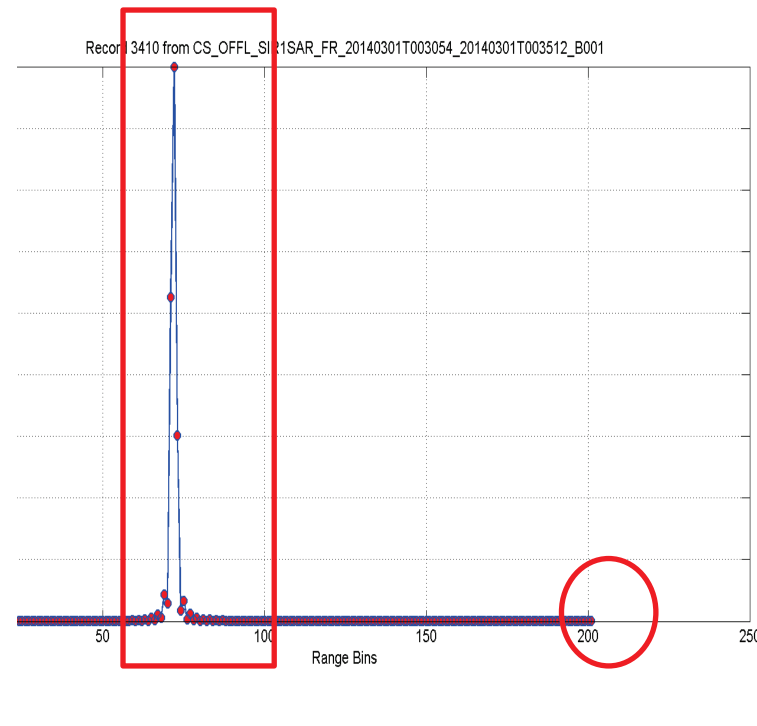

STACK EXPLOITATION →RIP (Range Integrated Power)

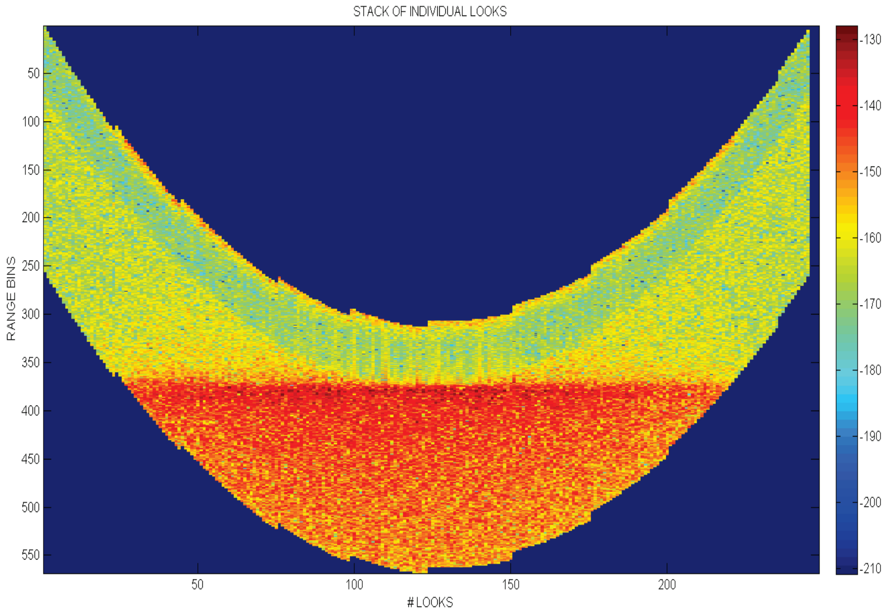

STACK EXPLOITATION → RIP (Range Integrated Power)

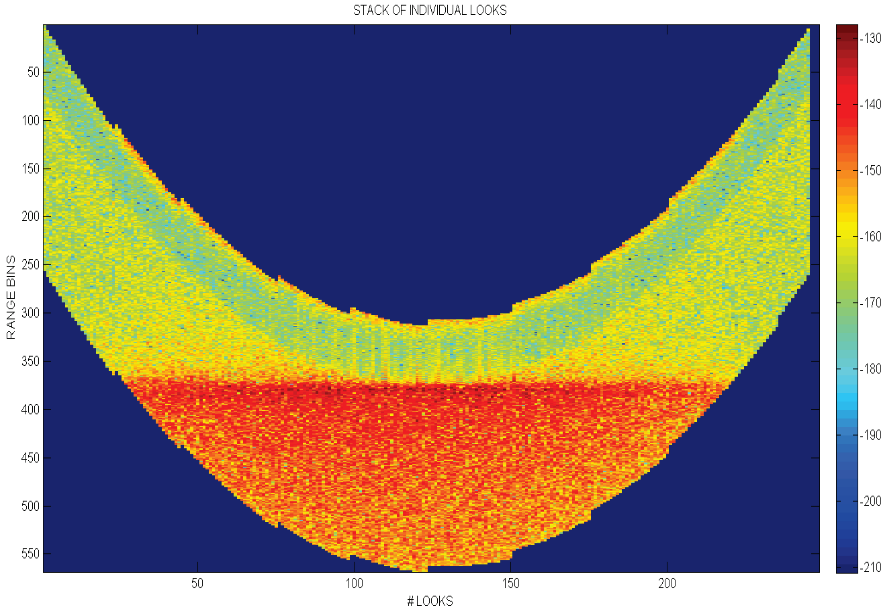

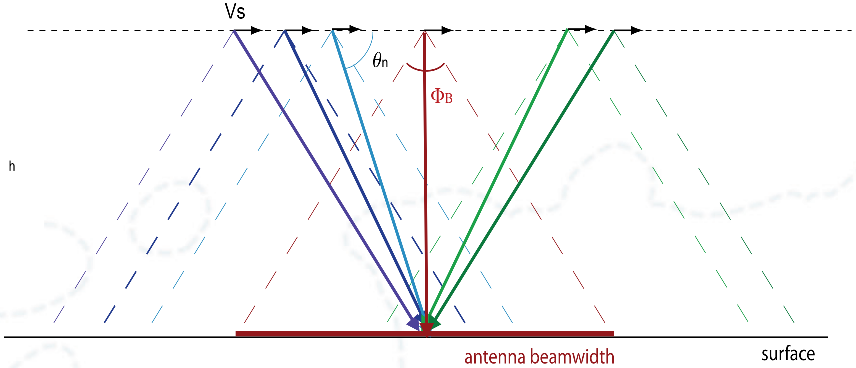

STACK EXPLOITATION →RIP (Range Integrated Power)

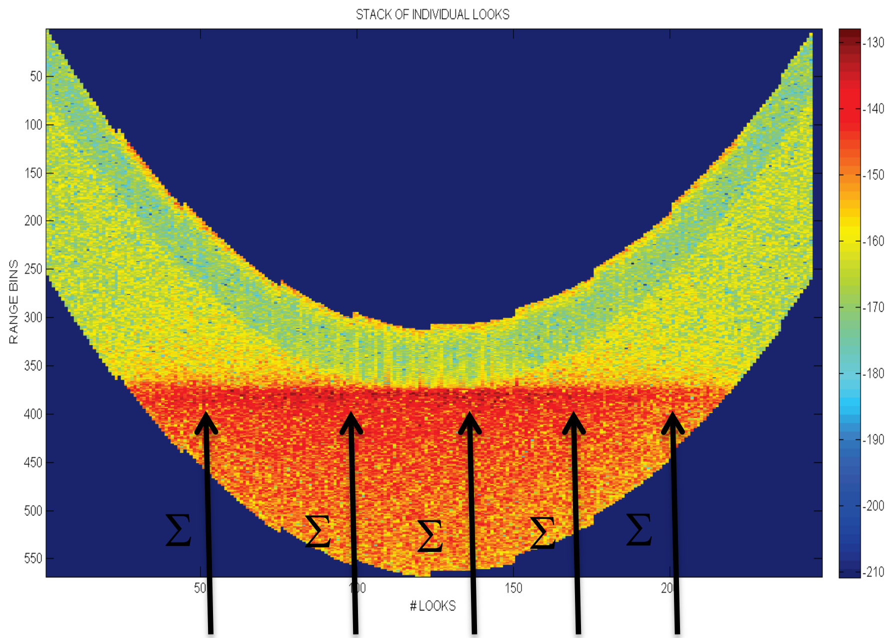

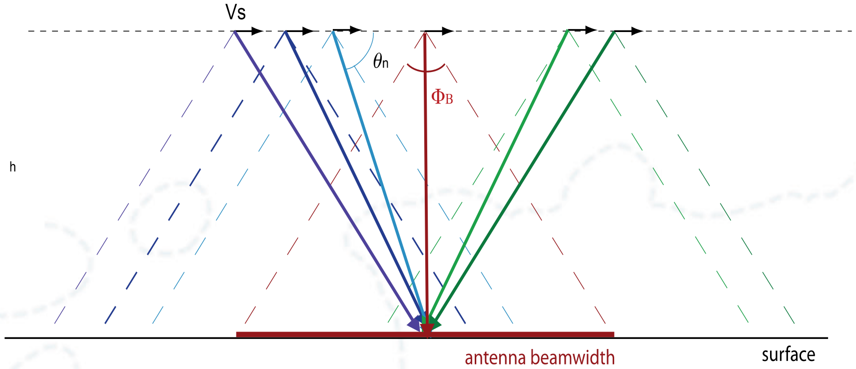

STACK EXPLOITATION →RIP (Range Integrated Power)

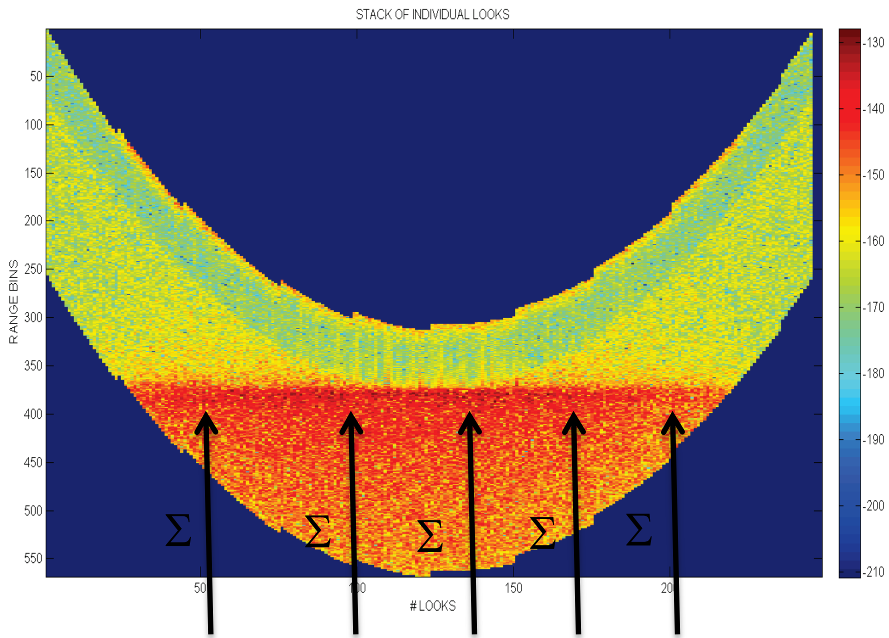

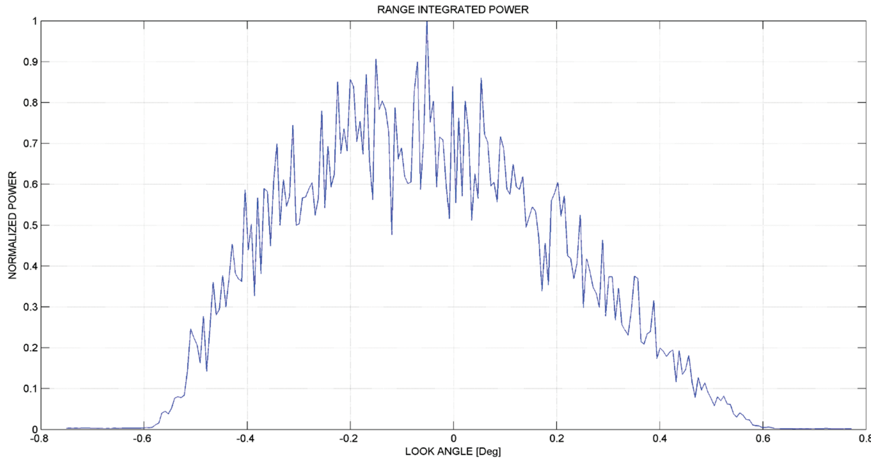

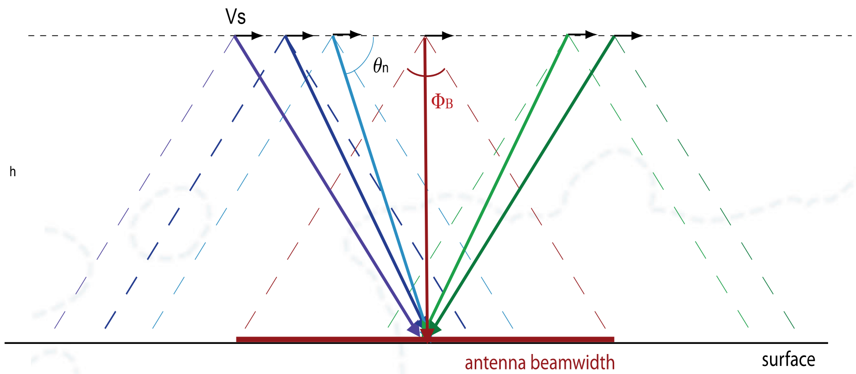

STACK EXPLOITATION →RIP (Range Integrated Power)

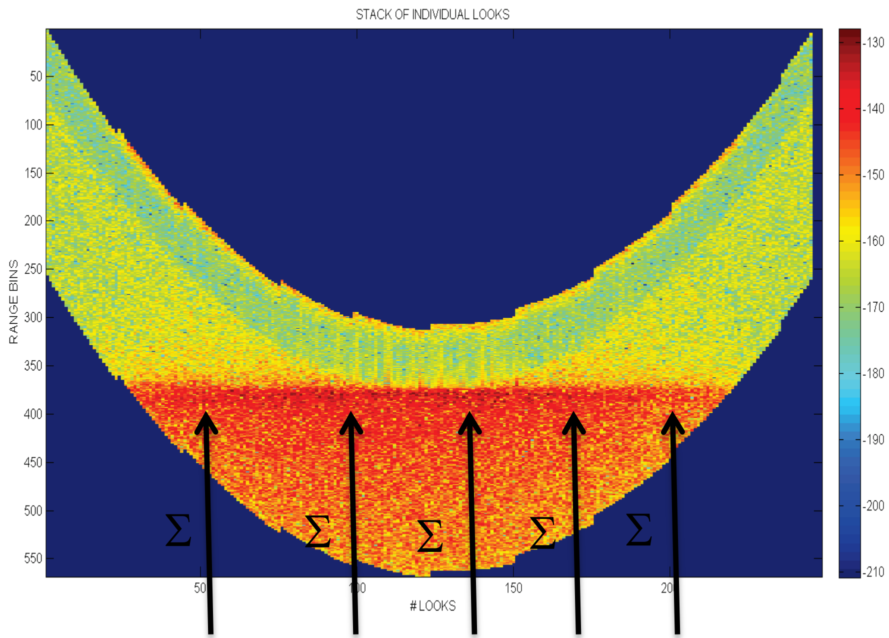

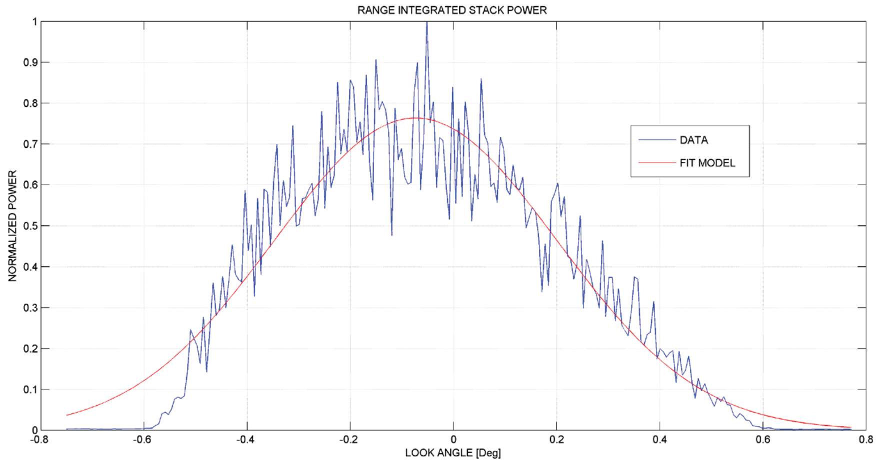

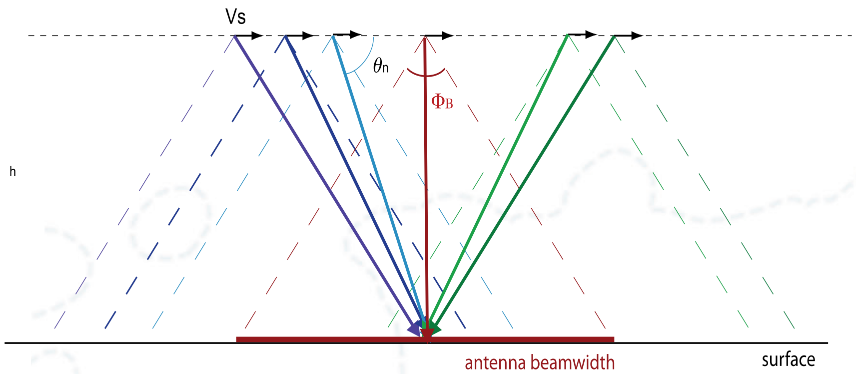

STACK EXPLOITATION →RIP (Range Integrated Power)

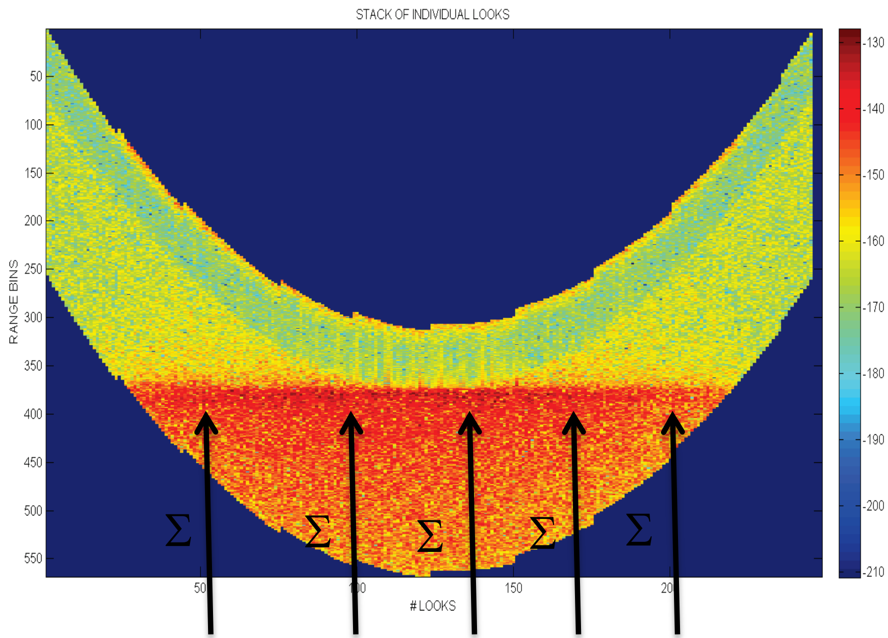

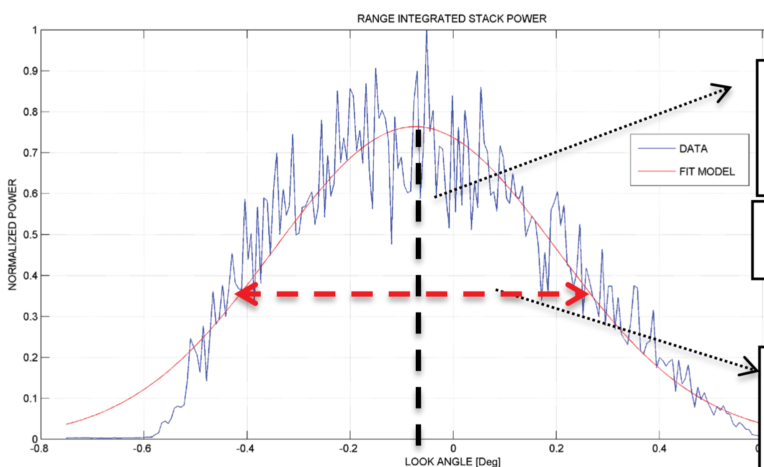

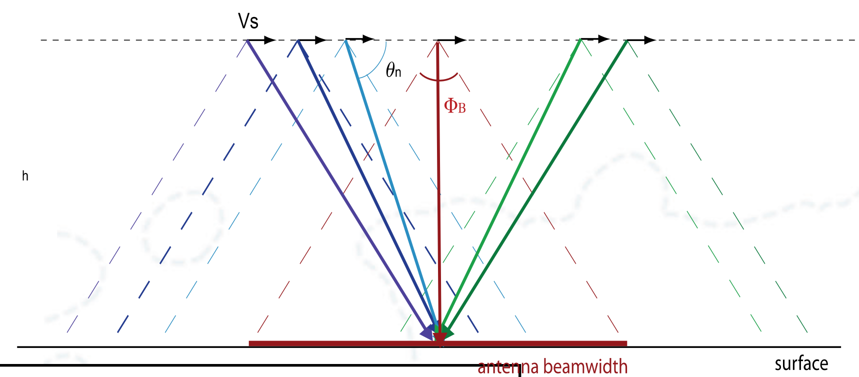

Offset depending on pitch mispointing

Power Distribution skewness and kurtosis.

3db aperture depending on sea surface mean square Slope

STACK EXPLOITATION →RIP (Range Integrated Power)

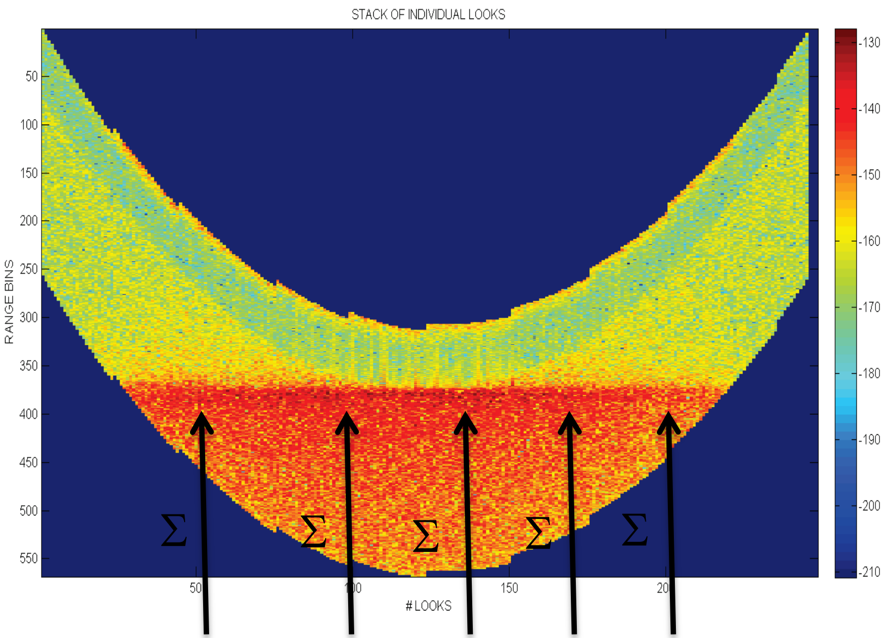

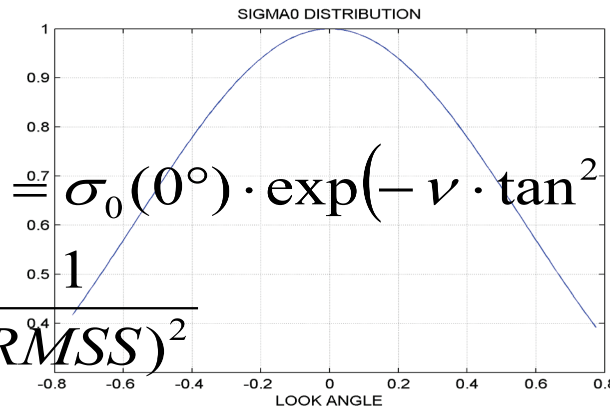

$$\sigma_0(\theta) = \sigma_0(0°) \cdot \exp\left(-\nu \cdot \tan^2 \theta\right)$$

$$\nu = \frac{1}{(RMSS)^2}$$

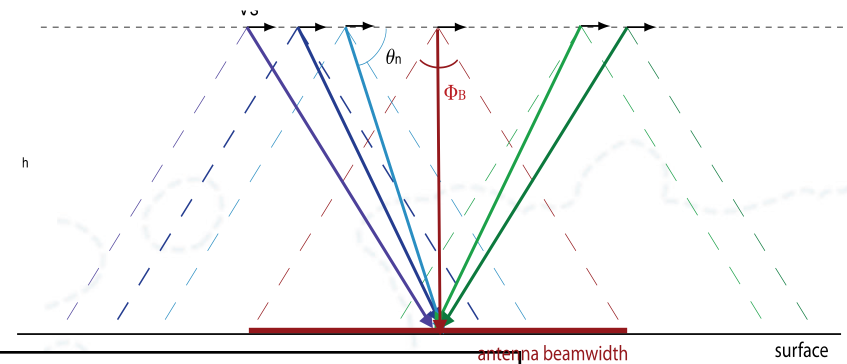

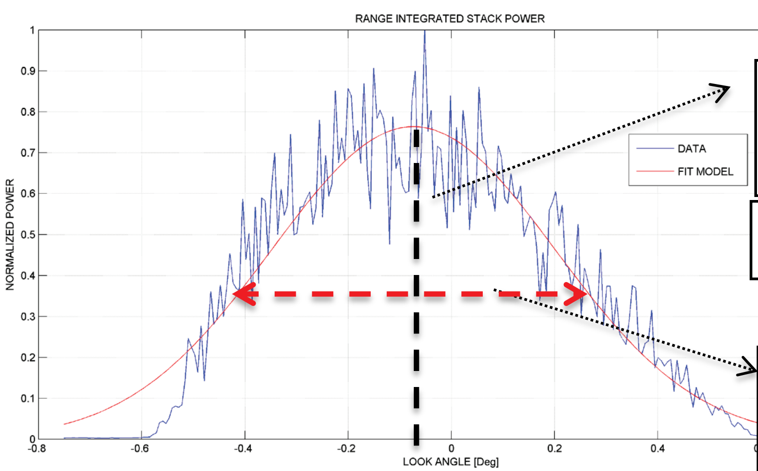

Offset depending on pitch mispointing

Power Distribution skewness and kurtosis.

3db aperture depending on sea surface mean square Slope

RIP Radargram for a sea ice pass

At the end, RIP is a new waveform independent from the multi-looked echo containing surface geophysical information (surface slope, mean square slope, surface skewness and peakness)

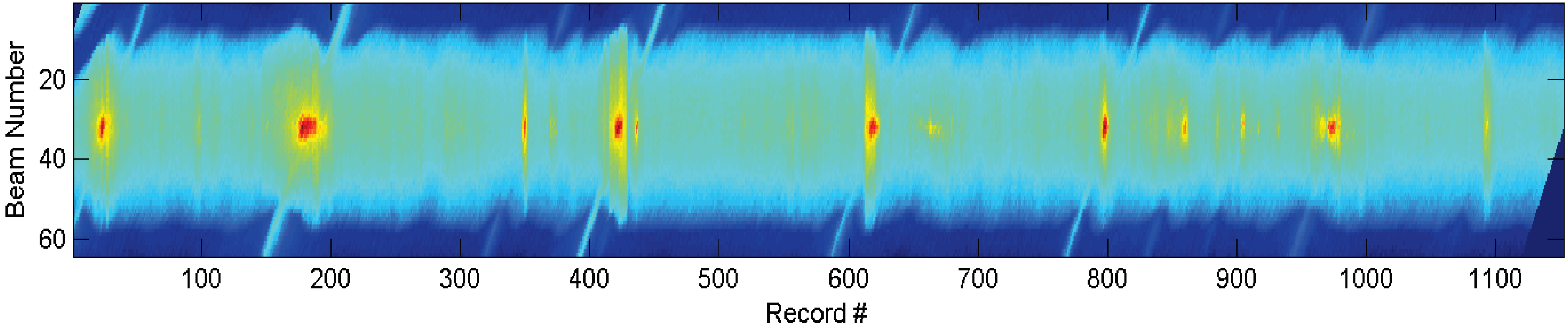

RIP Radargram for a sea ice pass

At the end, RIP is a new waveform independent from the multi-looked echo containing surface geophysical information (surface slope, mean square slope, surface skewness and peakness)

Sea-Ice leads, can be even recognized by visual inspection

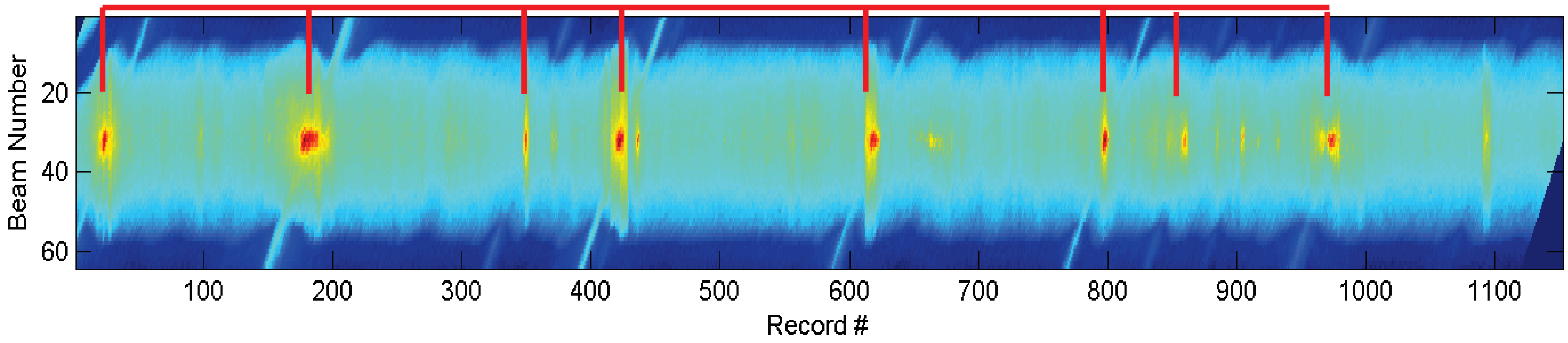

MULTILOOKING

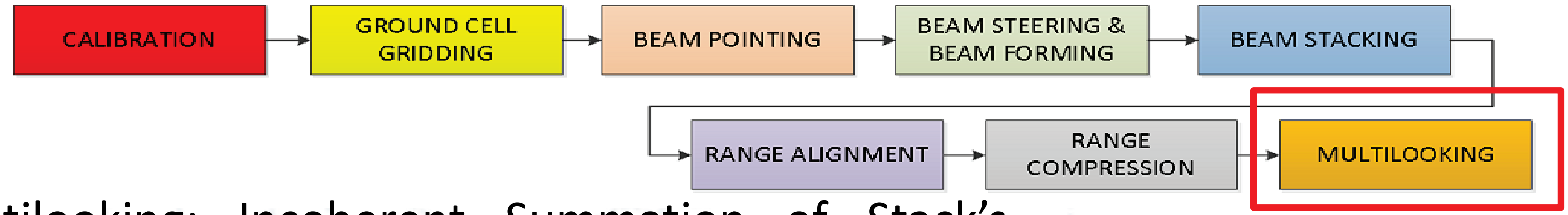

Multilooking: Incoherent Summation of Stack's looks in Azimuth direction.

The purpose of the multilooking is to knock down the speckle noise. Note that the "far from zero-Doppler" looks are not "complete" and hence not as much useful as "around zero-Doppler" looks

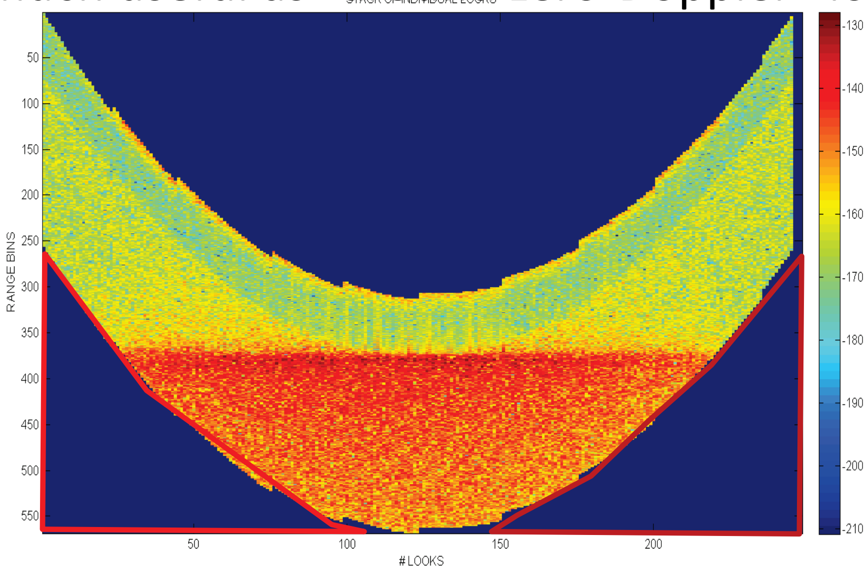

MULTILOOKING

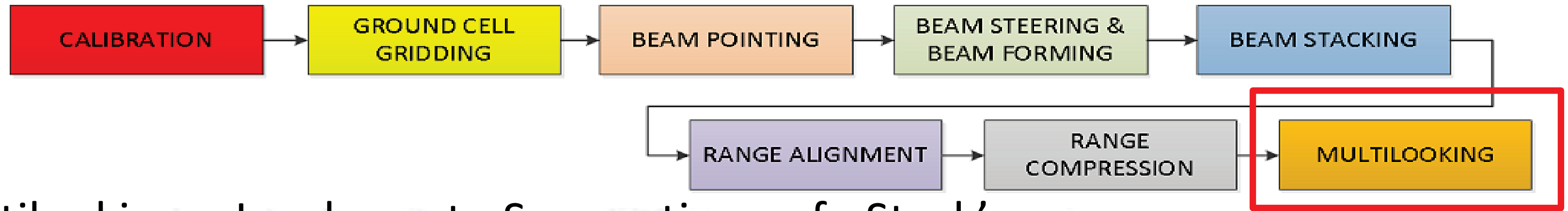

Multilooking: Incoherent Summation of Stack's looks in Azimuth direction.

The purpose of the multilooking is to knock down the speckle noise. Note that the "far from zero-Doppler" looks are not "complete" and hence not as much useful as "around zero-Doppler" looks

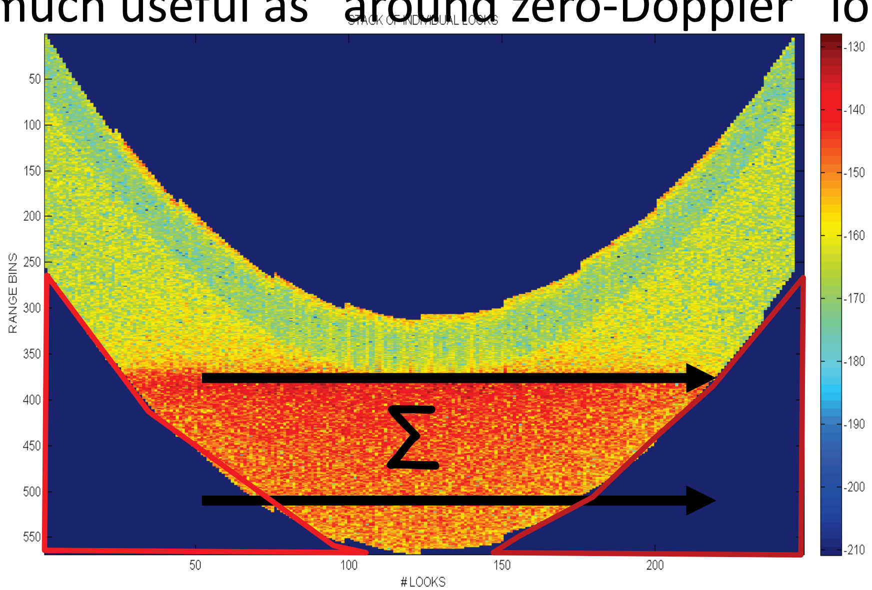

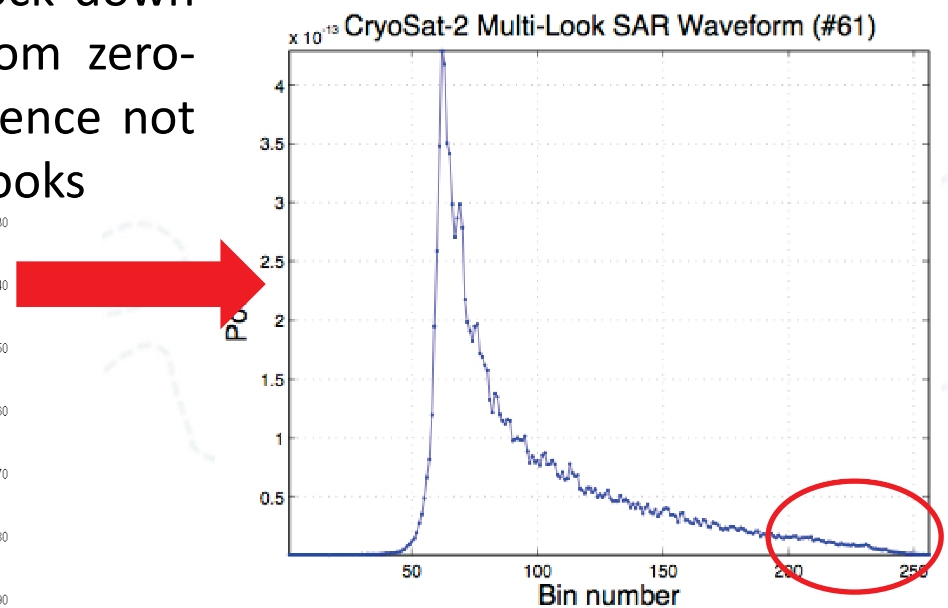

MULTILOOKING

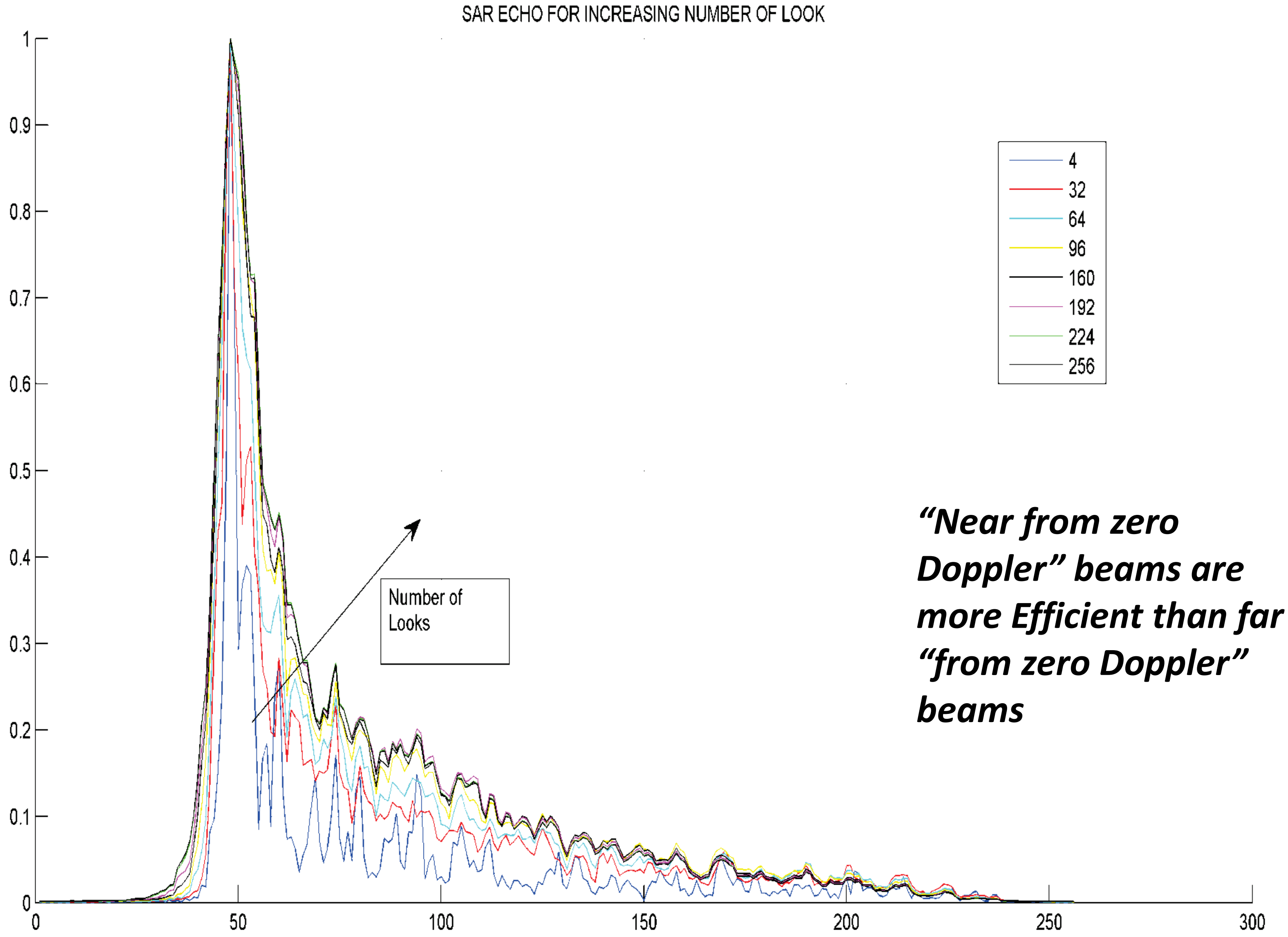

"Near from zero Doppler" beams are more Efficient than far "from zero Doppler" beams

MULTILOOKING Strategies

Different ways to perform multilooking are possible: for instance scaling the waveform by the number of not-zero in the stack (Scagliola et al.) or compensate the stack for the azimuth antenna pattern

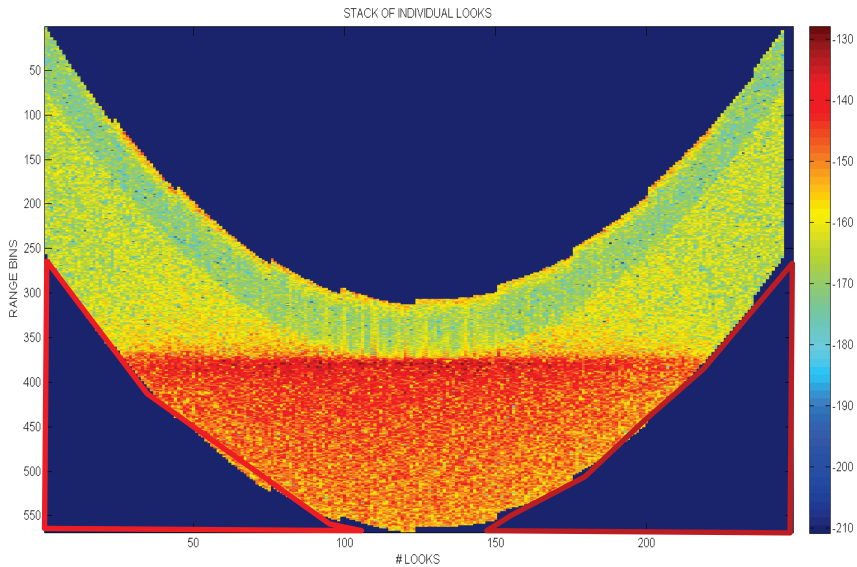

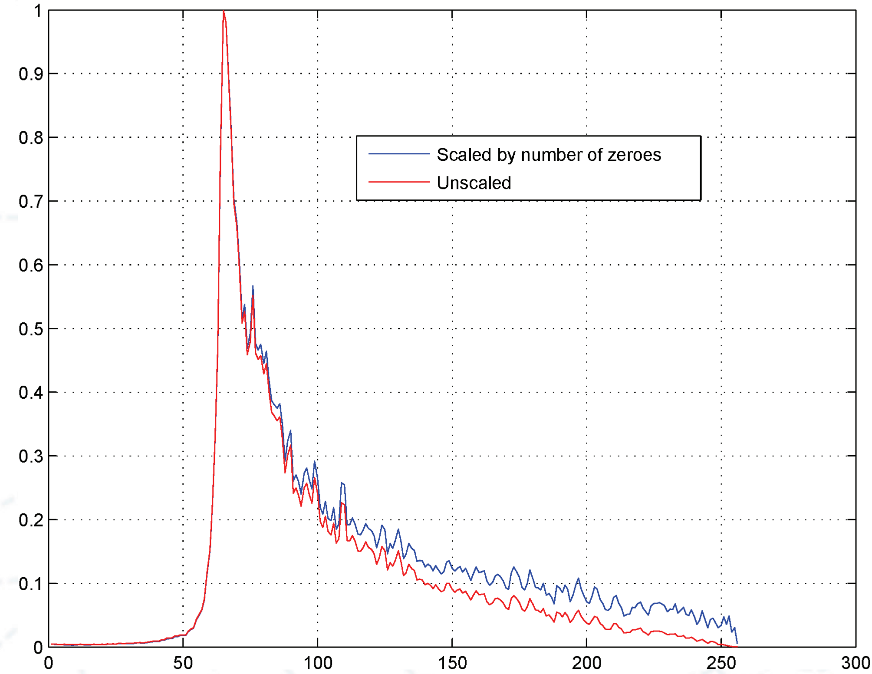

Range Window Expansion

Prior making multilooking, it necessary to decide which is the ´´center´´ of the stack in the range direction; If this decision can be simple for open ocean (using strongest power criterium), can be tricky over coastal zone and inland water.

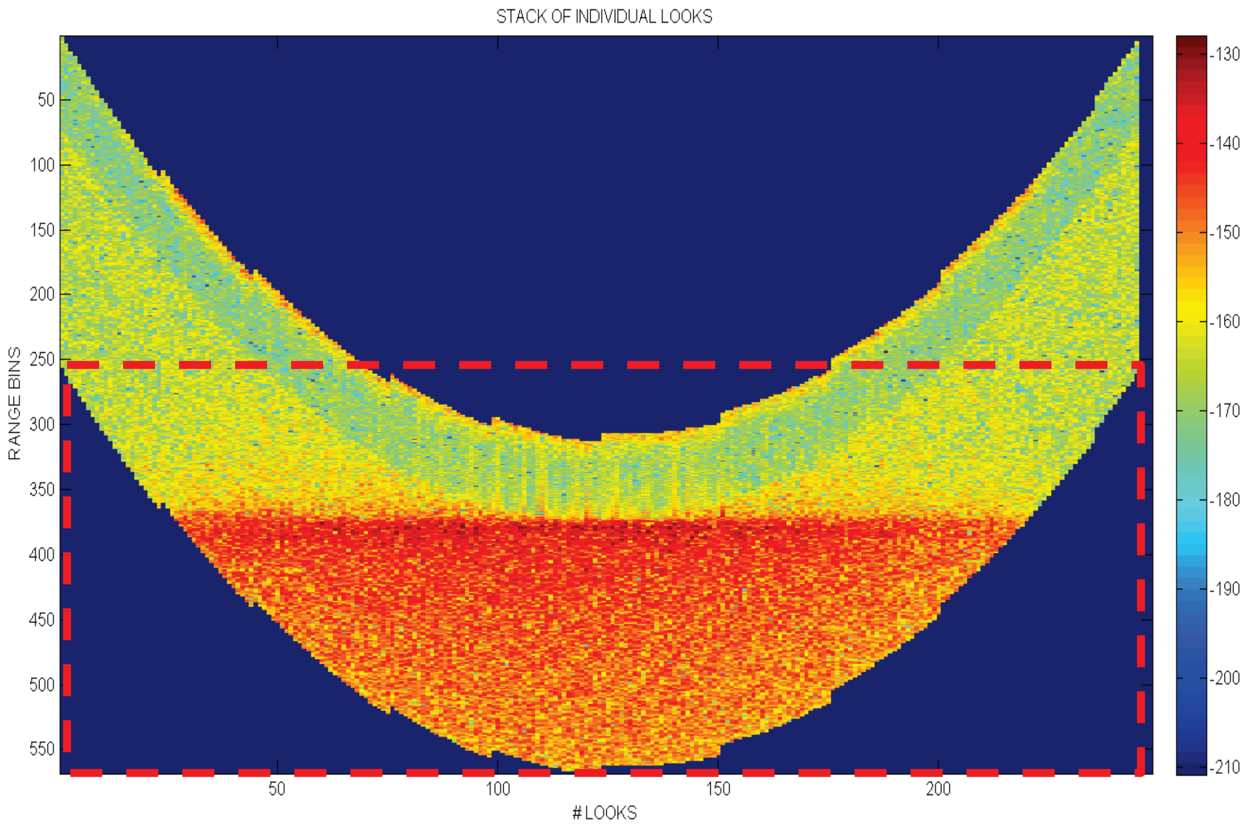

SAR with an Extended Range Window

PROBLEM:

Actually, in the CryoSat-2 L1b PDGS after range migration, a simple OCOG retracker is implemented to subset in range the “good” part of the SAR stack and accommodate the multilooked echo in a fixed product size (128 bins). Of course OCOG **can not discriminate properly between weak nadir and strong off-nadir return.**

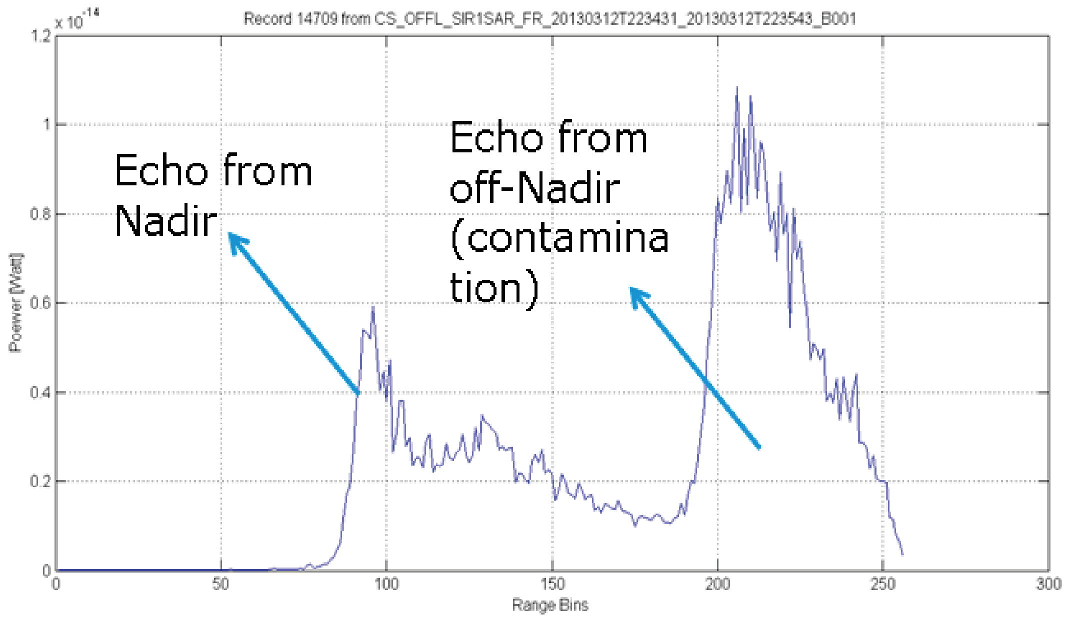

OPTIMAL SOLUTION:

Don’t subset the stack but double the size of the radar receiving window (i.e. extend the vertical swath) in the product and hence avoid the echo’s truncation

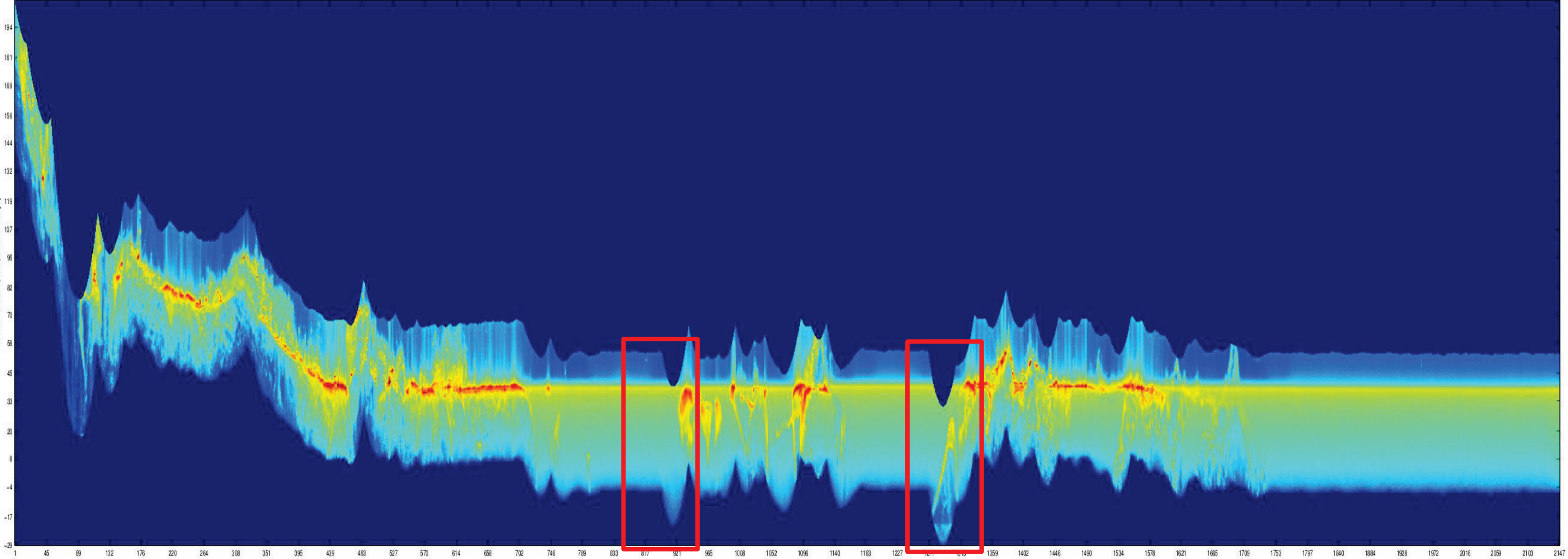

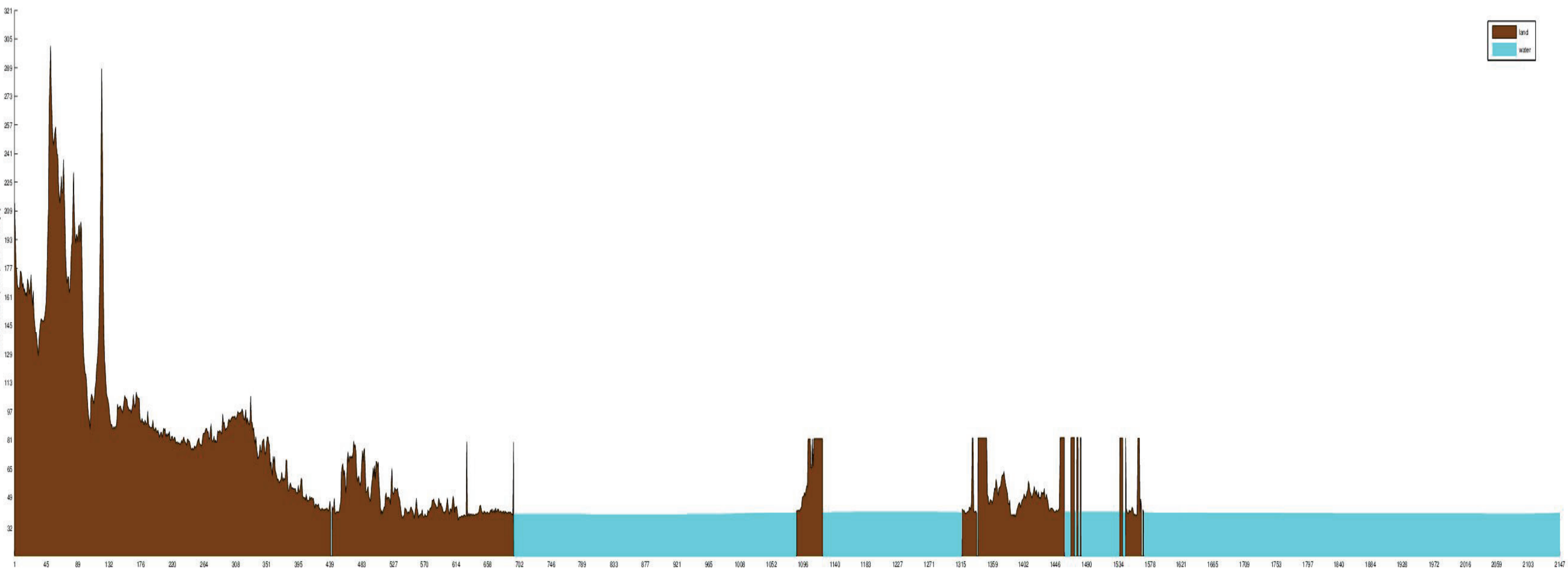
land
water

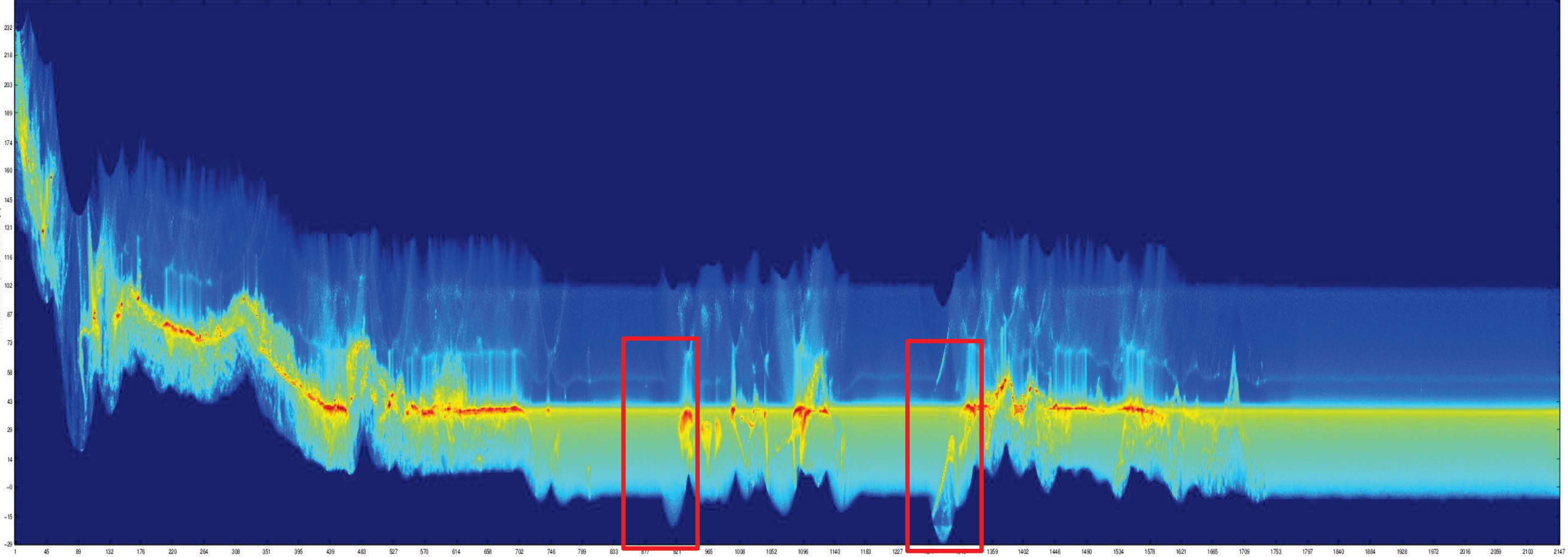

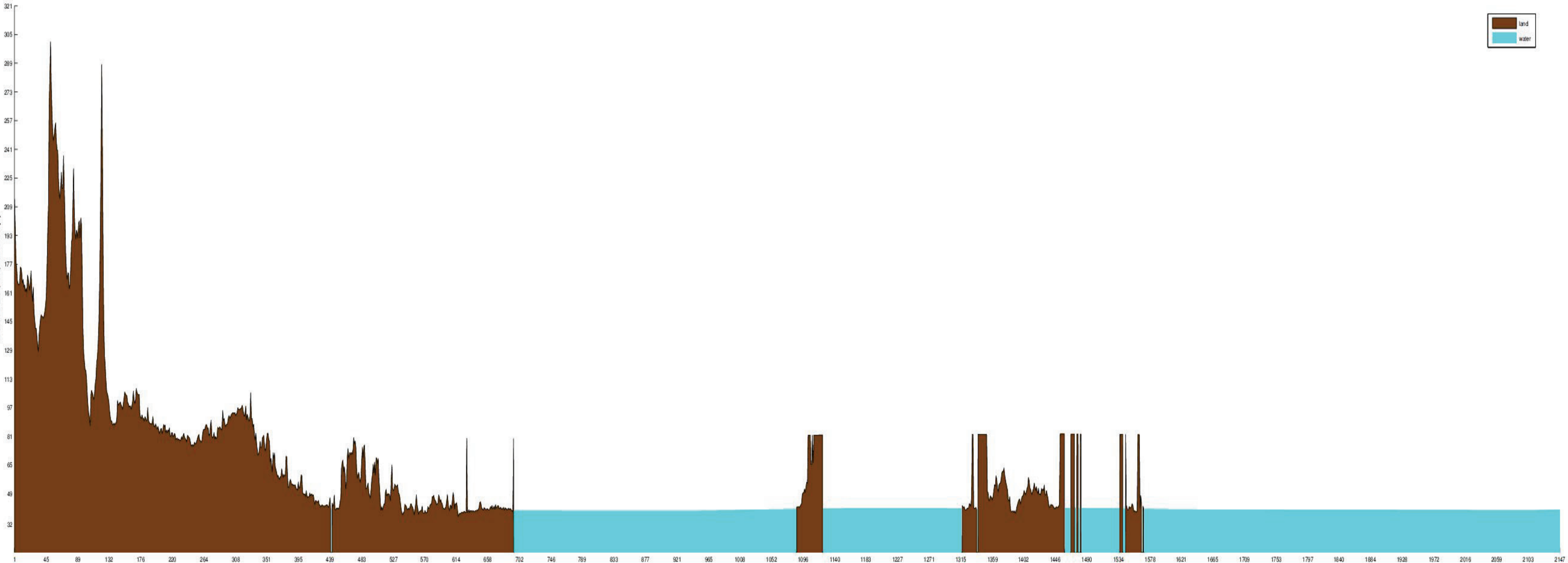
land
water

SAME PROBLEM OVER SEA-ICE

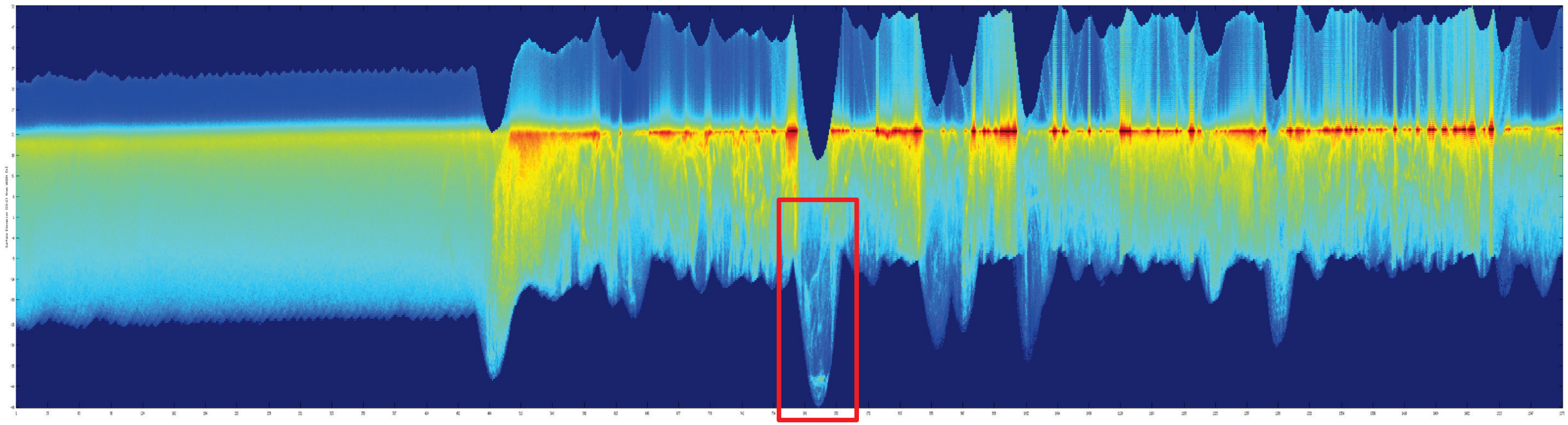

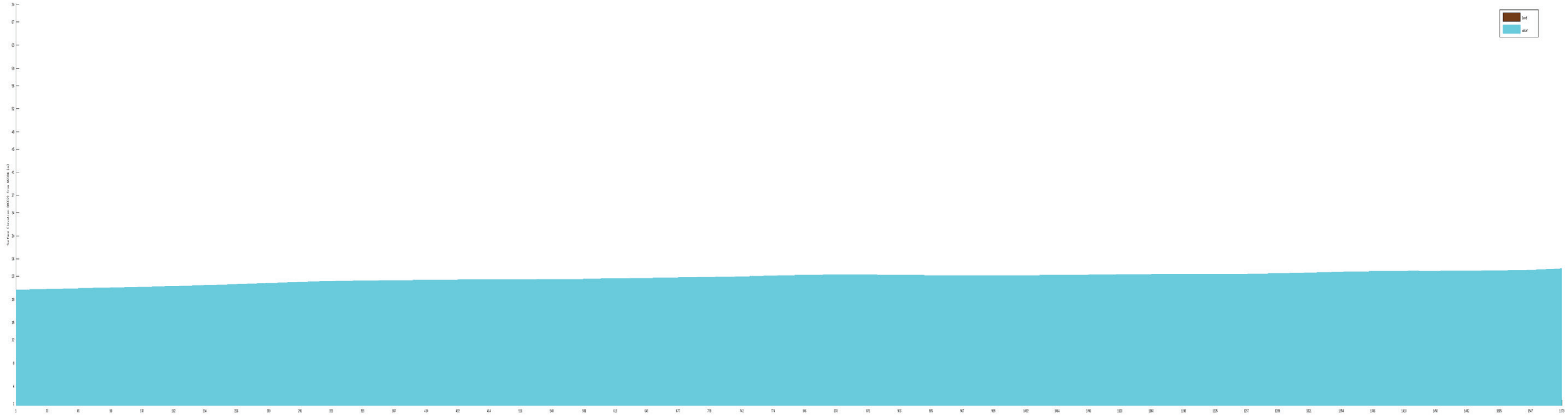

SAME PROBLEM OVER SEA-ICE

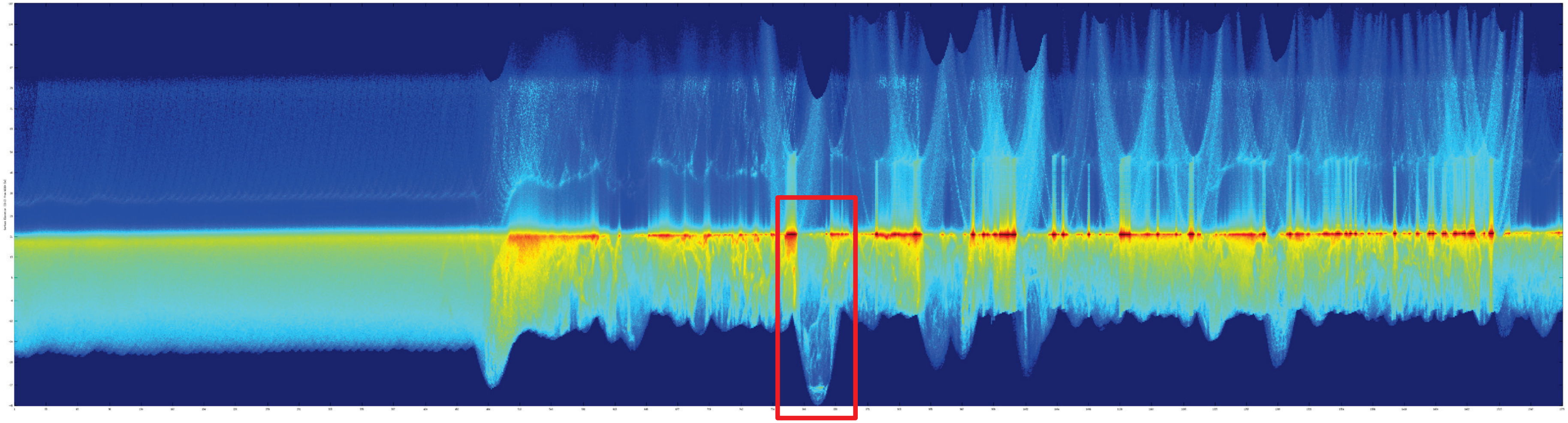

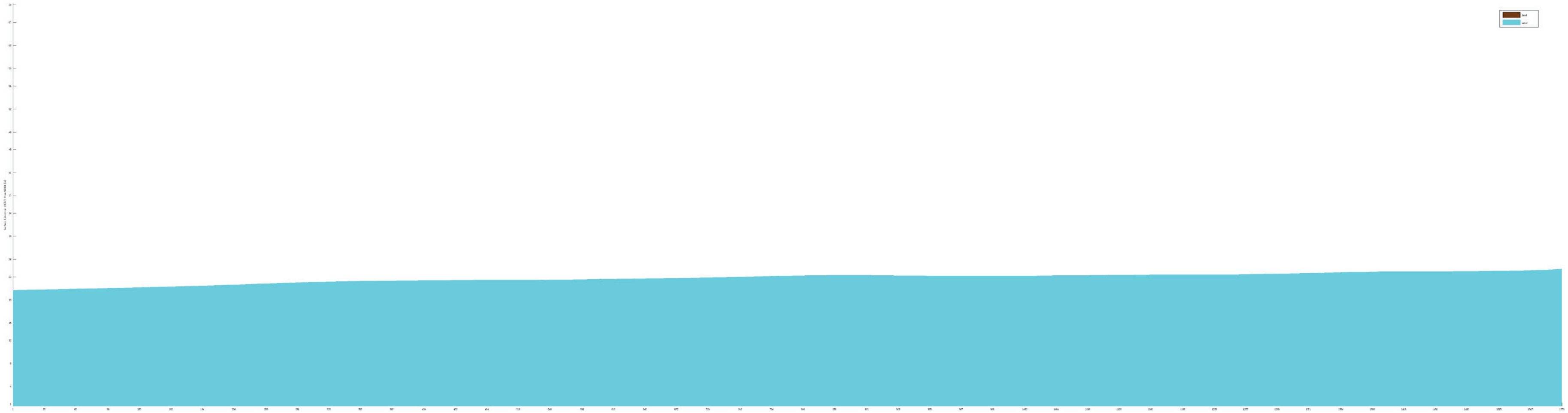

SPOTLIGHTED ALTIMETRIC MEASUREMENT

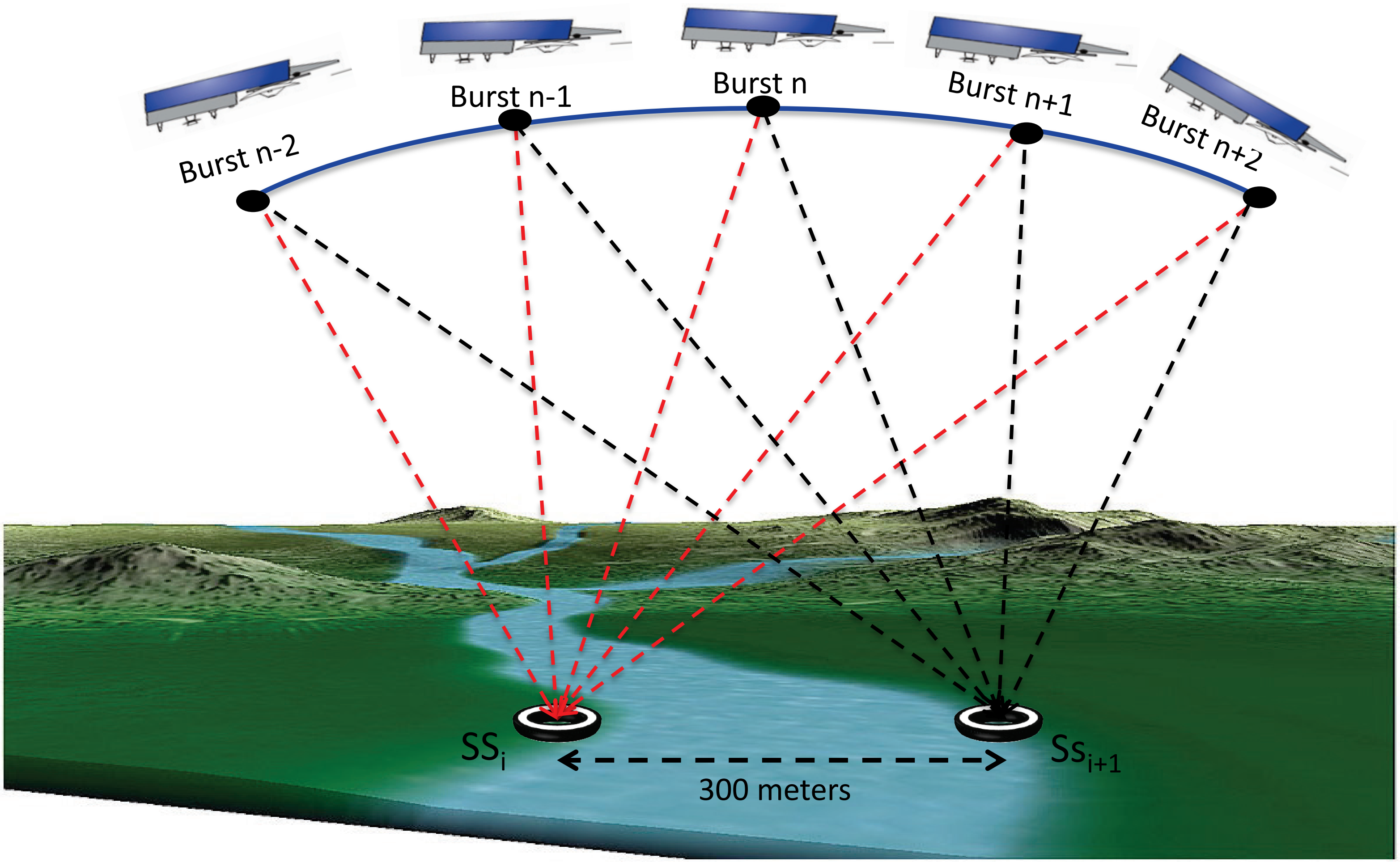

SPOTLIGHTED ALTIMETRIC MEASUREMENT

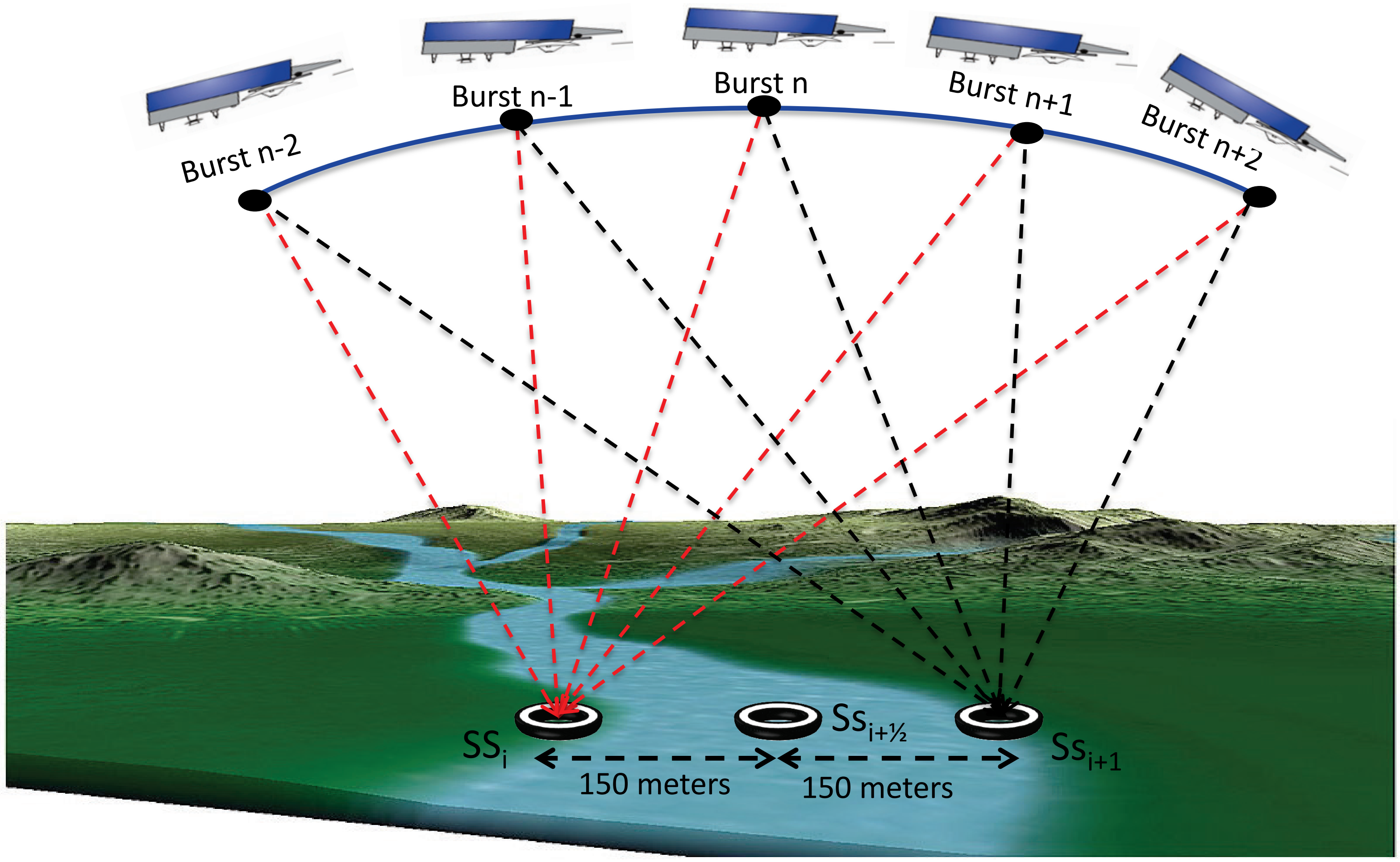

SPOTLIGHTED ALTIMETRIC MEASUREMENT

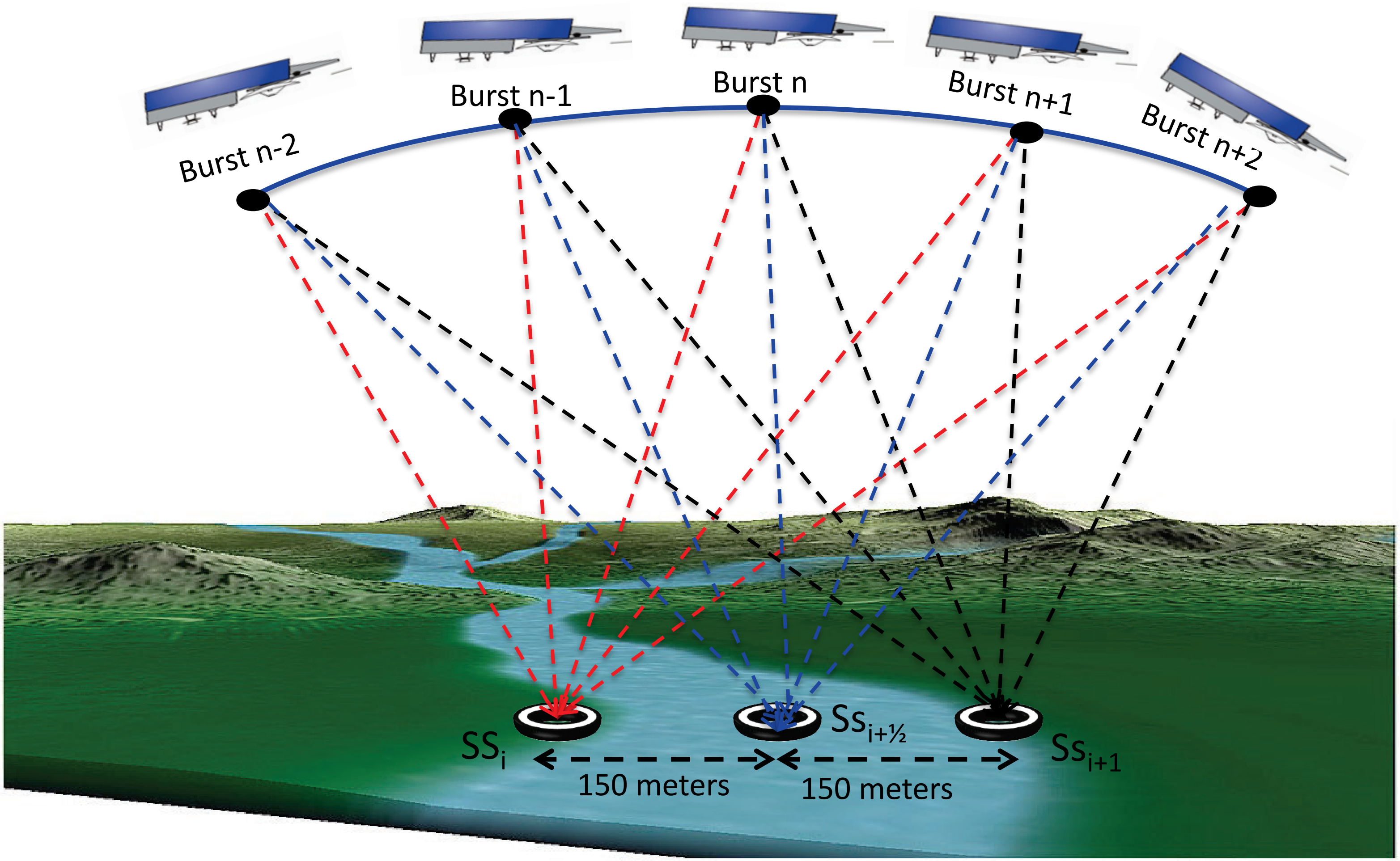

SPOTLIGHTED ALTIMETRIC MEASUREMENT

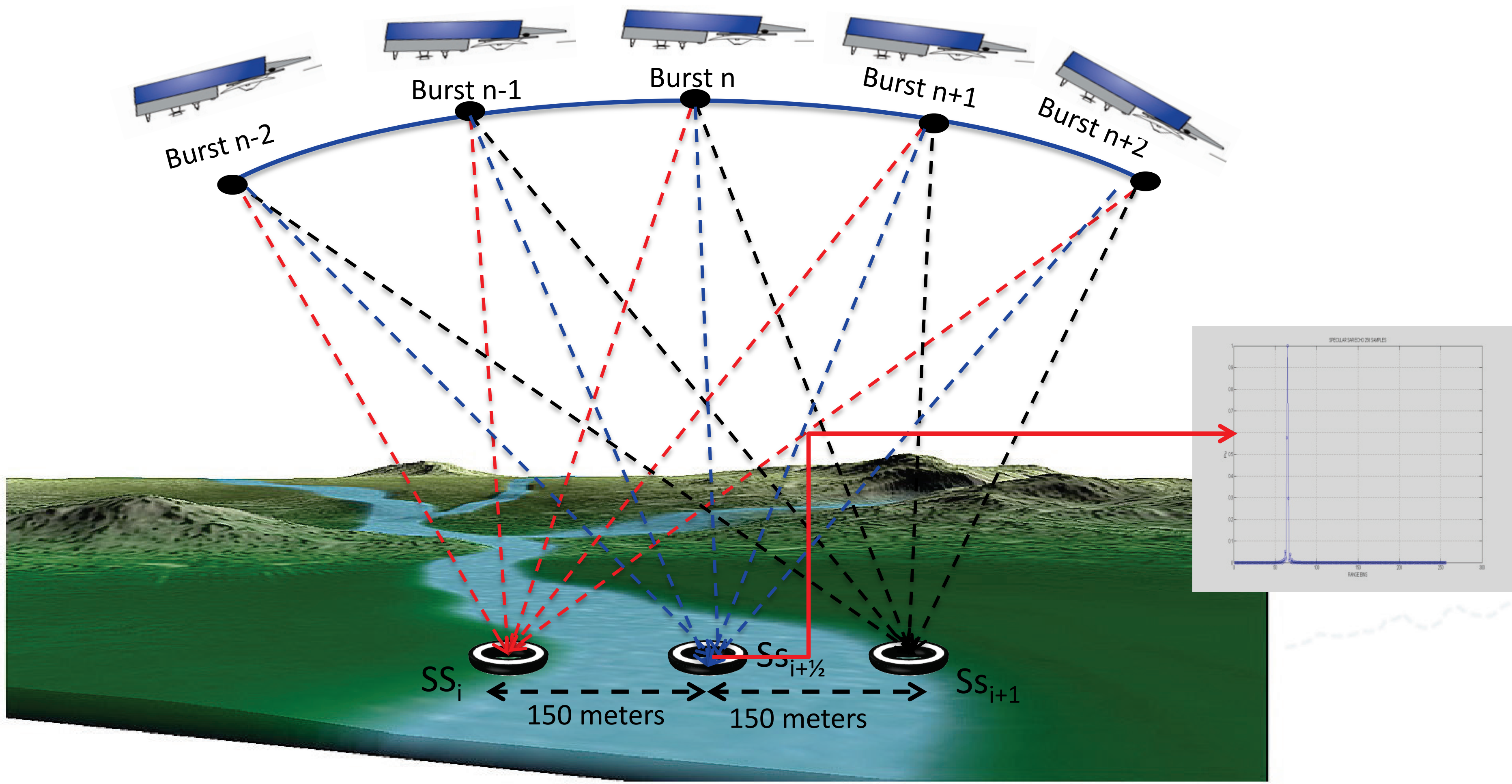

SPOTLIGHTED ALTIMETRIC MEASUREMENT

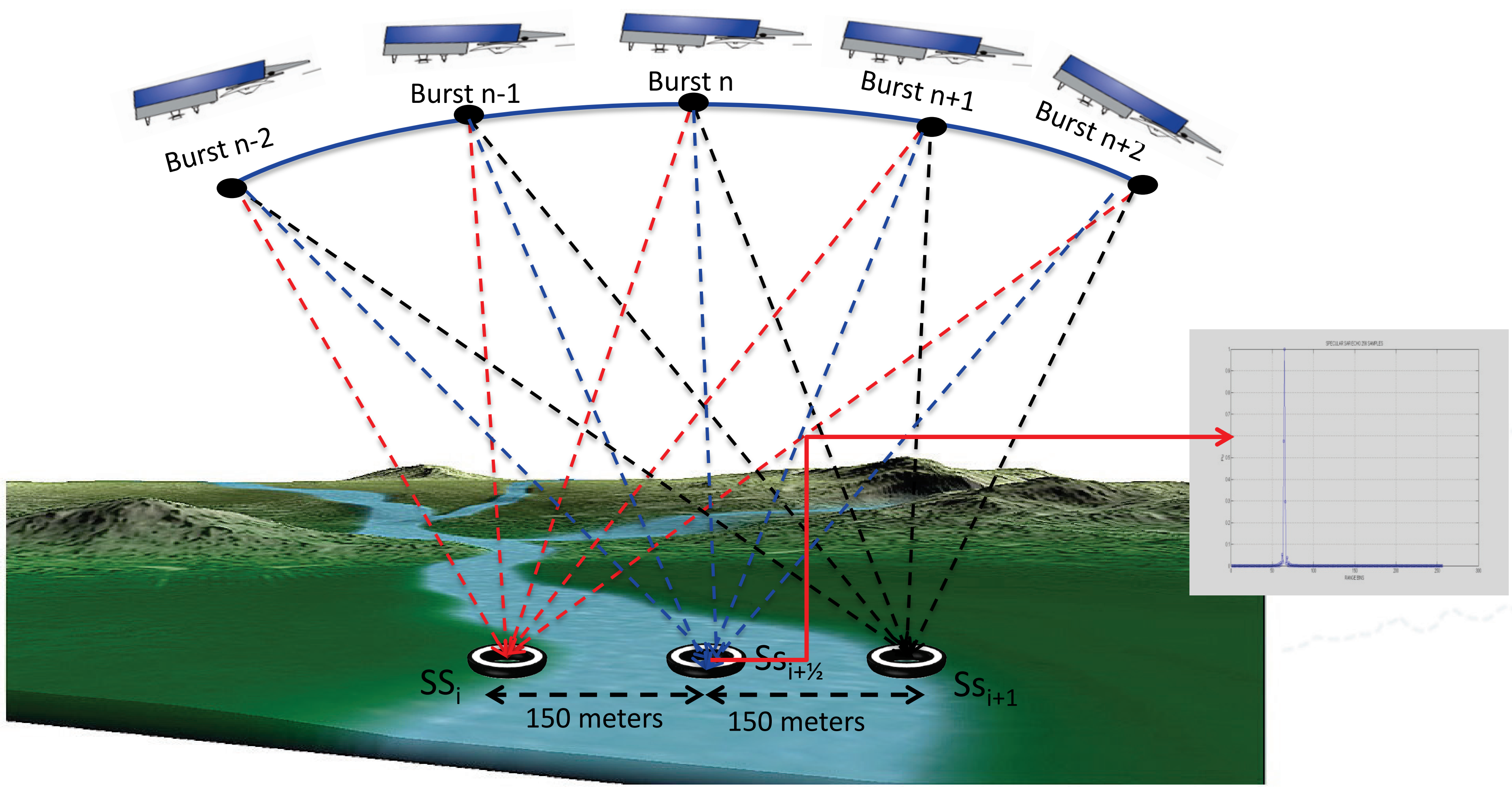

WE CAN HAVE A SAR ALTIMETRIC MEASUREMENT IN ANY GROUND POINT ALONG THE TRACK!

SPOTLIGHTED ALTIMETRIC MEASUREMENT

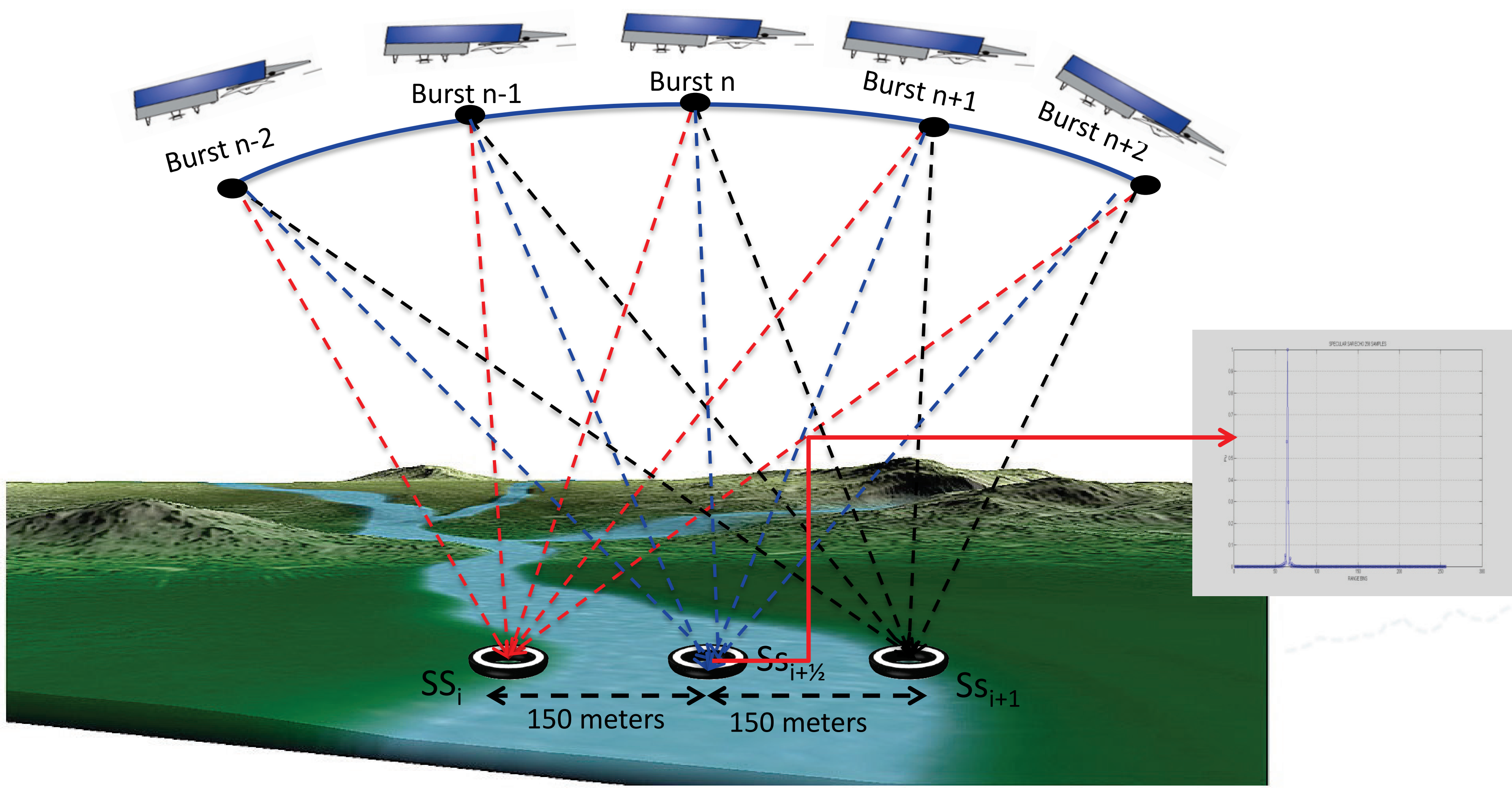

WE CAN HAVE A SAR ALTIMETRIC MEASUREMENT IN ANY GROUND POINT ALONG THE TRACK!

SAR ALTIMETRY @ FINER GRID STEP

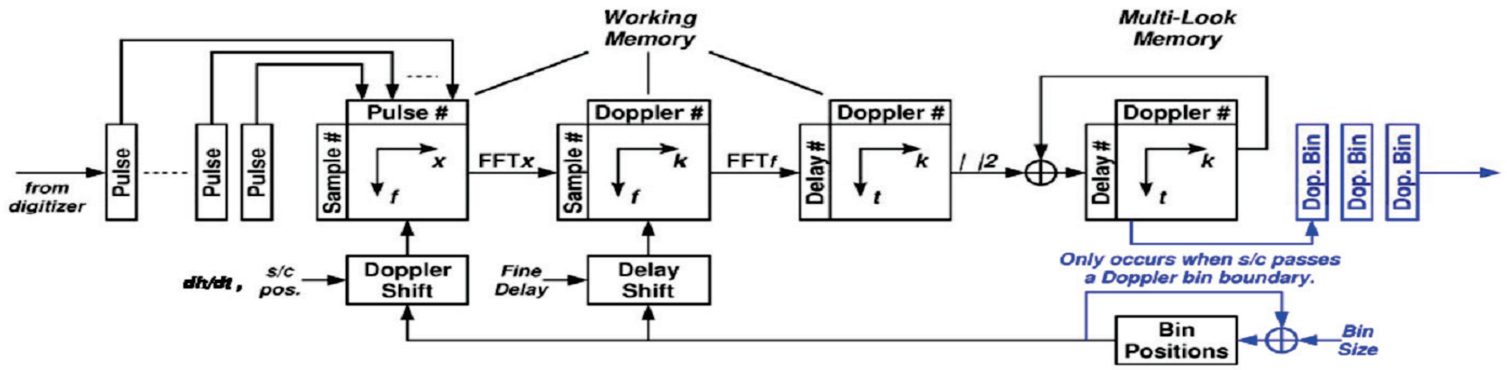

Above Image from Keith Raney

SAR ALTIMETRY @ FINER GRID STEP

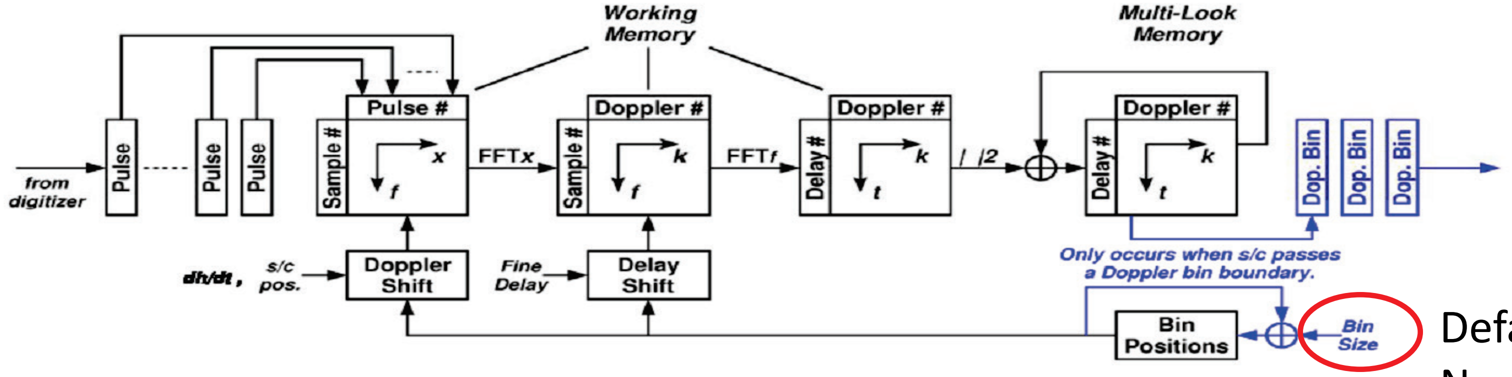

Default 300 m
Now fixed at 80 m

Above Image from Keith Raney

SAR ALTIMETRY @ FINER GRID STEP

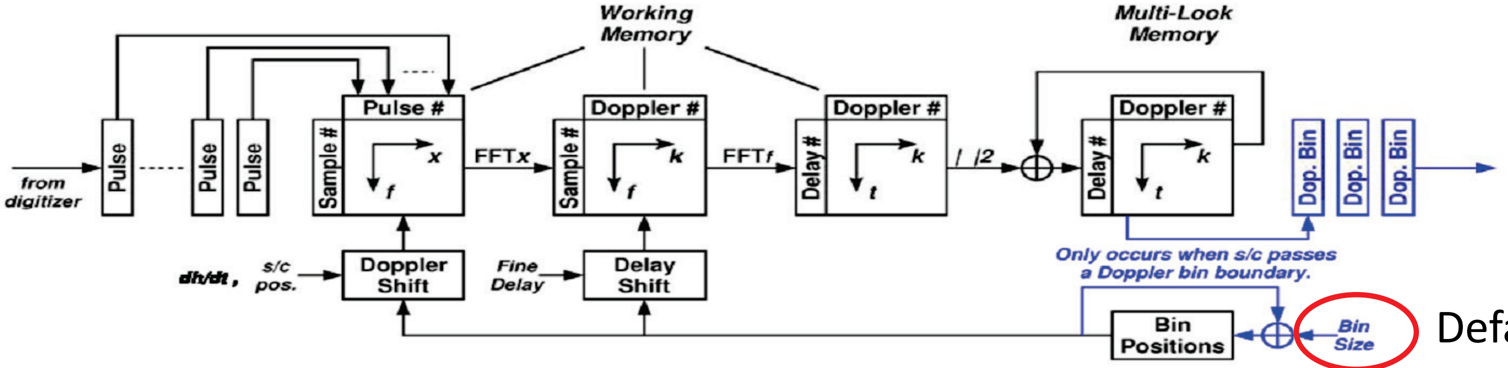

Default 300 m
Now fixed at 80 m

Above Image from Keith Raney

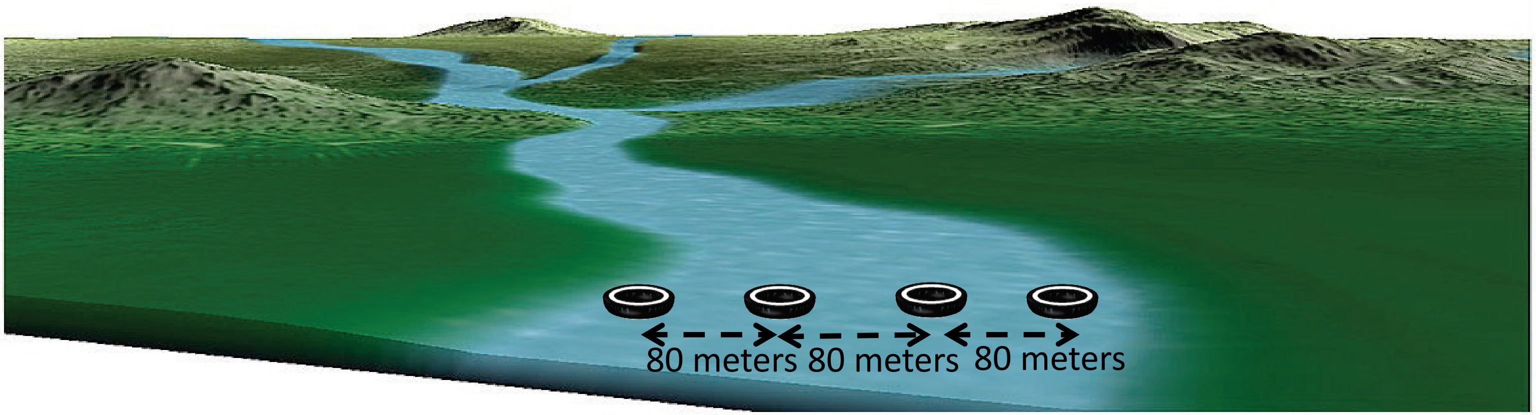

SAR ALTIMETRY @ FINER GRID STEP

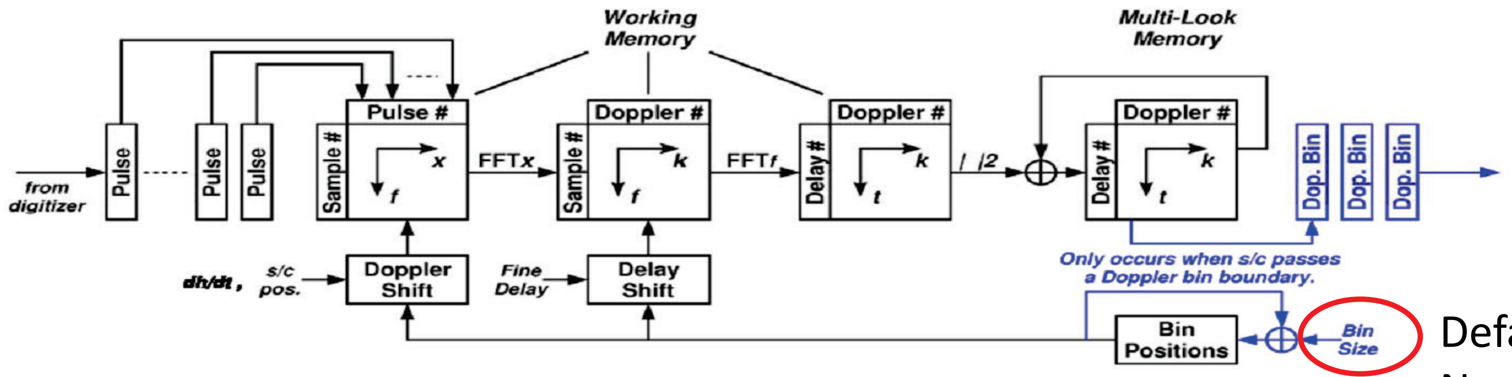

Default 300 m
Now fixed at
80 m

Above Image from Keith Raney

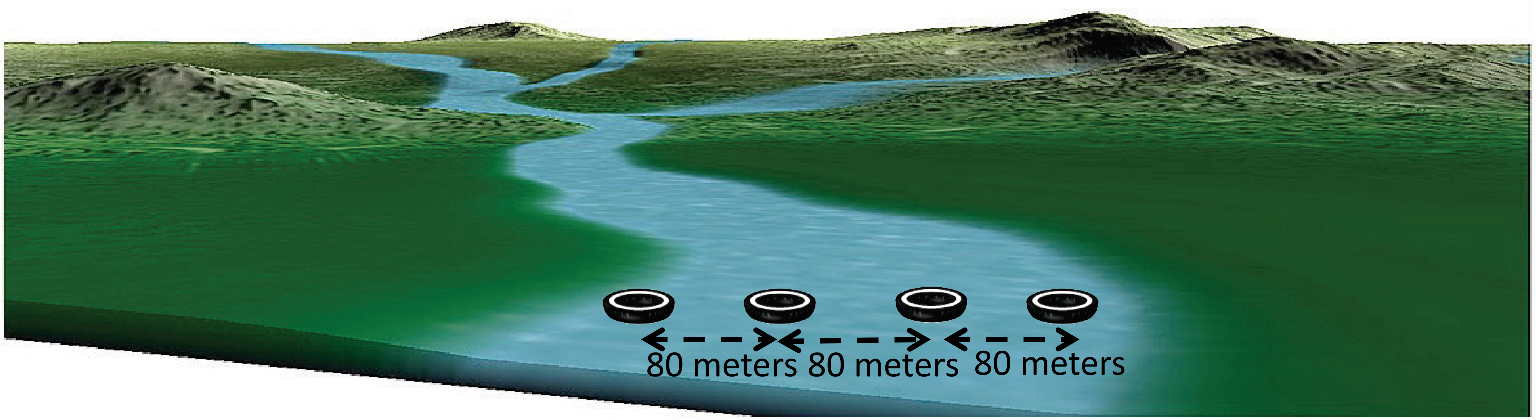

WE DONT CHANGE THE ALONG TRACK RESOLUTION, ONLY THE GRID STEP SIZE!

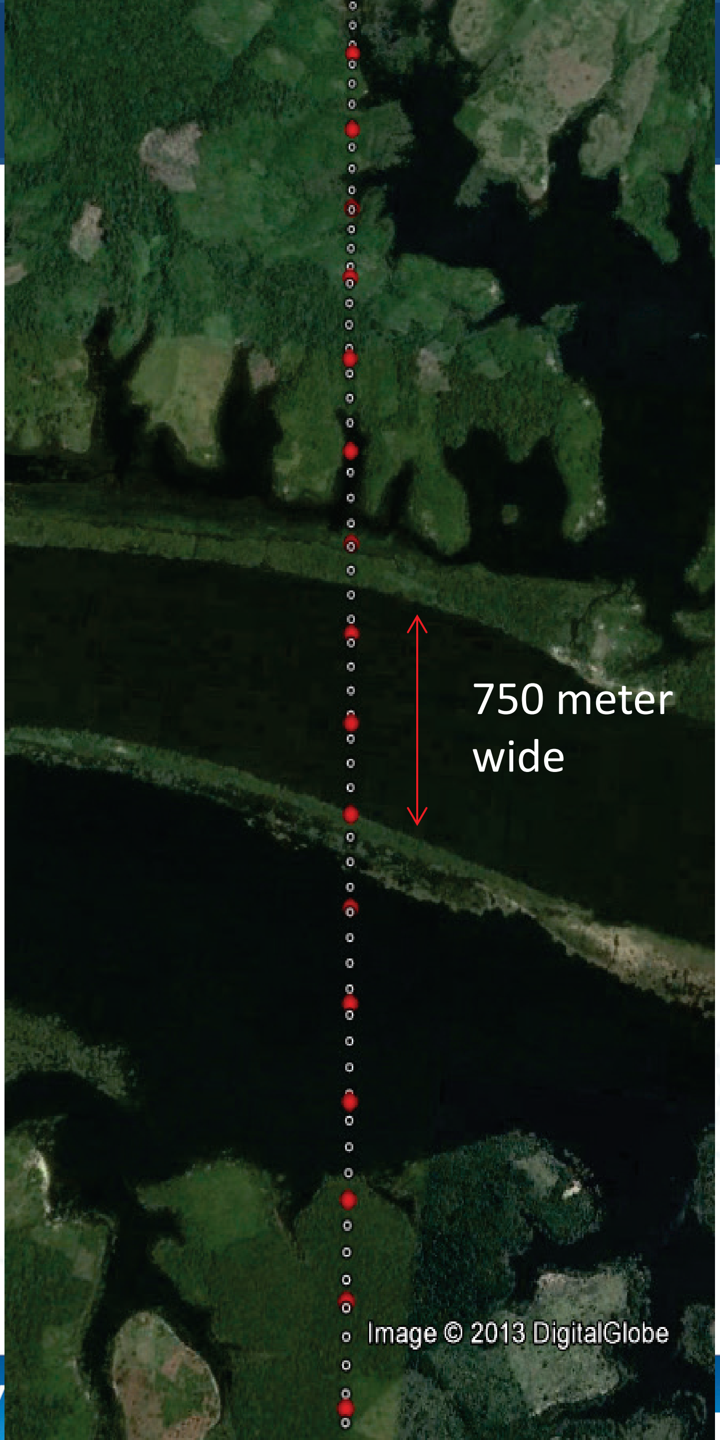
750 meter
wide
Image © 2013 DigitalGlobe

SAR ALTIMETRY 20 Hz

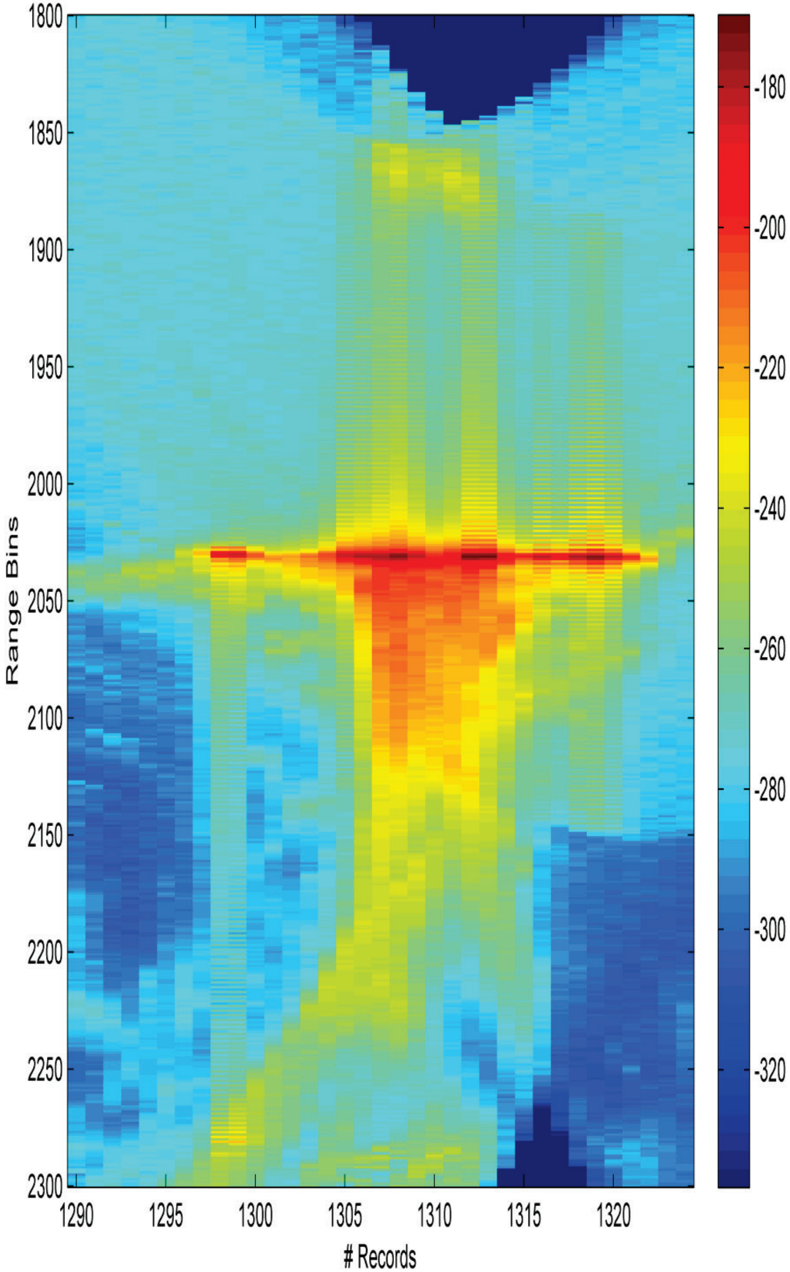

SAR ALTIMETRY 80 Hz

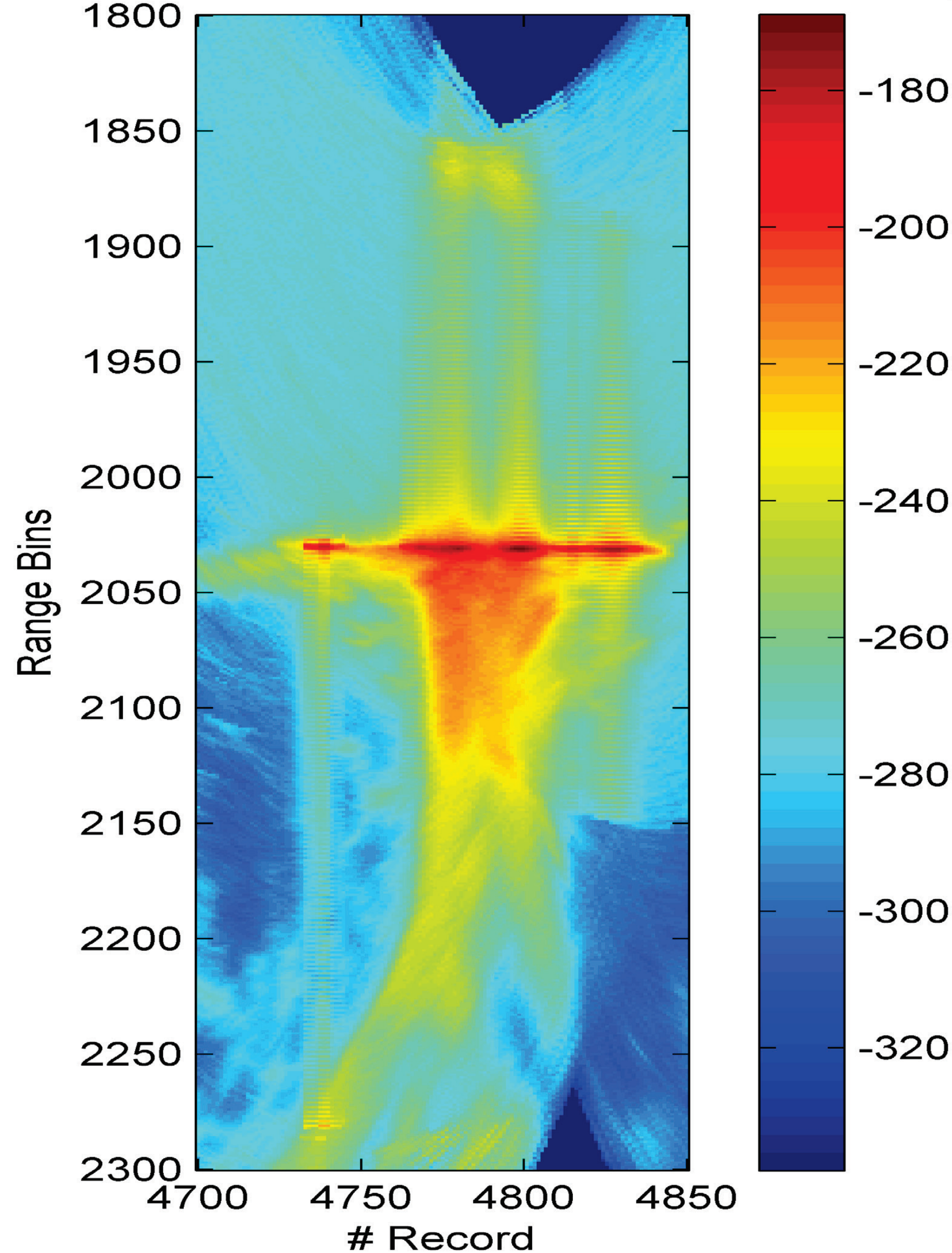

SAR Altimetry at 80 Hz for Sea-Ice

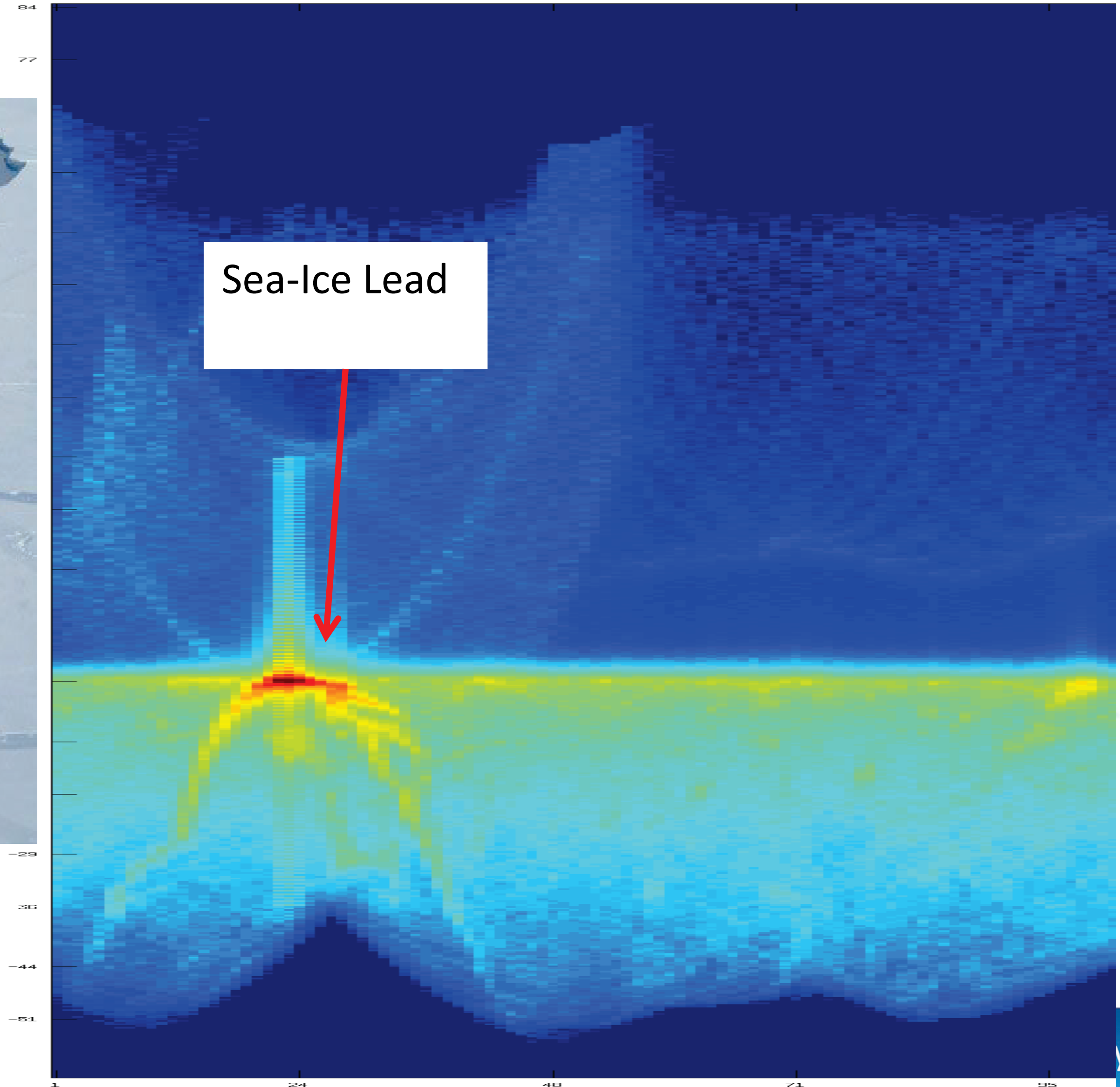

SAR Altimetry at 80 Hz for Sea-Ice

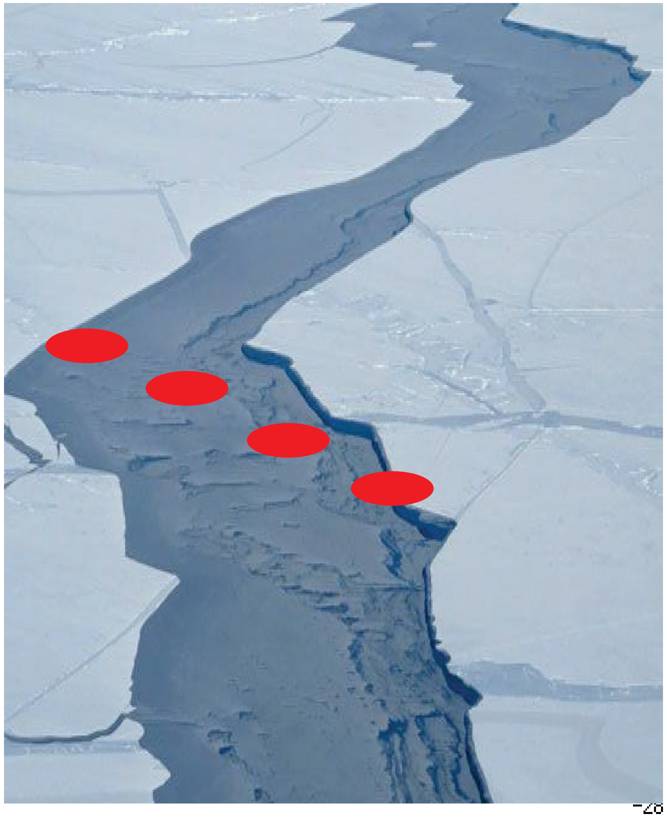

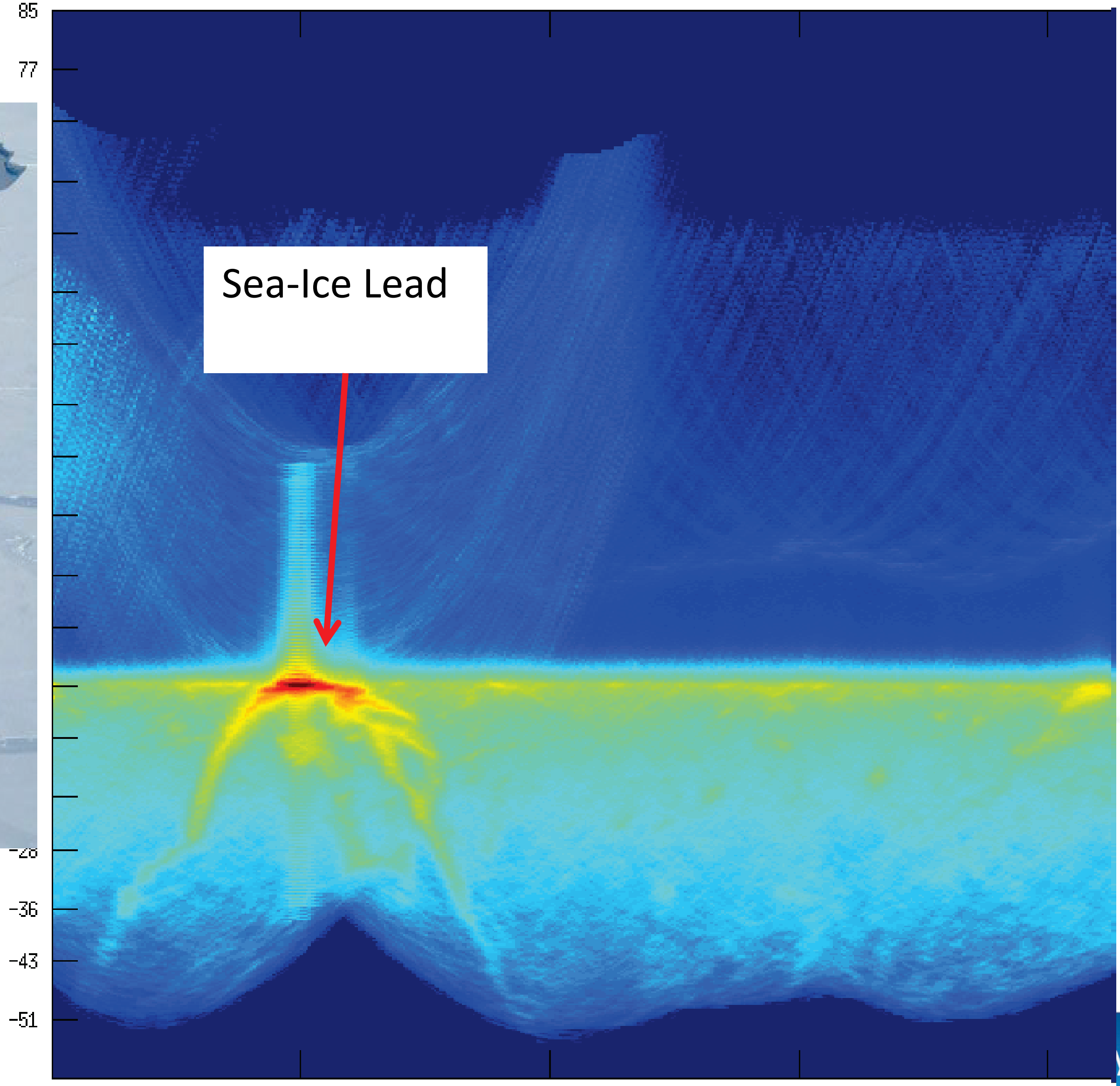

Waveform Model and Waveform Retracking

Altimetric Waveform Retracking

The process to retrieve from the received return waveform the three quantities:

- Two-way Travel Time
- Significant Wave Height
- Sigma zero (aka normalized back-scattering)

is referred as ***Waveform Retracking.***

This is achieved by fitting the shape of the sampled echo waveform to a model function or formulation which represents the form of the echo.

Altimetric Waveform Retracking

The process to retrieve from the received return waveform the three quantities:

- Two-way Travel Time
- Significant Wave Height
- Sigma zero (aka normalized back-scattering)

is referred as ***Waveform Retracking.***

This is achieved by fitting the shape of the sampled echo waveform to a model function or formulation which represents the form of the echo.

The retracking can be:

- Physical-based Model (analytical or numerical)
- Empirical (e.g. OCOG)

according if a model function or empirical formulations are used to retrieve the geophysical quantities from the waveform.

Altimetric Waveform Retracking

The process to retrieve from the received return waveform the three quantities:

- Two-way Travel Time
- Significant Wave Height
- Sigma zero (aka normalized back-scattering)

is referred as ***Waveform Retracking.***

This is achieved by fitting the shape of the sampled echo waveform to a model function or formulation which represents the form of the echo.

The retracking can be:

- Physical-based Model (analytical or numerical)
- Empirical (e.g. OCOG)

according if a model function or empirical formulations are used to retrieve the geophysical quantities from the waveform.

The final vertical resolution, after retracking, is generally more than an order of magnitude better than vertical resolution (we pass from 50 cm to few cms)

Altimetric Waveform Retracking

The process to retrieve from the received return waveform the three quantities:

- Two-way Travel Time
- Significant Wave Height
- Sigma zero (aka normalized back-scattering)

is referred as ***Waveform Retracking.***

This is achieved by fitting the shape of the sampled echo waveform to a model function or formulation which represents the form of the echo.

The retracking can be:

- Physical-based Model (analytical or numerical)
- Empirical (e.g. OCOG)

according if a model function or empirical formulations are used to retrieve the geophysical quantities from the waveform.

The final vertical resolution, after retracking, is generally more than an order of magnitude better than vertical resolution (we pass from 50 cm to few cms)

Typical Curve-Fitting schemes are Least Squares Estimation (LSE) or Maximum Likehood Estimator (MLE)

IN SAR Altimetry New Echo's Shape

=> we need a new model !

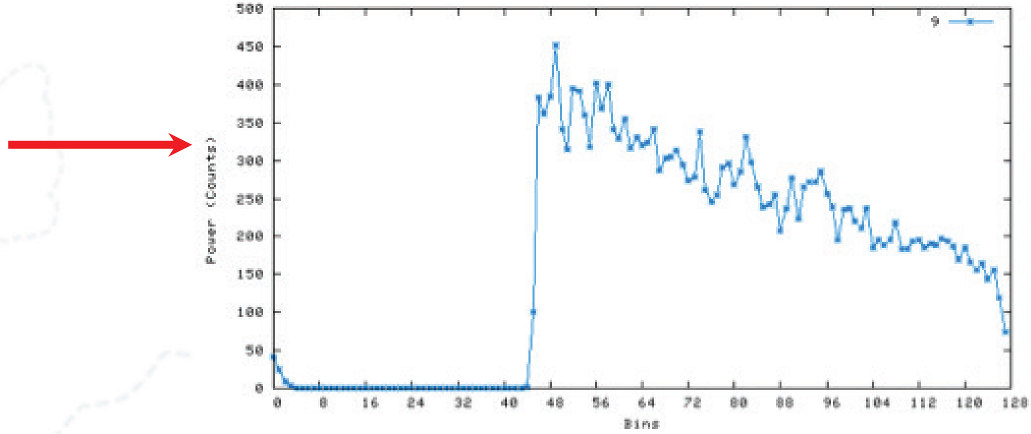

IN SAR Altimetry New Echo's Shape

=> we need a new model !

Classic Altimetry Echo (Brown Echo)

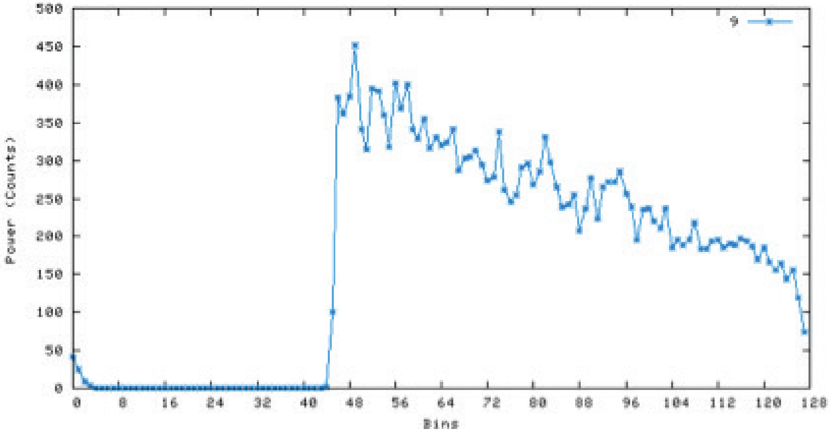

IN SAR Altimetry New Echo's Shape => we need a new model !

Classic Altimetry Echo (Brown Echo)

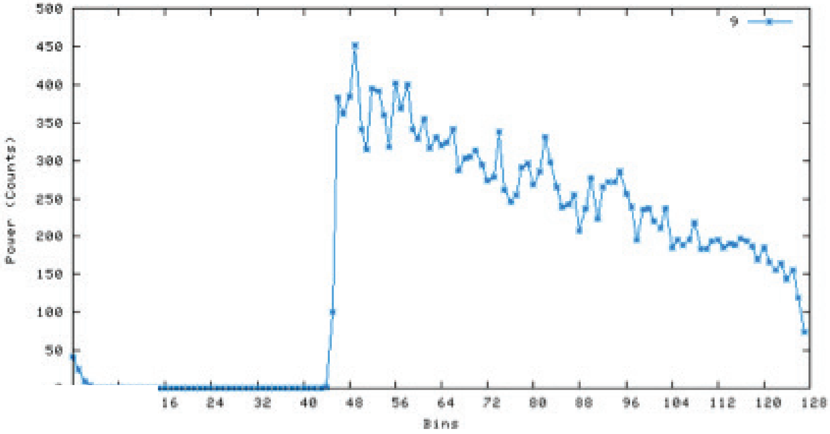

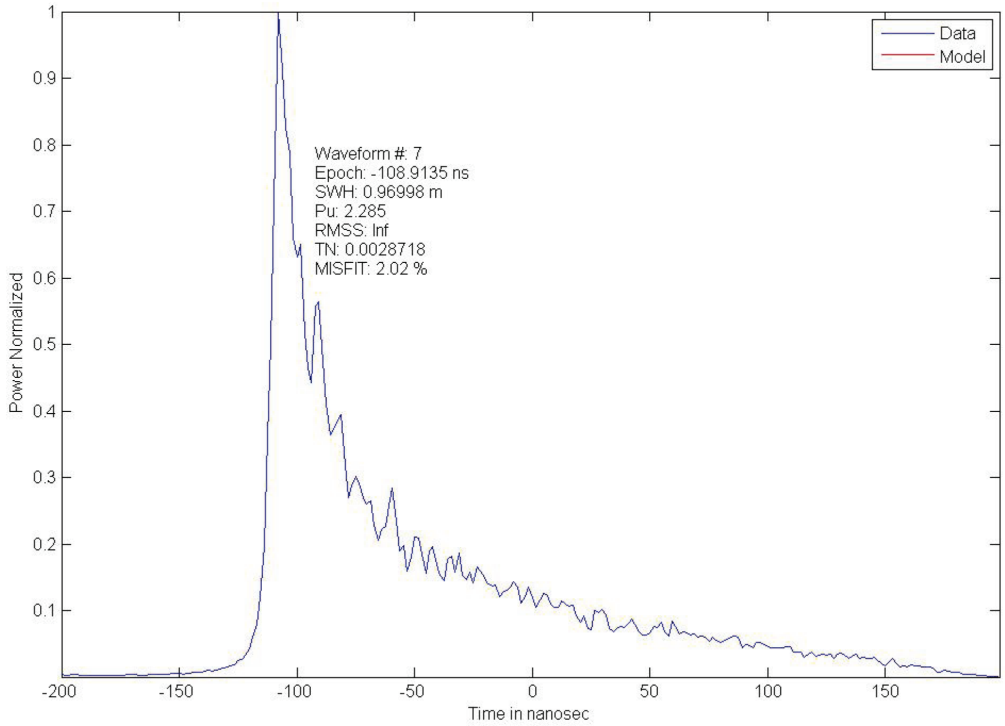

SAR Echo (Delay Doppler Echo)

IN SAR Altimetry New Echo's Shape => we need a new model !

Classic Altimetry Echo (Brown Echo)

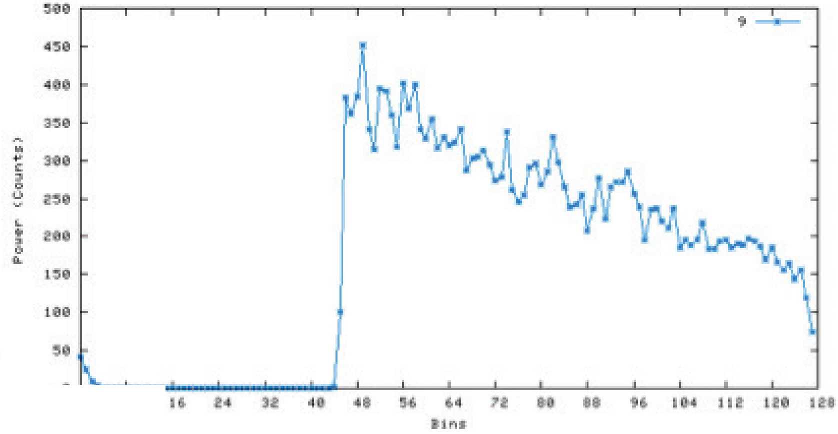

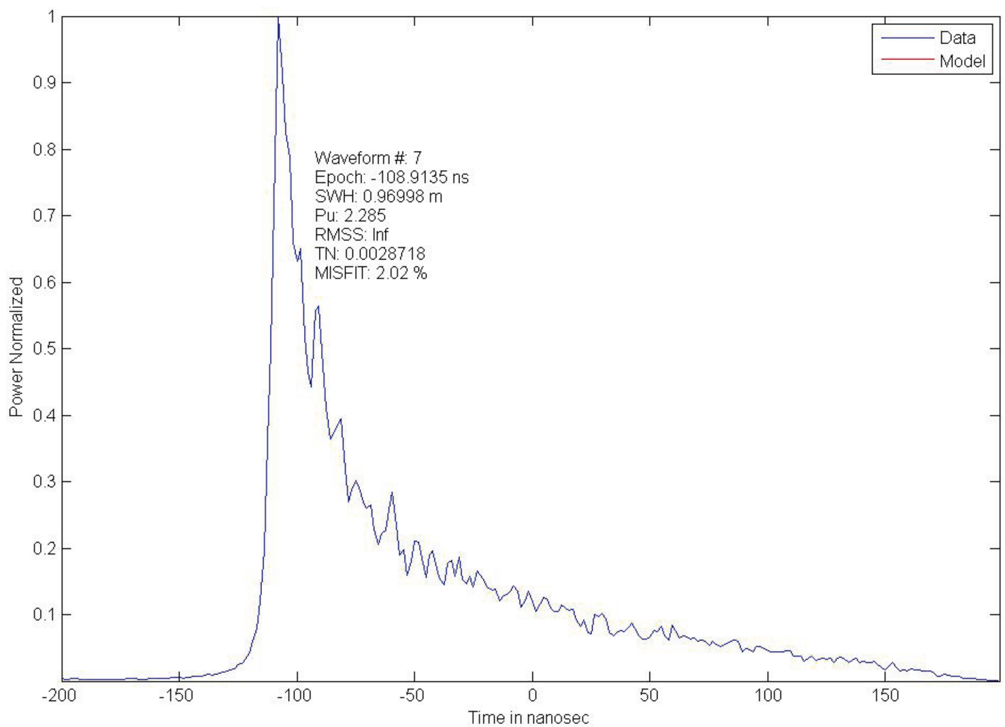

Total Different Shape => Problem, we need a new waveform model !

SAR Echo (Delay Doppler Echo)

THE SAMOSA PROJECT and HERITAGE

- Study funded by ESA, led by David Cotton (SatOC)
  - Starlab, NOC, De Montfort University, DTU Space & expert guidance from Keith Raney
- Initiated in March 2008
- First, the team worked with simulated data (CRYMPS), after CryoSat launch, the team started to work on real data
- SAMOSA Team succeeded to provide an all-comprehensive analytical model formulation for the SAR (Delay-Doppler) Echo
- SAMOSA Team laid the foundations for SAR Echo retracking SA over open ocean
- SAMOSA team firstly investigated the potential of SAR (Delay-Doppler) altimetry in coastal zone and inland water and sea floor bathymetry

SAMOSA WAVEFOM MODEL

SAMOSA MODEL: Physically-based model developed by Starlab from first principles.

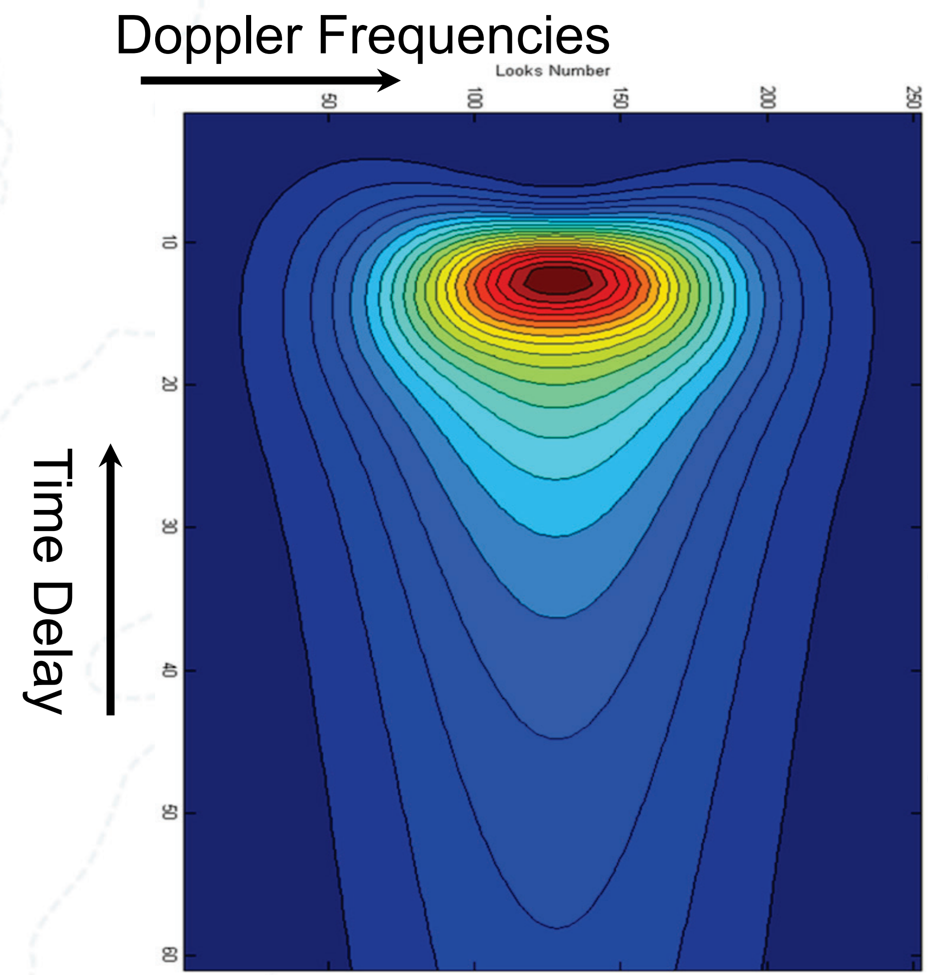

SAMOSA WAVEFOM MODEL

SAMOSA MODEL: Physically-based model developed by Starlab from first principles.

Fully-Analytical solution to model the Delay Doppler Maps (DDM) for the full span of Doppler Frequencies.

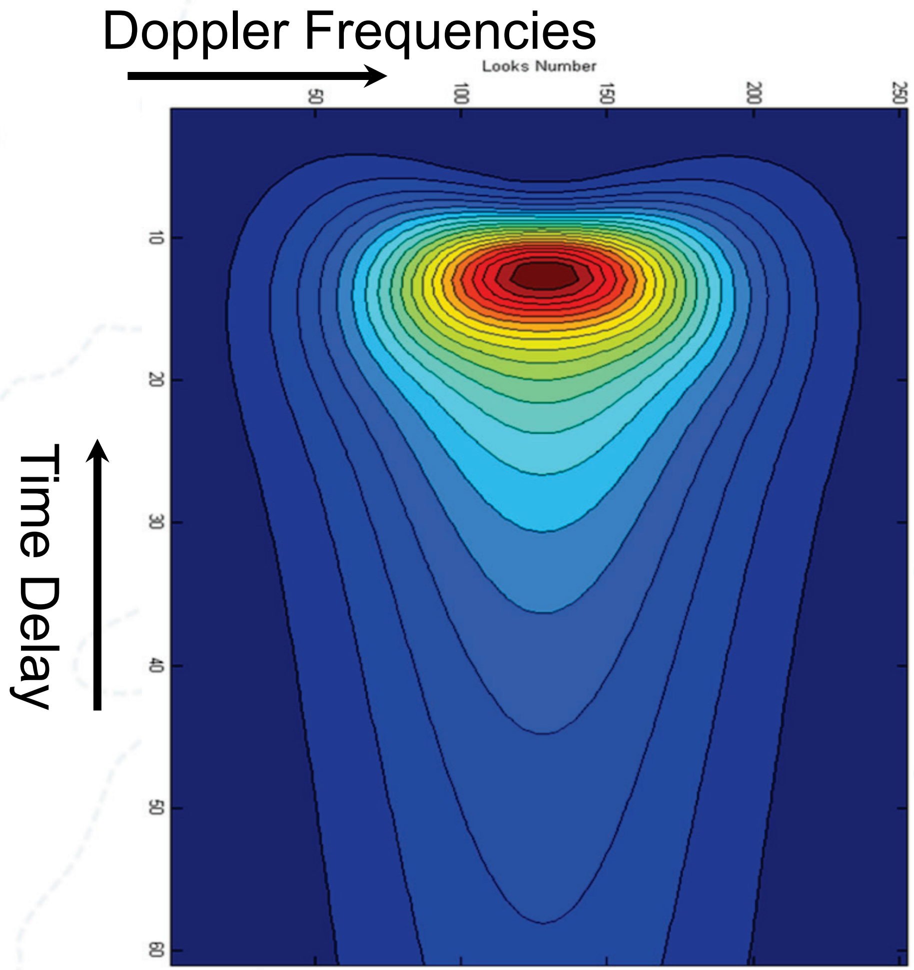

SAMOSA WAVEFOM MODEL

SAMOSA MODEL: Physically-based model developed by Starlab from first principles.

Fully-Analytical solution to model the Delay Doppler Maps (DDM) for the full span of Doppler Frequencies.

The model independent variables are the Doppler Frequency and the Time Delay (bi-dimensional model).

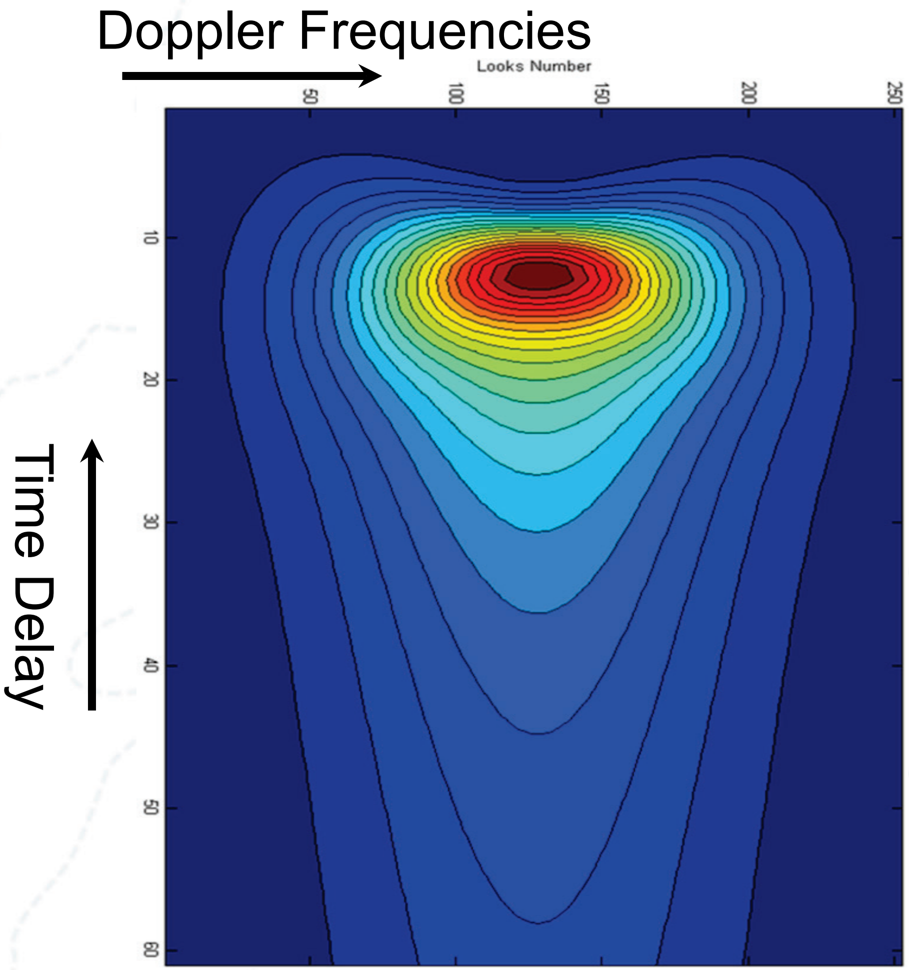

SAMOSA WAVEFOM MODEL

SAMOSA MODEL: Physically-based model developed by Starlab from first principles.

Fully-Analytical solution to model the Delay Doppler Maps (DDM) for the full span of Doppler Frequencies.

The model independent variables are the Doppler Frequency and the Time Delay (bi-dimensional model).

Model unknowns are epoch (time delay of the tracking point), significant wave height, Pu (waveform amplitude), mean square surface slope, and mispointing angles (pitch and roll).

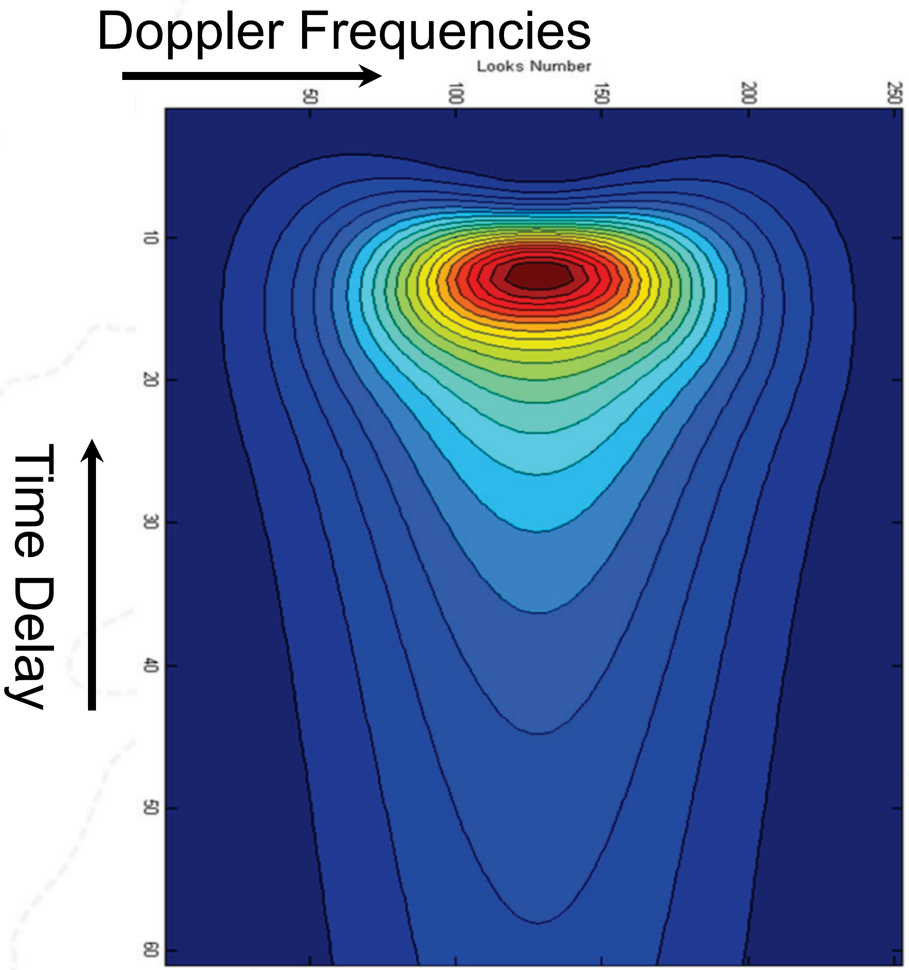

SAMOSA MODEL PAPER

All technical details, mathematical derivation and hypothesis can be found here

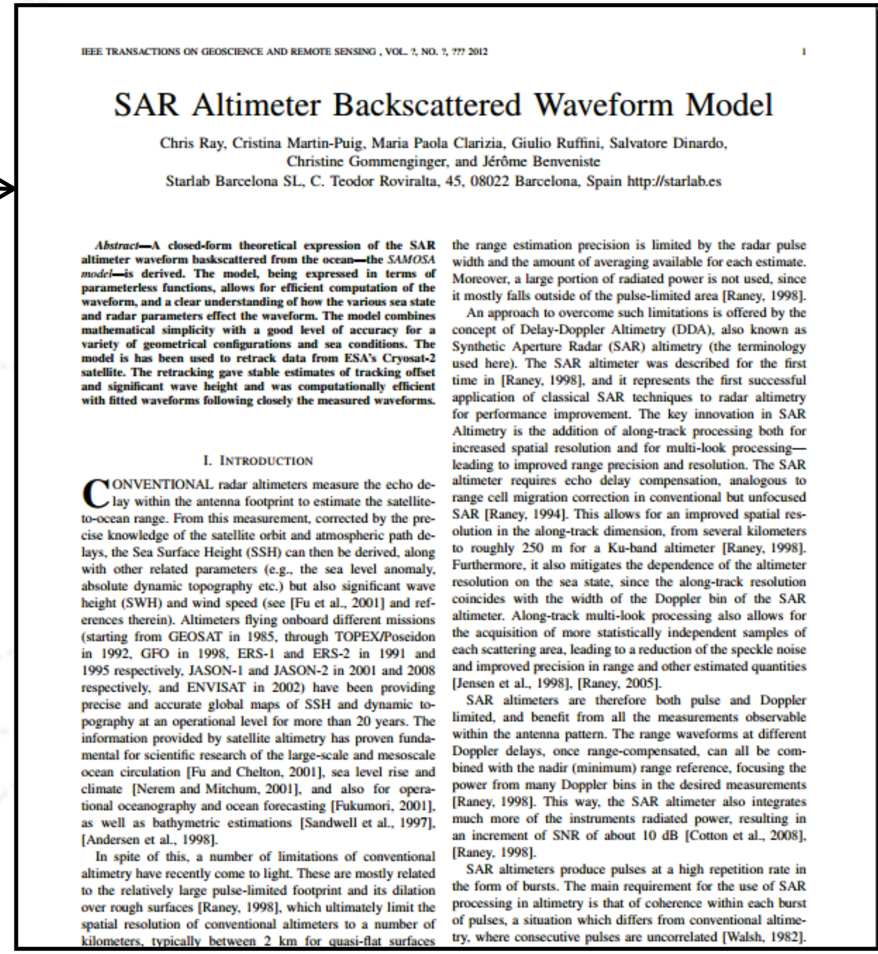
IEEE TRANSACTIONS ON GEOSCIENCE AND REMOTE SENSING , VOL. ?, NO. ?, ??? 2012

SAR Altimeter Backscattered Waveform Model

Chris Ray, Cristina Martin-Puig, Maria Paola Clarizia, Giulio Ruffini, Salvatore Dinardo, Christine Gommenginger, and Jérôme Benveniste
Starlab Barcelona SL, C. Teodor Roviralta, 45, 08022 Barcelona, Spain http://starlab.es

***Abstract*—A closed-form theoretical expression of the SAR altimeter waveform baskscattered from the ocean—the *SAMOSA model*—is derived. The model, being expressed in terms of parameterless functions, allows for efficient computation of the waveform, and a clear understanding of how the various sea state and radar parameters effect the waveform. The model combines mathematical simplicity with a good level of accuracy for a variety of geometrical configurations and sea conditions. The model is has been used to retrack data from ESA's Cryosat-2 satellite. The retracking gave stable estimates of tracking offset and significant wave height and was computationally efficient with fitted waveforms following closely the measured waveforms.**

I. Introduction

CONVENTIONAL radar altimeters measure the echo delay within the antenna footprint to estimate the satellite-to-ocean range. From this measurement, corrected by the precise knowledge of the satellite orbit and atmospheric path delays, the Sea Surface Height (SSH) can then be derived, along with other related parameters (e.g., the sea level anomaly, absolute dynamic topography etc.) but also significant wave height (SWH) and wind speed (see [Fu et al., 2001] and references therein). Altimeters flying onboard different missions (starting from GEOSAT in 1985, through TOPEX/Poseidon in 1992, GFO in 1998, ERS-1 and ERS-2 in 1991 and 1995 respectively, JASON-1 and JASON-2 in 2001 and 2008 respectively, and ENVISAT in 2002) have been providing precise and accurate global maps of SSH and dynamic topography at an operational level for more than 20 years. The information provided by satellite altimetry has proven fundamental for scientific research of the large-scale and mesoscale ocean circulation [Fu and Chelton, 2001], sea level rise and climate [Nerem and Mitchum, 2001], and also for operational oceanography and ocean forecasting [Fukumori, 2001], as well as bathymetric estimations [Sandwell et al., 1997], [Andersen et al., 1998].

In spite of this, a number of limitations of conventional altimetry have recently come to light. These are mostly related to the relatively large pulse-limited footprint and its dilation over rough surfaces [Raney, 1998], which ultimately limit the spatial resolution of conventional altimeters to a number of kilometers, typically between 2 km for quasi-flat surfaces the range estimation precision is limited by the radar pulse width and the amount of averaging available for each estimate. Moreover, a large portion of radiated power is not used, since it mostly falls outside of the pulse-limited area [Raney, 1998].

An approach to overcome such limitations is offered by the concept of Delay-Doppler Altimetry (DDA), also known as Synthetic Aperture Radar (SAR) altimetry (the terminology used here). The SAR altimeter was described for the first time in [Raney, 1998], and it represents the first successful application of classical SAR techniques to radar altimetry for performance improvement. The key innovation in SAR Altimetry is the addition of along-track processing both for increased spatial resolution and for multi-look processing—leading to improved range precision and resolution. The SAR altimeter requires echo delay compensation, analogous to range cell migration correction in conventional but unfocused SAR [Raney, 1994]. This allows for an improved spatial resolution in the along-track dimension, from several kilometers to roughly 250 m for a Ku-band altimeter [Raney, 1998]. Furthermore, it also mitigates the dependence of the altimeter resolution on the sea state, since the along-track resolution coincides with the width of the Doppler bin of the SAR altimeter. Along-track multi-look processing also allows for the acquisition of more statistically independent samples of each scattering area, leading to a reduction of the speckle noise and improved precision in range and other estimated quantities [Jensen et al., 1998], [Raney, 2005].

SAR altimeters are therefore both pulse and Doppler limited, and benefit from all the measurements observable within the antenna pattern. The range waveforms at different Doppler delays, once range-compensated, can all be combined with the nadir (minimum) range reference, focusing the power from many Doppler bins in the desired measurements [Raney, 1998]. This way, the SAR altimeter also integrates much more of the instruments radiated power, resulting in an increment of SNR of about 10 dB [Cotton et al., 2008], [Raney, 1998].

SAR altimeters produce pulses at a high repetition rate in the form of bursts. The main requirement for the use of SAR processing in altimetry is that of coherence within each burst of pulses, a situation which differs from conventional altimetry, where consecutive pulses are uncorrelated [Walsh, 1982].

SAMOSA MODEL PAPER

All technical details, mathematical derivation and hypothesis can be found here

Waveform Model Main Features
Handling Skewness in ocean SSH distribution
Handling Elliptical antenna (modeled as gaussian)
Handling Roll and Pitch mispointings
Handling Vertical speed and sea surface slope
Handling Earth's Sphericity
Handling mean square surface slope
Squared PTR approximated as Gaussian

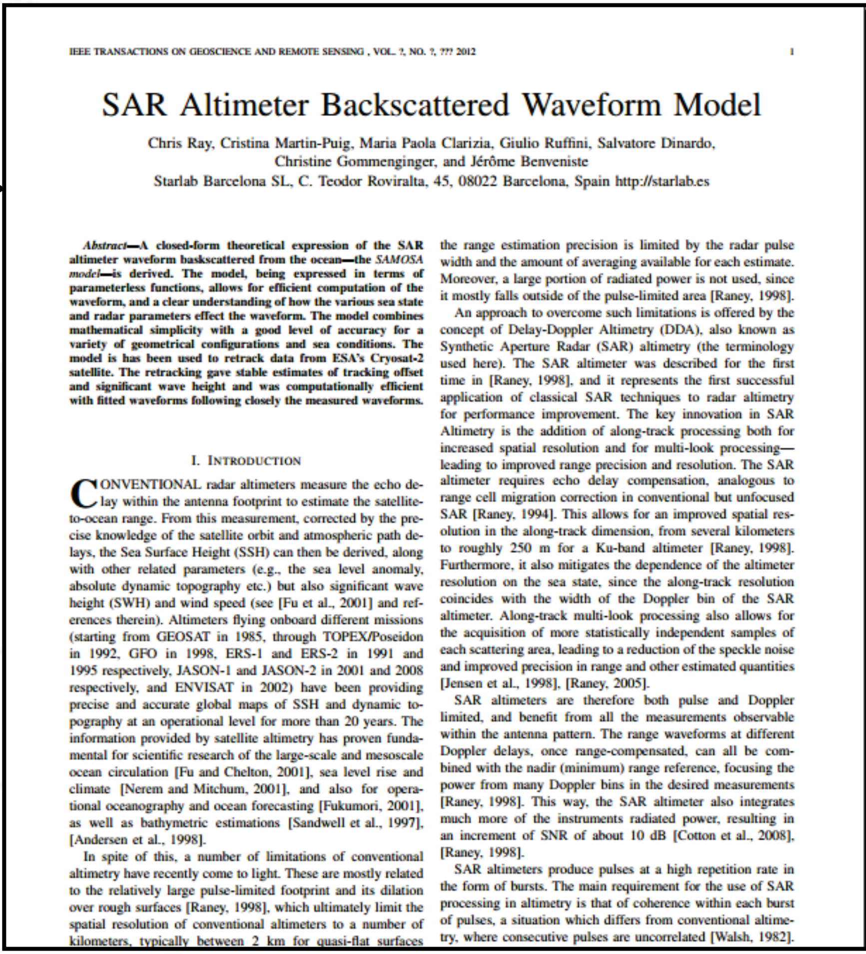

SAR Altimeter Backscattered Waveform Model

Chris Ray, Cristina Martin-Puig, Maria Paola Clarizia, Giulio Ruffini, Salvatore Dinardo, Christine Gommenginger, and Jérôme Benveniste
Starlab Barcelona SL, C. Teodor Roviralta, 45, 08022 Barcelona, Spain http://starlab.es

***Abstract*—A closed-form theoretical expression of the SAR altimeter waveform baskscattered from the ocean—the *SAMOSA model*—is derived. The model, being expressed in terms of parameterless functions, allows for efficient computation of the waveform, and a clear understanding of how the various sea state and radar parameters effect the waveform. The model combines mathematical simplicity with a good level of accuracy for a variety of geometrical configurations and sea conditions. The model is has been used to retrack data from ESA's Cryosat-2 satellite. The retracking gave stable estimates of tracking offset and significant wave height and was computationally efficient with fitted waveforms following closely the measured waveforms.**

I. Introduction

CONVENTIONAL radar altimeters measure the echo delay within the antenna footprint to estimate the satellite-to-ocean range. From this measurement, corrected by the precise knowledge of the satellite orbit and atmospheric path delays, the Sea Surface Height (SSH) can then be derived, along with other related parameters (e.g., the sea level anomaly, absolute dynamic topography etc.) but also significant wave height (SWH) and wind speed (see [Fu et al., 2001] and references therein). Altimeters flying onboard different missions (starting from GEOSAT in 1985, through TOPEX/Poseidon in 1992, GFO in 1998, ERS-1 and ERS-2 in 1991 and 1995 respectively, JASON-1 and JASON-2 in 2001 and 2008 respectively, and ENVISAT in 2002) have been providing precise and accurate global maps of SSH and dynamic topography at an operational level for more than 20 years. The information provided by satellite altimetry has proven fundamental for scientific research of the large-scale and mesoscale ocean circulation [Fu and Chelton, 2001], sea level rise and climate [Nerem and Mitchum, 2001], and also for operational oceanography and ocean forecasting [Fukumori, 2001], as well as bathymetric estimations [Sandwell et al., 1997], [Andersen et al., 1998].

In spite of this, a number of limitations of conventional altimetry have recently come to light. These are mostly related to the relatively large pulse-limited footprint and its dilation over rough surfaces [Raney, 1998], which ultimately limit the spatial resolution of conventional altimeters to a number of kilometers, typically between 2 km for quasi-flat surfaces the range estimation precision is limited by the radar pulse width and the amount of averaging available for each estimate. Moreover, a large portion of radiated power is not used, since it mostly falls outside of the pulse-limited area [Raney, 1998].

An approach to overcome such limitations is offered by the concept of Delay-Doppler Altimetry (DDA), also known as Synthetic Aperture Radar (SAR) altimetry (the terminology used here). The SAR altimeter was described for the first time in [Raney, 1998], and it represents the first successful application of classical SAR techniques to radar altimetry for performance improvement. The key innovation in SAR Altimetry is the addition of along-track processing both for increased spatial resolution and for multi-look processing—leading to improved range precision and resolution. The SAR altimeter requires echo delay compensation, analogous to range cell migration correction in conventional but unfocused SAR [Raney, 1994]. This allows for an improved spatial resolution in the along-track dimension, from several kilometers to roughly 250 m for a Ku-band altimeter [Raney, 1998]. Furthermore, it also mitigates the dependence of the altimeter resolution on the sea state, since the along-track resolution coincides with the width of the Doppler bin of the SAR altimeter. Along-track multi-look processing also allows for the acquisition of more statistically independent samples of each scattering area, leading to a reduction of the speckle noise and improved precision in range and other estimated quantities [Jensen et al., 1998], [Raney, 2005].

SAR altimeters are therefore both pulse and Doppler limited, and benefit from all the measurements observable within the antenna pattern. The range waveforms at different Doppler delays, once range-compensated, can all be combined with the nadir (minimum) range reference, focusing the power from many Doppler bins in the desired measurements [Raney, 1998]. This way, the SAR altimeter also integrates much more of the instruments radiated power, resulting in an increment of SNR of about 10 dB [Cotton et al., 2008], [Raney, 1998].

SAR altimeters produce pulses at a high repetition rate in the form of bursts. The main requirement for the use of SAR processing in altimetry is that of coherence within each burst of pulses, a situation which differs from conventional altimetry, where consecutive pulses are uncorrelated [Walsh, 1982].

SAR AVERAGED BACSKATTERED POWER WAVEFORM EQUATION

$$P_{k,l}(z_0) = \int_S d\vec{\rho}\ \frac{\lambda_0^2 G^4(\vec{\rho})\ \sigma_0(\vec{\rho})}{4\pi r^4}\ N_b^2 L_x L_y W_{k,l}(\vec{\rho}).$$

Instantaneous Backscattered DDM (Radar Equation)

SAR AVERAGED BACSKATTERED POWER WAVEFORM EQUATION

$$P_{k,l}(z_0) = \int_S d\vec{\rho}\ \frac{\lambda_0^2 G^4(\vec{\rho})\ \sigma_0(\vec{\rho})}{4\pi r^4}\ N_b^2 L_x L_y W_{k,l}(\vec{\rho}).$$

Antenna Pattern

Instantaneous Backscattered DDM (Radar Equation)

SAR AVERAGED BACSKATTERED POWER WAVEFORM EQUATION

$$P_{k,l}(z_0) = \int_S d\vec{\rho}\ \frac{\lambda_0^2 G^4(\vec{\rho})\ \sigma_0(\vec{\rho})}{4\pi r^4}\ N_b^2 L_x L_y W_{k,l}(\vec{\rho}).$$

Antenna Pattern

Squared Delay-Doppler PTR function

Instantaneous Backscattered DDM (Radar Equation)

SAR AVERAGED BACSKATTERED POWER WAVEFORM EQUATION

$$P_{k,l}(z_0) = \int_S d\vec{\rho}\ \frac{\lambda_0^2 G^4(\vec{\rho})\ \sigma_0(\vec{\rho})}{4\pi r^4}\ N_b^2 L_x L_y W_{k,l}(\vec{\rho}).$$

Antenna Pattern

Squared Delay-Doppler PTR function

Instantaneous Backscattered DDM (Radar Equation)

$$\begin{aligned} \langle P_{k,l}(z_0)\rangle_{z_0} &= \int d\eta\ p(\eta)\ P_{k,l}(\sigma_z\eta + \langle z_0\rangle - z_{\mathrm{EM}}) \\ &= K\Lambda_l\left(k + \frac{\langle z_0\rangle - z_{\mathrm{EM}}}{L_z}, \frac{\sigma_z}{L_z}\right). \qquad (49) \end{aligned}$$

Averaged Backscattered DDM

SAR AVERAGED BACSKATTERED POWER WAVEFORM EQUATION

$$P_{k,l}(z_0) = \int_{\mathrm{S}} d\vec{\rho}\, \frac{\lambda_0^2 G^4(\vec{\rho})\ \sigma_0(\vec{\rho})}{4\pi r^4}\ N_b^2 L_x L_y W_{k,l}(\vec{\rho}).$$

Antenna Pattern

Squared Delay-Doppler PTR function

Instantaneous Backscattered DDM (Radar Equation)

$$\begin{aligned} \langle P_{k,l}(z_0)\rangle_{z_0} &= \int d\eta\ p(\eta)\ P_{k,l}(\sigma_z\eta + \langle z_0\rangle - z_{\mathrm{EM}}) \\ &= K\Lambda_l\left(k + \frac{\langle z_0\rangle - z_{\mathrm{EM}}}{L_z}, \frac{\sigma_z}{L_z}\right). \qquad (49) \end{aligned}$$

Sea Surface PDF

Averaged Backscattered DDM

SAR AVERAGED BACSKATTERED POWER WAVEFORM EQUATION

$$P_{k,l}(z_0) = \int_S d\vec{\rho}\ \frac{\lambda_0^2 G^4(\vec{\rho})\ \sigma_0(\vec{\rho})}{4\pi r^4}\ N_b^2 L_x L_y W_{k,l}(\vec{\rho}).$$

Instantaneous Backscattered DDM (Radar Equation)

$$\begin{aligned}\langle P_{k,l}(z_0)\rangle_{z_0} &= \int d\eta\ p(\eta)\ P_{k,l}(\sigma_z\eta + \langle z_0\rangle - z_{\mathrm{EM}}) \\ &= K\Lambda_l\left(k + \frac{\langle z_0\rangle - z_{\mathrm{EM}}}{L_z}, \frac{\sigma_z}{L_z}\right). \qquad (49)\end{aligned}$$

Averaged Backscattered DDM

Antenna Pattern

Squared Delay-Doppler PTR function

Sea Surface PDF

SAR AVERAGED BACSKATTERED POWER WAVEFORM EQUATION

$$P_{k,l}(z_0) = \int_S d\vec{\rho}\, \frac{\lambda_0^2 G^4(\vec{\rho})\ \sigma_0(\vec{\rho})}{4\pi r^4}\ N_b^2 L_x L_y W_{k,l}(\vec{\rho}).$$

Antenna Pattern

Squared Delay-Doppler PTR function

Instantaneous Backscattered DDM (Radar Equation)

$$\langle P_{k,l}(z_0)\rangle_{z_0} = \int d\eta\ p(\eta)\ P_{k,l}(\sigma_z\eta + \langle z_0\rangle - z_{\mathrm{EM}}) = K\Lambda_l\left(k + \frac{\langle z_0\rangle - z_{\mathrm{EM}}}{L_z}, \frac{\sigma_z}{L_z}\right). \quad (49)$$

Sea Surface PDF

Averaged Backscattered DDM

$$\Lambda_l(x, \sigma_s) = \sqrt{\frac{\pi g_l}{2\alpha_g^2}}\Gamma_0\left\{ f_0(g_l x) + \frac{\sigma_z}{L_\Gamma} T_k(y_p) g_l \sigma_s f_1(g_l x) \right\}.$$

SAR AVERAGED BACSKATTERED POWER WAVEFORM EQUATION

$$P_{k,l}(z_0) = \int_S d\vec{\rho}\ \frac{\lambda_0^2 G^4(\vec{\rho})\ \sigma_0(\vec{\rho})}{4\pi r^4}\ N_b^2 L_x L_y W_{k,l}(\vec{\rho}).$$

Antenna Pattern

Squared Delay-Doppler PTR function

Instantaneous Backscattered DDM (Radar Equation)

$$\begin{aligned} \langle P_{k,l}(z_0)\rangle_{z_0} &= \int d\eta\ p(\eta)\ P_{k,l}(\sigma_z \eta + \langle z_0\rangle - z_{\text{EM}}) \\ &= K \Lambda_l \left(k + \frac{\langle z_0\rangle - z_{\text{EM}}}{L_z}, \frac{\sigma_z}{L_z}\right). \qquad (49) \end{aligned}$$

Sea Surface PDF

Averaged Backscattered DDM

$$\Lambda_l(x, \sigma_s) = \sqrt{\frac{\pi g_l}{2\alpha_g^2}}\Gamma_0 \left\{ f_0(g_l x) + \frac{\sigma_z}{L_\Gamma} T_k(y_p) g_l \sigma_s f_1(g_l x) \right\}.$$

SAR AVERAGED BACSKATTERED POWER WAVEFORM EQUATION

$$P_{k,l}(z_0) = \int_{\mathrm{S}} d\vec{\rho}\, \frac{\lambda_0^2 G^4(\vec{\rho})\ \sigma_0(\vec{\rho})}{4\pi r^4}\ N_b^2 L_x L_y W_{k,l}(\vec{\rho}).$$

Antenna Pattern

Squared Delay-Doppler PTR function

Instantaneous Backscattered DDM (Radar Equation)

$$\begin{aligned} \langle P_{k,l}(z_0)\rangle_{z_0} &= \int d\eta\ p(\eta)\ P_{k,l}(\sigma_z \eta + \langle z_0\rangle - z_{\mathrm{EM}}) \\ &= K \Lambda_l \left(k + \frac{\langle z_0\rangle - z_{\mathrm{EM}}}{L_z}, \frac{\sigma_z}{L_z} \right). \qquad (49) \end{aligned}$$

Sea Surface PDF

Averaged Backscattered DDM

$$\Lambda_l(x, \sigma_s) = \sqrt{\frac{\pi g_l}{2\alpha_g^2}}\, \Gamma_0 \left\{ f_0(g_l x) + \frac{\sigma_z}{L_\Gamma} T_k(y_p) g_l \sigma_s f_1(g_l x) \right\}.$$

F_0 and F_1 Terms

$$f_0(\xi) = \int_0^{+\infty} e^{-\frac{1}{2}(\xi - v^2)^2}\, dv = \frac{\pi}{4}(|\xi|)^{1/2}\left[I^{sc}_{-\frac{1}{4}}\left(\frac{1}{4}\xi^2\right) + \mathrm{sign}(\xi)\cdot I^{sc}_{\frac{1}{4}}\left(\frac{1}{4}\xi^2\right)\right]$$

$$f_1(\xi) = \int_0^{+\infty} e^{-\frac{1}{2}(\xi - v^2)^2}(\xi - v^2)\, dv = \frac{\pi}{8}|\xi|^{\frac{3}{2}}\left[\left(I^{sc}_{\frac{1}{4}}\left(\frac{1}{4}\xi^2\right) - I^{sc}_{-\frac{3}{4}}\left(\frac{1}{4}\xi^2\right)\right) + \mathrm{sign}(\xi)\cdot\left(I^{sc}_{-\frac{1}{4}}\left(\frac{1}{4}\xi^2\right) - I^{sc}_{\frac{3}{4}}\left(\frac{1}{4}\xi^2\right)\right)\right]$$

F_0 and F_1 terms can be expressed exactly in term of Bessel Function but ,for operational processor, better to tabulate them

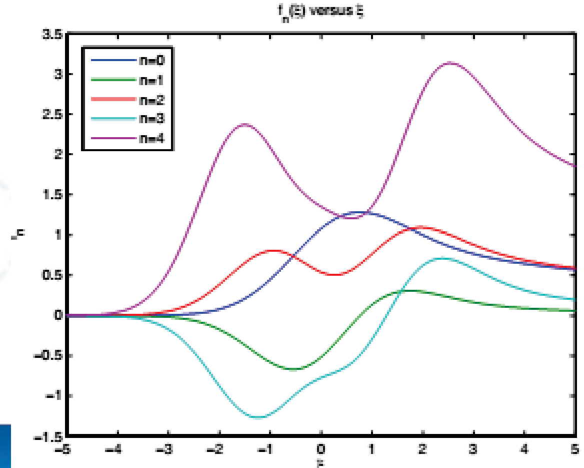

MODEL TRUNCATED VERSION

$$\Lambda_l(x,\sigma_s) = \sqrt{\frac{\pi g_l}{2\alpha_g^2}}\Gamma_0\left\{ f_0(g_l x) + \frac{\sigma_z}{L_\Gamma} T_k(y_p) g_l \sigma_s f_1(g_l x) \right\}.$$

Accumulating all the beams, we build the multilooked return waveform model. If we consider only the term for beam l=0, the model is termed as the Single-look waveform model.

$$\Lambda(x,\sigma) = \sum_l \Lambda_l(x,\sigma)$$

MODEL TRUNCATED VERSION

$$\Lambda_l(x,\sigma_s) = \sqrt{\frac{\pi g_l}{2\alpha_g^2}}\Gamma_0\left\{f_0(g_l x) + \frac{\sigma_z}{L_\Gamma}T_k(y_p)g_l\sigma_s f_1(g_l x)\right\}.$$

Accumulating all the beams, we build the multilooked return waveform model. If we consider only the term for beam l=0, the model is termed as the Single-look waveform model.

$$\Lambda(x,\sigma) = \sum_l \Lambda_l(x,\sigma)$$

MODEL TRUNCATED VERSION

$$\Lambda_l(x,\sigma_s) = \sqrt{\frac{\pi g_l}{2\alpha_g^2}}\Gamma_0\left\{f_0(g_l x) + \frac{\sigma_z}{L_\Gamma}T_k(y_p)g_l\sigma_s f_1(g_l x)\right\}.$$

Accumulating all the beams, we build the multilooked return waveform model. If we consider only the term for beam l=0, the model is termed as the Single-look waveform model.

$$\Lambda(x,\sigma) = \sum_l \Lambda_l(x,\sigma)$$

MODEL TRUNCATED VERSION

$$\Lambda_l(x,\sigma_s) = \sqrt{\frac{\pi g_l}{2\alpha_g^2}}\Gamma_0\left\{ f_0(g_l x) + \frac{\sigma_z}{L_\Gamma} T_k(y_p) g_l \sigma_s f_1(g_l x) \right\}.$$

Accumulating all the beams, we build the multilooked return waveform model. If we consider only the term for beam l=0, the model is termed as the Single-look waveform model.

$$\Lambda(x,\sigma) = \sum_l \Lambda_l(x,\sigma)$$

When considered only F_0 term (i.e. zero order only) in the model, the model itself is termed **SAMOSA 3**

MODEL TRUNCATED VERSION

$$\Lambda_l(x,\sigma_s) = \sqrt{\frac{\pi g_l}{2\alpha_g^2}}\Gamma_0\left\{f_0(g_l x) + \frac{\sigma_z}{L_\Gamma}T_k(y_p)g_l\sigma_s f_1(g_l x)\right\}.$$

Accumulating all the beams, we build the multilooked return waveform model. If we consider only the term for beam l=0, the model is termed as the Single-look waveform model.

$$\Lambda(x,\sigma) = \sum_l \Lambda_l(x,\sigma)$$

When considered only F_0 term (i.e. zero order only) in the model, the model itself is termed **SAMOSA 3**

When considered both terms (zero order and first order), the model is termed **SAMOSA 2**

SAMOSA 3 is more computational fast (for NRT products) but may **introduce errors**

Dependency on sea state (SWH)

Sea Level Anomalies differences between SAR and RDSAR (PLRM) shows a trend with SAMOSA 3

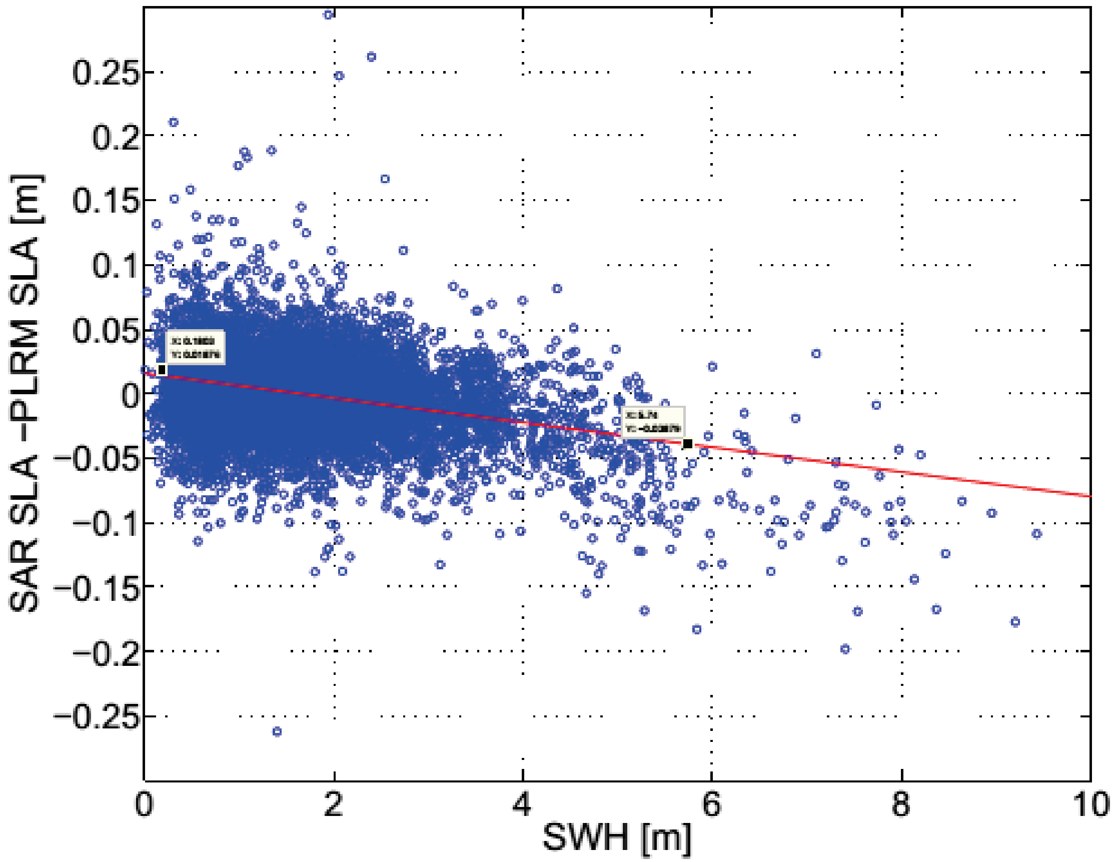

Dependency on sea state (SWH)

Trend disappears with SAMOSA 2

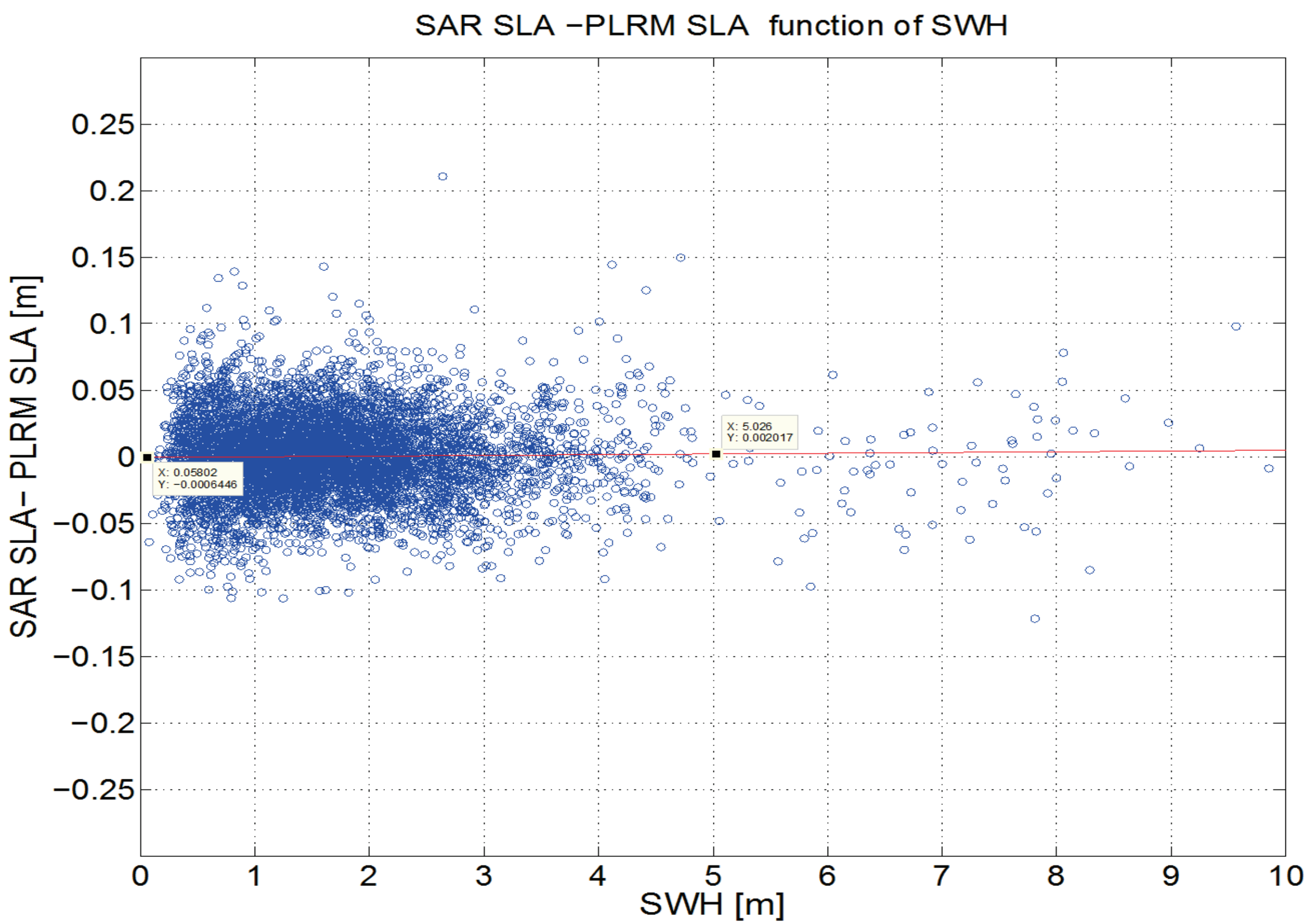

Model Doppler Beams

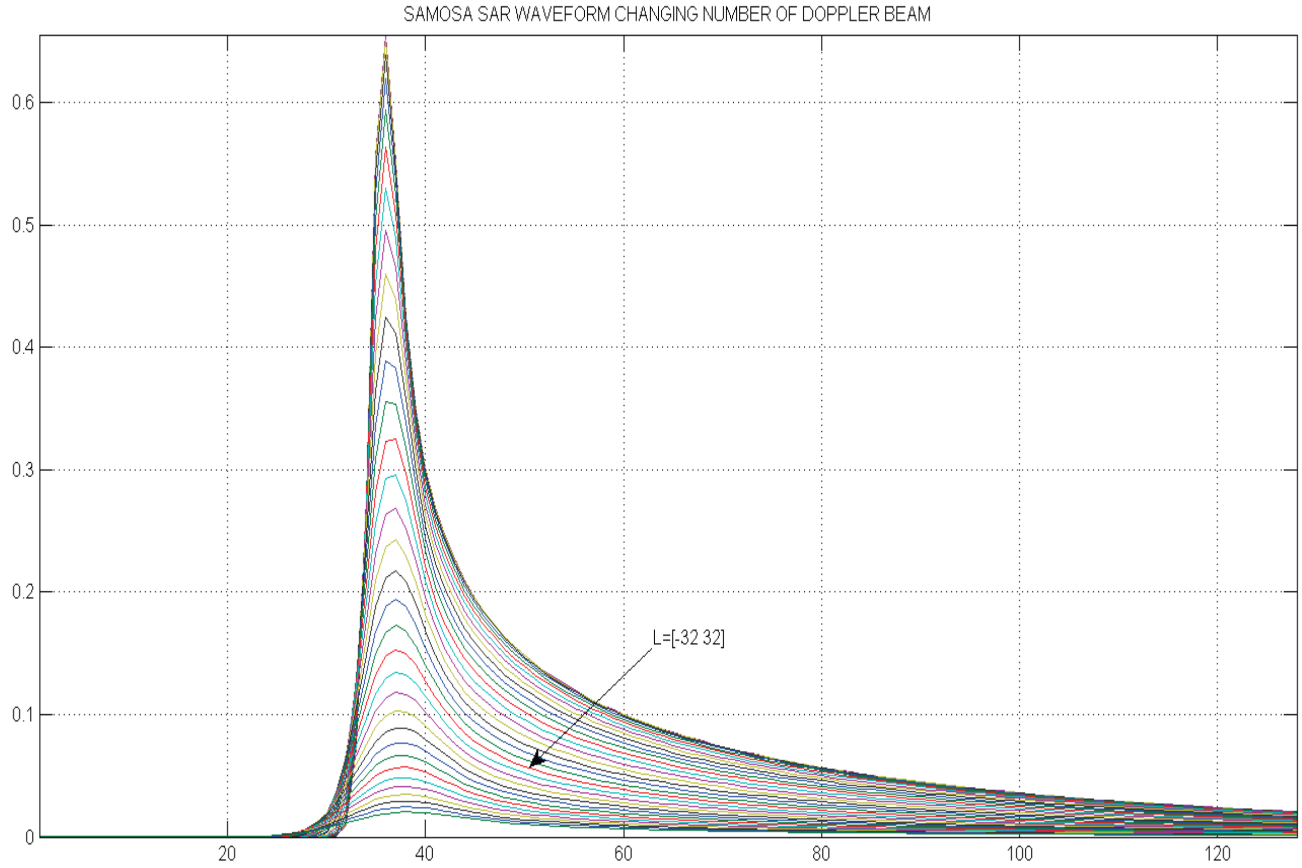

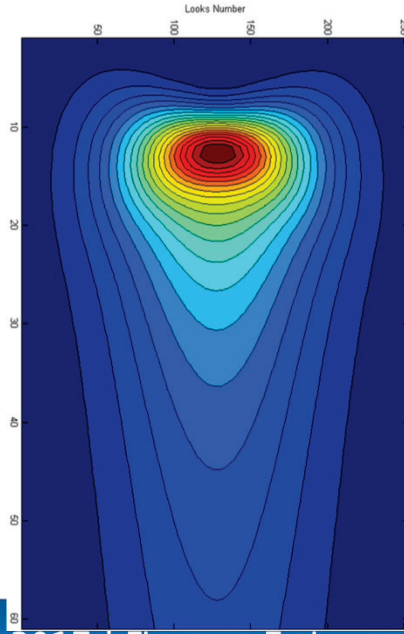

Dependency on SWH

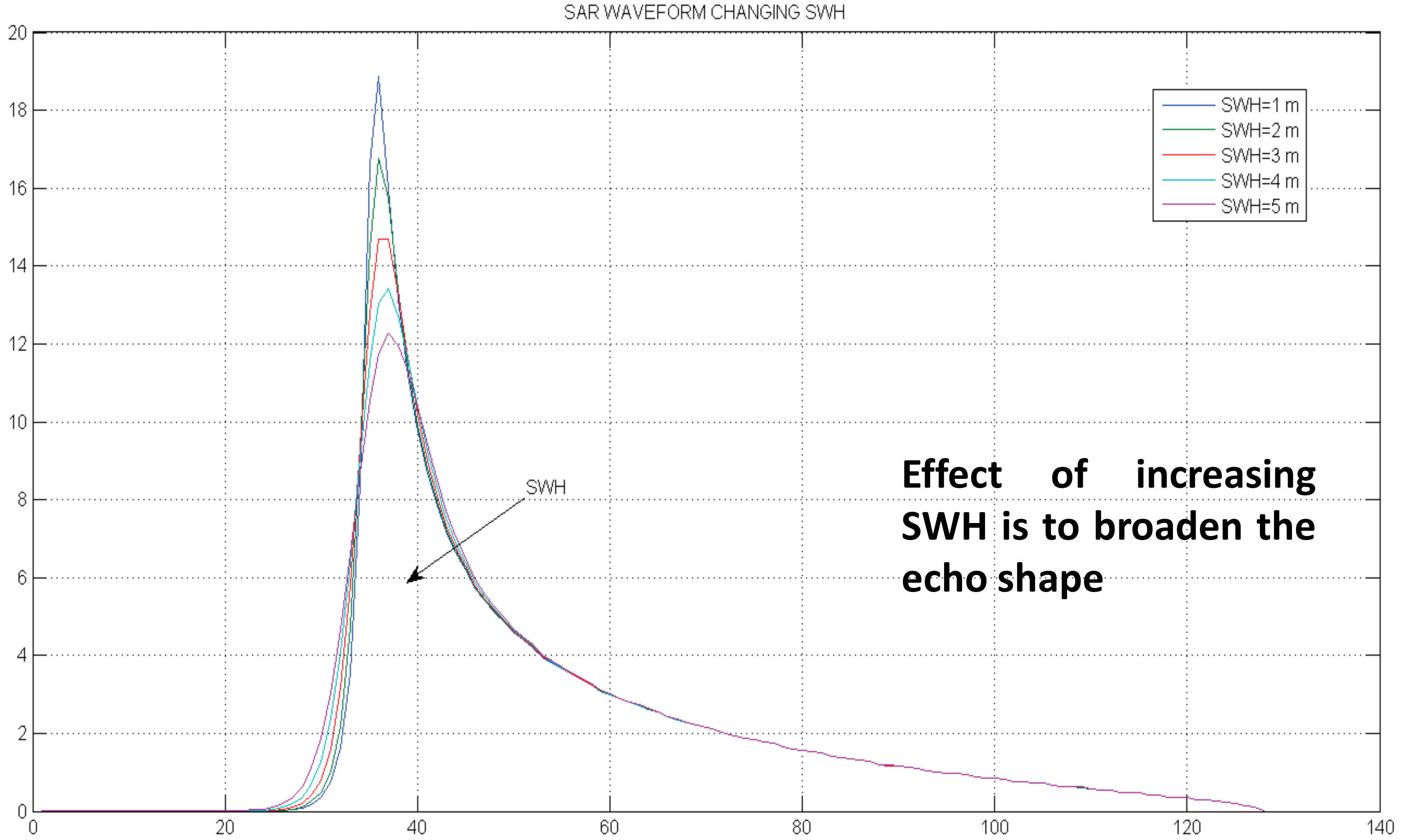

Effect of increasing SWH is to broaden the echo shape

Dependency on Roll Angle

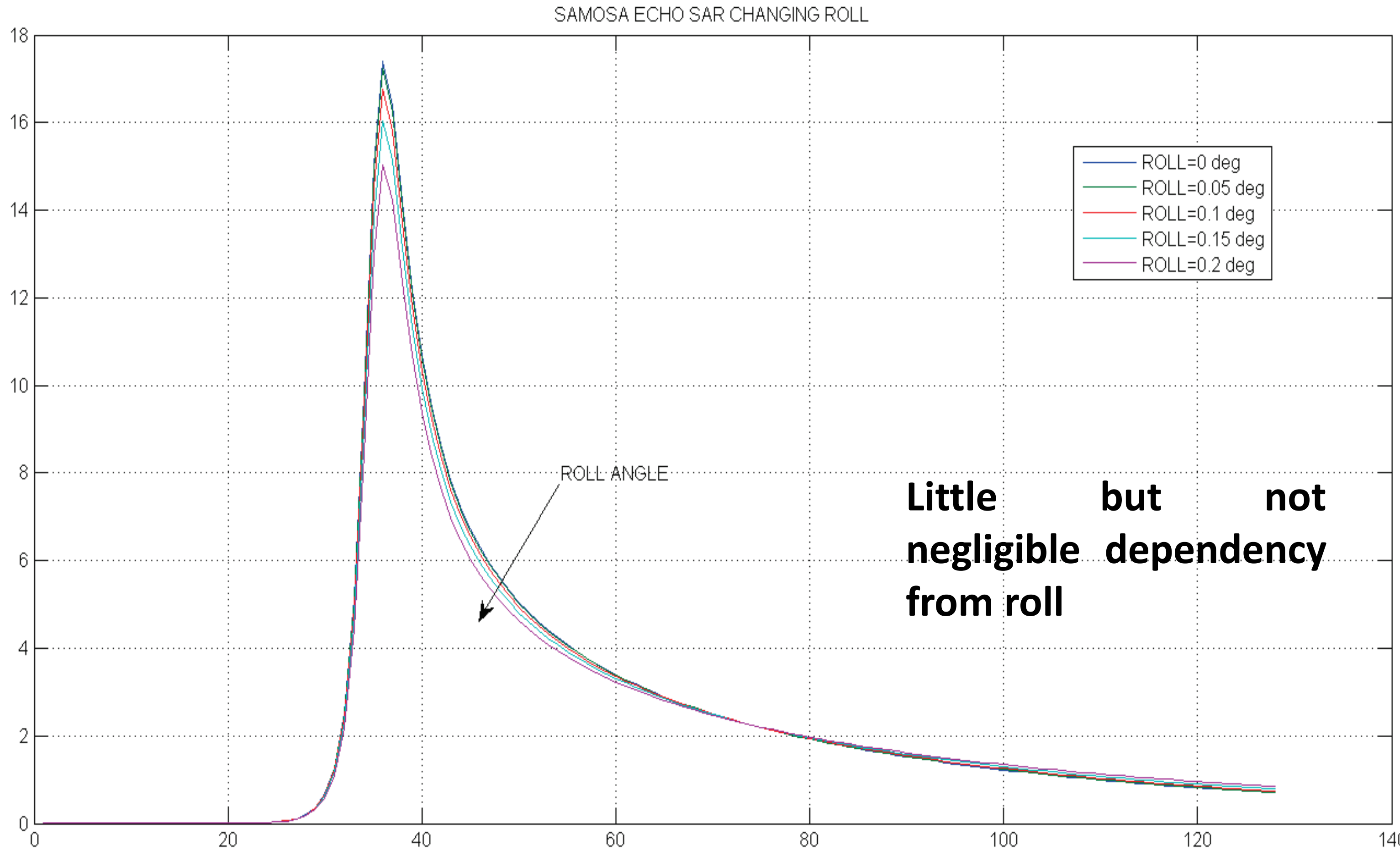

Little but not negligible dependency from roll

Dependency on Pitch Angle

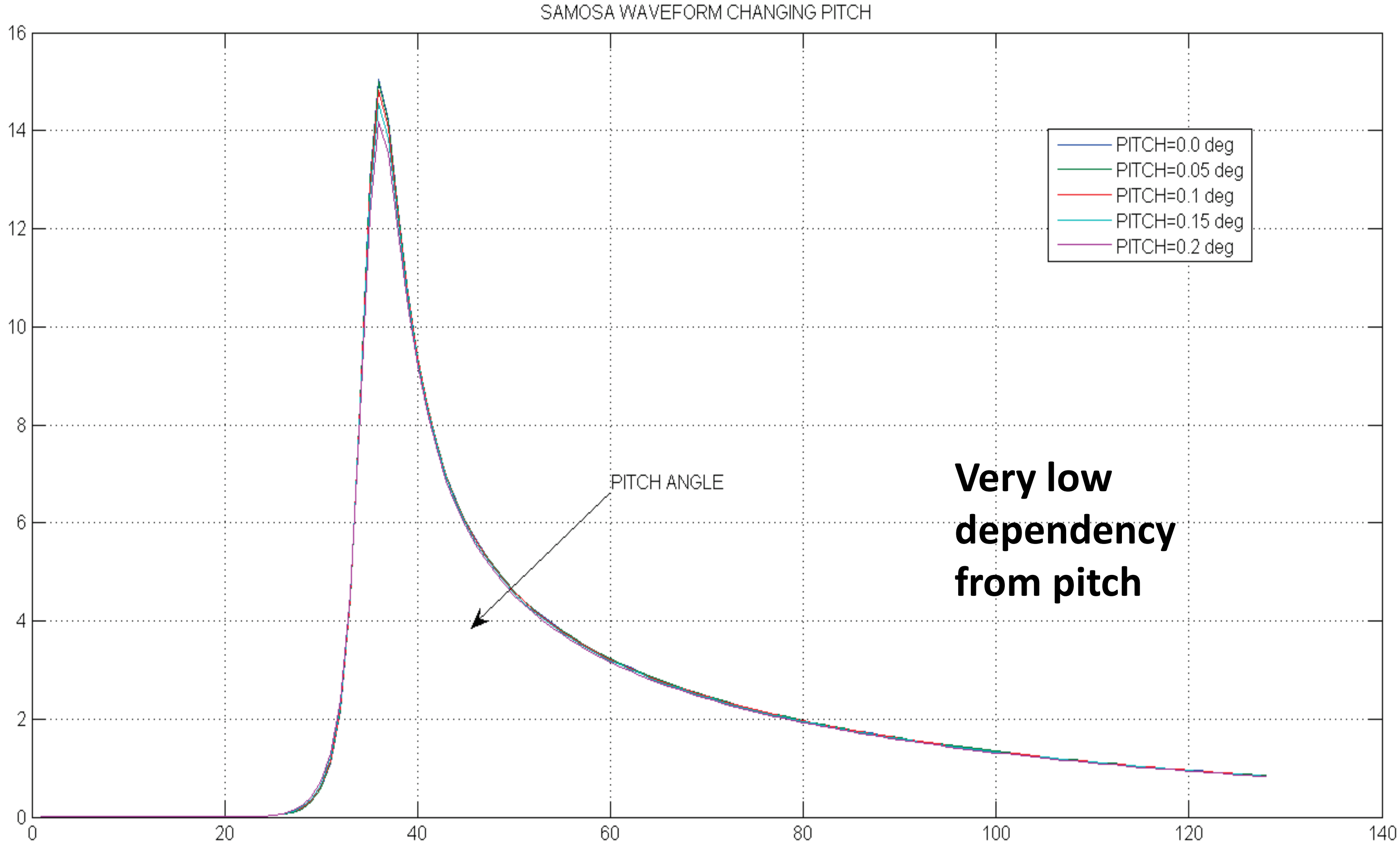

Very low dependency from pitch

Look-up Table for SAMOSA Model

Gaussian Approximation for squared Delay-Doppler PTR in the SAMOSA **Analytical** Model

$$\text{sinc}^2(x) \approx e^{-\left(\frac{x}{\sqrt{2}\cdot\alpha_p}\right)^2}$$

SAMOSA Model is function of alpha_p parameter (model's free parameter)

The question is: how to determine the best value for alpha_p ?

SAMOSA **Numerical** Model (SAMOSA Model not using the Gaussian approximation but a sinc^2 PTR and calculated solving numerical integration in 3-D space and time)

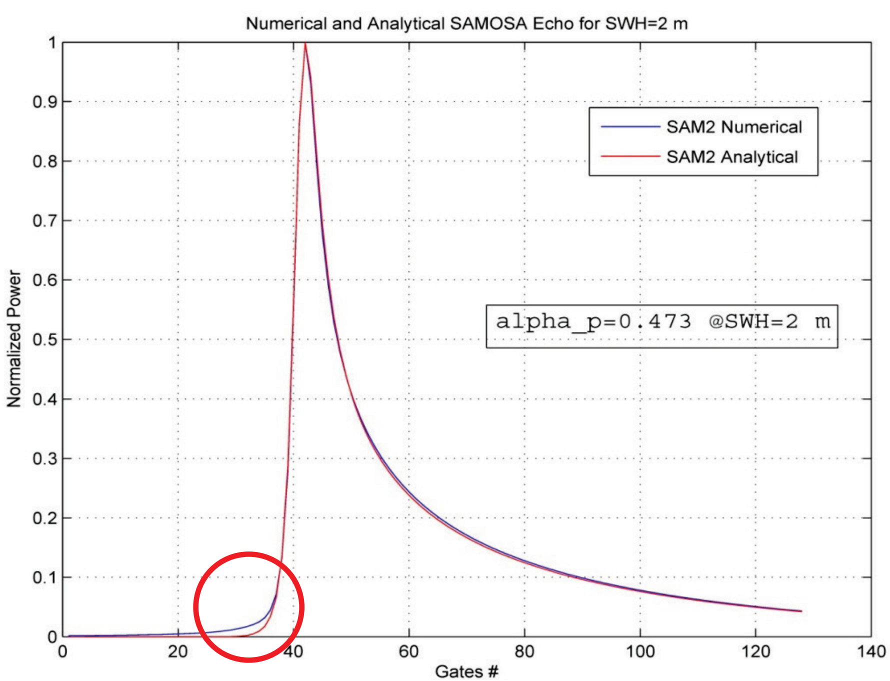

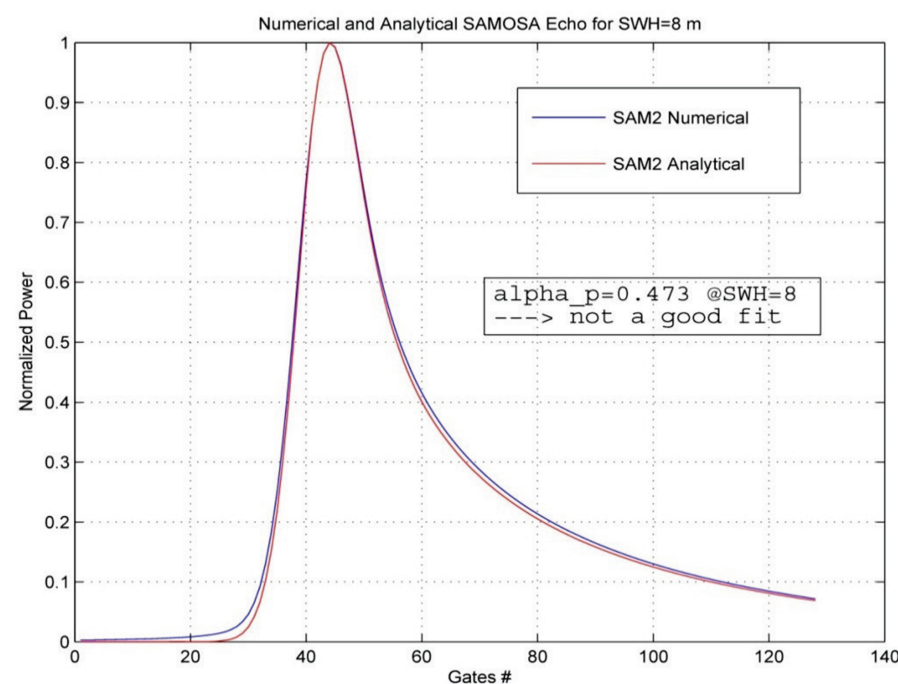

Look-up Table for SAMOSA Model

Gaussian Approximation for squared Delay-Doppler PTR in the SAMOSA **Analytical** Model

$$\operatorname{sinc}^2(x) \approx e^{-\left(\frac{x}{\sqrt{2}\cdot\alpha_p}\right)^2}$$

→ SAMOSA Model is function of alpha_p parameter (model's free parameter)

The question is: how to determine the best value for alpha_p ?

SAMOSA **Numerical** Model (SAMOSA Model not using the Gaussian approximation but a sinc^2 PTR and calculated solving numerical integration in 3-D space and time)

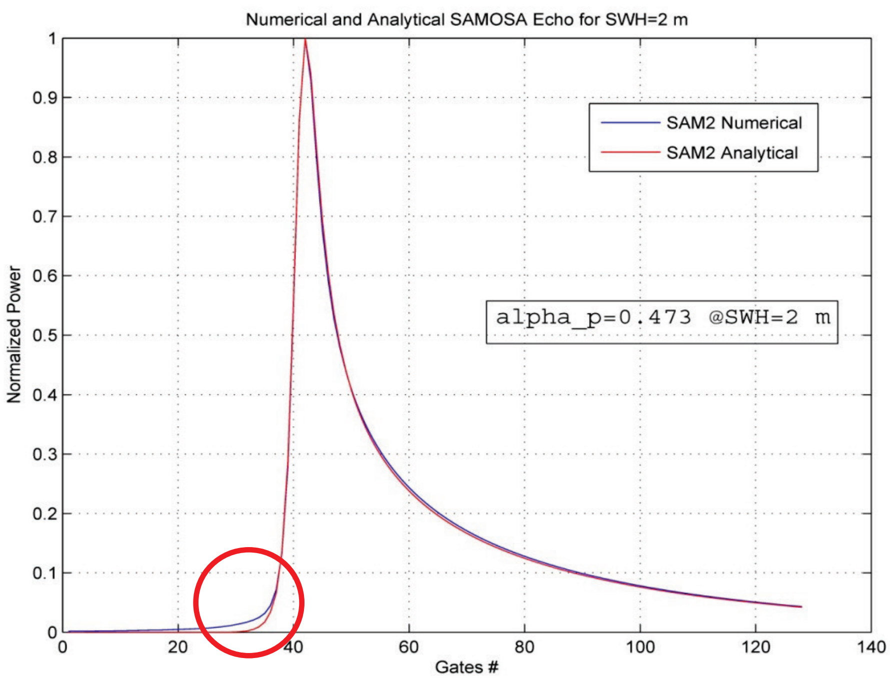

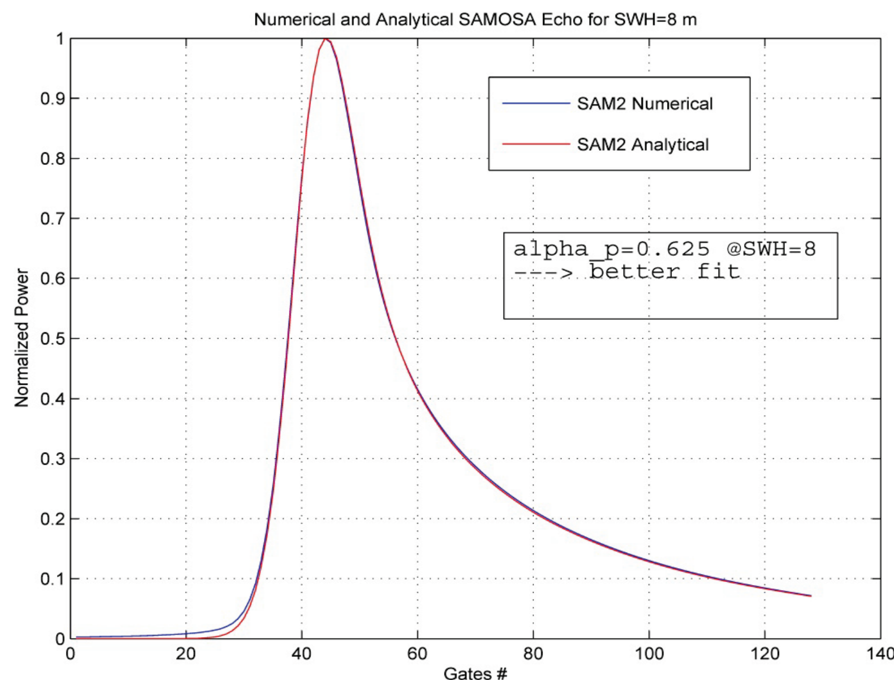

Look-up Table for SAMOSA Model

Gaussian Approximation for squared Delay-Doppler PTR in the SAMOSA **Analytical** Model

$$\mathrm{sinc}^2(x) \approx e^{-\left(\frac{x}{\sqrt{2}\cdot\alpha_p}\right)^2}$$

SAMOSA Model is function of alpha_p parameter (model's free parameter)

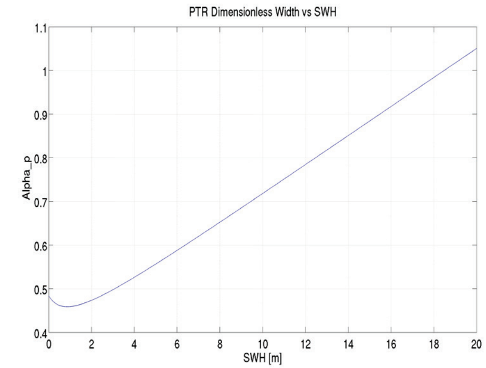

The question is: how to determine the best value for alpha_p ?

SAMOSA **Numerical** Model (SAMOSA Model not using the Gaussian approximation but a sinc^2 PTR and calculated solving numerical integration in 3-D space and time)

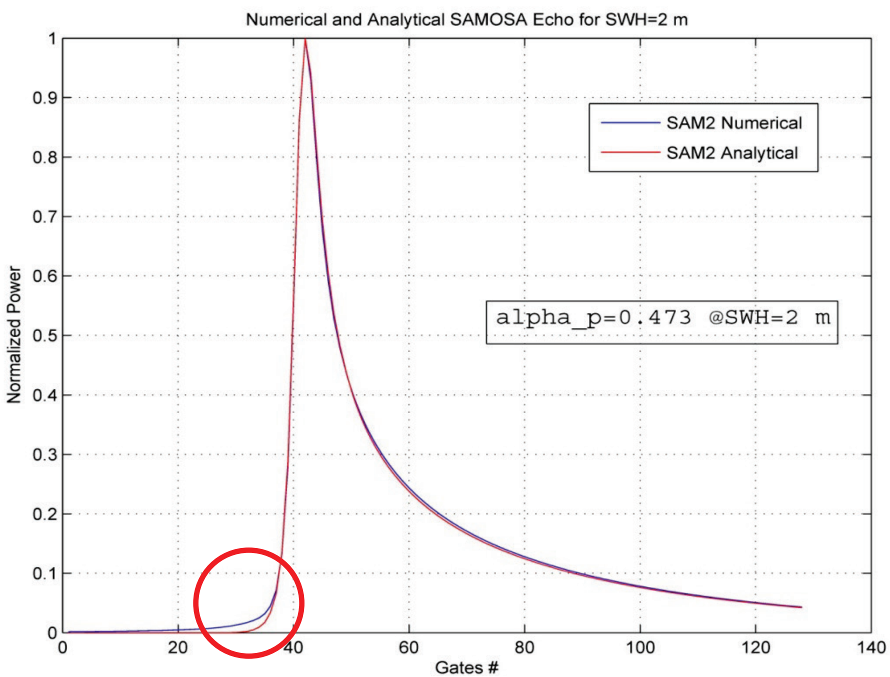

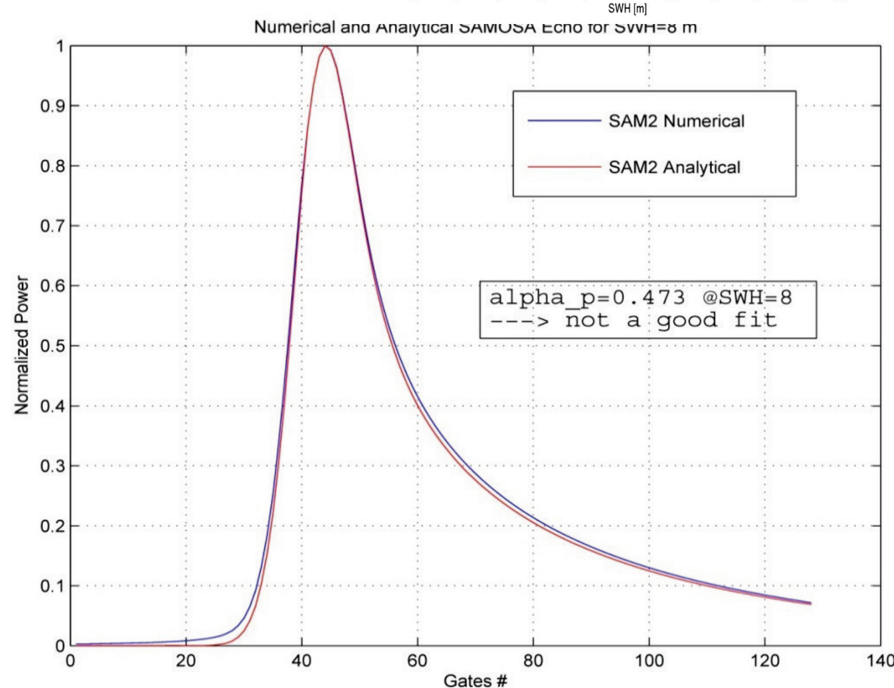

Look-up Table for SAMOSA Model

Gaussian Approximation for squared Delay-Doppler PTR in the SAMOSA **Analytical** Model

$$\mathrm{sinc}^2(x) \approx e^{-\left(\frac{x}{\sqrt{2}\cdot\alpha_p}\right)^2}$$

→ SAMOSA Model is function of alpha_p parameter (model's free parameter)

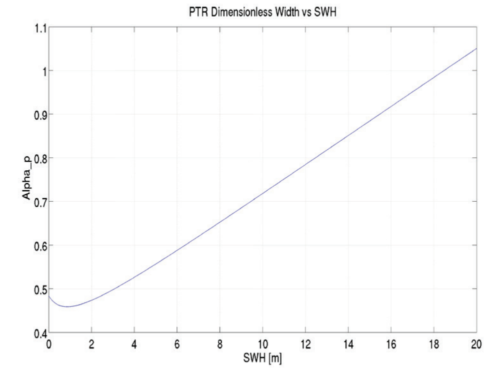

The question is: how to determine the best value for alpha_p ?

SAMOSA **Numerical** Model (SAMOSA Model not using the Gaussian approximation but a sinc^2 PTR and calculated solving numerical integration in 3-D space and time)

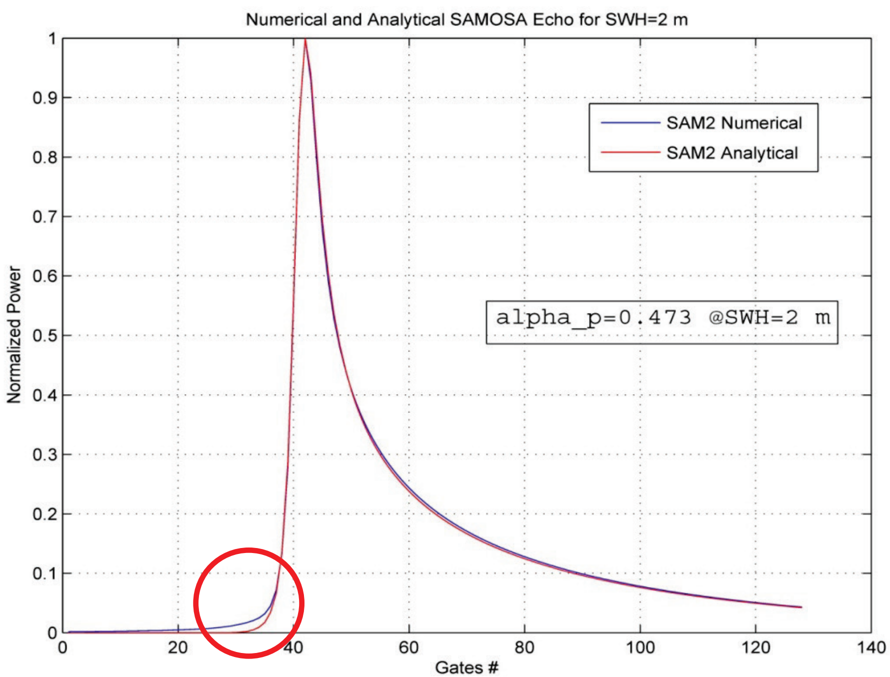

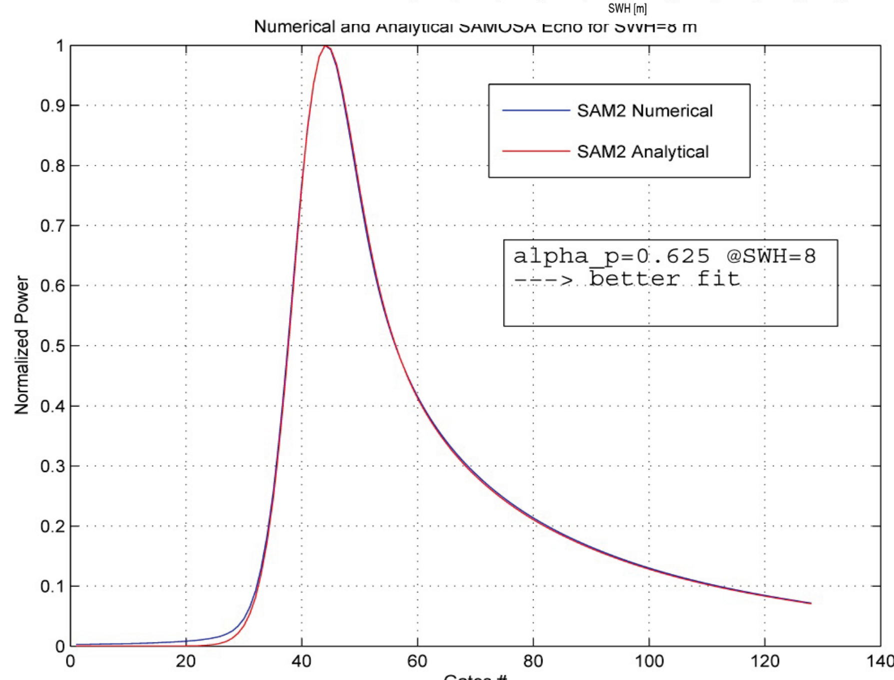

SAMOSA DDM ZERO MASKING

Due to the limited size of the radar receiving window (60 meters), after range alignment operation, the Delay –Doppler beam Stack gets filled with zeroes

At L2, a 1/0 mask is applied on Delay Doppler Map to build a echo waveform with tail decaying to zero

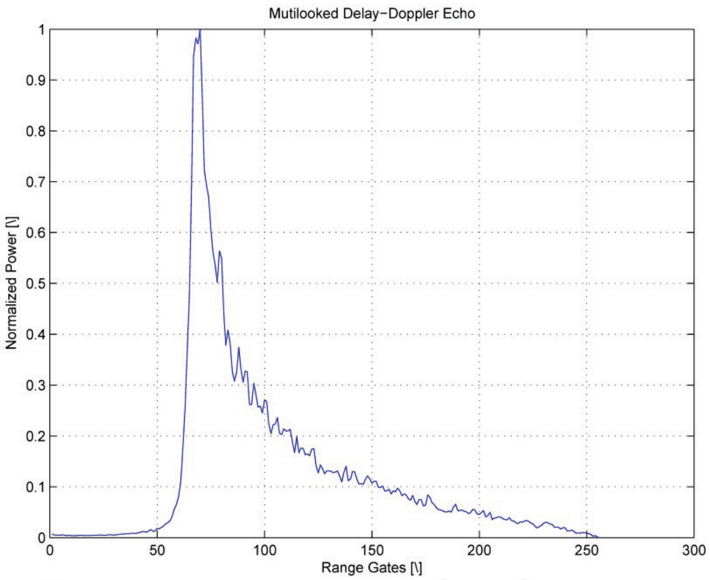

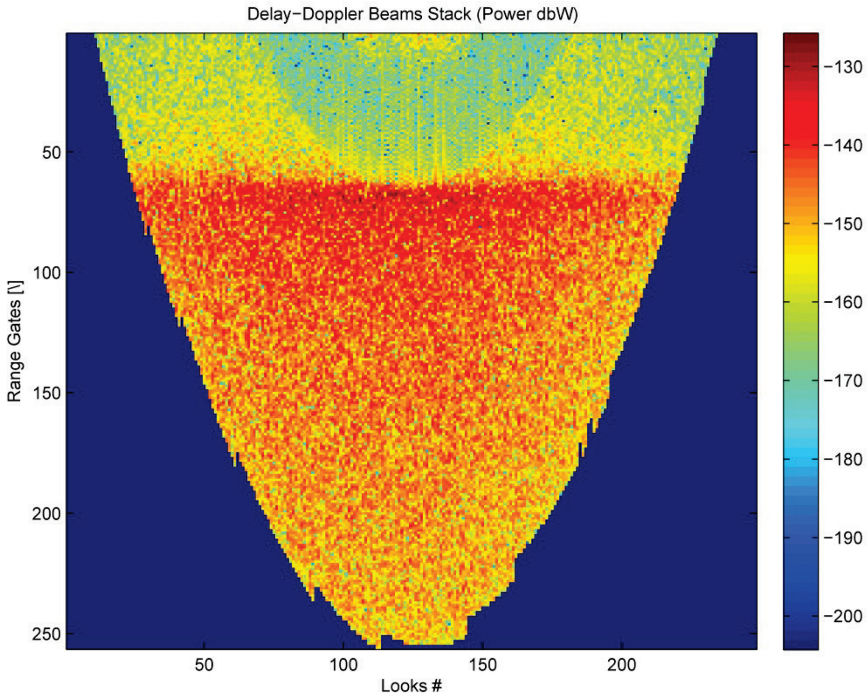

SAMOSA DDM ZERO MASKING

Due to the limited size of the radar receiving window (60 meters), after range alignment operation, the Delay –Doppler beam Stack gets filled with zeroes

At L2, a 1/0 mask is applied on Delay Doppler Map to build a echo waveform with tail decaying to zero

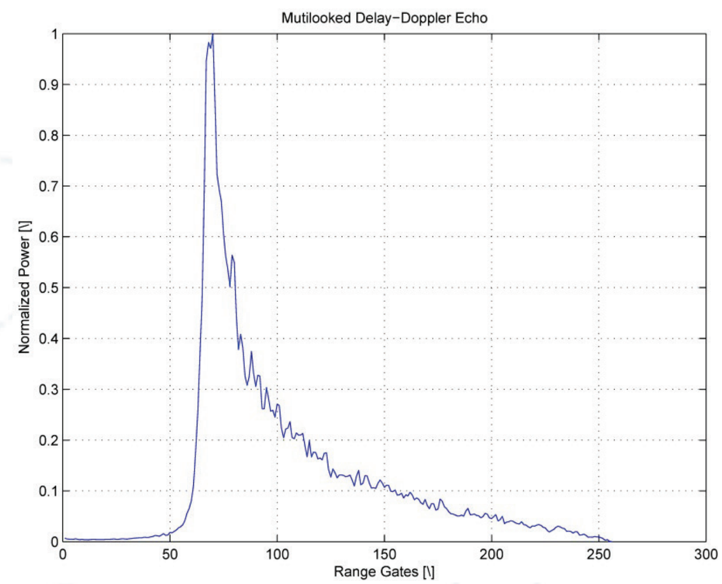

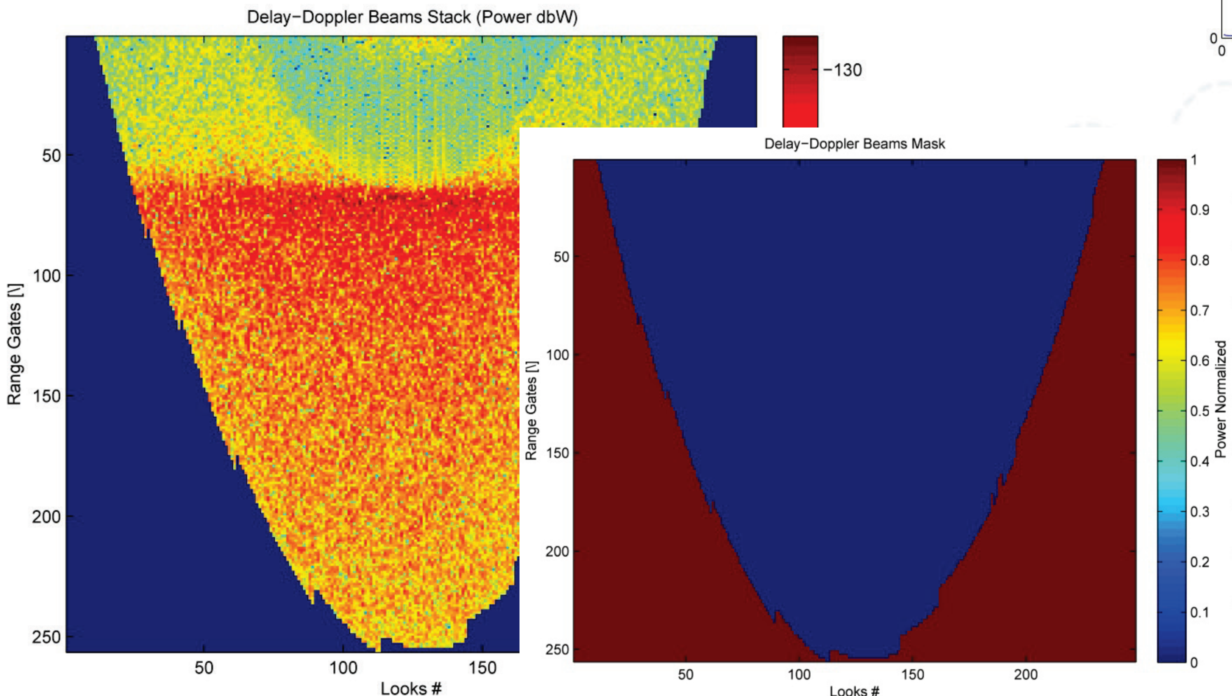

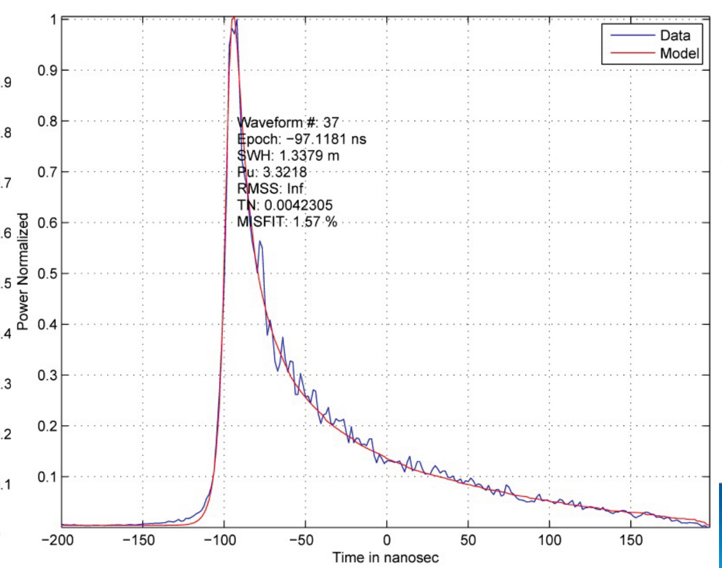

Waveform Retracking Scheme over open ocean

- The waveforms are retracked by Bounded Least-Square Curve Best-Fitting Algorithm (Levenberg-Marquard)
- Levenberg-Marquard implemented in C++ by LEVMAR Library
- Thermal noise floor is handled as parameter given in input to the retracking (estimated from early samples or from stack)
- Roll and Pitch mispointings are handled as parameters given in input to the retracking (from platform star trackers and corrected for biases)
- Mean square surface slope effect neglected
- Skewness set to zero

SAR Coastal Retracker

- Echo not contaminated/weakly contaminated/not specular, → SAMOSA 2 Model (C. Ray et al. 2014)
- Echo contaminated (high misfit) → SAMOSA 2 Model with Mean Square Surface Slope (mss) as free parameter and SWH set to zero

$$P_r^{SAR} = f_{SAMOSA}(t_0, SWH, P_u, mss)$$

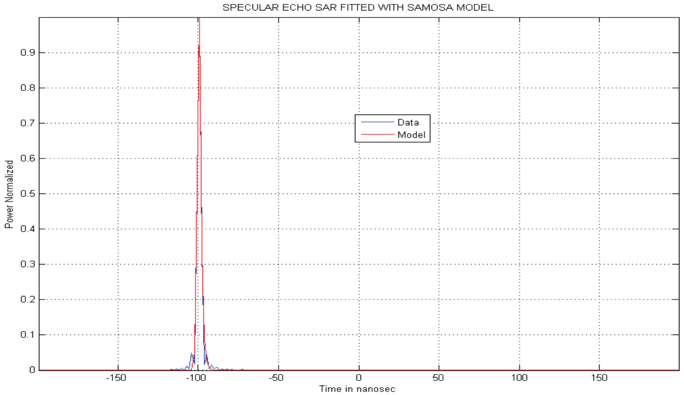

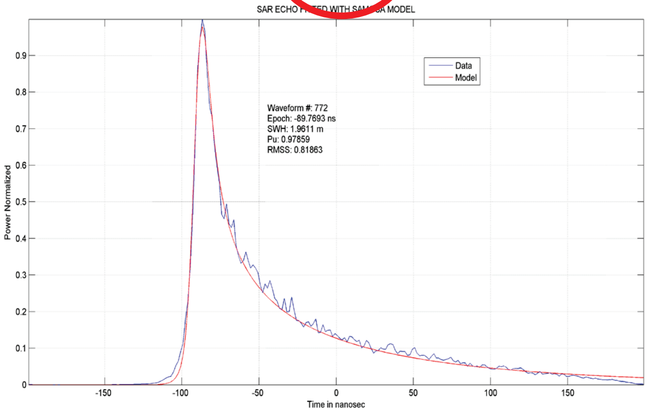

SAR Coastal Retracker

Fitting First-Guess epoch (retracker initialization) taken as position of the correlation's peak between 20 consecutive waveforms (to mitigate land contamination problem)

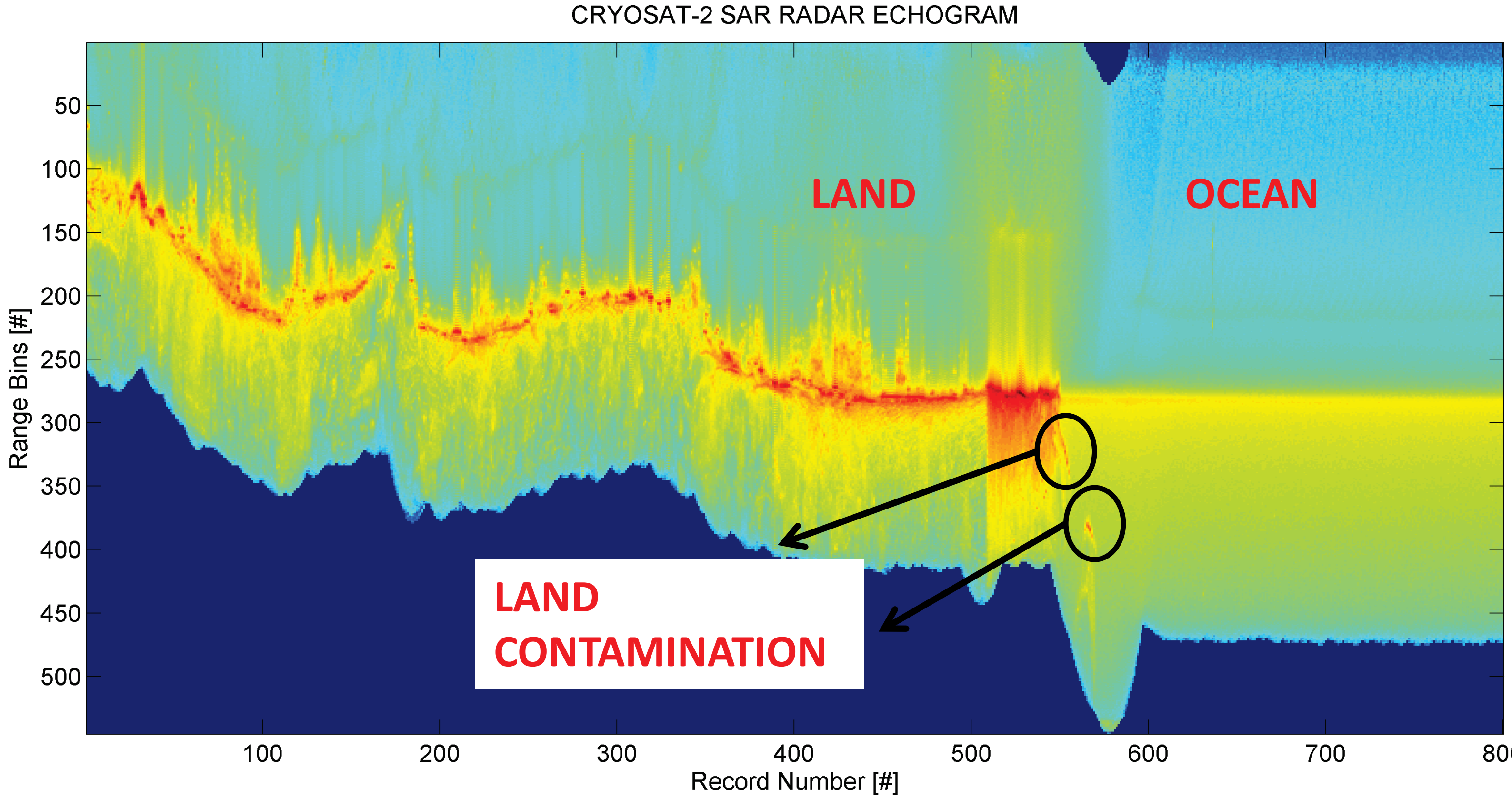

SAR Coastal Retracker

Fitting First-Guess epoch (retracker initialization) taken as position of the correlation's peak between 20 consecutive waveforms (to mitigate land contamination problem)

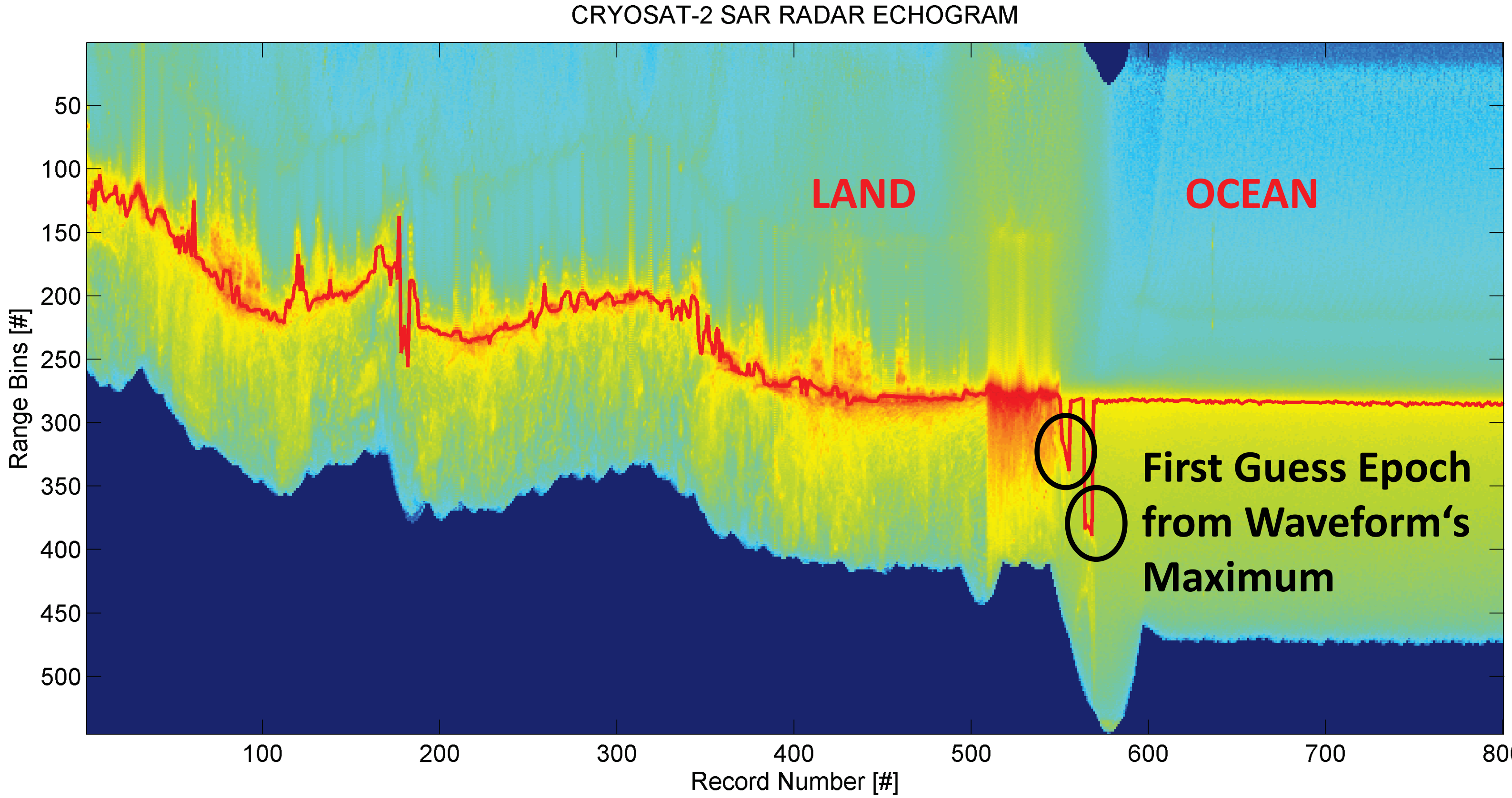

SAR Coastal Retracker

Fitting First-Guess epoch (retracker initialization) taken as position of the correlation's peak between 20 consecutive waveforms (to mitigate land contamination problem)

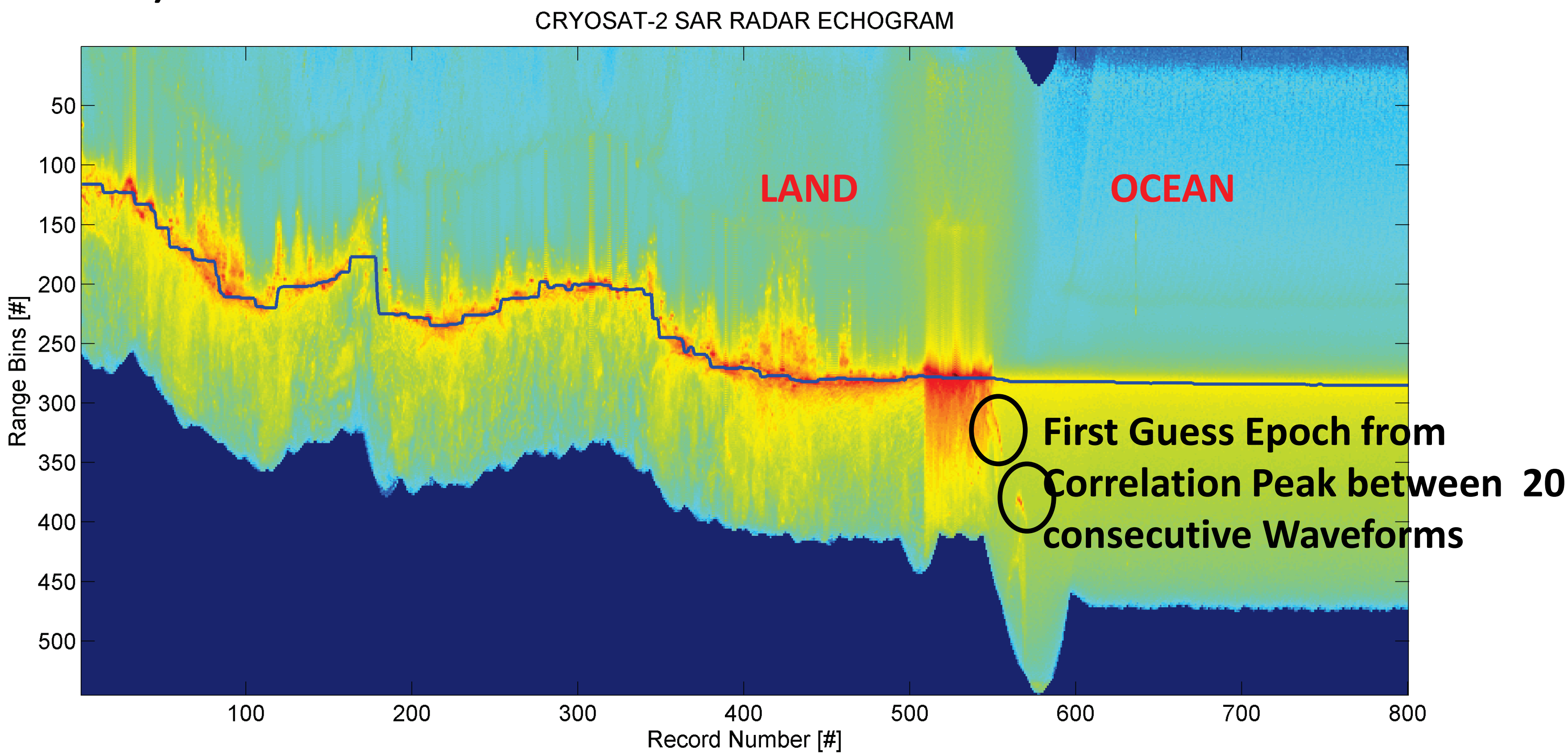

The Power Return depends on Wind Speed

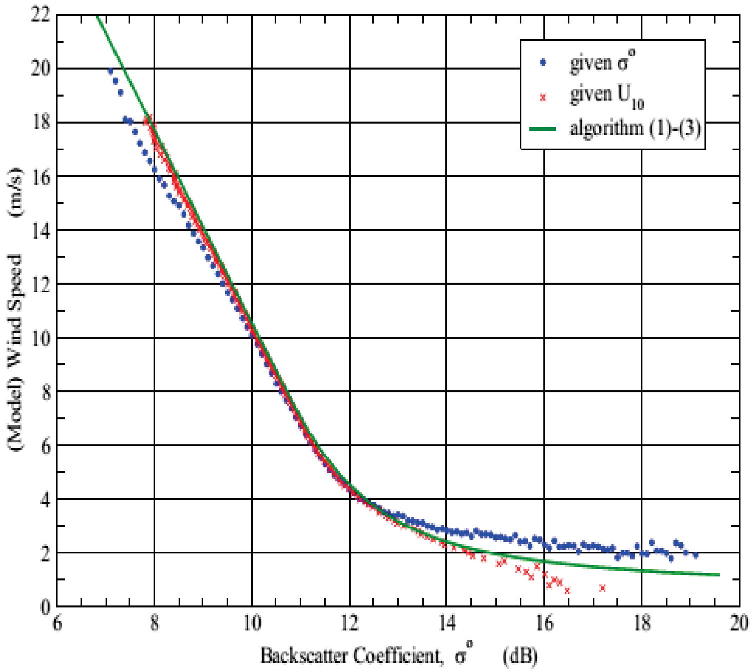

The wind speed model function is evaluated for **10 metres** above the sea surface. Only **speed intensity** can be retrieved

A standard model for Envisat is the Abdalla's Model (in the picture)

The retracking estimates the received power that is converted to backscattering applying the **SAR link budget equation.**

The waveform received power must be compensated for all the gain chain.

The nadir backscatter coefficient depends can be related to **wind speed**. Empirical models have established a relationship between the wind speed, the sea surface backscatter coefficient and significant wave height. Wind speed is calculated from an empirical mathematical relationship with the Ku-band backscatter coefficient and the significant wave height.

GPOD for CryoSat-2 and Sentinel-3

Follow hands on session this Friday:

- https://gpod.eo.esa.int/services/CRYOSAT_SAR/
- https://gpod.eo.esa.int/services/CRYOSAT_SARIN/
- https://gpod.eo.esa.int/services/SENTINEL3_SAR/

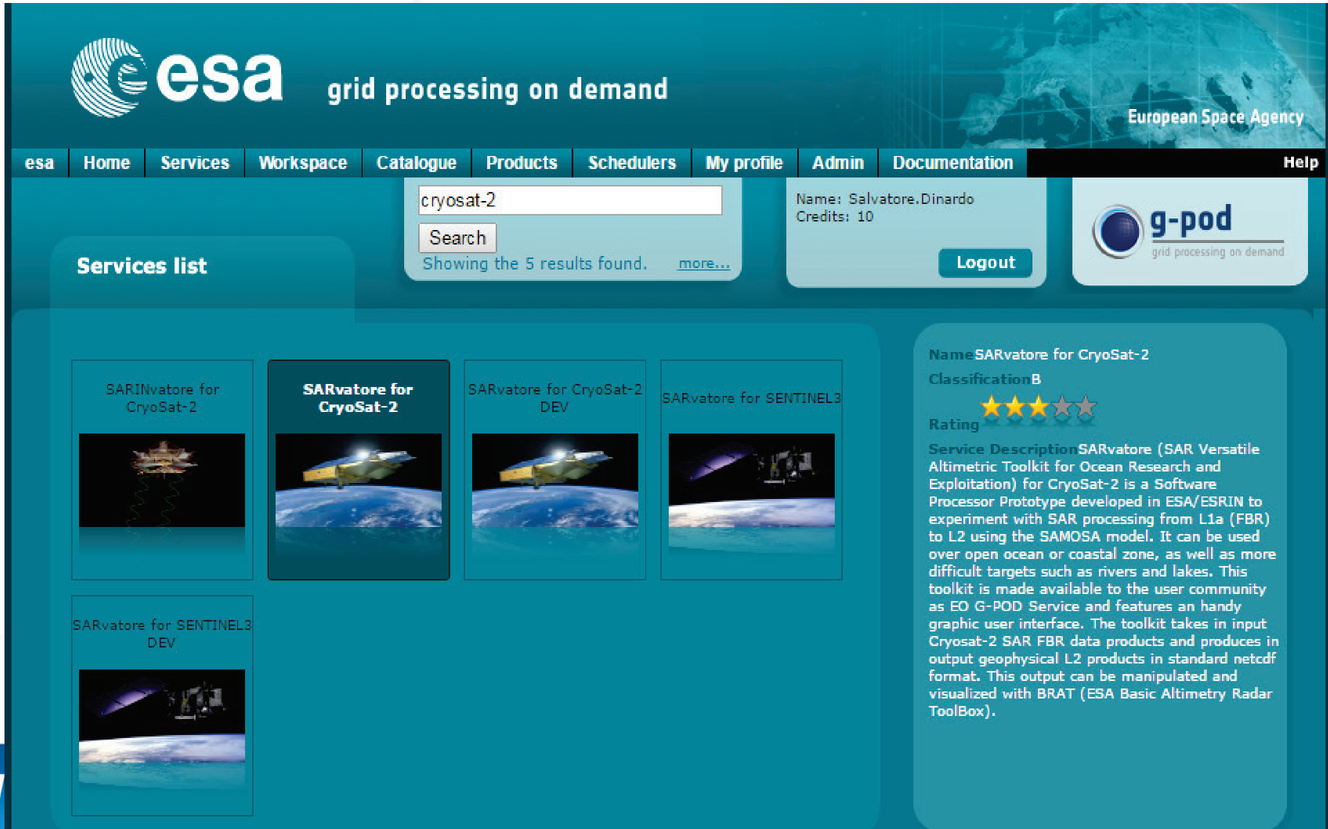

QUESTION TIME